The Role of Proteinase 3 in Chronic Obstructive Pulmonary Disease

By

Nicola Jane Sinden

A thesis submitted to

The University of Birmingham

For the degree of

Doctor of Philosophy

School of Clinical and Experimental Medicine

The University of Birmingham

November 2012

Synopsis

Chronic obstructive pulmonary disease (COPD) is a major cause of morbidity and mortality worldwide. In COPD, an imbalance is believed to exist between the activities of neutrophil serine proteinases (NSPs) such as neutrophil elastase (NE) and proteinase 3 (PR3), and their endogenous inhibitors such as alpha-1-antitrypsin (A1AT). Hence, a deficiency of A1AT predisposes to the development of COPD.

Following their release from neutrophils, NSPs may bind to local inhibitors depending on their concentrations and affinities, to substrate such as lung elastin or to the neutrophil cell membrane where they remain active. This work has demonstrated that; NSPs bound to the proteinase "inhibitor" alpha-2-macroglobulin (A2M) remain active, and A2M:NE complexes are able to degrade elastin *in vitro*; NE bound to elastin is poorly inhibited by A1AT; and PR3 binding to the neutrophil cell membrane is greater when the local concentration of A1AT is reduced.

The role of PR3 has not previously been studied in detail. However, PR3 activity was found to be present in sputum from clinically stable subjects with COPD or A1AT deficiency and was greater than NE activity. Hence, PR3 is likely to be important in the pathogenesis of COPD and could potentially be a target for therapeutic inhibitors.

Acknowledgements

Firstly, I would like to thank my supervisors Professor Robert Stockley and Professor Tim Dafforn for their support and encouragement throughout my PhD.

I would also like to thank my colleagues in both the Respiratory Research and Biosciences laboratories for their help with laboratory techniques; Gill McNab, Michael Ungurs, Dippica Mistry, Patti Bharadwa, Georgia Walton, Rosemary Parslow and Raul Pacheco-Gomez.

Many thanks also go to my clinical colleagues in the Lung Function and Sleep Department at Queen Elizabeth Hospital, to Peter Nightingale for providing statistical advice, and to Imran Haq at the University of Cambridge for performing the purification of the Z variant A1AT.

I would also like to thank my family for their love and support over the last 3 years; my husband Andy, and my mum, dad, brother and sister.

Finally, I wish to thank Grifols Therapeutics for funding this research.

List of abbreviations used throughout this thesis

A1AT	Alpha-1-antitrypsin
A1ATD	Alpha-1-antitrypsin deficiency
A2M	Alpha-2-macroglobulin
ADAPT	Antitrypsin Deficiency Assessment and Programme for Treatment
ANCA	Anti-neutrophil cytoplasmic antibody
ARDS	Acute respiratory distress syndrome
BAL	Bronchoalveolar lavage
BMI	Body mass index
BSA	Bovine serum albumin
CF	Cystic fibrosis
CFU	Colony forming units
CG	Cathepsin G
COPD	Chronic Obstructive Pulmonary Disease
CT	Computed Tomography
CV	Coefficient of variation
DMSO	Dimethyl sulfoxide
DNA	Deoxyribonucleic acid
EDTA	Ethylenediaminetetraacetic acid
ELISA	Enzyme linked immunosorbent assay
FEV1	Forced expiratory volume in one second
FITC	Fluorescein isothiocyanate
fMLP	N-formyl-methionine-leucine-phenylalanine
FRET	Förster Resonance Energy Transfer
FS	Forward scatter

FVC	Forced vital capacity
GPI	Glycosylphosphatidylinositol
HRCT	High resolution computed tomography
IL	Interleukin
iPSCs	Induced pluripotent stem cells
IQR	Inter-quartile range
Kass	Association rate constant
Kcat	Catalytic constant
KCO	Carbon monoxide transfer coefficient
Km	Michaelis constant
LPS	Lipopolysaccharide
LT	Leukotriene
LTOT	Long term oxygen therapy
MAPK	Mitogen-activated protein kinase
MFI	Mean fluorescence intensity
MMP	Matrix metalloproteinase
MNEI	Monocyte/neutrophil elastase inhibitor
MPO	Myeloperoxidase
MSaapvN	N-Methoxysuccinyl-Ala-Ala-Pro-Val p-nitroanilide
NE	Neutrophil elastase
NETs	Neutrophil extracellular traps
NICE	National Institute for Clinical Excellence
NSP	Neutrophil serine proteinase
OD	Optical density
PAS	Periodic acid Schiff

PBMC	Peripheral blood mononuclear cell
PBS	Phosphate buffered saline
PFTs	Pulmonary function tests
PGRN	Progranulin
Pi	Protease inhibitor
PMA	Phorbol myristate acetate
PMN	Polymorphonuclear leukocyte
PMSF	Phenylmethylsulphonyl fluoride
PPE	Porcine pancreatic elastase
PR3	Proteinase 3
RCL	Reactive centre loop
RPM	Revolutions per minute
RV	Residual volume
[S]	Concentration of substrate
SEM	Standard error of the mean
Serpin	Serine proteinase inhibitor
SGRQ	Saint George's Respiratory Questionnaire
SIRS	Systemic inflammatory response syndrome
SlaaapN	N-succinyl-ala-ala-ala-p-nitroanilide
SLPI	Secretory leukoproteinase inhibitor
SS	Side scatter
TIMP	Tissue inhibitor of metalloproteinases
TLC	Total lung capacity
TMB	Tetramethylbenzidine
TNFα	Tumour necrosis factor alpha

UK	United Kingdom
V	Reaction velocity
Vmax	Maximum rate of catalysis
WG	Wegener’s granulomatosis

Contents

List of Figures

List of Tables

1 Introduction

1.1 Chronic obstructive pulmonary disease

Chronic obstructive pulmonary disease (COPD) is a major cause of morbidity and mortality worldwide [1] and is estimated to kill around 25,000 people per year in England and Wales [2]. In the UK, it is estimated that 3 million people have COPD; approximately 900,000 cases have been diagnosed and a further 2 million people remain undiagnosed [3]. COPD is a major cause of hospital admissions and is estimated to be responsible for over one million hospital bed days per year [4]. For these reasons, further research into the pathophysiology and treatment of this condition is vital.

COPD is characterised by airflow obstruction that is not fully reversible following administration of short acting bronchodilators, and pulmonary inflammation in response to inhaled substances. The airflow obstruction is usually progressive over time. Airflow obstruction is diagnosed by performing spirometry and is defined by the ratio of the forced expiratory volume in one second (FEV1) to the forced vital capacity (FVC) being less than 0.7 [5], although depending on the subject's age and gender this may result in a slight over- or under-diagnosis of the condition, and some studies use alternative spirometric criteria (lower limit of normal) [6]. Severity is classified according to the post-bronchodilator FEV1 compared to that predicted by the subject's age, sex and height (FEV1 % predicted). The grades of severity of airflow obstruction are summarised in Table 1.1.

Table 1.1-Severity of airflow obstruction according to the National Institute for Clinical Excellence (NICE) 2010 clinical guidelines

Post-bronchodilator FEV1 (% predicted)	Severity of airflow obstruction
≥80%	Mild
50-79%	Moderate
30-49%	Severe
<30%	Very Severe

Although the main risk factor for the development of COPD is cigarette smoking [7], only around 20% of smokers develop clinically significant disease [8] indicating that other environmental and genetic risk factors are important in the aetiology. However, a deficiency of alpha-1-antitrypsin (A1AT) is the only widely accepted genetic predisposition to this disease.

1.1.1 Clinical features

COPD usually presents in middle age in subjects who are current or ex-smokers. Symptoms include exertional breathlessness, chronic cough, sputum production and wheeze. In addition, exacerbations occur which are associated with a rapid and sustained worsening of symptoms beyond normal day-to-day variability. Exacerbations can be infective (bacterial or viral) or non-infective (e.g. related to air pollution) in aetiology [9].

Significant heterogeneity exists within COPD and several pulmonary phenotypes have been recognised including; chronic bronchitis, emphysema, small airways disease and

bronchiectasis. These conditions can co-exist to varying degrees in affected individuals [10], with some showing a predominance of a particular phenotype. These pulmonary phenotypes are discussed in further detail below, and the pathophysiology is discussed further in sections 1.1.3 and 1.1.4, where the importance of the neutrophil and neutrophil-derived serine proteinases is considered.

Most subjects with COPD exhibit fixed airflow obstruction as measured by spirometry, although some may have an element of bronchodilator reversibility. Pulmonary function testing may also reveal an increase in lung volumes and gas trapping as measured by total lung capacity (TLC) and residual volume (RV). Small airways abnormalities may be identified by measurement of the forced mid expiratory flow (FEF25-75%). Emphysema is associated with the destruction of lung parenchyma and is associated with a reduction in gas transfer corrected for lung volumes (KCO).

In addition to pulmonary inflammation, COPD is associated with systemic inflammation [11]. It has been recognised that systemic features and other diseases are more common in COPD [12], including skeletal muscle dysfunction [13], cardiovascular disease [14], osteoporosis [15] and diabetes [16]. However, whether this represents independent physiological processes, common generalised processes or "overspill" inflammation [17] from one organ to another remains uncertain.

1.1.1.1 Chronic bronchitis

Chronic bronchitis is defined clinically as a cough productive of sputum for most days over at least a three month period in two consecutive years [18]. Subjects with the chronic bronchitis phenotype show a higher airway inflammatory burden compared to subjects who do not spontaneously expectorate sputum, which is not related to smoking status [19]. Chronic bronchitis is associated with several clinical consequences, including an accelerated decline in FEV1 [20], a predisposition to lower respiratory tract infections and greater exacerbation frequency [21], and increased mortality [22]. Chronic bronchitis is generally believed to be due to chronic mucus hypersecretion by goblet cells, which leads to worsening airflow obstruction by luminal obstruction of small airways, epithelial remodelling, and alteration of airway surface tension predisposing to collapse [23].

1.1.1.2 Emphysema

Emphysema is defined histologically as the destruction of alveolar walls and enlargement of airspaces distal to the terminal bronchioles [24]. More recently, emphysema has been diagnosed by computed tomography (CT) scanning [25]. Emphysema may be further sub-classified into centrilobular, panacinar and paraseptal emphysema, which may show different distributions throughout the lung [26]. For example, emphysema associated with cigarette smoking is typically centrilobular and predominantly affects the upper zones, whereas emphysema associated with A1AT deficiency (A1ATD) is typically panacinar in appearance and predominantly affects the lower zones [27]. These CT scan appearances are shown in Figure 1.1. Progressive destruction of lung parenchyma may lead to the formation of bullae, which are thin-walled air-filled spaces which do not take part in gas exchange.

1.1.1.3 Small airways disease

Small airways disease has been recognised as an important pathological finding associated with COPD [28]. The small airways are defined as non-cartilaginous airways with an internal diameter of 2mm or less [29]. In COPD, increased thickness of the small airway walls leads to luminal narrowing, which may be further occluded by mucus. These changes lead to increased peripheral airway resistance, air trapping and breathlessness on exertion. At present, the measurement of small airway function remains clinically difficult, and the delivery of inhaled drugs to the small airways requires further optimisation. A detailed review of the pathophysiology of the small airways in COPD can be found elsewhere [30].

1.1.1.4 Bronchiectasis

Bronchiectasis is usually diagnosed by high resolution CT (HRCT) scanning and clinical history. The condition is characterised by irreversible airway dilatation with chronic bronchial infection/inflammation [31]. Clinical features include a chronic productive cough, frequent exacerbations, fatigue and basal crepitations on respiratory examination. HRCT findings include bronchial dilatation and a lack of bronchial tapering [32]. Bronchiectasis may be sub-classified into cylindrical, varicose and cystic bronchiectasis according to CT scan appearance, and examples of such HRCT findings are shown in Figure 1.2.

Figure 1.1-CT scan appearances of centrilobular and panacinar emphysema

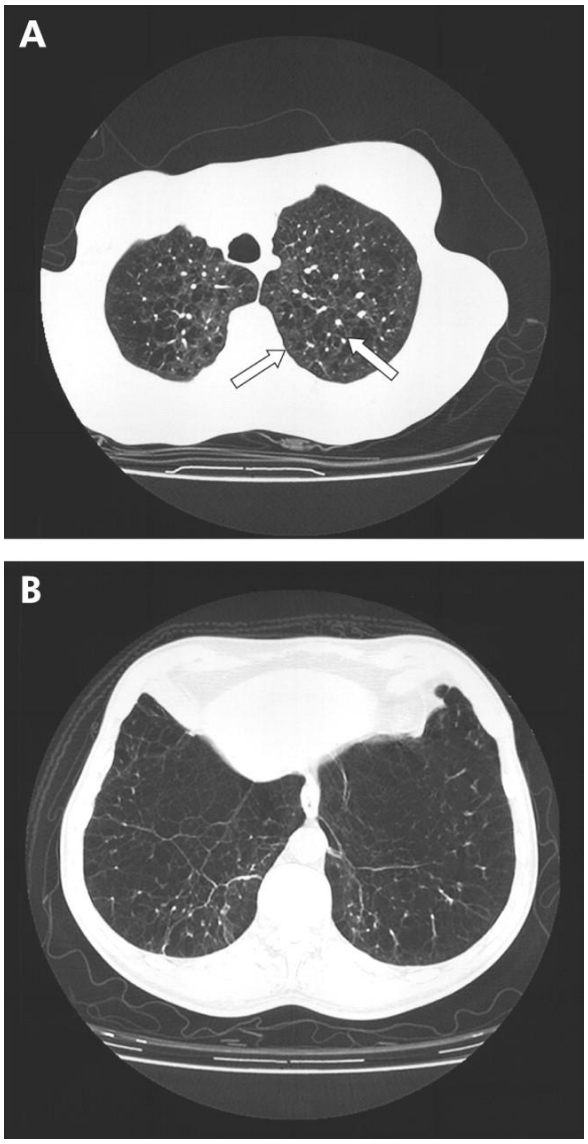

Figure 1.1: HRCT scans showing centrilobular emphysema in A with patchy low density areas (arrowed) and panacinar emphysema in B with a more diffuse pattern. Panacinar emphysema predominantly affects the lower zones and is associated with A1ATD. Images reproduced from [33].

Figure 1.2- CT scan appearances of bronchiectasis

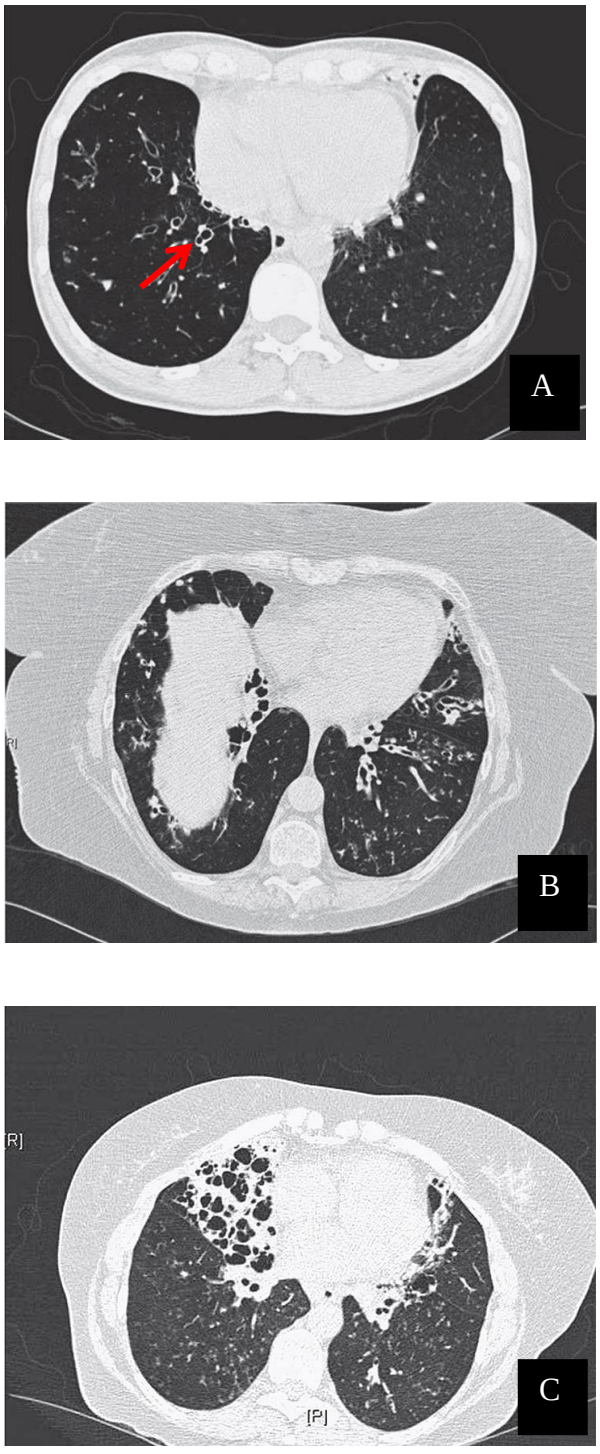

Figure 1.2: HRCT scans showing cylindrical bronchiectasis in A (with the classic signet ring sign arrowed), varicose bronchiectasis in B and cystic bronchiectasis in C. Images reproduced from [34].

1.1.2 Treatment options

Cigarette smoking is an important risk factor for COPD, and smoking cessation is one accepted intervention which reduces disease progression [35], as well as long term oxygen therapy (LTOT) in hypoxic patients which reduces mortality [36]. Inhaled therapies target airflow obstruction and inflammation, and include short or long-acting bronchodilators and corticosteroids. Non-pharmacological therapies such as pulmonary rehabilitation are also used [37]. Exacerbations are managed by using oral corticosteroids and/or antibiotic therapy. Pneumococcal and annual influenza vaccines also provide some benefit to patients with COPD [3].

At present, the pharmacological therapies available for COPD do not convincingly alter disease progression or mortality, and therefore there is an urgent need for novel therapies. Increasing our understanding of the complex pathophysiology of COPD will aid the development of specific therapies in the future. Some of the newer anti-inflammatory therapies for COPD in development are described elsewhere [38, 39].

1.1.3 The role of the neutrophil in COPD

Overall there is a strong body of evidence that the neutrophil and neutrophil-derived proteinases play a central role in the pathophysiology of COPD. Patients with COPD have increased numbers of neutrophils in sputum and bronchoalveolar lavage (BAL) fluid compared with asymptomatic smokers [40, 41]. Studies of neutrophilic factors in the airway at baseline have been shown to predict the subsequent progression of disease [42]

and rapid progression in COPD is associated with greater neutrophilic inflammation in the airways [43]. Furthermore, exacerbations of COPD are also associated with an increased neutrophilic inflammation [44] which could explain the greater progression of disease in individuals with frequent exacerbations [45]. Finally, both neutrophil numbers and the concentration of NE complex with A1AT are reduced following smoking cessation [46], consistent with the beneficial effects of this intervention.

In patients with COPD there is also evidence of altered circulating neutrophil function. For example; increased spontaneous adherence to endothelium under flow conditions [47], enhanced chemotaxis, increased spontaneous extracellular proteolysis [48], and greater production of reactive oxygen species [12]. More recent studies have confirmed that neutrophils show an aberrant chemotactic response at all degrees of severity of COPD which is not related to treatment or smoking habit, suggesting it is an inherent abnormality [49].

1.1.4 The role of serine proteinases in COPD

The serine proteinases are a diverse group of enzymes which possess a reactive serine residue within the active site. The family includes digestive enzymes such as trypsin and chymotrypsin, enzymes that participate in blood coagulation such as thrombin, and other bacterial enzymes [50]. The neutrophil serine proteinases (NSPs) are serine proteinases of the chymotrypsin family that are released from the azurophilic granules of activated neutrophils during inflammation. This family includes neutrophil elastase (NE), proteinase 3 (PR3) and cathepsin G (CG). The basic structure of chymotrypsin-like serine proteinases is shown in Figure 1.3. Their activities depend on a catalytic triad consisting of aspartate,

histidine and serine residues which are separated in their primary sequence but brought together at the enzyme's active site in their tertiary structures [51]. Substitution of amino acids at the active site gives individual proteinases their substrate specificities. The interactions between proteinases and their substrates were described by Schechter and Berger [52]; the S subsites of the enzyme accommodate P residues of the substrate upstream of the cleavage site, whilst S′ subsites accommodate P′ residues downstream of the cleavage site [51], as shown in Figure 1.4.

Figure 1.3-Structure of chymotrypsin-like serine proteinases

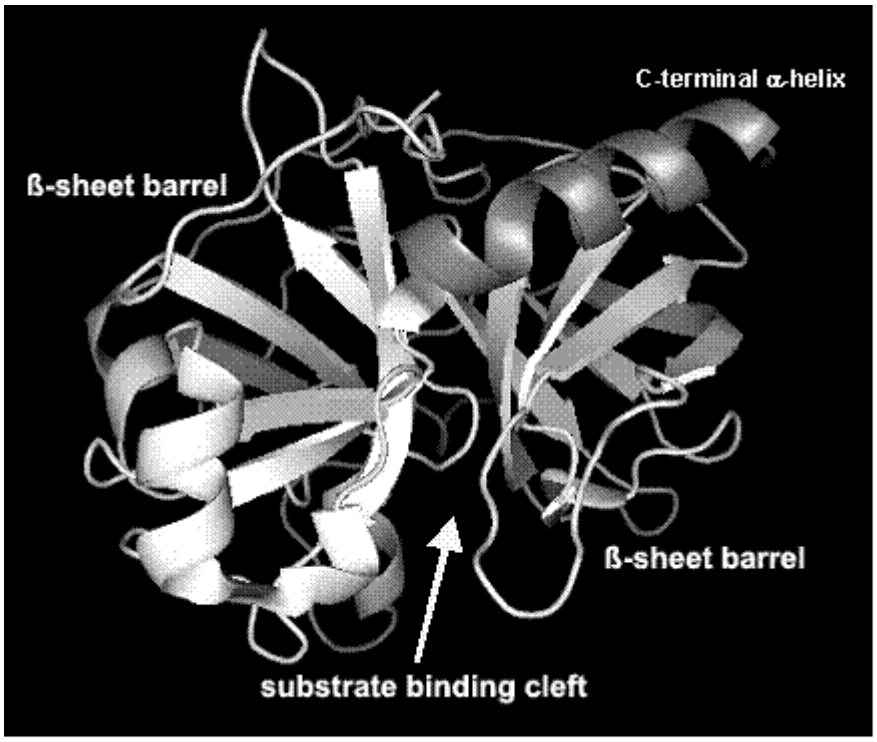

Figure 1.3: The serine proteinases are composed of two β-barrel domains (each consisting of six antiparallel β sheets) and a C-terminal α-helix. The catalytic triad of aspartate, histidine and serine is located within the substrate binding cleft. The structure of bovine chymotrypsin is shown as an example.

Figure 1.4- Interactions between proteinases and their substrates

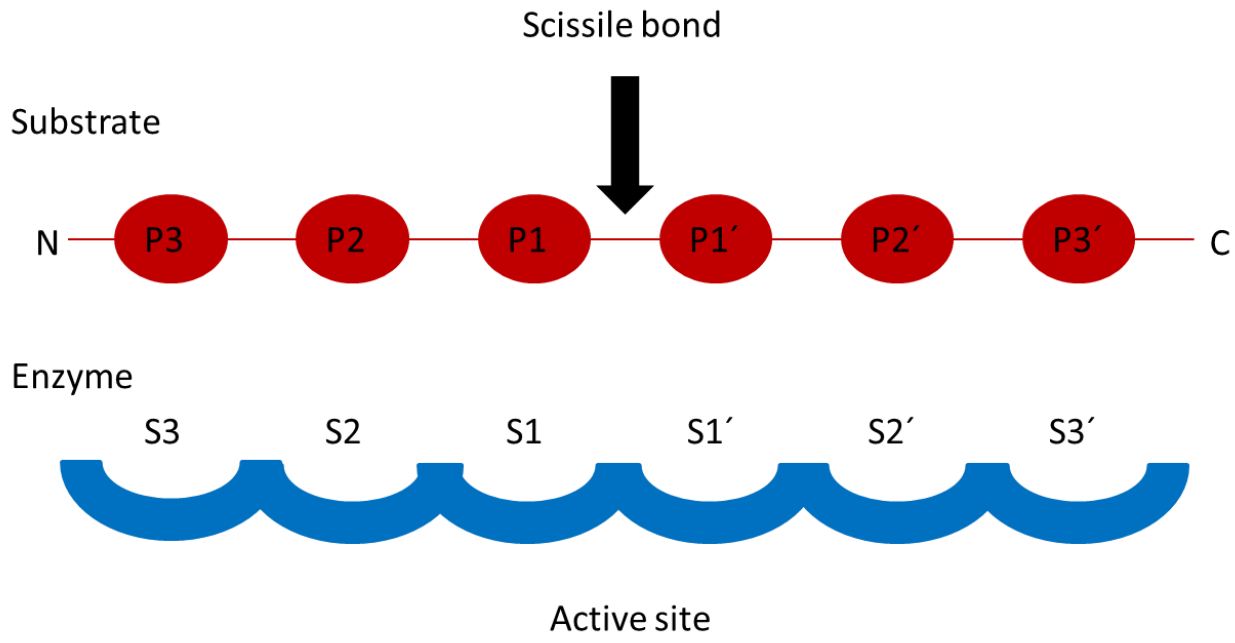

Figure 1.4: Nomenclature described by Schechter and Berger for interactions between enzymes and their substrates. The scissile bond of the substrate is subject to enzymatic cleavage. The S subsites of the enzyme accommodate P residues of the substrate towards the N-terminal and S´ subsites accommodate P´ residues towards the C-terminal of the substrate.

The NSPs have both intracellular and extracellular functions. They play an important role in the destruction of intracellular pathogens by digesting phagocytosed bacteria within phagolysosomes [53]. Enzymatically active NSPs are found on the cell membrane of activated neutrophils [54] which may facilitate penetration through tissue barriers and enable local degradation of extracellular matrix proteins without significant injury to surrounding tissues. Neutrophil activation and degranulation results in the extracellular

release of NSPs, which are involved in bacterial killing [55, 56] and local tissue damage during inflammation. Extracellular NSPs are important regulators of innate immunity, infection and inflammation [57, 58]. For example; they have bactericidal properties [56, 59, 60] which may be independent of their proteinase activities, and they can control cell signalling via the processing of chemokines, modulating cytokines and activating cell surface receptors [51]. Extracellular killing of pathogens by neutrophils can also occur following the formation of neutrophil extracellular traps (NETs) [61]. NETs are formed following neutrophil activation and consist of a DNA backbone with embedded antimicrobial peptides and enzymes [62]. NETs are believed to be produced by dying neutrophils in a process distinct from apoptosis [63], referred to as NETosis [64]. NSPs associated with NETs have extracellular roles in bacterial killing and degradation of virulence factors [65], and are more resistant to inhibition by proteinase inhibitors compared to free NSPs [66].

However, excessive proteinase activity is associated with damage to lung elastin and other critical components of the extracellular matrix in the lung parenchyma. This proteinase/anti-proteinase imbalance has dominated research in COPD as a result of observations from the 1960s [67, 68]. This hypothesis states that an imbalance exists, either from increased proteinase activity or a deficiency in their inhibitors (the anti-proteinases) resulting in excessive tissue destruction. To date, NSPs have been the best proven mediators replicating the pathological features of COPD and, in particular, emphysema.

The NSPs are both directly and indirectly implicated in the pathophysiology of lung tissue destruction (as observed in emphysema) due to their ability to degrade many components of the extracellular matrix including; elastin, type IV collagen, fibronectin and laminin [69-71], and to stimulate the release of pro-inflammatory cytokines [57, 72]. NE and PR3 have been shown directly to cause pathological changes consistent with emphysema in animal models [73, 74], and NSPs can produce other features of COPD including mucous gland hyperplasia, mucus hypersecretion and impaired mucociliary function (as observed in the chronic bronchitis phenotype) [75-77]. These observations are consistent with the susceptibility of individuals with a deficiency of the main plasma serine proteinase inhibitor (A1AT) to develop early onset severe emphysema [67]. Together these findings have provided the crucial support to the proteinase/anti-proteinase hypothesis.

Characteristics of the individual NSPs and their roles in the pathophysiology of lung disease are discussed in further detail below.

1.1.4.1 Neutrophil elastase

NE is a 29.5KDa glycoprotein which is coded for by the ELA2 (or more recently named ELANE) gene and is predominantly localised to neutrophil azurophilic granules, although it is also found in a subset of monocytes [78]. Its substrate specificity is determined not only by the P1 amino acid but also by its interactions with S and S´ subsites due to its extended substrate binding site [79]. NE shows a preference for small hydrophobic residues such as Ala, Val, Ser or Cys as the P1 amino acid [51]. The hydrophobic properties of the S2 subsite explain why proline is preferred at the P2 position, whilst

substrates with charged residues at P2 are less well cleaved. Additionally, Ala residues are preferentially accommodated at P3 and P4, rather than positively charged residues [51].

Animal and *in vitro* studies have shown that exogenous NE causes mucous gland hyperplasia [80] and mucus secretion [81], which are features of human chronic bronchitis. NE deficient mice exposed to cigarette smoke are 60% protected from airspace enlargement and show impaired recruitment of neutrophils and monocytes into the lung compared to smoke-exposed wild type control mice [82]. Wright *et al* [83] showed that a synthetic NE inhibitor could reduce cigarette smoke-induced emphysema in guinea pigs. The specific NE inhibitor sivelestat (ONO-5046) has been shown to reduce endotoxin-induced lung injury in guinea pigs [84] and suppress bleomycin-induced pulmonary fibrosis by blocking neutrophil chemotaxis and by inhibiting NE-induced lung cell apoptosis [85]. These studies suggest that sivelestat treatment reduces inflammation, and may act through NF-kB inhibition [86]. An oral reversible inhibitor of NE, AZD9668, has been shown in animal models to reduce human NE-induced lung injury, and prevent airspace enlargement and small airway wall remodelling in guinea pigs exposed to tobacco smoke [87]. The oral NE inhibitor ONO-6818 has also been shown to inhibit the development of emphysematous changes in rats, including lung hyperinflation, reduction of elastic recoil, and airspace enlargement [88].

In human studies, sputum positive for NE from subjects with bronchiectasis has been shown to reduce ciliary beat frequency of epithelial cells [89]. There is a direct relationship between the severity of emphysema in human tissue and the amount of NE in the interstitium [90], and subjects with high levels of A1AT:NE complex in BAL fluid have a

significantly accelerated decline in lung function as measured by FEV1, suggesting that NE in the lung is related to progression in COPD [91, 92]. Furthermore, a fibrinogen cleavage product detectable in plasma which is a marker of pre-inhibition NE activity showed a positive correlation with A1AT:NE complexes and a negative correlation with FEV1 % predicted [93].

In human clinical studies, the NE inhibitor sivelestat reduces lung injury associated with systemic inflammatory response syndrome (SIRS) [94] and can reduce serum cytokine levels [95] in patients with acute respiratory distress syndrome (ARDS) although it is not associated with a reduction in mortality of these patients in a meta-analysis [96]. Studies of NE inhibitors in COPD patients have shown that midesteine (MR889), a reversible NE inhibitor, has low toxicity when given over a 4 week period in a randomised placebo controlled study [97]. However, the development of ONO-6818 was discontinued when data from a phase IIa study in COPD patients revealed abnormalities in liver function related to the treatment [98]. More recently, Kuna *et al* [99] demonstrated in a 12 week randomised placebo controlled phase IIb trial of 615 COPD patients that the reversible NE inhibitor AZD9668 was well tolerated. However, in this short-term study, there was no improvement in lung function, respiratory signs and symptoms or quality of life scores when added to budesonide/formoterol maintenance therapy in COPD patients.

Despite the above evidence many uncertainties remain; the association of NE with human emphysema has been inconsistent, and limited short-term studies of selective NE inhibitors have not been fully effective in controlling neutrophil-mediated damage in the airways,

suggesting that other proteinases implicated in experimental models of emphysema [100] may play a role.

1.1.4.2 Proteinase 3

PR3 is a multifunctional serine proteinase mainly located in the azurophilic granules and on the cell surface of neutrophils [101]. PR3 can also be found in specific granules and secretory vesicles in contrast to NE [102]. It is a 29KDa glycoprotein alternatively named myeloblastin, AGP7 and p29b [60, 103]. The PR3 gene (PRTN3) is found in the same region of chromosome 19p13.3 as NE [104] and its structure is similar to that of NE with 57% sequence homology [105]. PR3 has an extended substrate binding site that influences substrate specificity. The S2, S1′, S2′, and S3′ subsites predominantly determine the substrate specificity of PR3, and explain its difference from NE [106]. PR3 shows a preference for small hydrophobic residues such as Cys, Ala, Val and norVal as the P1 amino acid [51]. The main structural differences between NE and PR3 are described in detail elsewhere [107].

PR3 is the most abundant serine proteinase in the neutrophil with each cell being estimated to store 3, 1.1, and 0.85 pg of PR3, NE, and CG, respectively [108]. Another study reported that neutrophils release more PR3 than NE during phagocytosis [109]. Its biological roles are diverse and include its ability to cleave the human cathelicidin hCAP-18 to generate the antibacterial peptide LL-37 [110], and a pro-inflammatory role for PR3 has been suggested by its ability to activate TNFα, IL-8, IL-1β, IL-18 and IL-32 [58, 111-113]. Kuckleburg *et al* [114] reported that PR3 may also play a role in neutrophil transmigration via its cell membrane interaction with the NB1 receptor, as the interaction

between endothelial cell PECAM-1 and neutrophil NB1 plays an important role in neutrophil transmigration. The authors found that neutrophils expressing NB1 and PR3 on their surface were selectively recruited, and that the efficiency of transmigration positively correlated with PR3 activity. In addition, PR3 is the main antigenic target of antineutrophil cytoplasmic antibodies (ANCAs) in Wegener's granulomatosis (WG), a systemic disease associated with small vessel vasculitis and necrotising granulomatosis of the respiratory tract [115]. ANCAs can bind to PR3 expressed on neutrophil cell membranes and amplify cell activation [116].

The role of PR3 in respiratory diseases has been less well studied. In animal and *in vitro* studies, PR3 can degrade extracellular matrix proteins such as elastin and fibronectin, resulting in tissue injury (as observed in human emphysema) [117] and can induce mucus secretion (as observed in human chronic bronchitis) [75]. Intra-tracheal administration of PR3 to hamsters leads to the development of bullous emphysema [74]. Knockout mice for both PR3 and NE demonstrate less neutrophilic inflammation compared to wild-type mice and mice deficient in NE alone [118]. In this study, the defects in mice lacking both PR3 and NE were directly linked to the accumulation of the anti-inflammatory protein, progranulin. The authors concluded that PR3 and NE may enhance neutrophil activation by degrading oxidative burst-suppressing progranulin. However, species differences in physico-chemical properties, substrate specificities and enzyme kinetics towards synthetic peptide substrates have been shown [119] and therefore results from animal models should be interpreted with caution when considering human disease. *In vivo* studies have indicated that apoptosis of lung endothelial cells can lead to emphysematous changes [120] and PR3 has been shown to be pro-apoptotic [121, 122]. The pro-apoptotic mechanism of PR3 is likely to be due to cleavage of NF-κB and the cell cycle inhibitor p21 [58].

Studies in human disease have been few, which may reflect the paucity of specific reagents to quantify PR3 and its activity. However, Witko-Sarsat *et al* [75] found that PR3 concentration exceeded NE concentration in sputum from patients with cystic fibrosis (CF) and showed a negative correlation with FEV1 % predicted.

The anti-proteinase screen for PR3 in the lungs is less efficient than that for NE since PR3 is not inhibited by secretory leukoproteinase inhibitor (SLPI) [109], and the remaining airway inhibitors A1AT and elafin bind to NE more readily than to PR3 [123]. This together with the greater concentration of PR3 suggests it may play a more significant role in neutrophil mediated lung damage. To date, there have been no studies of specific PR3 inhibitors in animal or human models of respiratory disease. Table 1.2 summarises the biological functions of PR3 and its potential roles in the pathophysiology of COPD.

Table 1.2- Functions of PR3 and its potential roles in the pathophysiology of COPD

Function of PR3	**References**
Degradation of components of the extracellular matrix	[117]
Activation of chemokines/cytokines	[58, 111-113]
Mucus secretion from airway submucosal gland serous cells	[75]
Endothelial cell apoptosis	[121, 122, 124]
Bactericidal properties	[125]
Platelet activation	[126]
Inactivation of proteinase inhibitors	[127]
Neutrophil transendothelial migration	[114]
Target of autoantibodies in Wegener's granulomatosis	[128]

1.1.4.3 Cathepsin G

CG is a 28.5KDa glycoprotein which is coded for by the CTSG gene on chromosome 14q11.2 [129] and is predominantly located in neutrophil azurophilic granules. The role of CG in lung diseases may also be clinically relevant and distinct from other NSPs. In animal and *in vitro* studies, CG does not produce emphysema-like lesions but has been shown to induce mucous gland hyperplasia [73] and mucus secretion [81]. Further evidence for the role of CG in the pathogenesis of suppurative lung diseases has been shown in animal models of endobronchial inflammation where ability to clear *Pseudomonas aeruginosa* is inhibited [130], and a dual inhibitor of CG and chymase has been shown to reduce airway inflammation [131]. To date, the role of CG in COPD has not been studied in human subjects, so the relevance and mechanisms involved remain largely unknown.

1.1.5 Inhibitors of serine proteinases

Endogenous inhibitors of serine proteinases include the serpins, chelonianin inhibitors and alpha-2-macroglobulin (A2M), and are discussed in further detail below.

1.1.5.1 The serpins

The serine proteinase inhibitors (serpins) are a diverse family of proteins found in several species. The family includes A1AT, α1-antichymotrypsin, monocyte/neutrophil elastase inhibitor (MNEI or serpin B1), antithrombin, C1 inhibitor and plasminogen activator inhibitor-1 [132]. These proteins are key regulators of inflammation, coagulation and the complement and fibrinolytic pathways. They account for around 2% of total protein in human plasma, the most common being A1AT [51]. The serpins share a similar conserved tertiary structure and the superfamily is classified into sixteen clades, with human serpins belonging to the first nine clades (A to I) [132]. The structure of serpins consists of three β-sheets (A-C) and eight or nine α-helices (hA-hI) with an exposed mobile reactive centre loop (RCL) between β-sheets A and C, as shown in Figure 1.5. The RCL typically contains 20 residues that act as a pseudo-substrate for the target proteinase [133]. The enzyme and serpin initially form a Michaelis complex [134] followed by cleavage of the RCL between P1 and P1′. This allows insertion of the cleaved RCL into the β-sheet A of the serpin and movement of the enzyme from the upper to the lower pole of the serpin with distortion of the active site of the enzyme [133, 135]. This suicide substrate inhibition mechanism renders both molecules inactive. The serpin-proteinase complex is then rapidly cleared from the circulation [136].

Figure 1.5- Serpin structure

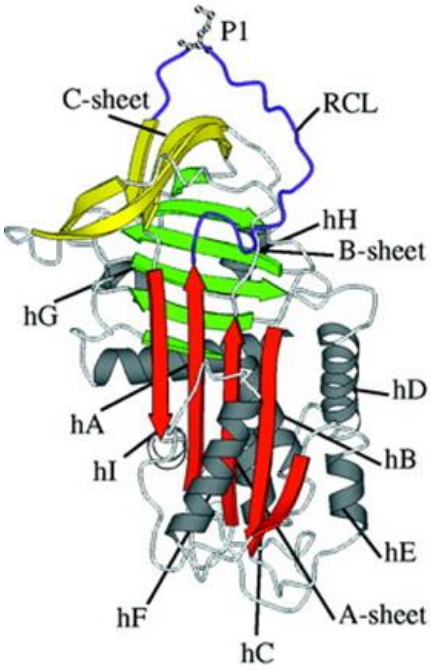

Figure 1.5: The structure of A1AT. The α-helices are shown in grey and labelled hA to hI. The three β-sheets are shown; the A sheet in red, the B sheet in green and the C sheet in yellow. The RCL is between β-sheets A and C. The position of P1 is shown. Reproduced from [132].

Dysfunction of serpins leads to diseases such as emphysema, thrombosis, angioedema, cancer and dementia [137]. The so-called "serpinopathies" result from point mutations within members of the serpin family and are characterised by the formation of polymers that are retained in the cell of synthesis [138, 139]. Pathological consequences result from a "toxic gain of function" from the accumulated polymers and a loss of function from the deficiency of the inhibitor. This is exemplified by A1ATD which is described in further detail below.

Alpha-1-antitrypsin

A1AT is a 52 kDa circulating glycoprotein mostly secreted by hepatocytes [140] and, to a much lesser extent, by lung epithelial cells [141] and phagocytes [142]. It enters the lungs primarily by passive diffusion from plasma. A1AT is coded for by the protease inhibitor (Pi) locus on chromosome 14 at q32.1. [143]. A1AT is able to inhibit the NSPs NE, PR3 and CG as well as other serine proteinases including thrombin, trypsin and chymotrypsin [144]. Circulating levels of A1AT are in the range 20-53μM/L in healthy (PiMM) individuals [145] and can increase during the acute phases of infection and inflammation [146]. The RCL of A1AT is cleaved at the Met358-Ser359 bond by target NSPs [135]. NE is irreversibly inhibited with 1:1 stoichiometry, whereas with PR3 and CG the inhibitor/enzyme stoichiometry is slightly greater than 1 due to partial proteolytic inactivation of some A1AT during the interaction (the "substrate pathway") [129]. The normal M variant of A1AT is a less competent inhibitor of PR3 and CG compared to NE with the second order association rate constants (Kass) being ten-fold and one hundred-fold lower for PR3 and CG respectively [117, 147]. The activity of A1AT can be modulated by genetic and environmental factors, for example, lung A1AT is potentially

susceptible to local oxidation of methionine residues in its RCL (P1 Met358 and P8 Met351) by cigarette smoke and myeloperoxidase released from activated neutrophils [148]. Oxidised A1AT has a greatly reduced inhibitory capacity, with its Kass for NE being reduced by a factor of more than 2000 [147].

A1ATD was first described in 1963 [67] and is inherited as an autosomal co-dominant disorder. Over 100 naturally occurring genetic variants of A1AT have been described. Each variant is named according to its speed of migration in an isoelectric pH gradient. The slower migrating variants are named with letters towards the end of the alphabet, for example, M (medium), S (slow) and Z (very slow). The normal variant is M (of which there are at least four subtypes) which is associated with normal levels of A1AT. The most common allele associated with marked deficiency of A1AT is the Z variant which results from a single amino acid substitution where glutamate at residue 342 is replaced by lysine [149, 150]. The Z variant results in a marked reduction in secretion, releasing approximately 20% of that produced by the M variant, and accumulation of the protein in the rough endoplasmic reticulum of hepatocytes [151, 152] forming periodic acid Schiff (PAS) positive hepatic inclusions. This accumulation can lead to liver disease including hepatitis, cirrhosis and hepatocellular carcinoma [153]. The resulting deficiency in circulating A1AT means that the lungs are not adequately protected from NSP activity leading to an increased risk of developing emphysema. Previous studies of the Kass of A1AT have shown that Z variant A1AT is a less competent inhibitor of NE than normal M A1AT [154]. Thus, individuals with the PiZZ genotype not only have lower concentrations of A1AT, but it is also less functional as an inhibitor of NE [155]. A review of genotype frequencies has suggested that the homozygous PiZZ genotype occurs in approximately 1 in 3500 individuals in the UK, with the heterozygous PiMZ genotype occurring in

approximately 1 in 25 individuals [156]. Population and *in vitro* studies [157] suggest a minimum serum A1AT threshold of 11μM is critical, and below this level A1AT is decreasingly able to protect the lungs, leading to an increasing risk of developing emphysema. This concept of a protective threshold emerged following the observation that a subset of individuals with the PiSZ phenotype (with serum A1AT levels below 11μM) were at increased risk of emphysema, whereas those with concentrations exceeding this threshold (including PiMZ heterozygotes) were not deemed at increased risk [158, 159].

Other A1AT variants described in this thesis include the S, F and I variants. The S variant results from a single amino acid substitution where glutamate at residue 264 is replaced by valine [160, 161] and is associated with a serum protein level of approximately 60% of that produced by the M allele due to reduced secretion from hepatocytes [162]. The F variant has an allelic frequency of approximately 0.002 in the Caucasian population and was first identified in 1965 [163, 164]. The F variant results from a single amino acid substitution where arginine at residue 223 is replaced by cysteine. Serum levels of A1AT in individuals carrying the F allele are usually normal, although there have been reports of an increased risk of emphysema in PiFZ heterozygotes [165]. To date, no PiFF homozygotes have been reported in the literature, although there is one case report of an individual with COPD and the PiFnull phenotype [166]. The observation of emphysema in PiFZ individuals raises the question about the function of F variant A1AT. The I variant results from a single base substitution where arginine at position 39 is replaced by cysteine [167]. The PiIZ phenotype was first reported in 1987 and has also been associated with both respiratory disease [168] and liver cirrhosis [169] perhaps because that is where it is most assessed. Nevertheless, these observations suggest that the I variant of A1AT may

also be less functional than the normal M variant. Several null allelic variants have also been described which result in an absence of A1AT and are reviewed elsewhere [170].

The Z variant of A1AT (and to a lesser extent the S and I variants [169]) has an increased tendency to fold aberrantly and form polymers in the liver. However, the formation of polymers is not only restricted to the liver, and polymers have been found in the circulation [171] and in BAL fluid [172]. Furthermore, Z type A1AT purified from plasma can form polymers under physiological conditions [173]. Polymeric A1AT does not function as an enzyme inhibitor, thereby further reducing the anti-proteinase protection in PiZZ homozygotes beyond that expected by the depleted A1AT levels. Co-inheritance of an S or I allele with a Z allele can lead to interaction between the A1AT variants and the formation of heteropolymers within hepatocytes [169]. The Z mutation of A1AT is at residue P17 at the head of strand 5 of the A sheet and the base of the mobile RCL [151]. This substitution of glutamate by lysine leads to a conformational change in the protein and formation of an unstable intermediate characterised by partial insertion of the RCL and opening of β-sheet A [174]. The A sheet is then more able to accept the RCL of a second A1AT molecule to form a dimer, which can extend to form a polymer, as shown in Figure 1.6. Alternative mechanisms of polymerisation have been described, including C sheet linkages, although the A sheet linkage is thought to be most likely *in vivo* [173]. Formation of polymers is accelerated by exposure of Z A1AT to cigarette smoke and its resultant oxidation [175]. Polymers of A1AT in the lung have chemotactic properties *in vivo* and act as pro-inflammatory stimuli leading to neutrophil recruitment [176]. These findings are consistent with the processes resulting in the early onset and progression of emphysema in PiZZ homozygotes, particularly those who smoke.

Figure 1.6- Polymerisation of A1AT

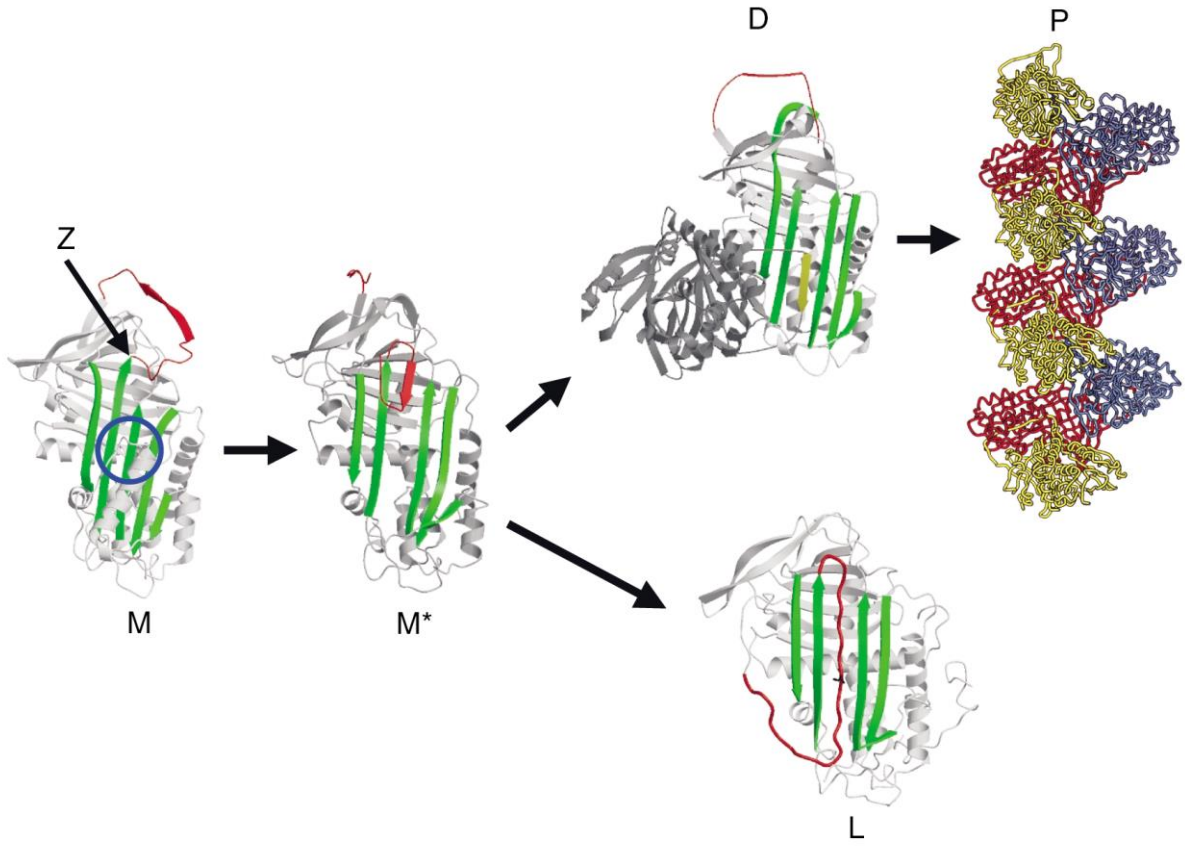

Figure 1.6: Mutations such as the Z mutation (arrowed) or mutations within the shutter domain (blue circle) such as Mmalton or Siiyama lead to a conformational change in the monomer (M) and opening of β-sheet A (green) to form an unstable intermediate (M*). The A sheet can accept the RCL (red) of a second A1AT molecule to form a dimer (D) and can extend to form a polymer (P). Alternatively, the open A sheet can accept its own RCL resulting in latent A1AT (L). Image reproduced from [151].

Inhibitors of polymerisation could potentially play a therapeutic role in A1ATD and other serpinopathies. Small molecule peptides that can inhibit polymerisation of Z A1AT have been studied *in vitro* [152, 177]. However, further *in vivo* studies are now warranted to determine any therapeutic benefit for subjects with PiZZ A1ATD related diseases.

Other serpins

Other serpins relevant to NSPs include MNEI and α1-antichymotrypsin. MNEI is found in the cytoplasm of neutrophils and monocytes [178], and is able to irreversibly inhibit all 3 NSPs by forming a 1:1 complex [179]. It is a 42KDa intracellular serpin which has two functional sites in the RCL (Phe343-Cys344 and Cys344-Met345) [129]. α1-antichymotrypsin (also known as SERPINA3) is a 68KDa glycoprotein produced in the liver and secreted into the circulation. Its reactive site is at the Leu358-Ser359 bond and it inhibits CG but not PR3 or NE [129].

1.1.5.2 Chelonianin inhibitors

The chelonianin inhibitors are a family of canonical inhibitors which bind to their target enzymes through an exposed convex binding loop with a conformation which is complementary to the active site of the enzyme [180]. Endogenous chelonianin inhibitors that are important in controlling the activities of NSPs include SLPI, and elafin and its precursor trappin-2.

Secretory leukoproteinase inhibitor

SLPI is an 11.7KDa protein produced locally in the lungs by epithelial cells, alveolar type 2 cells, Clara cells and by phagocytes [181, 182]. It is a reversible inhibitor of NE and CG but does not inhibit PR3 [109]. Bacterial proteinases, human cysteine proteinases and PR3 can inactivate SLPI [127, 183, 184] hence potentiating the activities of other NSPs normally inhibited by SLPI. Unlike A1AT, SLPI can inhibit NE bound to elastin [185].

Elafin

Elafin is a 6KDa inhibitor produced locally in the lungs by alveolar type 2 cells and Clara cells [182]. Elafin and its precursor trappin-2 can reversibly inhibit NE and PR3 but not CG [186]. It can also inhibit NE and PR3 expressed on the cell surface of activated neutrophils [187]. In addition to its role as a proteinase inhibitor, elafin has anti-microbial activity against both gram positive and gram negative respiratory pathogens [188]. Elafin can be cleaved by NE, and although cleaved fragments of the inhibitor can still inhibit NE activity, its anti-microbial role is diminished [189].

1.1.5.3 Alpha-2-macroglobulin

A2M is a 725 kDa glycoprotein produced by the liver and composed of four identical subunits of approximately 185 kDa [190]. All four classes of proteinases (serine, aspartic acid, cysteine and matrix metalloproteinases) can be irreversibly trapped by A2M. The normal blood levels of A2M are around 2mg/ml [191]. The ultrastructure of A2M shows the molecule to be a twin trap capable of binding 2 NE molecules when the concentration of NE is high [192]. A2M predominantly enters the lungs by diffusion, although some local production may occur [193]. Diffusion from the blood may be restricted by the large molecular size of A2M, but increases in the presence of inflammation [194].

A2M has a 25 amino acid stretch known as the "bait region" which can be cleaved by different proteinases [195]. Cleavage of the bait region results in a conformational change of the A2M molecule which mediates "trapping" of the proteinase and physical exclusion of large substrates from the active site of the enzyme. Therefore "inhibition" of proteinases by A2M does not block the active site and the proteinase retains activity towards small substrates [196]. This is in contrast to other mechanisms of proteinase-inhibitor complex formation, which involves irreversible active site inhibition [197]. Cleavage of the bait region also results in exposure of new sites that are recognised by receptors on several cell types [198, 199]. Therefore, A2M may function predominantly to remove proteinases from the circulatory system by steric shielding and rapid clearance [200], rather than inhibiting their activity. Complexes of NE with A2M can retain their activity even in the presence of other inhibitors such as A1AT [201].

1.1.6 The role of other proteinases in COPD

The proteinase/anti-proteinase hypothesis has predominantly highlighted the importance of NSPs in the pathogenesis of COPD due to direct experimental and clinical observations. There are, however, other enzyme systems that have been explored as potential mechanisms in COPD and particularly emphysema. These include the matrix metalloproteinases (MMPs) and the cysteine proteinases. Proteinases implicated in the pathophysiology of COPD are summarised in Table 1.3. In addition, complex interactions exist between NSPs, MMPs, cysteine proteinases and proteinase inhibitors. These interactions are summarised in Figure 1.7.

Table 1.3- Proteinases implicated in the pathogenesis of COPD

Proteinase	**Class**	**Source**	**Inhibitors**	**References**
NE	Serine proteinase	PMN Pro-inflammatory monocytes	A1AT A2M SLPI Elafin	[80-82, 90-92, 202]
PR3	Serine proteinase	PMN	A1AT A2M Elafin	[74, 75, 117]
CG	Serine proteinase	PMN	A1AT A2M SLPI Alpha-1 antichymotrypsin	[73, 81]
MMP-1	Matrix metalloproteinase	Macrophages Fibroblasts Epithelial cells Endothelial cells	TIMP 1-4 A2M	[203, 204]
MMP-2	Matrix metalloproteinase	PMN Macrophages Fibroblasts Epithelial cells Endothelial cells	TIMP 1-4 A2M	[205]
MMP-8	Matrix metalloproteinase	PMN Fibroblasts Endothelial cells	TIMP 1-4 A2M	[206, 207]
MMP-9	Matrix metalloproteinase	PMN Macrophages Eosinophils Fibroblasts Epithelial cells Endothelial cells	TIMP 1-4 A2M	[205, 207-209]
MMP-12	Matrix metalloproteinase	Macrophages	TIMP 1-4 A2M	[208, 210, 211]
Cathepsin B	Cysteine proteinase	Macrophages Epithelial cells Endothelial cells	Cystatins A, C, S A2M Kininogens	[212, 213]
Cathepsin L	Cysteine proteinase	Macrophages Endothelial cells Fibroblasts	Cystatins A, C, S A2M Kininogens	[214]
Cathepsin S	Cysteine proteinase	Macrophages Endothelial cells	Cystatins A, C, S A2M Kininogens	[215]

Figure 1.7- Interactions between different classes of proteinases and their biological inhibitors

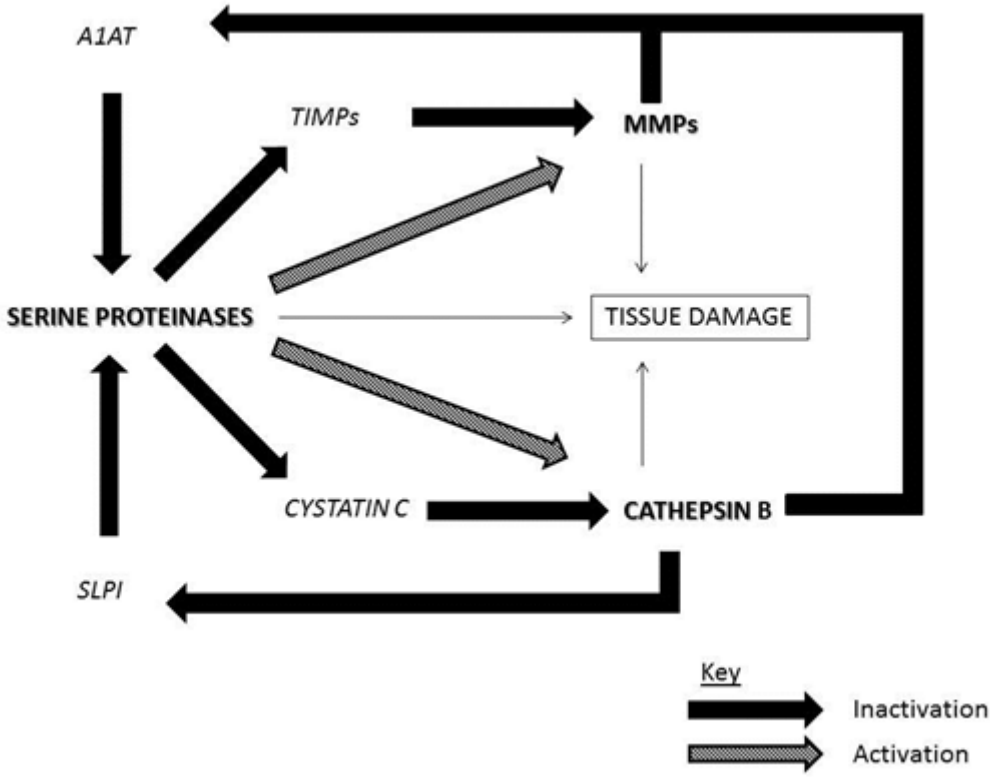

Figure 1.7: The complex interactions between proteinases (shown in bold) and their inhibitors (shown in italics). The serine proteinases NE and PR3, MMPs and cathepsin B are capable of producing tissue damage leading to emphysema. MMPs indirectly enhance the activity of serine proteinases by inactivating A1AT [216, 217]. In a complex relationship, NE further activates MMPs [218] and inactivates their inhibitors, the TIMPs [219]. The cysteine proteinases, including cathepsin B, have been shown to inactivate SLPI [184], and cathepsins B and L can inactivate A1AT [220, 221]. NE can activate cathepsin B [222] and inactivate its inhibitor, cystatin C [223]. This inflammatory cascade facilitates the activity of proteinases in the presence of neutrophilic inflammation.

1.2 Alpha-1-antitrypsin deficiency

1.2.1 Clinical features

A1ATD is associated with panacinar emphysema which is usually of an earlier onset than in patients with usual COPD and shows a lower zone predominance. Disease severity is often out of proportion to the smoking history [27]. Other respiratory features include chronic bronchitis and bronchiectasis [224], although not all subjects develop respiratory disease suggesting that environmental and other genetic factors may play a role.

In addition to respiratory disease, A1ATD has been associated with liver disease in some subjects due to the accumulation of aggregated protein [153], including neonatal cholestasis, cirrhosis and hepatocellular carcinoma. Evidence to support the "toxic gain of function" from the polymers accumulated in the hepatocytes is provided by the recognition that null alleles, which do not produce A1AT, are not associated with cirrhosis [225]. Polymerisation of A1AT is accelerated with increasing temperature [139] and it has been hypothesized that febrile illness in infancy is a predisposing factor for infantile hepatitis [226]. A1ATD has also been associated with panniculitis [227] and Wegener's granulomatosis [228].

1.2.2 Treatment options

Treatment for A1ATD depends on the individual presentation. For most subjects this will involve standard treatments for COPD such as inhaled bronchodilators and corticosteroids. Bacterial exacerbations should be identified and especially treated promptly, since they are associated with a greater proteinase/anti-proteinase imbalance [229] and hence more tissue

damage than in usual COPD. Indications for LTOT and pulmonary rehabilitation are the same as those in usual COPD. There is also even more emphasis on avoidance of cigarette smoking, maintenance of nutrition, and preventative vaccination against influenza and pneumococcus. Lung transplantation may be considered in subjects with very severe respiratory disease [230].

Newer approaches targeting the molecular basis of the disease are the subject of current research. These include A1AT augmentation therapy (discussed in Chapter 7), inhibitors of polymerisation within hepatocytes and gene therapy. A1AT augmentation therapy does not affect polymerisation of Z A1AT in the liver and is therefore not effective for liver disease associated with A1ATD. Similarly, it does not prevent the local production of Z A1AT polymers in the lungs which act as neutrophil chemoattractants [231]. Small molecule peptides that can inhibit polymerisation of Z A1AT have been studied *in vitro* [177]. However, *in vivo* studies are still awaited to determine their efficacy.

Numerous strategies for gene therapy have been employed including recombinant adeno-associated viral vectors, non-viral vectors and induced pluripotent stem cells (iPSCs). A phase 2 clinical study of a recombinant adeno-associated viral vector expressing A1AT [232] administered intramuscularly to 9 A1ATD subjects showed that vector-derived expression of normal M A1AT was dose-dependent and persisted for at least 90 days. Vector administration was well tolerated in these subjects with no serious adverse events. All subjects developed antibodies to adeno-associated virus (which may influence long term efficacy of this approach) but not to A1AT. Further research will be required into the design or delivery of viral vectors in order to achieve therapeutic efficacy in A1ATD.

Human iPSCs have been used to correct the point mutation in Z A1AT in both *in vitro* and animal studies [233]. However, stem cells accumulate mutations within their genome which can occur at random, and therefore there are concerns about the long-term risks of malignancy with stem cell therapy, as previously highlighted in a patient who received stem cell therapy for ataxia telangiectasia [234]. These safety concerns will need to be addressed before stem cell therapy can be considered in clinical practice.

Liver transplantation from a PiMM individual can return A1AT levels to normal and is associated with favourable outcomes [235], but is only available to subjects with end stage liver disease at present due to a shortage of donor organs.

Newer anti-inflammatory treatments for usual COPD may also be of particular benefit to subjects with lung disease associated with A1ATD. These include antioxidants, inhibitors of p38 mitogen-activated protein kinase (MAPK) and antagonists of the interleukin (IL)-8 receptor CXCR2 and are reviewed elsewhere [39]. In particular, inhibitors of NSPs could be beneficial due to the greater proteinase/anti-proteinase imbalance in subjects with A1ATD. However, the roles of individual NSPs need to be established to determine their relative importance to the overall proteolytic burden.

1.2.3 Alpha 1 antitrypsin deficiency as a model for usual COPD

A1ATD is associated with all the clinical features of usual COPD including symptoms, recurrent exacerbations and development of emphysema. Neutrophilic inflammation is

increased in these individuals and reflects an exaggerated form of that seen in usual COPD [229]. The condition is easily monitored, and due to its more rapid progression, allows the validation of neutrophilic biomarkers over a shorter period of time. Studies in A1ATD have pioneered the use of CT scanning as a tool to assess degree and progression of emphysema. CT scan appearance has been shown to be the best predictor of mortality in A1ATD [236], and this has subsequently been confirmed in usual COPD [237], providing further support for A1ATD as a predictive model for usual COPD.

1.3 Aims and structure of this thesis

The predominant aims of this thesis are twofold; firstly to study the interactions of the NSPs NE and PR3 with their biological inhibitors of varying efficacies and substrates of different molecular sizes, and secondly to explore the potential role of PR3 in COPD, both with and without A1ATD.

In Chapter 3, the potential for serum samples from both healthy controls and subjects with A1ATD to inhibit NE or PR3 activities has been examined. Serum contains the proteinase inhibitors A1AT and A2M. The partitioning of NSPs between these inhibitors is of interest because NE bound to A2M can retain its proteolytic activity towards low molecular weight peptide substrates [196], whereas NE bound to A1AT is inactivated. The proteolytic potential of PR3 complexes with A2M has not previously been explored. In this section, serum samples of different A1AT genotypes (e.g. PiMM, PiSZ, PiFZ, PiZZ) have been used to assess how NSPs partition between the two serum inhibitors in the presence of different A1AT variants, and any resultant effects on their activities. These results have been explored further in Chapter 4 where the activities of NE and PR3 bound to A2M have

been studied, and the partitioning of NSPs has been studied by using purified inhibitors (A2M and A1AT) in the equivalent concentrations found in the serum samples.

In Chapter 5, elastin degradation by NE and PR3 has been studied. Elastin is a large molecular weight natural substrate of both NE and PR3 and its destruction *in vivo* leads to the development of emphysema. Elastin degradation has been examined both in the presence of serum from subjects with different A1AT genotypes, and with pure A1AT and A2M. Any biological relevance of complexes between A2M and NE or PR3 has been studied by determining their ability to degrade elastin *in vitro*. In addition, the inhibitory ability of A1AT towards NE and PR3 in the presence of elastin has been considered.

The focus of Chapter 6 is on the association rate constants between NE or PR3 and different variants of A1AT. Previous work has suggested that Z variant A1AT is a less competent inhibitor of NE than M variant A1AT [154], and M variant A1AT is a less competent inhibitor of PR3 than NE [117]. Therefore, in the presence of neutrophilic inflammation in usual COPD, A1AT will preferentially inhibit NE. This together with the greater amount of neutrophil PR3 may potentially increase the damaging potential of this enzyme. The association rate constants of PR3 and A1AT variants (other than M A1AT) have not been studied previously. The clinical consequences of co-inheriting a "dysfunctional" AlAT variant with the Z variant are also considered by studying the clinical phenotypes of PiFZ heterozygotes.

At present, the only specific therapy available for A1ATD is A1AT augmentation therapy but randomised controlled studies to date have not convincingly demonstrated its efficacy in clinical practice [238]. In Chapter 7, the *in vitro* effects of augmenting A1ATD serum with normal M A1AT and the altered distribution of NSPs between the serum inhibitors have been assessed. In addition, elastin degradation by augmented and non-augmented serum samples has been measured.

Activated neutrophils express NSPs on their cell surfaces that remain enzymatically active [54, 108], and therefore may play a role in the tissue damage associated with COPD. In Chapter 8, the neutrophil cell surface expression of NE and PR3 has been measured in subjects with A1ATD or usual COPD, and healthy controls. In addition, the influence of local proteinase inhibitor concentrations on the cell membrane expression of NE and PR3 has been evaluated by incubating and stimulating neutrophils in either normal or A1ATD plasma and determining the effect of local A1AT concentration on NSP expression.

Finally, the role of NE in lung diseases has previously been studied in detail [239]. However, PR3 has not been well studied. The amino acid sequence and crystal structure of PR3 is similar to that of NE [105], and until recently no substrates or inhibitors were available that could discriminate between the two proteinases [240]. In Chapter 9, recently developed specific NE and PR3 substrates have been used to measure the activities of these NSPs in sputum samples from subjects with A1ATD or usual COPD. This has allowed comparisons to be made of the activities of individual proteinases. Results have been related to other inflammatory markers, bacterial colonisation and clinical status.

Overall, the data presented here provides new information on the contribution of PR3 to the proteinase/anti-proteinase imbalance found in A1ATD and COPD. Such knowledge may provide novel insights into therapeutic targets for these important medical conditions.

2 General methods

This section provides a general overview of methods used for subject selection, sample collection, diagnostic tests, buffers used for experiments, active site titration of enzymes and statistical analyses. Specific methods are described in the relevant chapters.

2.1 Subject selection

Subjects with A1ATD were identified from the UK national registry. The Antitrypsin Deficiency Assessment and Programme for Treatment (ADAPT) reviews subjects with A1ATD on an annual basis, and is located in Birmingham, UK. It is funded by a non-commercial grant from Grifols Therapeutics. All subjects registered with ADAPT have their diagnosis confirmed by phenotyping and genotyping (Heredilab, Salt Lake City, USA). Presently, the UK database contains over 1,000 patients who have been assessed annually for up to 16 years. These well characterised patients have full demographic data recorded including; medical history, clinical examination, quality of life measures, full lung physiology, biochemical and haematological parameters, radiology, and stored plasma, serum and sol-phase sputum. All patients provided written informed consent and ethical approval was obtained for all aspects of this project (South Birmingham Research Ethics Committee LREC3359).

Subjects with usual COPD (normal PiMM A1AT phenotype) were recruited from primary care at the start of an acute exacerbation (infective or non-infective). These subjects had a clinical diagnosis of COPD based on a history of chronic bronchitis and exertional breathlessness, with or without supportive spirometry at presentation. Exacerbations were

defined by increased breathlessness, cough and sputum production. Subjects were assessed at the start of an acute exacerbation (day 1) and provided blood samples and a spontaneous sample of sputum. The sputum samples were analysed using a standardised colour chart (Bronkotest, Heredilab, USA) and subjects with mucopurulent or purulent sputum were treated with antibiotics, whilst those with mucoid sputum were not. Subjects were followed up after resolution of the episode during convalescence (day 56). At this visit, blood and spontaneously produced sputum samples were collected and full pulmonary function tests (PFTs) and HRCT scans were performed. Additional subjects with usual COPD were recruited from hospital outpatient clinics when clinically stable. These subjects had their diagnosis confirmed by spirometry and provided blood samples for research during their visit. All subjects provided written informed consent to participate in this study.

Healthy controls who were partners of patients with A1ATD (and therefore age-matched) were also recruited. The healthy controls had a normal PiMM A1AT phenotype, no significant medical history and normal spirometry, were on no regular medication and were non- or ex-smokers. The healthy controls provided blood samples for research purposes and had plasma and serum stored. All subjects gave written informed consent to participate.

2.2 Sample collection, processing and storage

2.2.1 Plasma and serum samples

Venous blood was collected from all subjects and processed within 30 minutes of collection. Plasma was obtained using ethylenediaminetetraacetic acid (EDTA)-containing Vacuette® tubes (Greiner bio-one, UK) and serum was obtained using Vacuette® serum tubes, allowing clot formation. The tubes were centrifuged at 1800 x g for ten minutes at room temperature. Plasma and serum were harvested and stored at -70 ºC until analysis.

2.2.2 Neutrophil extraction

Neutrophils were isolated in a biological safety class 2 cabinet to ensure a sterile environment. Venous blood was collected into heparinised Vacuette® tubes and placed in a 50ml Falcon tube (Becton Dickinson, UK). A 2% dextran solution was prepared by adding 2g of dextran 500 (Sigma, UK) to 0.9% saline and the solution was filter sterilised. For every 6ml of blood collected, 1ml of the 2% dextran solution was added and the contents were mixed. The blood was then left for 30-40 minutes to allow sedimentation of the red cells. The top layer was the "buffy layer" which contained the leukocytes.

A Percoll® gradient was prepared in a 15ml Falcon tube (Becton Dickinson, UK) as shown in Figure 2.1. The "100%" Percoll® was made by adding 45ml of pure Percoll® (Sigma, UK) to 5ml of 9% saline. The 9% saline was prepared by dissolving 9g of NaCl in 100ml of deionised water and then sterilised by autoclaving. Subsequently, 80% Percoll® solution was made by adding 40ml of "100%" Percoll® to 10ml of 0.9% saline, and 56% Percoll® solution was made by adding 28ml of "100%" Percoll® to 22ml of 0.9% saline.

A gradient was formed by adding 5ml of 56% Percoll® to a 15ml Falcon tube. Slowly, 2.5ml of 80% Percoll® was added beneath the 56% Percoll® solution. The buffy layer from the blood was then added slowly onto the surface of the 56% Percoll® solution. Caution was taken to avoid air bubbles, which can lead to neutrophil activation. The tube was centrifuged at 220 x g for 20 minutes at room temperature with minimal acceleration and no brake. Following separation of the cells in the Percoll® gradient, the top plasma layer was removed and discarded. Next, the peripheral blood mononuclear cell (PBMC) layer was removed with a small pipette and discarded. The neutrophil layer was then removed from the interface between the 80% and 56% Percoll® and added to sterile phosphate buffered saline (PBS) in a 50ml Falcon tube. The tube was topped up to 30ml with PBS and the cells washed by centrifuging the tube at 460 x g for 10 minutes at room temperature. The excess PBS was poured out of the tube to leave a pellet of neutrophils. The neutrophil pellet was then re-suspended in RPMI 1640 medium (Sigma, UK).

In order to count the number of cells present, 10µL of the solution was extracted and examined on a haemocytometer. The dilution of the neutrophils was varied to achieve a final neutrophil concentration of 2 million cells per ml. To confirm purity of the neutrophil preparation, a cytospin was prepared with 100µL of the cell solution and spun at 500 RPM for 3 minutes. Using a Reastain® quick-diff kit (Reagena Ltd, UK) the cells were examined for purity. All neutrophil preparations used were >95% pure, the remaining cells being predominantly eosinophils.

Methods for isolating neutrophils from blood are associated with a risk of activation and modification of the cell surface properties. The use of dextran increases cell attachment

and reduces subsequent cell movement, whereas greater cell motility has been observed when the cells are separated in the presence of Percoll® [241]. Another study comparing the anticoagulant used during blood collection showed that heparin and citrate increased phorbol myristate acetate (PMA)-induced activation compared to EDTA [242]. The methods used throughout this thesis for neutrophil isolation were standardised and designed to minimise cell activation whilst preserving yield and purity. Therefore any differences in cell surface expression observed between subject groups are likely to reflect basic rather than activated differences.

Figure 2.1- Neutrophil isolation using a Percoll® gradient

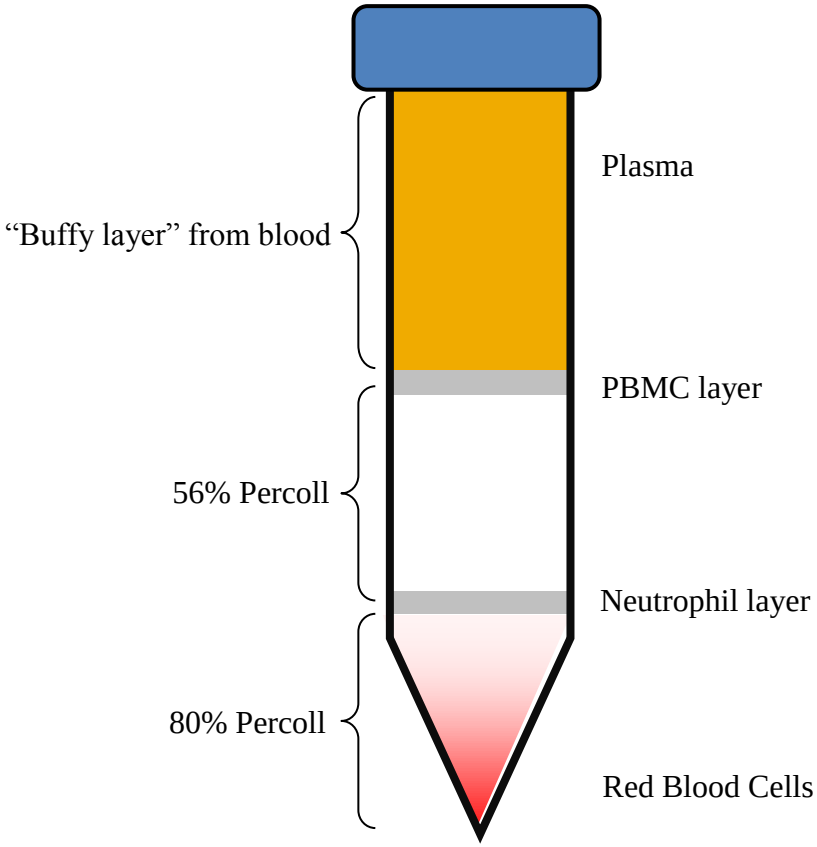

Figure 2.1: A Percoll® gradient was prepared as shown on the left side of the Figure and the buffy layer from the blood was added onto the surface of the 56% Percoll® solution. Following centrifugation, cell separation occurred as shown on the right hand side of the diagram. A full description is given in the text.

2.2.3 Processing sputum samples and quantitative sputum culture

Spontaneously produced sputum samples were collected into a sterile container from waking over a four hour period. A mouthwash was used prior to obtaining the sample to minimise contamination by saliva. Each sputum sample was analysed by its macroscopic

appearance using a standardised colour chart (Bronkotest, Heredilab, USA) and allocated a number. Values of 1-2 (colourless-white) were classed as mucoid whilst values of 3-5 (yellow-green) were classed as mucopurulent or purulent. Sputum samples were analysed within two hours of arrival and were divided into three aliquots. One aliquot (with a minimum weight of 1g) was used to obtain quantitative microbiological culture as described previously [243], and results were expressed as colony forming units per millilitre of sputum (cfu/ml). The second aliquot (minimum 1g) was ultracentrifuged (50,000 x g for 90 minutes at 4°C) to obtain the sol-phase which was stored at -70°C until analysis. The third aliquot was used for cytospin preparation to obtain cell counts and viability as described previously [244].

2.3 Pulmonary function tests

PFTs were performed in the stable clinical state following the administration of bronchodilators by trained Respiratory Physiologists at the Lung Function Department, Queen Elizabeth Hospital, Birmingham, UK. Post-bronchodilator (salbutamol 400 mcg and ipratropium 60 mcg via a spacer) spirometry was performed using a wedge bellows spirometer (Vitalograph, Buckinghamshire, UK), static lung volume measurements including TLC and RV were assessed using helium dilution [245] and gas transfer by the single breath carbon monoxide method. The European Community for Steel and Coal reference equations [246] were used to derive predicted values for spirometry and static lung volumes, and Cotes reference equation [247] was used for KCO.

2.4 High resolution CT scanning

HRCT scans of the thorax were performed using Prospeed and Lightspeed scanners (General Electrical Systems, Milwaukee, USA) to determine the presence or absence of emphysema (Figure 1.1) or bronchiectasis (Figure 1.2), and were reported by a single radiologist.

2.5 Buffers used for experiments

The buffers used commonly in subsequent experiments are listed in Table 2.1. Further buffers used in specific chapters are described in the relevant sections.

Table 2.1- Buffers used for experiments

Name of buffer	**Description**
Porcine pancreatic elastase (PPE) buffer	0.2M Tris-HCl, pH 8.6, 0.1% v/v Triton X100
PPE substrate buffer	0.1M Hepes, pH 7.5, 9.5% DMSO
NE assay buffer	0.01M Tris-HCl, 0.5M NaCl, 0.1% Triton X100, pH 8.6
NSP assay buffer	50mM Hepes, pH 7.4, 150mM NaCl, 0.05% Igepal CA-630 (v/v)
Elastin buffer	0.2M Tris base, pH 8.8

2.6 Active site titration of enzymes

The experiments described in this thesis depend on using pure enzymes of known specific activity. NE and porcine pancreatic elastase (PPE) obey the Michaelis-Menten model of enzyme kinetics [248] in that the rate of catalysis (V) is a function of the concentration of substrate [S]. At a fixed concentration of enzyme, the rate of substrate catalysis (V) is related to [S] in a linear fashion provided that V is significantly below its maximal value (Vmax). The Michaelis constant (Km) is the concentration of substrate at which the reaction rate is at half of its maximal value (Vmax/2) and is an inverse measure of the substrate's affinity for the enzyme. The Km value is independent of the enzyme and substrate concentrations. The Michaelis-Menten model is given by the following formula (equations taken from [248]);

$$E + S \underset{K_{-1}}{\overset{K_1}{\rightleftharpoons}} ES \xrightarrow{K_2} E + P \quad (1)$$

The enzyme E combines with substrate S to form as ES complex with a rate of K_1. The ES complex may then dissociate to E and S with a rate of K_{-1} or form the product with a rate of K_2. The initial rate of catalysis (V) is equal to the product of the concentration of the ES complex and K_2;

$$V = K_2[ES] \quad (2)$$

The quantity of ES is given by its rates of formation and breakdown;

$$Rate\ of\ ES\ formation = K_1[E][S] \quad (3)$$

$$Rate\ of\ ES\ breakdown = (K_{-1} + K_2)[ES] \quad (4)$$

In the steady state, the concentration of ES stays constant and the rate of formation equals the rate of breakdown. Therefore;

$$K_1[E][S] = (K_{-1} + K_2)[ES] \tag{5}$$

Rearranging equation 5 gives;

$$\frac{[E][S]}{[ES]} = \frac{(K_{-1}+K_2)}{K_1} \tag{6}$$

This equation can be simplified by defining the Michaelis constant Km;

$$Km = \frac{K_{-1} + K_2}{K_1} \tag{7}$$

Combining equations 6 and 7 and solving for ES gives;

$$[ES] = \frac{[E][S]}{Km} \tag{8}$$

In equation 8, [S] is very nearly equal to the total substrate concentration provided that the concentration of the enzyme is much lower than that of the substrate, and the concentration of the enzyme [E] is equal to the total enzyme concentration $[E]_T$ minus the concentration of the ES complex. This gives the equation;

$$[E] = [E]_T - [ES] \tag{9}$$

Substituting [E] from equation 9 into equation 8 gives;

$$[ES] = \frac{([E]_T - [ES])[S]}{Km} \tag{10}$$

Rearranging equation 10 gives;

$$[ES] = [E]_T \frac{[S]}{[S] + Km} \tag{11}$$

Substituting this expression for ES into equation 2 gives;

$$V = K_2[E]_T \frac{[S]}{[S] + Km} \tag{12}$$

When Vmax is achieved, the active sites of the enzyme are saturated with substrate and therefore $[ES]=[E]_T$. Putting this information into equation 2 gives;

$$Vmax = K_2[E]_T \tag{13}$$

The Michaelis-Menten equation is obtained by substituting equation 13 into equation 12 where V_0 is the initial reaction velocity;

$$V_0 = Vmax \frac{[S]}{[S] + Km} \tag{14}$$

The definition of Km can be derived from equation 14; when [S]=Km, then V_0=Vmax/2. The Km value for an enzyme depends on the substrate used as well as conditions such as pH and temperature. The Vmax gives the turnover number of an enzyme which is the number of molecules of substrate converted to product in unit time when the enzyme is fully saturated with substrate. This is equal to K_2 and is also known as Kcat. When the substrate concentration is much less than Km, V depends on the values of Kcat/Km, [S] and $[E]_T$. In these circumstances, Kcat/Km is the rate constant for the interaction of the enzyme and the substrate and may be used as a measure of catalytic efficiency. Therefore it is possible to compare an enzyme's preference for different substrates [248].

It is possible to derive the specific enzyme activity from values of Vmax which can in turn be derived from measurements of the dependence of V on [S]. These data can be analysed by construction of a Lineweaver-Burk double reciprocal plot (Figure 2.2).

The activity assays described in this Chapter were repeated at regular time intervals to ensure consistency.

Figure 2.2- Lineweaver-Burk double reciprocal plot

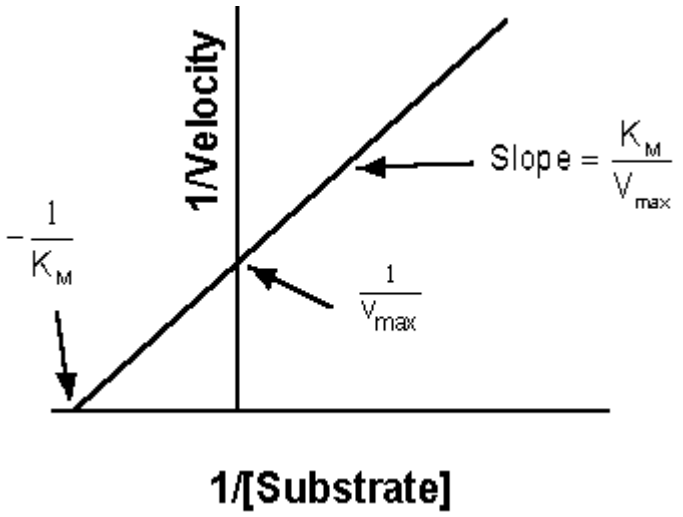

Figure 2.2: Example of a Lineweaver-Burk double reciprocal plot- a graphical method for analysis of the Michaelis-Menten equation. 1/V is plotted on the y-axis against 1/[S] on the x-axis. The y intercept is equivalent to the inverse of Vmax and the x intercept represents -1/Km. The slope represents Km/Vmax.

2.6.1 Methods for active site titration experiments

2.6.1.1 Active site titration of PPE by Lineweaver-Burk double reciprocal plot analysis

PPE (Sigma, UK) was prepared at a stock concentration of 1mg/ml in PPE buffer (the molecular weight of PPE is 25.9KDa). All buffers used for PPE activity experiments were free of sodium chloride (NaCl) as it has previously been suggested that this can affect the specific activity of PPE, although this is not the case for human NE [79, 249]. Stock PPE was aliquoted, rapidly frozen with liquid nitrogen and stored at -70 ºC until required. Fresh aliquots were used for all assays and freeze/thaw cycles were avoided. The elastase

substrate N-succinyl-ala-ala-ala-p-nitroanilide (SlaaapN, Sigma, UK) was used for PPE activity assays in PPE substrate buffer at the following concentrations; 7.5mM, 5mM, 2.5mM, 1mM and 0.5mM. One ml of each concentration of substrate was added to a polystyrene cuvette with a 1cm pathlength. The spectrophotometer (Jasco V550) was blanked against the assay buffer, and the absorbance of the substrate solution was measured at 410nm. PPE was diluted to 10µg/ml, and 10µL was added to the substrate. The change in optical density (absorbance) was measured over a 10 minute period. Each experiment was performed in triplicate and average results taken.

The reaction velocity (V) was calculated by substituting the absorbance (410nm) values into the Beer-Lambert equation;

$$A = ecl$$

Where;

A= Absorbance (410nm)

e= Extinction coefficient [8,800 M^{-1} cm^{-1} for SlaaapN [250]]

c= Concentration of product (M)

l= cell pathlength (cm)

The reaction velocity (V) was determined in terms of moles of product produced per unit time, and was used to construct a Lineweaver Burk plot of 1/V against 1/[S]. The y intercept gives 1/Vmax.

The molar concentration of active enzyme is equal to Vmax/Kcat (by rearranging equation 13). The kinetic constants under these conditions have previously been published [251].

2.6.1.2 Activity assessment of PPE with PiMM plasma

Once the activity of PPE was determined it was then titrated against healthy (PiMM) plasma of known A1AT concentration (where the A1AT is assumed to be predominantly functional) to provide further support to the results obtained by Lineweaver-Burk double reciprocal plot analysis. The A1AT concentration was measured using a modified version of an in-house enzyme linked immunosorbent assay (ELISA), as described below.

A1AT ELISA

This was performed by adding 200µL of 2µL/ml goat anti-human A1AT antibody (Binding site, Birmingham UK) in coating buffer (0.05M Na_2CO_3, 0.05M $NaHCO_3$, pH 9.6) to a Maxisorp microtitre plate (Nunc, Glasgow UK) using only the inner wells. The plate was incubated over night at 4ºC, and then washed 3 times with 300µL wash buffer [phosphate buffered saline (PBS), albumin 0.1% (w/v), Tween 0.05% (v/v)]. Next, 200µL of blocking solution [50mM Tris base, 0.14M NaCl, 1% bovine serum albumin (BSA), pH 8] was added to each well and incubated for 1 hour at room temperature, followed by washing as before. A human serum protein calibrator (Dako, UK) containing 1.24g/L A1AT was used as a standard. This was serially diluted in wash buffer to generate standards ranging from 62ng/ml to 1.94ng/ml. The plasma or serum samples were diluted in wash buffer in the range of 1 in 20,000 to 1 in 60,000. Then 200µL of standard or

sample was added to the plate, left to incubate for 2 hours at room temperature, and then the plate was washed as previously. Next, 200µL of 2.6µL/ml goat anti-human A1AT peroxidase conjugate (Binding site, Birmingham UK) in wash buffer was added to the plate and allowed to incubate for two hours at room temperature. Following a washing step, 200µL of tetramethylbenzidine (TMB) solution (Sigma, UK) was added to the plate and incubated in the dark until a colour change occurred. The reaction was stopped with 50µL per well of 0.1M H_2SO_4. The absorbance was then read at 450nm with a 570nm wavelength correction using a Biotek Synergy HT plate reader. The concentration of A1AT in the samples was determined by interpolation from the linear portion of the standard curve using Microsoft Excel 2007. Samples with values falling outside of the standard curve were repeated at a more appropriate dilution. The intra- and inter- assay coefficients of variation (CVs) were 4.66% and 4.35% respectively.

Titration of PPE with PiMM plasma

The major elastase inhibitors in plasma include A1AT and A2M. Elastase that is bound to A2M can retain its proteolytic activity towards low molecular weight nitroanilide substrates [252], and therefore inhibition of PPE by plasma largely reflects the inhibitory capacity due to A1AT.

PPE was diluted to 10µg/ml and fresh PiMM plasma was diluted 1 in 200 in PPE buffer. PPE (10µL) was added to a 96 well plate (Costar, USA) in triplicate sets. Control wells did not contain any PPE, but contained all other components. Reducing volumes of diluted plasma (18-0µL) were added to the wells, to give reducing concentrations of inhibitor

(A1AT present in plasma irreversibly inhibits PPE) until the final wells contained no plasma. PPE buffer was then added to each set of wells to make up to a final volume of 110µL. The plate was covered and incubated with gentle shaking at 37ºC for 20 minutes to allow the enzyme to form a complex with the inhibitor. Residual activity was measured by adding 100µL SlaaapN at a concentration of 1mg/ml in PPE substrate buffer. The absorbance at 410nm was then read at 5 minute intervals up to 60 minutes using a Biotek Synergy HT plate reader at 37ºC. Mean results were taken of all triplicates and control values were subtracted.

An inhibition curve was constructed by plotting the percentage of remaining enzyme activity against the molar ratio of A1AT:PPE. The linear portion of the curve was extrapolated to the x-axis, and the number of moles of A1AT required to inhibit each mole of PPE was determined.

This method was optimised by including control wells for every volume of plasma. This was important since the inherent colour of diluted plasma could interfere with the optical density (OD) measured. Also, the substrate solution was added to all of the wells (including the control wells) since the substrate solution had a different OD to the buffer. For these reasons, the control wells contained all of the components of the other wells apart from the enzyme. Extra buffer (10µL) was added to control wells to ensure that the total volumes of the wells were the same.

The specific activity of PPE was therefore calculated using Lineweaver-Burk double reciprocal plot analysis and confirmed by titration with PiMM plasma. This specific activity value was then used in all subsequent calculations. Lineweaver-Burk double reciprocal plot analysis can be prone to errors since the y-axis uses the inverse of V which may increase any small errors in measurement. To reduce potential errors, experiments were performed in triplicate and mean results taken, and more points were plotted for larger values of [S] and hence smaller values for 1/[S] to increase the accuracy of extrapolation to the y-axis. Similar data may also be obtained by computational data fitting using non-linear regression.

2.6.1.3 Activity of pure A1AT by titration with PPE

Pure A1AT (Athens Research and Technology, USA) was titrated with PPE of known specific activity. A1AT is an irreversible inhibitor of PPE and forms a complex with 1:1 stoichiometry. PPE was diluted to 10µg/ml in PPE buffer and A1AT was diluted to 20µg/ml in the same buffer. The inhibition assay was performed as described in section 2.6.1.2.

2.6.1.4 Activities of pure NE and PR3

Pure NE (Athens Research and Technology, USA) and pure PR3 (Merck, UK) were titrated with the pure A1AT, which had been titrated with PPE of known activity (as above). Both NE and PR3 were taken as forming complexes with A1AT with 1:1 stoichiometry, and their specific activities were determined by performing enzyme inhibition assays as described below.

All enzyme and inhibitor concentrations quoted in subsequent experiments refer to active concentrations.

NE inhibition assay with pure A1AT

Pure NE was diluted in NE assay buffer to 10µg/ml. Pure A1AT of known activity was diluted so that the concentration of active inhibitor was equal to the concentration of NE. NE (10µL) was added to a 96 well plate (Costar, USA) in triplicate sets. Increasing volumes of pure A1AT (0-18µL) were added to the wells. Each triplicate had an appropriate control containing no enzyme. All wells were made up to 110µL with NE assay buffer. The plate was then covered and incubated with gentle shaking at 37ºC for 20 minutes. Residual activity was measured by adding 100µL SlaaapN at a concentration of 1mg/ml in NE assay buffer. The absorbance at 410nm was read at 5 minute intervals up to 60 minutes using a Biotek Synergy HT plate reader at 37ºC. Mean results were taken of all triplicates and control values were subtracted. The activity of NE was determined by constructing an inhibition curve and determining the intercept with the known amount of active A1AT.

PR3 inhibition assay with pure A1AT

Pure PR3 was diluted in NSP assay buffer. The detergent was added to the buffer to minimise adherence of free proteinases to plastic and glass surfaces when in dilute solution [240]. The PR3 was diluted to a concentration of 1.5µM and pure A1AT of known activity was diluted so that the concentration of active inhibitor was equal to the concentration of

PR3. The method was carried out as described for NE, except a different buffer (above) and substrate were used. The elastase substrate SlaaapN is not a suitable substrate for PR3 experiments as it shows no significant hydrolysis. However, an alternative elastase substrate, N-Methoxysuccinyl-Ala-Ala-Pro-Val p-nitroanilide (MSaapvN) (Sigma, UK) which is not specific for NE, can also be used for pure PR3 experiments. The catalytic efficiencies are different for the two enzymes and are shown in Table 2.2. For these experiments, 150µL of MSaapvN was used per well at a concentration of 0.2mg/ml in NSP assay buffer. The activity of PR3 was determined by constructing an inhibition curve and determining the intercept with the known amount of active A1AT.

Table 2.2- Kinetic parameters for NE and PR3 enzyme activities

(adapted from reference [119])

Substrate	**Parameter**	**NE**	**PR3**
SlaaapN	K_{cat}/K_m ($M^{-1}s^{-1}$)	465	Very low activity
MSaapvN	K_{cat}/K_m ($M^{-1}s^{-1}$)	33915	499

2.6.2 Results of active site titration experiments

2.6.2.1 Active site titration of PPE by Lineweaver-Burk double reciprocal plot analysis

The mean results of three experiments are summarised in Table 2.3 and Figure 2.3.

Table 2.3- Reaction velocities for PPE at different substrate concentrations (SlaaapN)

[S] (mM/L)	1/[S] (mM/L^{-1})	V (mM/L/s)	1/V (mM/L/s^{-1})
7.5	0.133	0.0001	10000
5	0.2	0.0000933	10741
2.5	0.4	0.0000833	12037
1	1	0.00004	26111
0.5	2	0.0000267	38889

Figure 2.3- Lineweaver-Burk double reciprocal plot for PPE

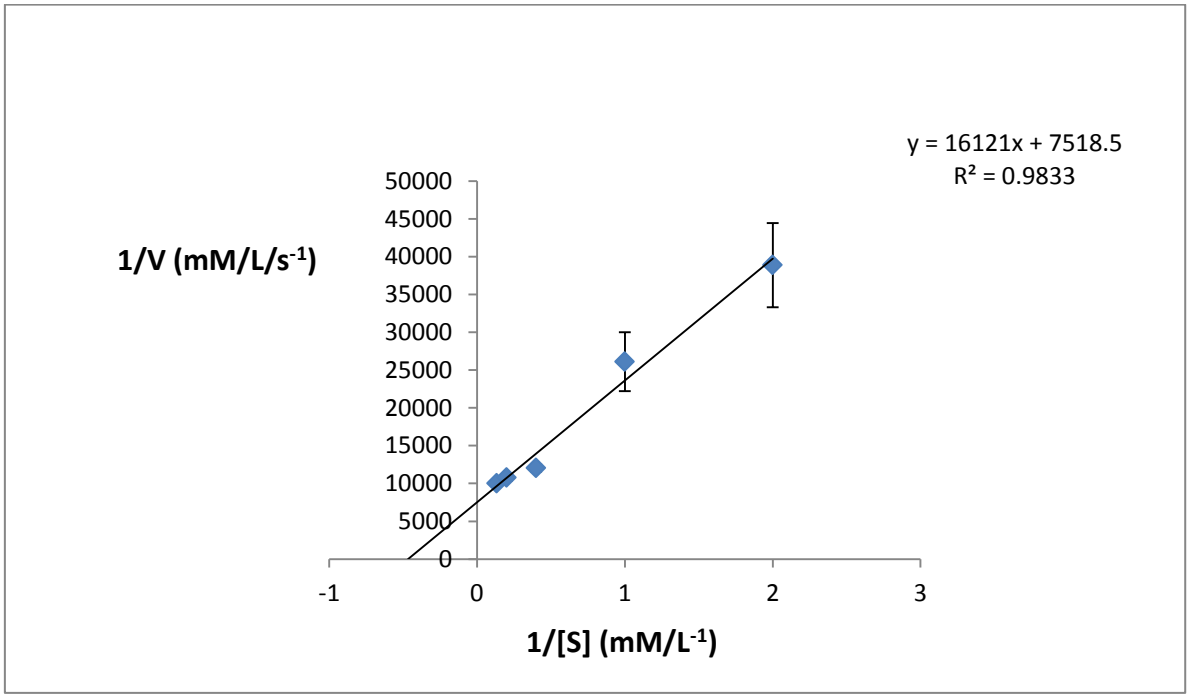

Figure 2.3: Lineweaver-Burk double reciprocal plot for PPE. The points show the mean results of three experiments ± standard error of the mean (SEM).

From these results, Vmax was calculated as 0.133µM/L/s. Using the equation of active enzyme=Vmax/Kcat (where the Kcat for PPE with this substrate is 37s^{-1} [251]) the

concentration of active enzyme was found to be 0.36µM/L. The total concentration of enzyme was 0.39µM/L and therefore the PPE was 92% active as determined by this method.

2.6.2.2 Active site titration of PPE with PiMM plasma

The concentration of A1AT in the PiMM plasma sample was found to be 30.3µM by ELISA. The intra-assay and inter- assay CVs for the A1AT ELISA were 4.66% and 4.35% respectively. The inhibition slope of PPE by PiMM plasma is shown in Figure 2.4.

Figure 2.4- Inhibition of PPE by PiMM plasma (SlaaapN)

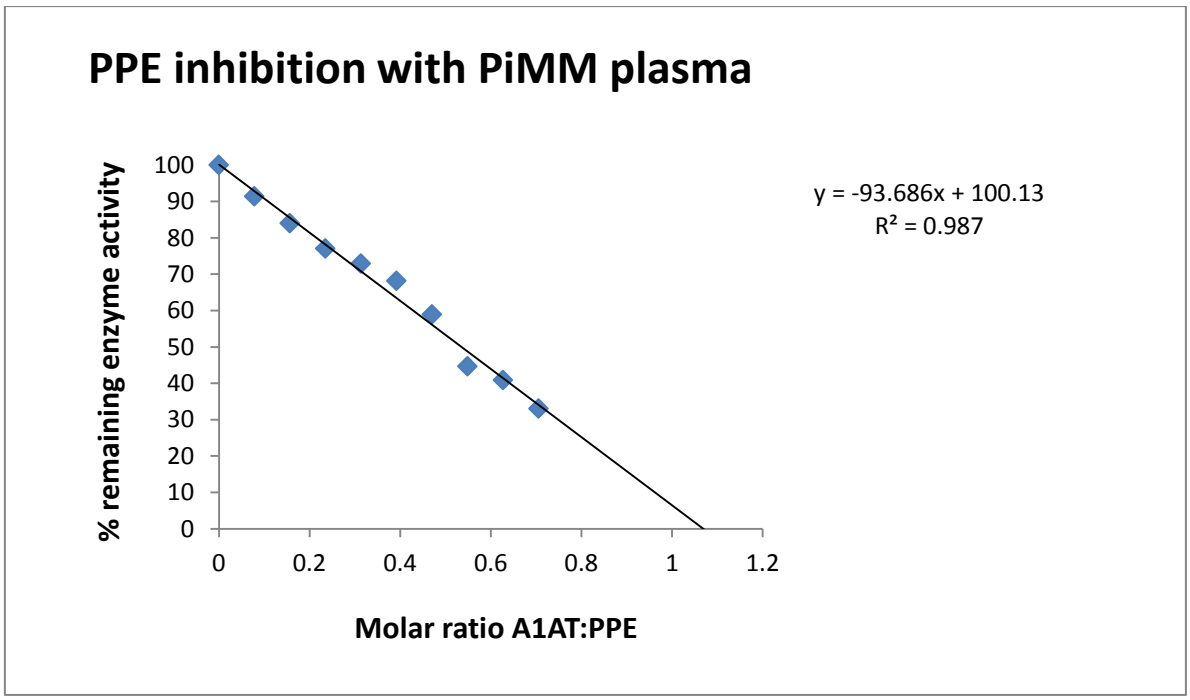

Figure 2.4: Inhibition slope of PPE with PiMM plasma. Each point shows the mean result from 3 experiments. The SEM was small and fell within the points plotted.

Extrapolation of the slope shows that the A1AT in PiMM plasma inhibits PPE at a molar ratio of 1.07:1. Therefore the results confirm the PPE to be almost fully active. Since this result is in keeping with the result obtained by Lineweaver-Burk double reciprocal plot analysis, 92% activity for PPE has been used throughout the following experiments.

2.6.2.3 Activity of pure A1AT by titration with PPE

The inhibition slope of PPE by pure A1AT is shown in Figure 2.5. Extrapolation of the slope shows that the pure A1AT inhibited PPE at a molar ratio of 1.1:1. Therefore the pure A1AT was 84% active. This value was used for subsequent experiments.

Figure 2.5- Inhibition of PPE by pure A1AT (SlaaapN)

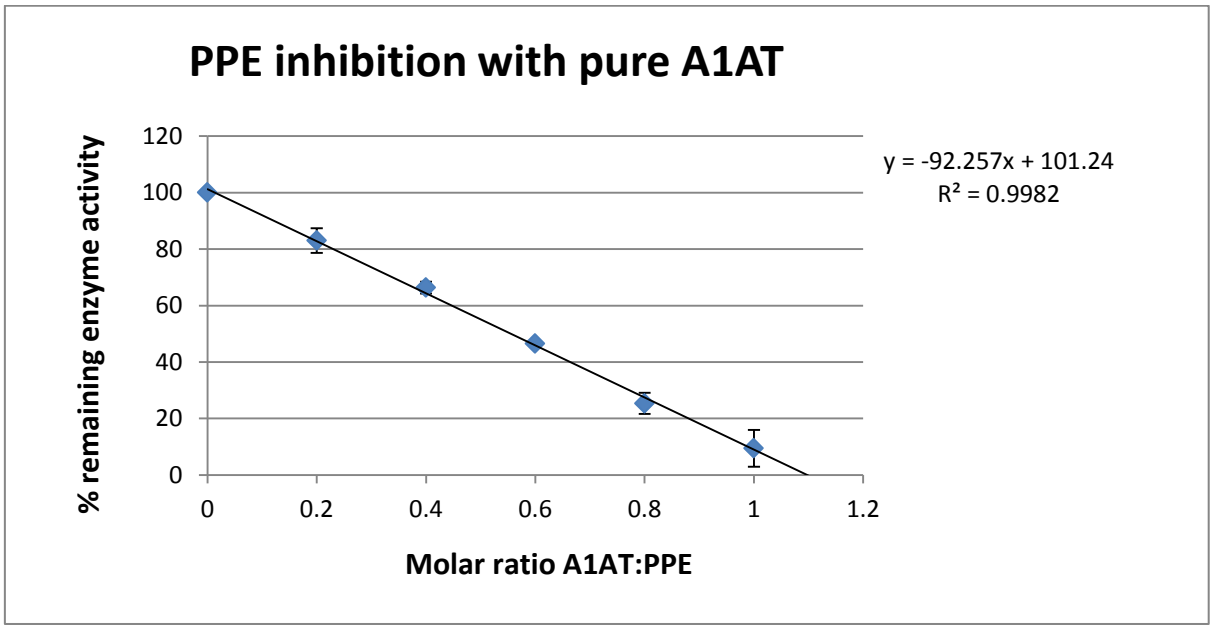

Figure 2.5: Inhibition slope of PPE activity with pure A1AT with SlaaapN used as the substrate. The points show the mean results ± SEM.

2.6.2.4 Activities of pure NE and PR3

The inhibition slopes of NE and PR3 activities by pure A1AT are shown in Figures 2.6 and 2.7. Extrapolation of the slopes demonstrates that the pure A1AT inhibited NE at a molar ratio of 0.87:1 and PR3 at a molar ratio of 0.85:1. Therefore, the NE and PR3 were 87% and 85% active respectively. These results were used for all subsequent experiments.

Figure 2.6- Inhibition of NE by pure A1AT (SlaaapN)

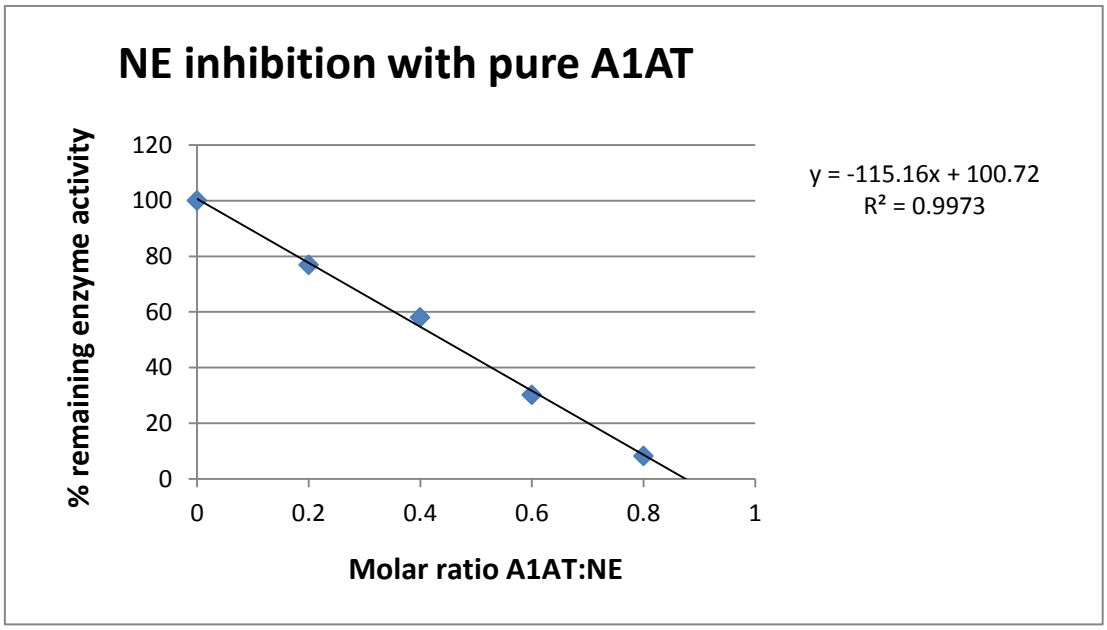

Figure 2.6: Inhibition of NE activity with pure A1AT with SlaaapN used as the substrate. Each point shows the mean result from three experiments. The SEM was small and fell within the points plotted.

Figure 2.7- Inhibition of PR3 by pure A1AT (MSaapvN)

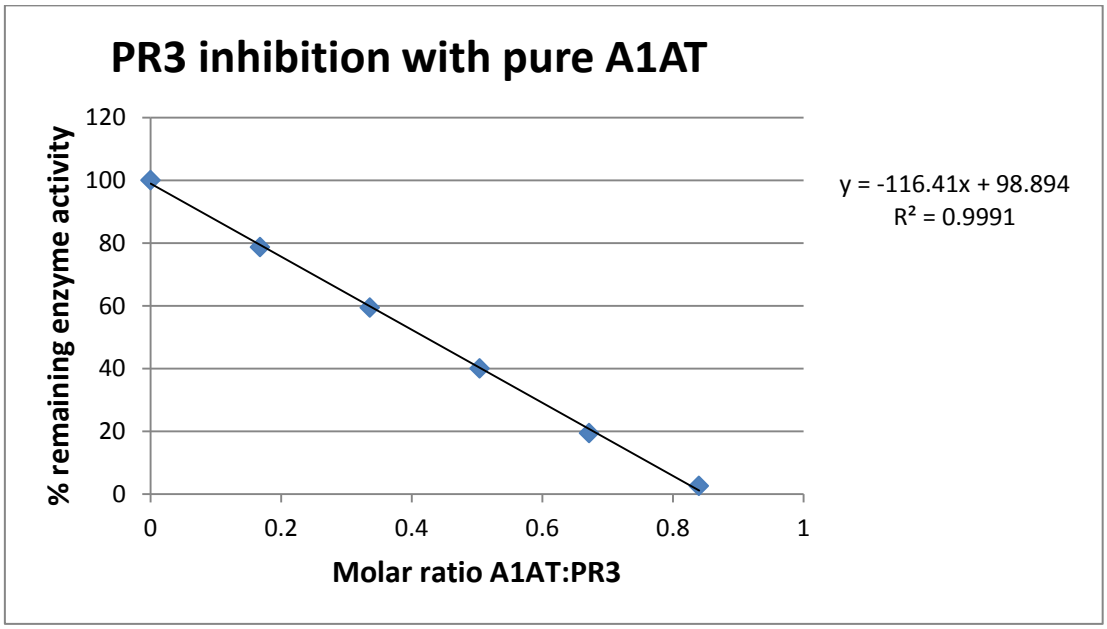

Figure 2.7: Inhibition of PR3 activity with pure A1AT with MSaapvN used as the substrate. Each point shows the mean result from three experiments. The SEM was small and fell within the points plotted.

2.6.3 Conclusions of active site titration experiments

The experiments described in this thesis depend on using proteins of known activity, rather than known concentration. Lineweaver-Burk double reciprocal plot analysis was used as the standard for determining PPE activity and these results were confirmed by using A1AT in PiMM plasma where most of the A1AT is functional. The methods for determining the activities of pure A1AT, NE and PR3 are summarised in Figure 2.8.

Enzyme activity can be influenced by many factors including salt concentration, temperature, pH and freeze/thaw cycles. For these reasons, experimental conditions were kept consistent throughout and fresh aliquots of enzyme were used for all experiments.

The baseline experiments described here were repeated at regular time intervals to ensure consistency of results. All concentrations referred to in subsequent chapters represent the active protein concentration unless otherwise stated.

Figure 2.8- Summary of active site titration experiments

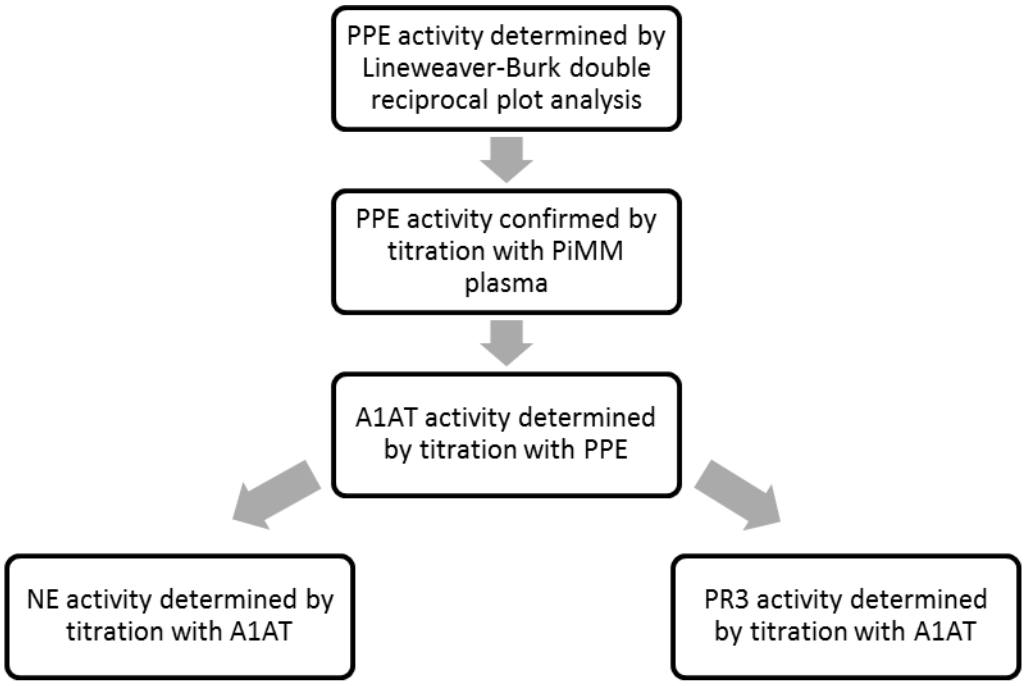

Figure 2.8: Series of experiments performed in order to determine the activities of enzymes and inhibitors used throughout this thesis.

2.7 Statistical analysis

Statistical analyses were performed using PASW statistics 18 for Windows. Normality was tested using the Kolmogorov-Smirnov test. Parametric data are presented as mean ±standard error of mean (SEM) and independent or paired T-tests were used for comparisons of data for independent or related measures respectively. Non-parametric data are presented as medians and inter-quartile ranges (IQR). Mann-Whitney U tests or Wilcoxon signed rank tests were used for comparisons of independent or related data respectively. Correlations were assessed using Spearman's rank correlation coefficient. Results were deemed statistically significant if $p \leq 0.05$.

3 The ability of serum samples to inhibit proteinase activity

3.1 Introduction

Excessive proteolytic activity of NSPs is associated with tissue damage in COPD [100]. The major serum inhibitors of NE and PR3 are A1AT and A2M which differ in their mechanism of inhibition. Complex formation between A1AT and NSPs results in the enzyme being inactivated. However, the inhibitory mechanism of A2M is predominantly by steric hindrance and NE that is bound to A2M retains its proteolytic activity towards low molecular weight nitroanilide substrates [252]. The proteolytic potential of PR3 complexes with A2M has not been previously studied. In this Chapter, serum samples from subjects with different A1AT genotypes have been used to assess how NE and PR3 partition between these two serum inhibitors in the presence of different A1AT variants, and any resultant effects on their activities.

3.2 Methods

3.2.1 SlaaapN assays

3.2.1.1 Inhibition of NE with serum from various A1AT genotypes

Pure NE of pre-determined activity was diluted in NE assay buffer to 1.5µM active enzyme. Serum samples from subjects with various A1AT genotypes (PiMM, PiSZ, PiFZ and PiZZ) were taken and the A1AT concentration was measured by ELISA as described in section 2.6.1.2. Each serum sample was then diluted in NE assay buffer so that the concentration of A1AT was 1.5µM. Ten µL of NE was added to a 96-well plate (Costar,

USA) in triplicate sets and increasing volumes of serum were then added to each set of wells. Each experimental set had an appropriate control containing no NE, but containing all other components including diluted serum. This was important because the inherent colour of diluted serum affects the OD. All wells were made up to 110µL with NE assay buffer, and the plate was covered and incubated with gentle shaking at 37ºC for 20 minutes to allow the NE to form complexes with the serum inhibitors. Residual activity was measured by adding 100µL of the NE specific substrate SlaaapN at a concentration of 1mg/ml in NE assay buffer. The absorbance at 410nm was read at 5 minute intervals up to 60 minutes using a Biotek Synergy HT plate reader at 37ºC. Average results were taken for all triplicates and control values were subtracted. Inhibition slopes were constructed by plotting the percentage of remaining enzyme activity against the molar ratio of A1AT:NE. Each experiment was performed in triplicate to ensure consistency.

These experiments were also performed once in the presence of EDTA (Sigma, UK) at a final concentration of 5mM (an inhibitor of MMPs) and E-64 (Sigma, UK) at a final concentration of 10µM (an inhibitor of cysteine proteinases) to ensure that measured enzyme activity could not be attributable to other classes of proteinase. The experiments were also repeated once in NSP assay buffer (at a physiological pH of 7.4) rather than NE assay buffer (pH 8.6) to determine whether this change in pH would influence the pattern of results.

3.2.2 MSaapvN assays

3.2.2.1 Inhibition of NE with serum from various A1AT genotypes

These experiments were performed using NSP assay buffer to facilitate comparison of results between NE and PR3 assays. MSaapvN was made at a concentration of 0.2mg/ml in this buffer. Initially, it was necessary to determine the optimal concentration of NE for these experiments due to different kinetic parameters between SlaaapN and MSaapvN (Table 2.2). A range of NE concentrations were made (0.03-1.5µM) and 10µL of NE was added to each well of a 96 well plate. MSaapvN (150µL) was added to each well and the absorbance at 410nm was read at 5 minute intervals up to 60 minutes using a Biotek Synergy HT plate reader at 37ºC. The OD was plotted against time, and the optimal concentration of NE was selected where the graph remained linear, indicating that the reaction was not limited by [S]. Subsequent experiments were performed using this concentration of NE with this substrate.

It was also necessary to establish whether any other proteinases in the serum samples could affect the results, since MSaapvN is not specific for NE. To do this, 20µL of each diluted serum sample was added to a 96 well plate and 150µL of MSaapvN was added. The OD was measured as described above and plotted against time.

The NE inhibition assays were performed in a similar manner to the SlaaapN assays with the following exceptions; NE was diluted to 0.1µM, serum samples were diluted so that the concentration of A1AT was 0.1µM, NSP assay buffer was used, and 150µL of MSaapvN was used at a concentration of 0.2mg/ml.

3.2.2.2 Inhibition of PR3 with serum from various A1AT genotypes

These experiments were carried out as described in section 2.6.1.4 for pure A1AT, except diluted serum samples were used with an A1AT concentration of 1.5µM. Briefly, 10µL of 1.5µM active PR3 was added to a 96-well plate in triplicate sets. Increasing volumes (0-16µL) of diluted serum (A1AT concentration 1.5µM) were added to each triplicate set and the total volume of each well was made up to 110µL with NSP assay buffer. Control wells for each triplicate set contained all components except for the PR3. An extra 10µL of buffer was added to control wells to ensure that the volumes were equal. The plate was covered and incubated with gentle shaking at 37ºC for 20 minutes to allow the PR3 to form complexes with the serum inhibitors. Residual PR3 activity was measured by adding 150µL of MSaapvN at a concentration of 0.2mg/ml in NSP assay buffer. The absorbance at 410nm was read at 5 minute intervals up to 60 minutes using a Biotek Synergy HT plate reader at 37ºC. Mean results were taken of all triplicates and control values were subtracted. Inhibition slopes were constructed by plotting the percentage of remaining enzyme activity against the molar ratio of A1AT:PR3.

3.3 Results

3.3.1 A1AT ELISA

The A1AT concentrations (measured by ELISA) of the serum samples used throughout this thesis are shown in Table 3.1. Values are consistent with published ranges [145].

Table 3.1- A1AT concentrations in serum of different A1AT genotypes

A1AT genotype	Serum A1AT concentration (µM)
PiMM	30.3
PiMZ	19.8
PiSZ	16.2
PiSS	14.4
PiFZ	21.6
PiFM	35.2
PiIZ	16.6
PiZZ	4.3

3.3.2 SlaaapN assays

3.3.2.1 Inhibition of NE with PiMM serum

The inhibition slope of NE with PiMM serum is shown in Figure 3.1. For comparison, the inhibition slope of NE with pure A1AT is also shown. The results show that pure A1AT fully inactivated NE when the molar ratio of A1AT:NE exceeded 1:1, as would be expected. PiMM serum also inhibited NE activity in a linear fashion until the molar ratio of A1AT:NE reached 1:1. However, when the A1AT in PiMM serum was in a molar excess of NE, 17.1 ± 0.1% (mean ± SEM) residual NE activity was still observed, suggesting that PiMM serum did not completely inactivate NE even when the main inhibitor A1AT was in a molar excess. Possible reasons for this finding are discussed in section 3.4 (Discussion).

Figure 3.1- Inhibition assays of NE with PiMM serum and pure A1AT (SlaaapN)

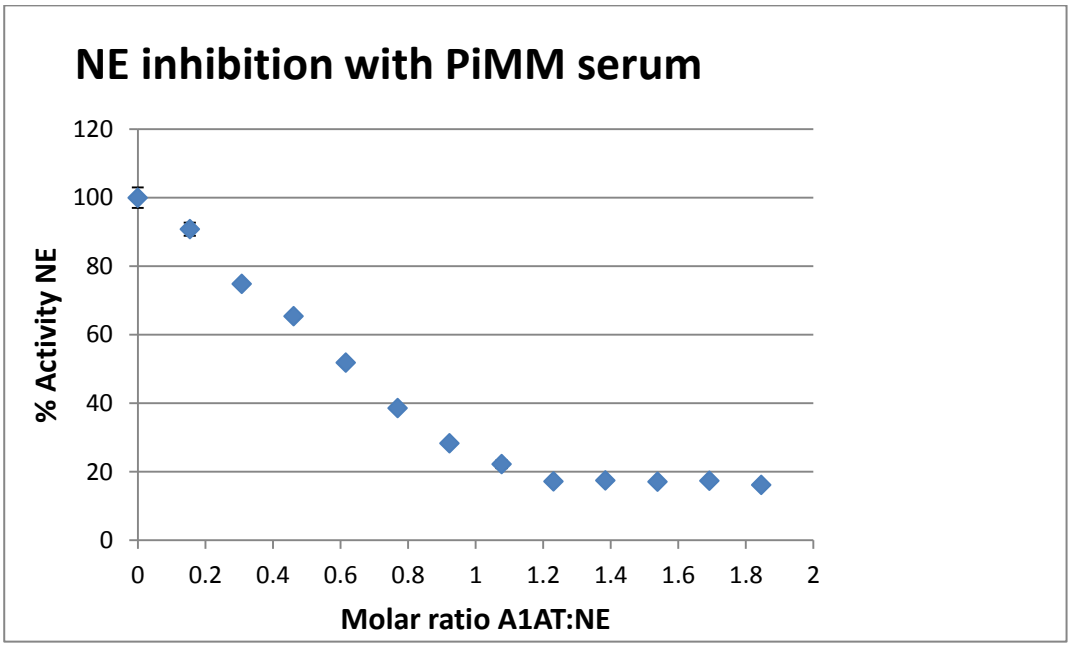

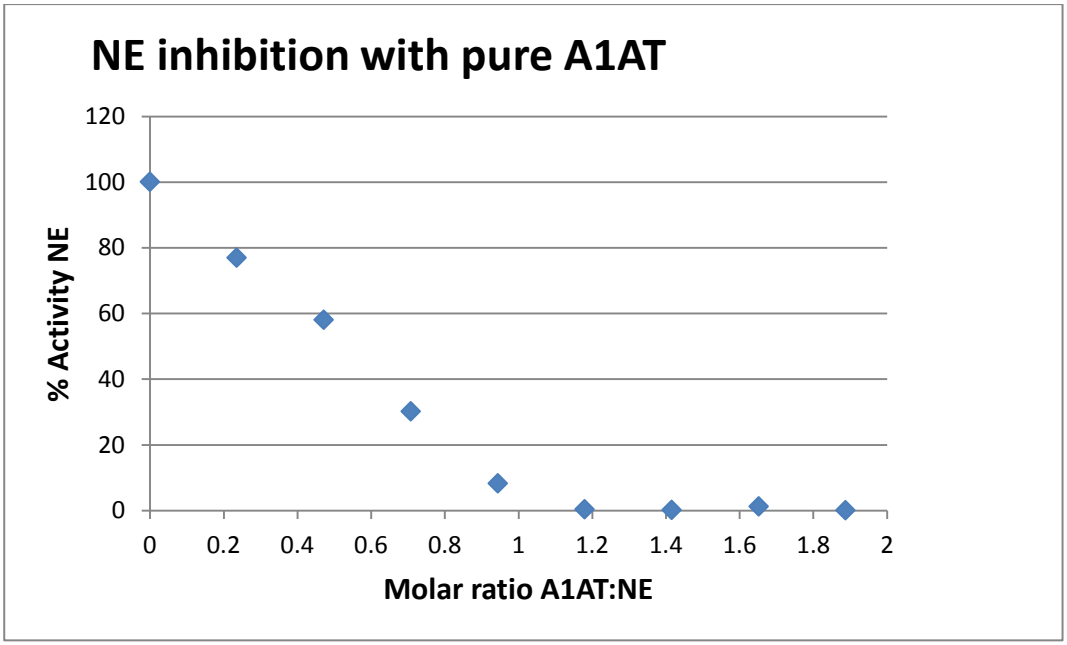

Figure 3.1: Inhibition assays of NE activity with PiMM serum and pure A1AT. Points show the mean values and the SEM falls within the symbol for most of these data points.

3.3.2.2 Inhibition of NE with PiSZ serum

The inhibition slope of NE with PiSZ serum is shown in Figure 3.2. Initially, NE activity was increasingly inhibited by PiSZ serum as the molar ratio of A1AT:NE approached 1:1. However, even when the A1AT in the serum was in a molar excess of the NE, residual NE activity remained at 60.6 ± 1.0% which was greater than the residual NE activity observed with PiMM serum.

Figure 3.2-Inhibition of NE with PiSZ serum (SlaaapN)

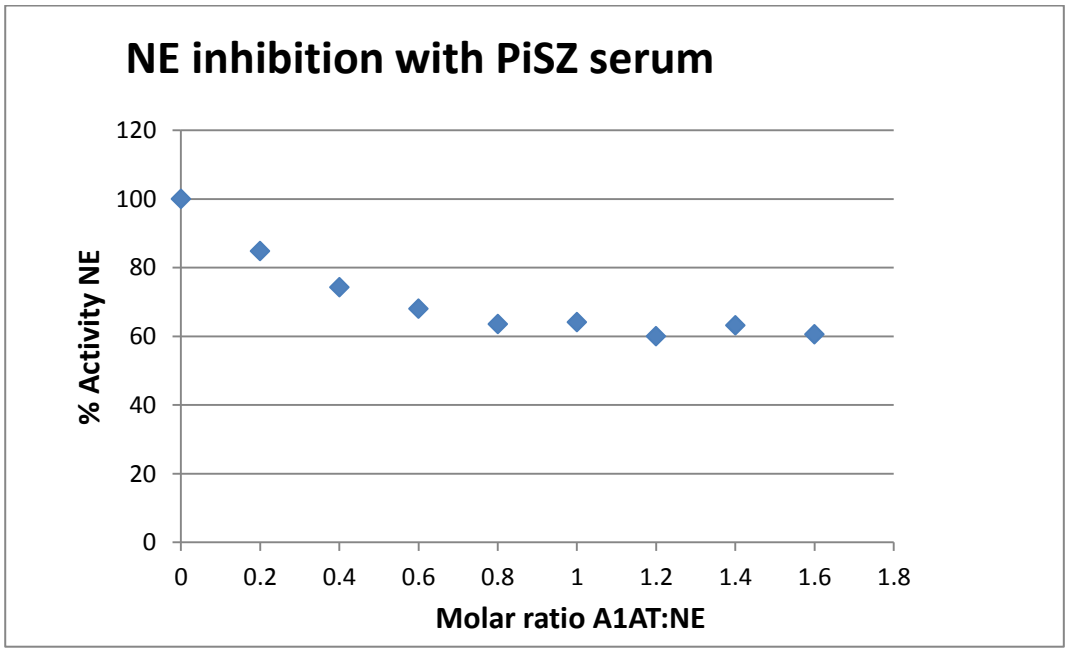

Figure 3.2: Inhibition of NE activity with PiSZ serum using SlaaapN as the substrate. Points show the mean values and the SEM falls within the points plotted.

3.3.2.3 Inhibition of NE with PiFZ serum

The inhibition slope of NE with PiFZ serum is shown in Figure 3.3. As observed with PiSZ serum (Figure 3.2), PiFZ serum also did not fully inactivate NE when the serum A1AT was in a molar excess, and 56.0 ± 0.5% residual NE activity was observed.

Figure 3.3-Inhibition of NE with PiFZ serum (SlaaapN)

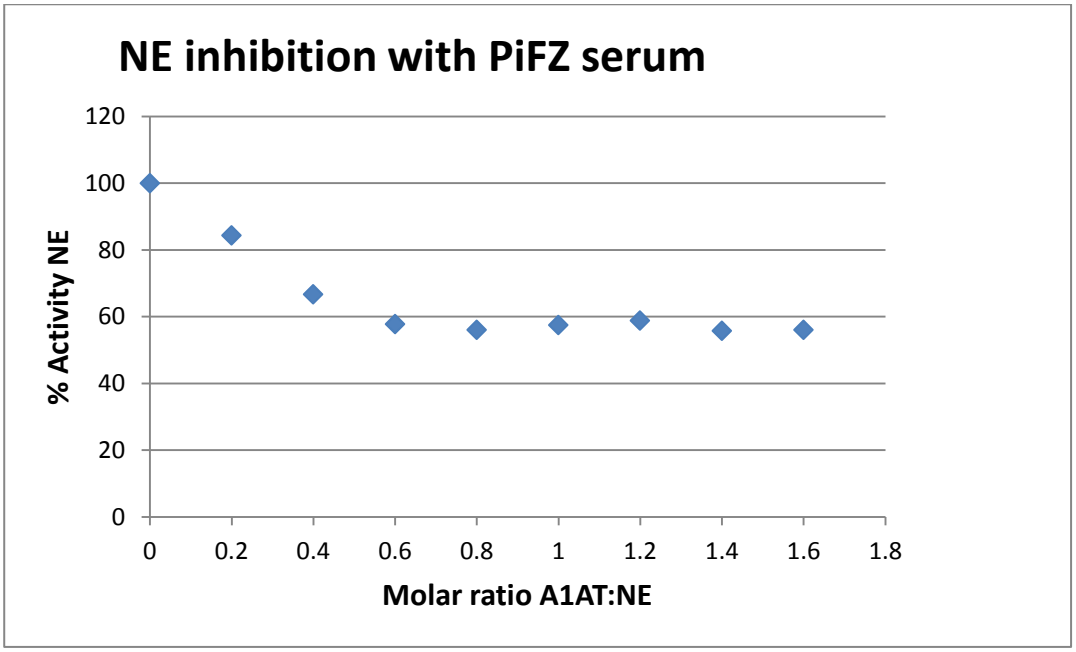

Figure 3.3: Inhibition of NE activity with PiFZ serum using SlaaapN as the substrate. Points show the mean values and the SEM falls within the points plotted.

3.3.2.4 Inhibition of NE with PiZZ serum

The inhibition slope of NE with PiZZ serum is shown in Figure 3.4. These results were different to those observed with PiMM, PiSZ and PiFZ sera. Initially, inhibition of NE activity was observed, but as the molar ratio of A1AT:NE increased, enhanced NE activity was seen above that measured with NE alone. This experiment was therefore repeated in the presence of inhibitors of MMPs and cysteine proteinases (Figure 3.6) to establish whether this effect could be attributable to other classes of proteinases, and the experiment was also performed at a different pH to determine whether pH changes could influence the results (Figure 3.7).

Figure 3.4-Inhibition of NE with PiZZ serum (SlaaapN)

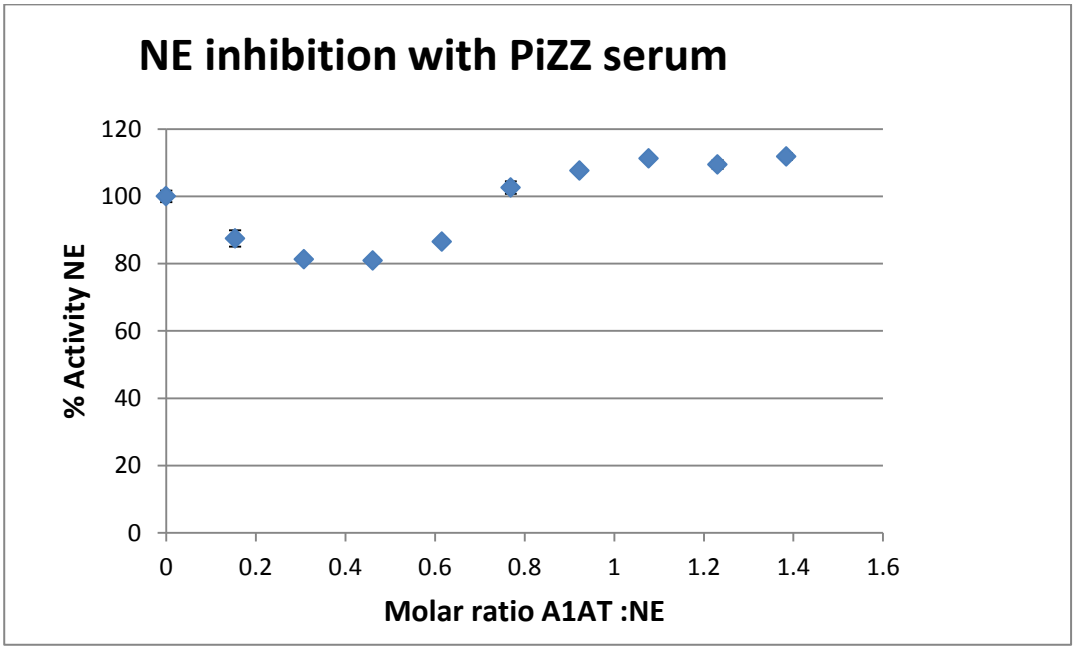

Figure 3.4: Inhibition of NE activity with PiZZ serum using SlaaapN as the substrate. Points show the mean values and the SEM falls mostly within the points plotted.

3.3.2.5 Summary of SlaaapN assays

Figure 3.5 shows a summary of the NE inhibition slopes described above. These results have used pure A1AT or serum samples from different A1AT genotypes as the inhibitors, and SlaaapN as the substrate. Table 3.2 summarises the amount of residual NE activity observed when the different serum samples were used and the A1AT was in a molar excess. The molar ratio of serum A2M to NE is also shown for the different serum samples. Lower serum concentrations of A1AT were associated with a greater molar ratio of A2M:NE and also greater residual NE activity when A1AT was in a molar excess.

Figure 3.5- Comparison of NE inhibition slopes with pure A1AT and serum samples from different A1AT genotypes (SlaaapN)

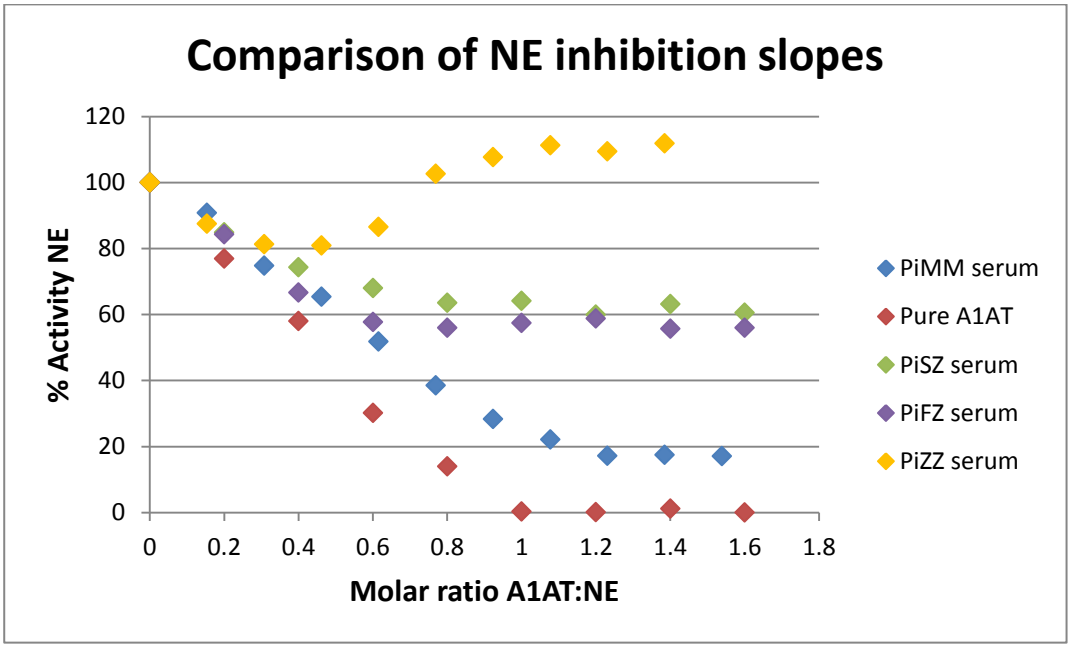

Figure 3.5: A comparison of inhibition slopes of NE activity with pure A1AT and PiMM, PiSZ, PiFZ and PiZZ sera. SlaaapN was used as the substrate for these experiments.

Table 3.2- Residual NE activity observed when serum samples from different A1AT genotypes were used and the A1AT was in a molar excess (SlaaapN)

A1AT genotype	**Residual NE activity observed when A1AT was in a molar excess**	**Molar ratio of A2M:NE when the ratio of A1AT:NE was 1:1**
PiMM	17.1 ± 0.1%	0.09:1
PiFZ	56.0 ± 0.5%	0.12:1
PiSZ	60.6 ± 1.0%	0.16:1
PiZZ	111.2 ± 0.7%	0.60:1

3.3.2.6 Inhibition of NE with PiMM or PiZZ serum in the presence of EDTA & E-64

The inhibition slopes of NE with PiMM or PiZZ serum in the presence of the MMP and cysteine proteinase inhibitors are shown in Figure 3.6. The enhanced activity of NE with increasing volumes of PiZZ serum was still observed.

Figure 3.6- Inhibition of NE with PiMM or PiZZ serum in the presence of EDTA & E-64 (SlaaapN)

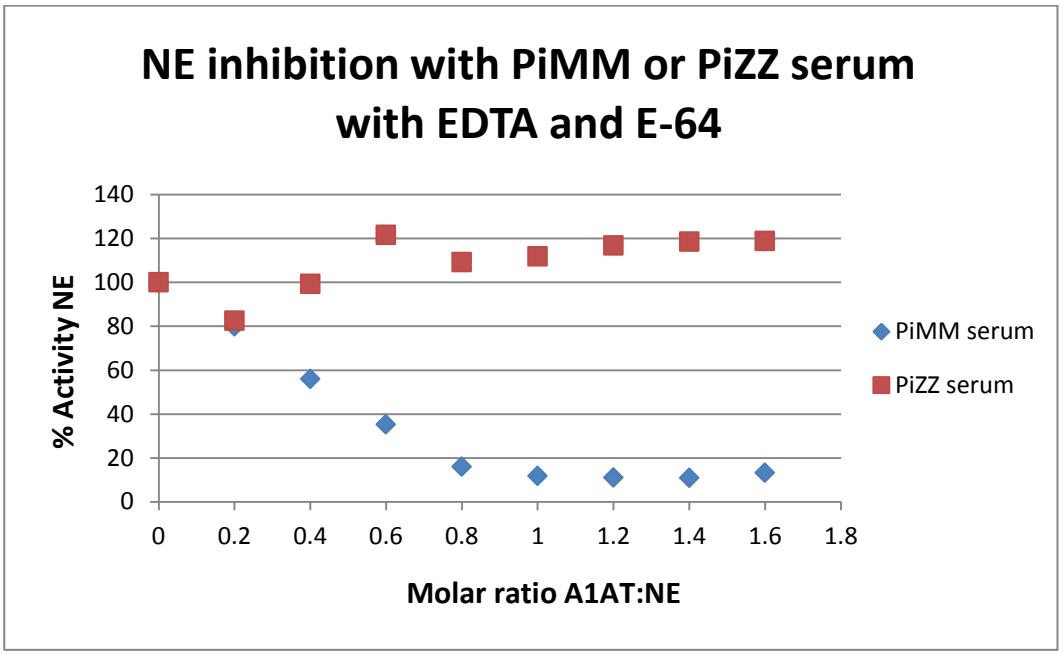

Figure 3.6: Inhibition of NE activity with PiMM or PiZZ serum in the presence of inhibitors of MMPs and cysteine proteinases. SlaaapN was used as the substrate. The results of single experiments for each serum sample are shown.

3.3.2.7 Inhibition of NE with PiMM or PiZZ serum in NSP assay buffer (pH 7.4)

The inhibition slopes of NE with PiMM or PiZZ serum in NSP assay buffer are shown in Figure 3.7. The pattern of results was not significantly different to those obtained using NE assay buffer and the enhanced activity of NE with increasing volumes of PiZZ serum was still observed.

Figure 3.7- Inhibition of NE with PiMM or PiZZ serum in NSP assay buffer (SlaaapN)

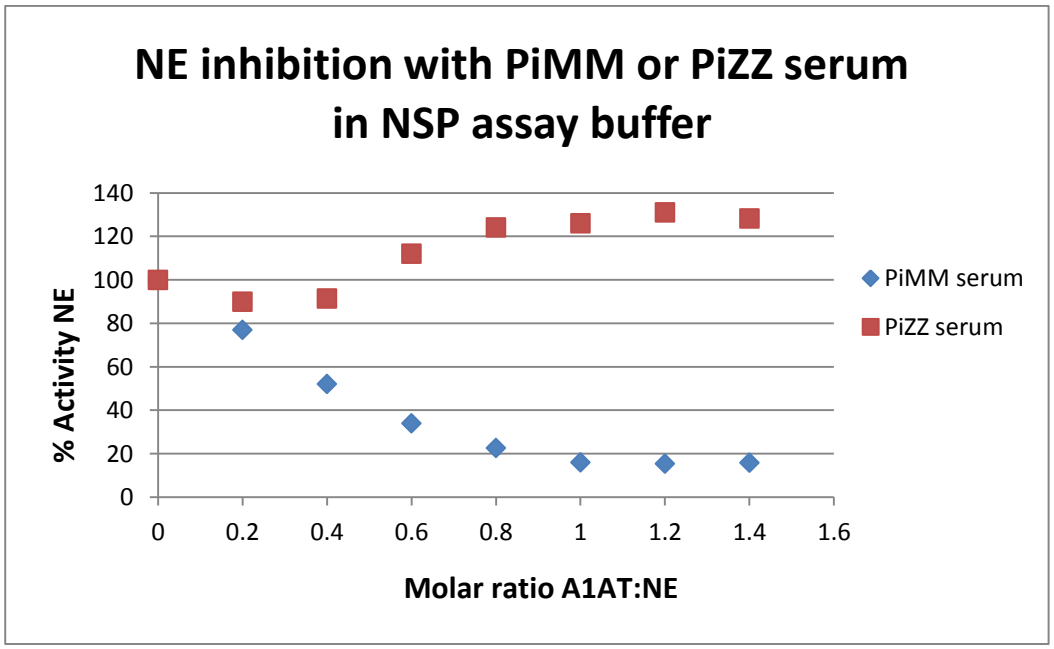

Figure 3.7: Inhibition of NE activity by PiMM or PiZZ serum in a buffer with a physiological pH of 7.4. SlaaapN was used as the substrate. The results of single experiments for each serum sample are shown.

3.3.3 MSaapvN assays

Initially, these assays were optimised by establishing suitable concentrations of enzymes to be used, and to determine the suitability of MSaapvN for experiments involving serum

since MSaapvN is not a specific substrate and is hydrolysed by more than one proteinase. Data was then collected following these optimisation experiments.

3.3.3.1 Determining the optimal concentration of NE for MSaapvN assays

The optimal concentration of NE which produced a reasonable change in OD at 60 minutes was found to be 0.1µM. At this concentration, the graph remained linear throughout the time course used, indicating that the reaction was not limited by [S]. These results are shown in Figure 3.8.

Figure 3.8- Determination of the optimal concentration of NE for MSaapvN experiments

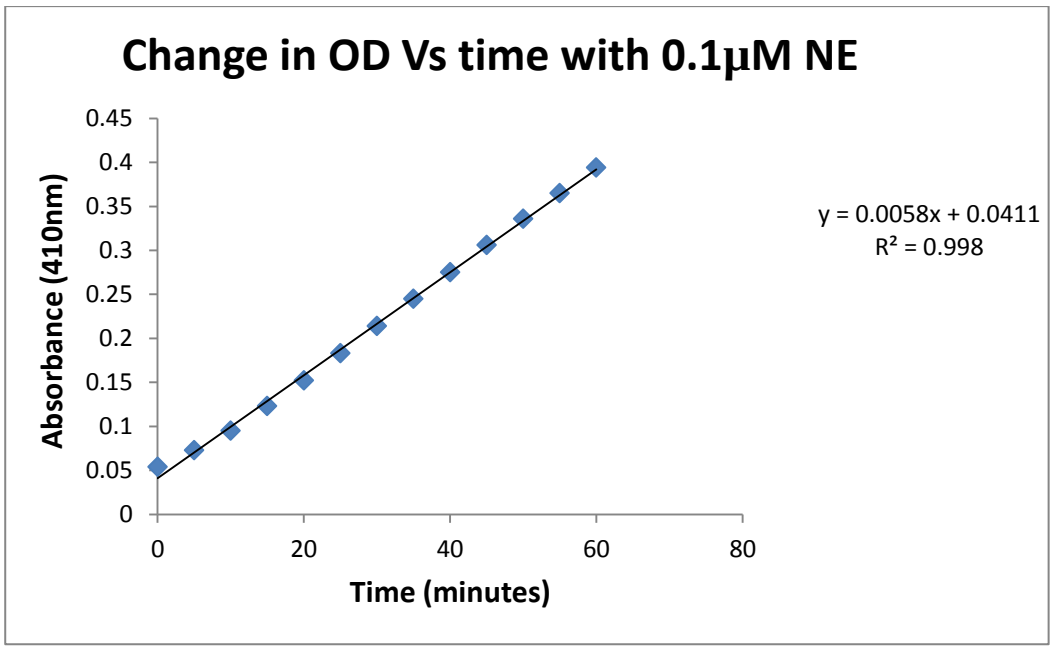

Figure 3.8: The optimal concentration of NE for MSaapvN assays was 0.1µM. At this concentration, the slope remained linear throughout the time course used indicating that the reaction was not limited by [S], and an acceptable change in absorbance was observed over this time course. The results from a single experiment are shown.

3.3.3.2 Determining the suitability of MSaapvN for use with serum samples

When MSaapvN was added to the diluted serum samples to be used in subsequent experiments, there was no change in OD over the time course of the experiments. These results showed that there was no detectable free proteinase activity in the serum samples that could affect the results of the NE and PR3 inhibition assays. The results from a single experiment using PiMM serum are shown in Figure 3.9. The results were similar for other A1AT genotype serum samples (data not shown).

Figure 3.9-Determining the change in OD over time using PiMM serum and MSaapvN

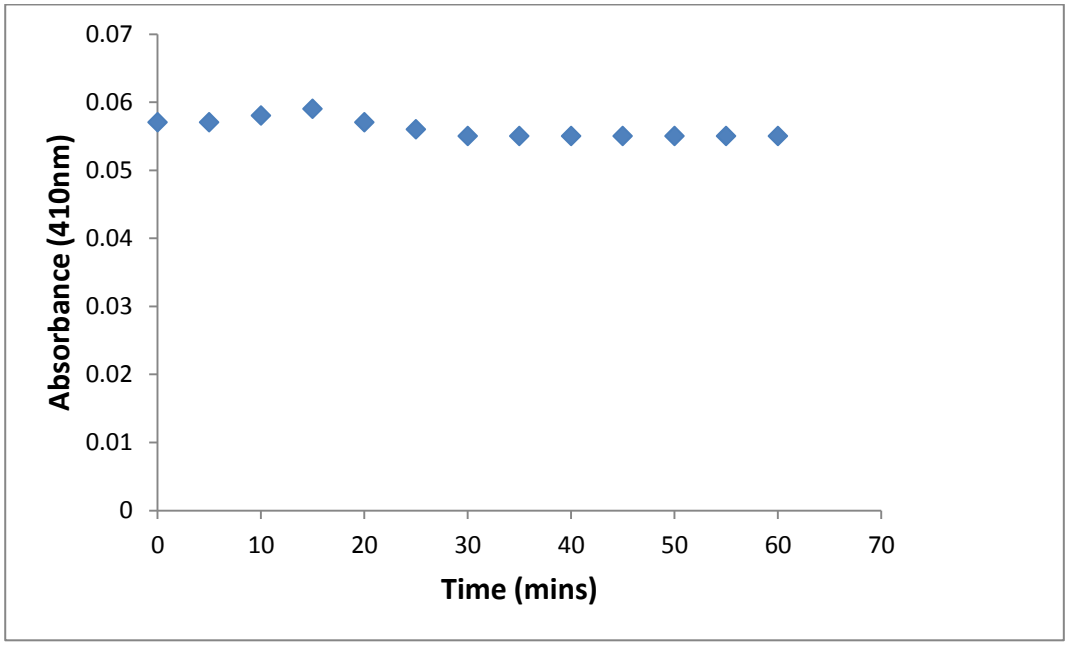

Figure 3.9: When MSaapvN was added to diluted PiMM serum there was no change in absorbance noted over the time course of the experiment, indicating that no other proteinases in the serum could interfere with the serine proteinase assays. The results from a single experiment are shown.

3.3.3.3 Inhibition of NE and PR3 with PiMM serum

The inhibition slopes of NE and PR3 with PiMM serum are shown in Figure 3.10. For comparison, the inhibition slope of PR3 with pure A1AT is also shown. The results show that pure A1AT fully inactivated PR3 when the molar ratio of A1AT:PR3 exceeded 1:1, as would be expected. PiMM serum was initially able to inhibit NE or PR3 activity in a linear pattern as the molar ratio of A1AT to the enzyme increased. Experiments were performed separately for each proteinase but the results are presented together for comparison. When the A1AT in PiMM serum was in a molar excess, 5.4 ± 1.1% residual NE activity remained and 7.7 ± 0.8% residual PR3 activity remained, suggesting that PiMM serum was not able to fully inactivate either NE or PR3 even when the predominant inhibitor A1AT was in a molar excess of the enzyme. The inhibition assays using PiMM serum and NE or PR3 were similar to each other. The residual NE activity observed was less when MSaapvN was used as the substrate than when SlaaapN was used (Figure 3.1).

Figure 3.10-Inhibition assays of NE and PR3 with PiMM serum and PR3 with pure A1AT (MSaapvN)

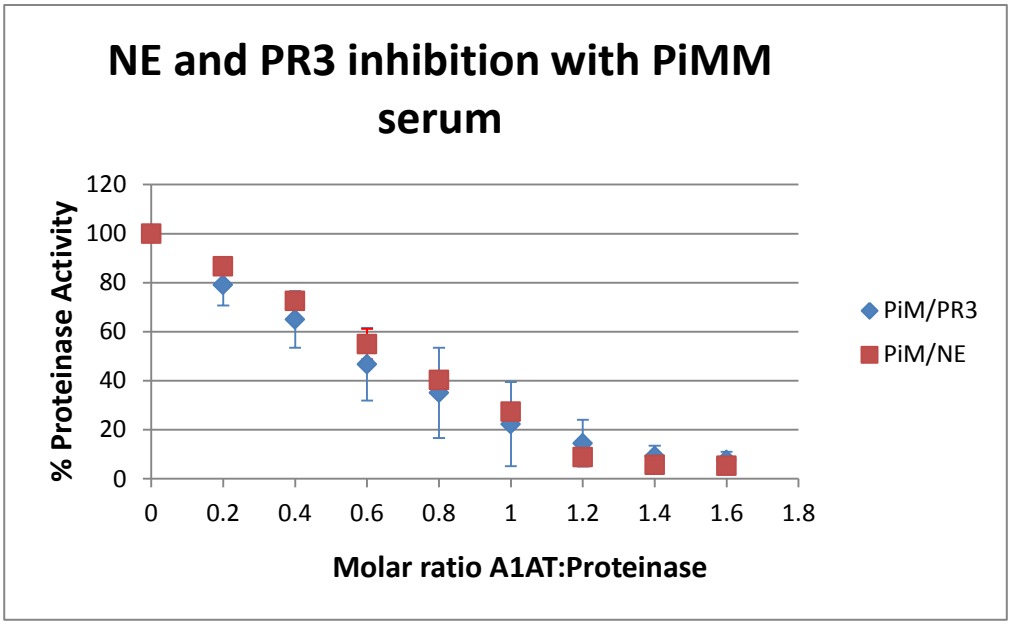

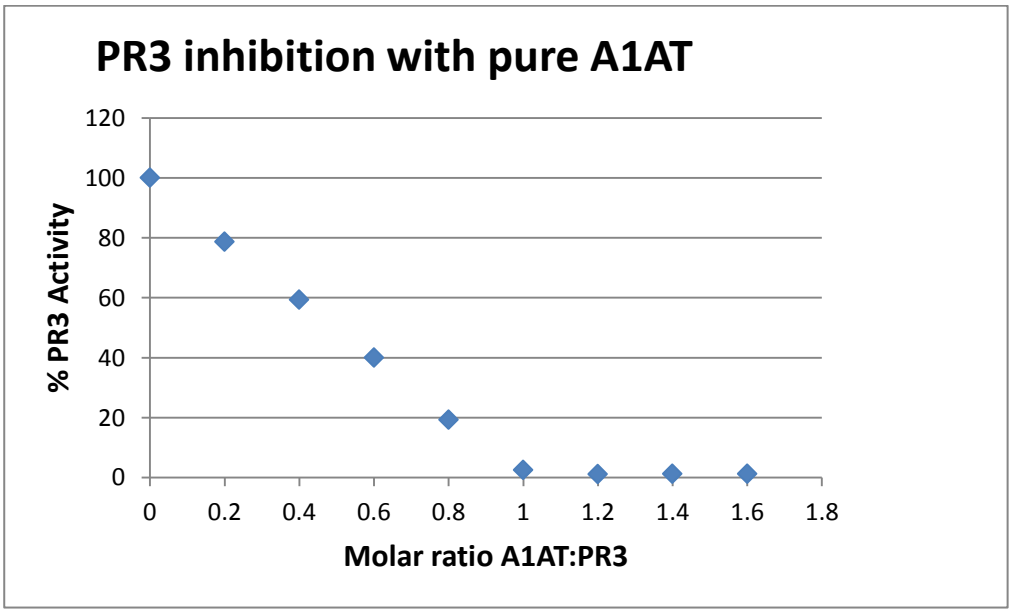

Figure 3.10: Inhibition of NE and PR3 activities by PiMM serum with MSaapvN as the substrate. Individual experiments were performed using a single proteinase and the data for NE and PR3 are presented together for comparison. The points show the mean ± SEM. The inhibition slope of PR3 with pure A1AT is also shown for comparison.

3.3.3.4 Inhibition of NE and PR3 with PiSZ serum

The inhibition slopes of NE and PR3 with PiSZ serum are shown in Figure 3.11. The results show that NE or PR3 were both initially inhibited by PiSZ serum as the molar ratio of A1AT to the enzyme increased but neither enzyme was fully inactivated by PiSZ serum even when A1AT was in a molar excess. Separate experiments were performed for each proteinase but the results are presented together for comparison. The residual activities for NE and PR3 were 13.6 ± 1.2% and 18.2 ± 0.7% respectively.

Figure 3.11- Inhibition of NE and PR3 with PiSZ serum (MSaapvN)

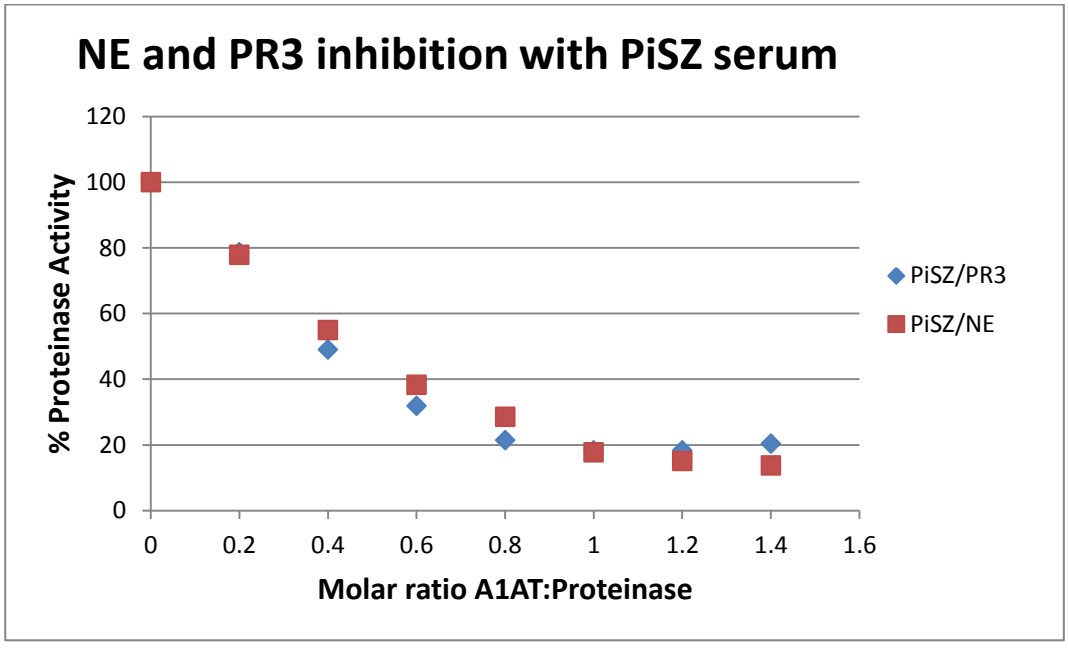

Figure 3.11: Inhibition of NE and PR3 activities by PiSZ serum with MSaapvN as the substrate. Single experiments were performed for each proteinase and the data for NE and PR3 are presented together for comparison.

3.3.3.5 Inhibition of NE and PR3 with PiFZ serum

The inhibition slopes of NE and PR3 with PiFZ serum are shown in Figure 3.12. The initial linear portion of the slope shows that PiFZ serum was able to inhibit NE and PR3 as the molar ratio of serum A1AT to the enzyme increased. However, residual NE activity at 56.4 ± 0.5% was observed which was greater than the 36.8 ± 0.3% residual PR3 activity.

Figure 3.12- Inhibition of NE and PR3 with PiFZ serum (MSaapvN)

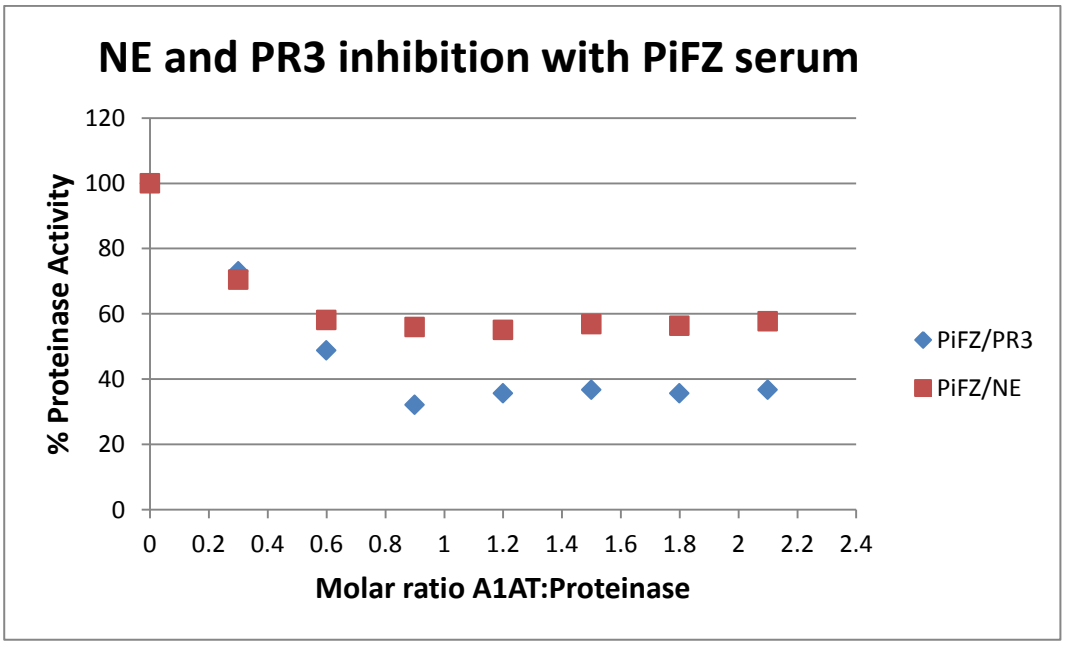

Figure 3.12: Inhibition of NE and PR3 activities by PiFZ serum with MSaapvN as the substrate. Individual experiments were performed for each proteinase and the data for NE and PR3 are presented together for comparison.

3.3.3.6 Inhibition of NE and PR3 with PiFM serum

The inhibition slopes of NE and PR3 with PiFM serum are shown in Figure 3.13. Again, the initial linear portion of the slope shows that PiFM serum was able to inhibit NE and PR3 as the molar ratio of serum A1AT to the enzyme increased. However, residual NE activity at 41.9 ± 1.6% was observed which was greater than the 9.6 ± 0.6% residual PR3 activity. Experiments with each proteinase were performed separately but the data are presented together for comparison.

Figure 3.13- Inhibition of NE and PR3 with PiFM serum (MSaapvN)

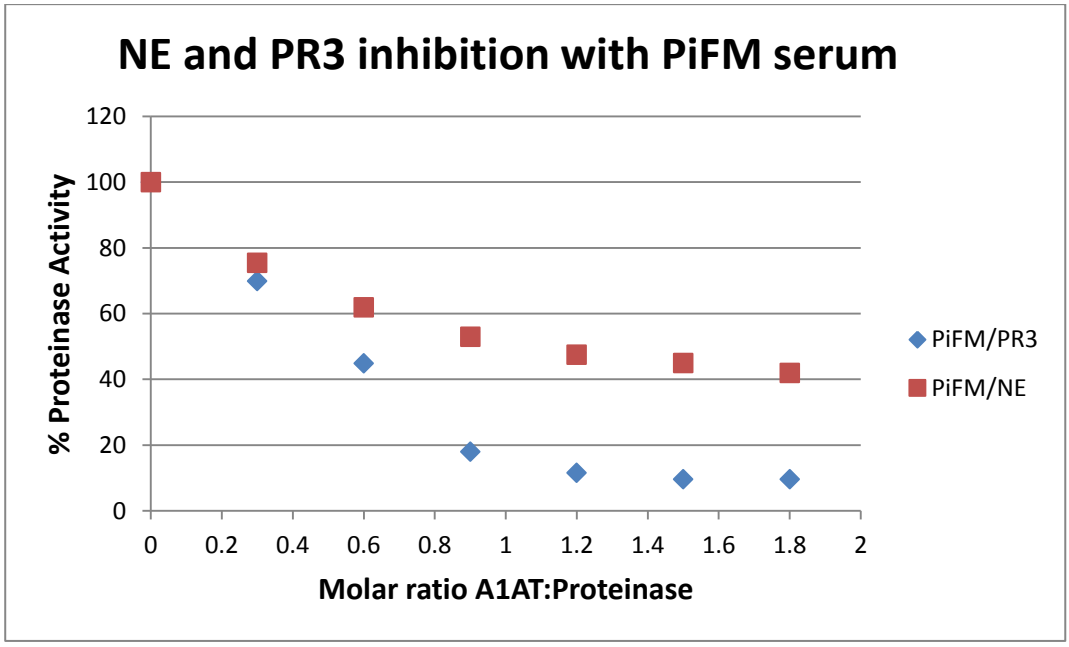

Figure 3.13: Inhibition of NE and PR3 activities by PiFM serum with MSaapvN as the substrate. Individual experiments were performed for each proteinase and the data for NE and PR3 are presented together for comparison.

3.3.3.7 Inhibition of NE and PR3 with PiIZ serum

The inhibition slopes of NE and PR3 with PiIZ serum are shown in Figure 3.14. The residual activity of NE (when the serum A1AT was in a molar excess of the enzyme) was greater than the residual activity observed with PR3 (47.8 ± 1.4% vs 19.5 ± 1.0%).

Figure 3.14- Inhibition of NE and PR3 with PiIZ serum (MSaapvN)

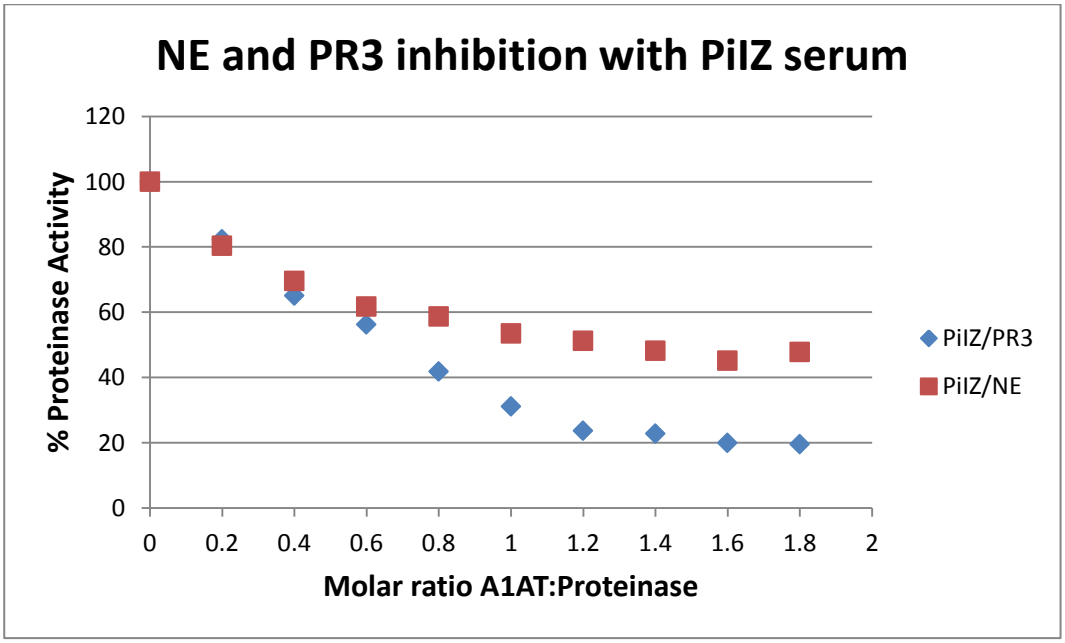

Figure 3.14: Inhibition of NE and PR3 activities by PiIZ serum with MSaapvN as the substrate. Individual experiments were performed for each proteinase and the data for NE and PR3 are presented together for comparison.

3.3.3.8 Inhibition of NE and PR3 with PiZZ serum

The inhibition slopes of NE and PR3 with PiZZ serum are shown in Figure 3.15. The initial linear portion of the slopes shows that PiZZ serum increasingly inhibited NE and PR3 activities as the molar ratio of serum A1AT to enzyme increased. However, PiZZ serum did not fully inactivate NE or PR3 even when the serum A1AT was in a molar excess and the residual activities were 35.7 ± 0.5% for NE and 44.2 ± 0.8% for PR3. Unlike the PiZZ serum experiments using SlaaapN as the substrate (Figure 3.4), no enhancement of enzyme activity (above that measured with free enzyme) was observed with this substrate.

Figure 3.15- Inhibition of NE and PR3 with PiZZ serum (MSaapvN)

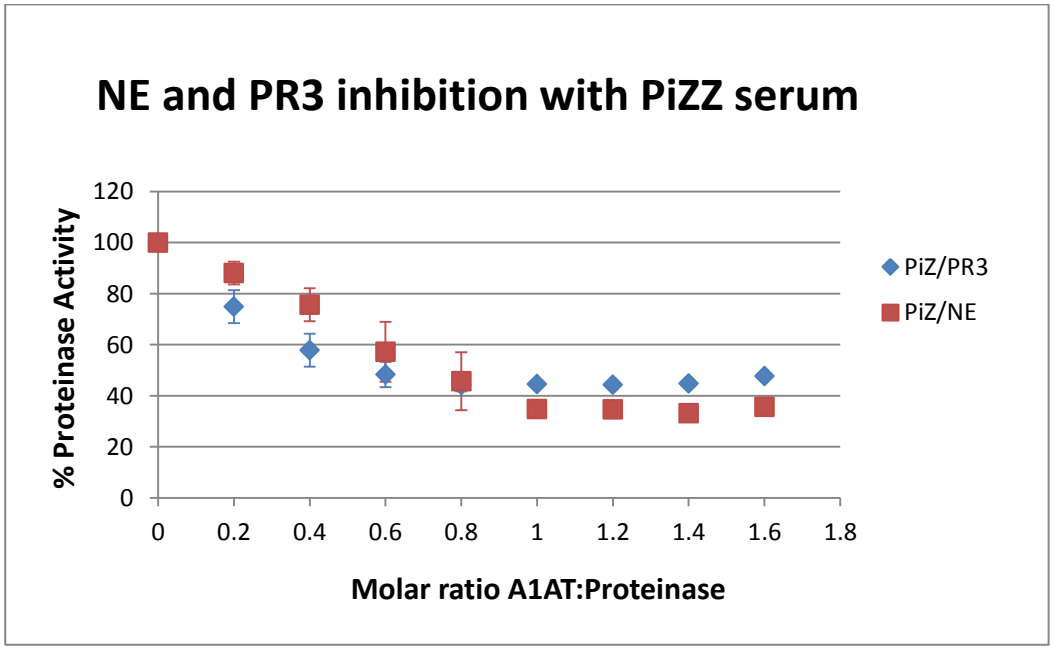

Figure 3.15: Inhibition of NE and PR3 activities by PiZZ serum with MSaapvN as the substrate. Individual experiments were performed using a single proteinase and the data for NE and PR3 are presented together for comparison. The points show the mean of 3 experiments ± SEM.

3.3.3.9 Summary of MSaapvN assays

Table 3.3 summarises the residual NE and PR3 activities observed when the different serum samples were used and the A1AT was in a molar excess.

Table 3.3- Residual NE and PR3 activities observed when serum samples from different A1AT genotypes were used and the A1AT was in a molar excess (MSaapvN)

A1AT genotype	**Residual NE activity observed when A1AT was in a molar excess.**	**Residual PR3 activity observed when A1AT was in a molar excess.**
PiMM	5.4 ± 1.1%	7.7 ± 0.8%
PiSZ	13.6 ± 1.2%	18.2 ± 0.7%
PiFZ	56.4 ± 0.5%	36.8 ± 0.3%
PiFM	41.9 ± 1.6%	9.6 ± 0.6%
PiIZ	47.8 ± 1.4%	19.5 ± 1.0%
PiZZ	35.7 ± 0.5%	44.2 ± 0.8%

3.4 Discussion

The NE inhibition assays using SlaaapN as the substrate presented in this Chapter have given differing results. As shown in Figure 3.1, pure A1AT completely inactivated NE when the molar ratio of A1AT:NE exceeded 1:1, as expected. However, this was not the case with PiMM serum which increasingly inhibited NE activity as the molar ratio of A1AT:NE approached 1:1, but when A1AT was in a molar excess of NE, 17.1 ± 0.1% residual NE activity was still observed. This suggests that PiMM serum could not

completely inactivate NE even when the main inhibitor A1AT was in a molar excess. When partially A1AT deficient (PiSZ) serum was used to inhibit NE, the activity of NE decreased initially as the molar ratio of A1AT:NE increased (Figure 3.2). However, NE activity was inhibited less effectively than with PiMM serum, and when A1AT was in a molar excess, 60.6 ± 1.0% NE activity remained. Figure 3.3 shows that the results were similar when PiFZ serum was used, with 56.0 ± 0.5% of the NE activity remaining. These results indicate a failure of serum to completely inactivate NE and most likely reflect ongoing activity of NE bound to A2M. Binding of NE to A2M does not involve direct interaction with the enzyme's active site, and animal studies have shown that A2M:NE complexes retain proteolytic potential whereas A1AT:NE complexes do not [201]. The results obtained could have clinical significance. Indeed, active A2M:NE complexes have been implicated in the pathogenesis of emphysema in animal models [201]. Other studies have shown that A2M:NE complexes may also play a role in the adult respiratory distress syndrome in humans [253], and the degradation of cartilage matrix in rheumatoid arthritis [254]. These concepts are explored further in Chapters 4 and 5.

The NE inhibition assays using SlaaapN as the substrate and PiZZ serum as the inhibitor gave different results to those described above. Figure 3.4 shows that PiZZ serum initially inhibited NE activity, but as the ratio of A1AT:NE increased and greater volumes of serum were added, enhanced activity of NE was detected (>100% of that seen with free NE). This result was consistently obtained and was believed to be correct for several reasons. Firstly, the result could not be due to an artefact relating to the inherent colour of the serum interfering with the OD measurements because the control wells contained the same volume of diluted serum. Secondly, for the same reasons, the results could not be due to free NE activity in the serum samples. Thirdly, Figure 3.6 shows that the effect was not

due to the activity of another class of proteinase, since the same effect was seen in the presence of inhibitors of MMPs and cysteine proteinases. In addition, Figure 3.7 shows that the effect was not due to experimental changes in pH, since the same effect was seen when the experiment was performed at a physiological pH of 7.4. Overall, the enhanced activity is likely to result from NE bound to A2M. Previous authors have reported enhanced activity of NE bound to A2M compared to free NE when using small peptide substrates such as SlaaapN [255]. These interactions between NE and A2M are discussed further in Chapter 4.

PR3 activity was also not completely inhibited by PiMM serum (Figure 3.10) even when A1AT was in a molar excess (7.7 ± 0.8% of PR3 activity remained), whereas pure A1AT completely inactivated PR3 as expected. When PiSZ serum was used as an inhibitor of PR3, Figure 3.11 shows that initially its activity decreased as the molar ratio of A1AT:PR3 increased, but total inhibition of PR3 activity was less efficient than with PiMM serum, and 18.2 ± 0.7% residual PR3 activity was observed when the A1AT was in a molar excess. When PiZZ serum was used, the residual activity of PR3 was 44.2 ± 0.8% (Figure 3.15). This pattern of results was similar to that of NE, and again most likely reflects ongoing activity of PR3 bound to A2M in the serum samples. The proteolytic activity of PR3 complexes with A2M has not been explored previously, but may have clinical significance particularly since PR3 has a lower Kass for M type A1AT compared to NE [117]. Therefore in situations where the concentration of A1AT is inadequate to inhibit both proteinases, NE would be preferentially inhibited by A1AT, and PR3 may be more likely to form a complex with A2M. This scenario could be even more relevant in situations where A1AT is deficient or dysfunctional.

When PiFZ, PiFM or PiIZ sera (Figures 3.12, 3.13 and 3.14 respectively) were used to inhibit NSP activities, the baseline activities of NE (when the A1AT was in a molar excess) were greater than that of PR3. The partitioning of proteinases between their inhibitors is influenced by the differences in their rates of association and their concentrations. The association rate constants of A1AT variants and NSPs are discussed further in Chapter 6. However, these factors are unlikely to fully explain the differences observed because the residual NE activities when PiFZ, PiFM or PiIZ sera were used were greater than that observed with PiZZ serum, in addition to being greater than PR3 activities. The exact reasons for these findings remain uncertain, but several hypotheses will be discussed. Firstly, it is possible that the A1AT:NE complexes formed by F or I variant A1AT can dissociate in the presence of A2M resulting in the transfer of the enzyme from A1AT to A2M. This phenomenon has previously been described by Ohlsson [256] using trypsin in dog serum, and Meyer *et al* [257] using PPE in the presence of the two inhibitors. Secondly, it could be hypothesized that F or I variant A1AT may be proteolytically inactivated to some degree by NE during the interaction (the "substrate pathway"), resulting in inactivated A1AT and free NE (which could then bind to A2M). Further studies into the function of F and I variants of A1AT and the stability of their complexes with NE are therefore necessary.

The inhibition assays of NE with PiZZ serum (Figures 3.4 and 3.15) demonstrated differing interactions between enzymes and their substrates. When SlaaapN was used as the substrate, an enhancement of NE activity was observed in the presence of higher volumes of serum, consistent with enhanced activity of NE bound to A2M compared to

activity of free NE. However, this enhancement of NE activity was not seen when MSaapvN was used as the substrate. Twumasi *et al* [255] previously demonstrated that the degree of activation of NE bound to A2M varied depending on the synthetic peptide substrate used, and varied from little or no activation to 15-fold activation. Interestingly, they also showed that the activity of PPE towards SlaaapN was inhibited by human A2M, thus highlighting species differences in enzyme inhibition and kinetics towards synthetic peptide substrates, and reinforcing the observation that results from animal studies should be interpreted with caution when considering human disease.

The partitioning of NSPs between their serum inhibitors is dependent on several factors including local concentrations of inhibitors and their functional activities. Mutant variants of A1AT have different rates of association with NSPs (as discussed further in Chapter 6) which affect their anti-proteinase capabilities. In addition, mutant variants of A1AT are susceptible to conformational transitions which may further reduce the levels of functional proteinase inhibitor *in vivo*. For example, the formation of loop sheet polymers reduces the anti-proteinase capabilities of mutant variants of A1AT beyond that expected for the reduced concentration and Kass. Other conformational transitions of mutant variants of A1AT which may affect their anti-proteinase function include the formation of unstable intermediates and latent A1AT (as shown in Figure 1.6), or cleaved A1AT following its interaction with NSPs. To gain further insight into the relative importance of these factors affecting the anti-proteinase capacity of A1AT, PiMZ serum could be studied in future experiments. In PiMZ heterozygotes, the serum A1AT concentration is within the same range as that for PiFZ and PiIZ heterozygotes, but the M variant is less susceptible to conformational transitions. Therefore, studying the partitioning of NSPs in PiMZ serum

would assist in determining the relative importance of A1AT concentration against other factors (described above) that influence its anti-proteinase capability.

This Chapter has studied how NE and PR3 partition between their two serum inhibitors in the presence of different A1AT variants, and has suggested that proteinases bound to A2M are not inactivated and retain their proteolytic potential. Further studies to consolidate these findings are discussed in Chapter 4 when pure A1AT and A2M are used in equivalent concentrations to those found in serum samples with different A1AT genotypes. The physiological relevance of active proteinases bound to A2M is then explored in Chapter 5 when elastin is used as a biologically relevant substrate.

4 Interactions of serine proteinases with A2M

4.1 Introduction

Results from Chapter 3 have suggested that both NE and PR3 retain their proteolytic activities towards synthetic peptide substrates when bound to A2M. When NE or PR3 are added to serum, they partition between the two serum inhibitors A1AT and A2M depending on the local concentrations of inhibitors and their association rate constants as shown in Figure 4.1. In addition, the susceptibility of mutant variants of A1AT to form polymers or other conformations may further influence partitioning.

The aim of this Chapter is to establish whether the residual activities of NE or PR3 observed in Chapter 3 are due to binding to A2M, and not due to other features of the serum. This will be determined by using mixtures of pure A1AT and A2M in the concentrations found in serum samples, and comparing the results with those obtained in Chapter 3.

Figure 4.1- Partitioning of NSPs between their serum inhibitors

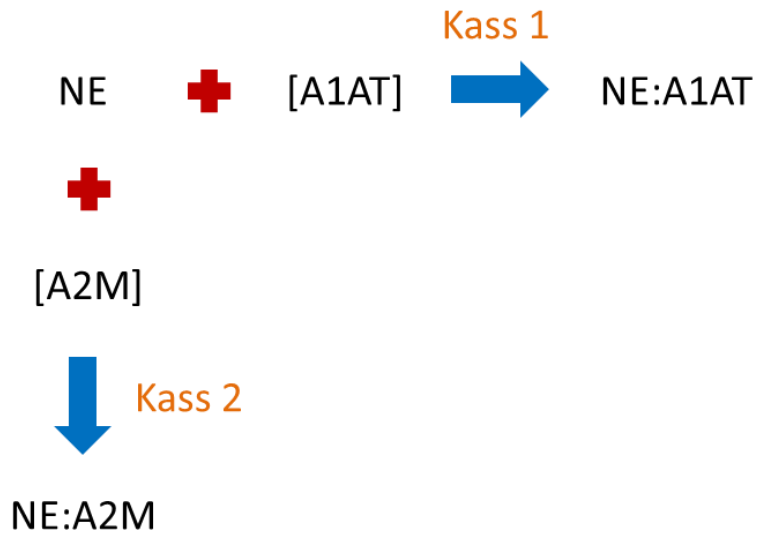

Figure 4.1: When NE is released in the presence of serum, it will partition between the serum inhibitors A1AT and A2M. The amounts of NE:A1AT or NE:A2M complexes formed will be dependent on the concentrations of these inhibitors and their association rate constants (Kass). The same applies to PR3.

4.2 Methods

4.2.1 Inhibition of pure proteinases with pure A2M

Pure A2M (Sigma, UK) was diluted in NE assay buffer at a concentration of 1mg/ml or 1.38µM. This stock A2M was then aliquoted, rapidly frozen with liquid nitrogen and stored at -70ºC until required. Pure NE or PR3 were diluted to an active concentration of 1.38µM, and 10µL of proteinase was added per well to a 96 well plate in triplicate sets with appropriate controls. Increasing volumes of A2M were added to each triplicate set, and all wells were made up to a total volume of 110µL with buffer. For NE experiments, NE assay buffer was used. For PR3 experiments, NSP assay buffer was used. The plate

was covered and incubated with gentle shaking at 37ºC for 20 minutes to allow the proteinases to form complexes with the A2M. The NE experiments were performed with both SlaaapN (100µL of 1mg/ml) and MSaapvN (150µL of 0.2mg/ml) as substrates. The PR3 experiments were performed with MSaapvN only. The absorbance at 410nm was read at 5 minute intervals up to 60 minutes using a Biotek Synergy HT plate reader at 37ºC. Mean results were taken of all triplicate sets and control values were subtracted. Inhibition slopes were constructed by plotting the percentage of remaining enzyme activity against the molar ratio of A2M:proteinase.

4.2.2 A2M ELISA

The A2M concentrations of serum samples were determined using a commercially available A2M ELISA kit (Universal Biologicals Cambridge, UK). Serum samples with the following A1AT genotypes were used; PiMM, PiMZ, PiFZ, PiFM and PiZZ. The ELISA used a quantitative competitive sandwich enzyme immunoassay technique to measure A2M and was performed at room temperature. A polyclonal antibody specific for human A2M was pre-coated onto a 96 well microplate. Serum samples were diluted 1 in 400 in the diluent provided. Standards of pure human A2M were prepared by performing serial dilutions of the top standard (40µg/ml). Standards and samples (25µL) were added to the 96-well plate in triplicate, with the diluent being used as a blank for the assay. Immediately following this step, 25µL of biotinylated A2M was added to each well and mixed gently with the standard or sample. The plate was then covered and incubated for two hours. After incubation, the plate was washed six times with 300µL per well of the wash buffer provided using a labtech LT-3500 microplate washer. Next, 50µL of streptavidin-peroxidase conjugate was added to each well followed by a 30 minute incubation. The plate was washed as described above, and then 50µL of TMB substrate

was added to each well. The plate was incubated in the dark until a colour change occurred (approximately 10 minutes) and then 50µL of the stop solution (0.5N hydrochloric acid) was added to each well. The colour then changed from blue to yellow. The absorbance was read using a Biotek Synergy HT plate reader at 450nm with 570nm wavelength correction. The mean of the triplicate sets was calculated and a standard curve generated. The sample concentrations were determined from the standard curve and multiplied by the dilution factor. The minimum detectable level of A2M was 1µg/ml and the intra- and inter- assay CVs were 5% and 7.2% respectively.

4.2.3 Inhibition of proteinases with mixtures of pure A2M and pure A1AT

Using the values obtained from the A2M and A1AT ELISAs (section 2.6.1.2) for serum samples, mixtures of pure A2M and pure M variant A1AT were created in the same concentrations as would be found in some of the serum samples from Chapter 3 (PiMM, PiFZ and PiZZ). NE or PR3 were diluted to an active concentration of 1.5µM. The mixtures of pure inhibitors were diluted so that they contained 1.5µM of active A1AT. NE or PR3 (10µL) was added to a 96-well plate, and increasing volumes of the mixtures were added to the proteinases with appropriate controls. The total well volume was then made up to 110µL with buffer. For the NE experiments, NE assay buffer was used and for the PR3 experiments, NSP assay buffer was used. The proteinase and inhibitors mixtures were then incubated for 30 minutes with gentle shaking at 37ºC, followed by the addition of the substrate. The NE experiments were performed using either SlaaapN (100µL of 1mg/ml) or MSaapvN (150µL of 0.2mg/ml) as the substrate, and the PR3 experiments were performed using MSaapvN. The NE experiments using MSaapvN as the substrate were performed using NE and A1AT at active concentrations of 0.1µM. The absorbance at 410nm was read at 5 minute intervals up to 60 minutes using a Biotek Synergy HT plate

reader at 37ºC. Control values were subtracted and inhibition slopes were constructed by plotting the percentage of remaining enzyme activity against the molar ratio of A1AT:proteinase.

In addition, the above experiments were repeated using Z variant A1AT purified from human plasma instead of pure M A1AT. The pure Z A1AT was a kind gift from the research group of Professor Lomas at the University of Cambridge, UK, and was purified as described previously [258]. The Z A1AT was active site titrated against NE as described in section 2.6 and was found to be 54% active. Active concentrations of Z A1AT were used in these experiments.

Purified variants of A1AT other than M and Z (for example, S or F variants) were not available for these experiments due to both time constraints and lack of availability of sufficient volumes of plasma for the purification process. Therefore, the experiments described in this Chapter were predominantly performed to assess the effects of altering the relative concentrations of A1AT and A2M on the partitioning of NSPs. The limitations of this approach are discussed further in section 4.4 (Discussion).

4.3 Results

4.3.1 Inhibition of pure proteinases with pure A2M

The relationship between NE activity and increasing volumes of pure A2M using SlaaapN as the substrate is shown in Figure 4.2. These results demonstrate that NE showed enhanced activity (compared to free NE) as the concentration of A2M increased. When MSaapvN was used as the substrate, A2M did not inhibit NE or PR3 activities up to a molar ratio of 1.4:1, but no enhancement of proteinase activity was observed. These results are shown in Figure 4.3.

Figure 4.2-"Inhibition" of NE with pure A2M (SlaaapN)

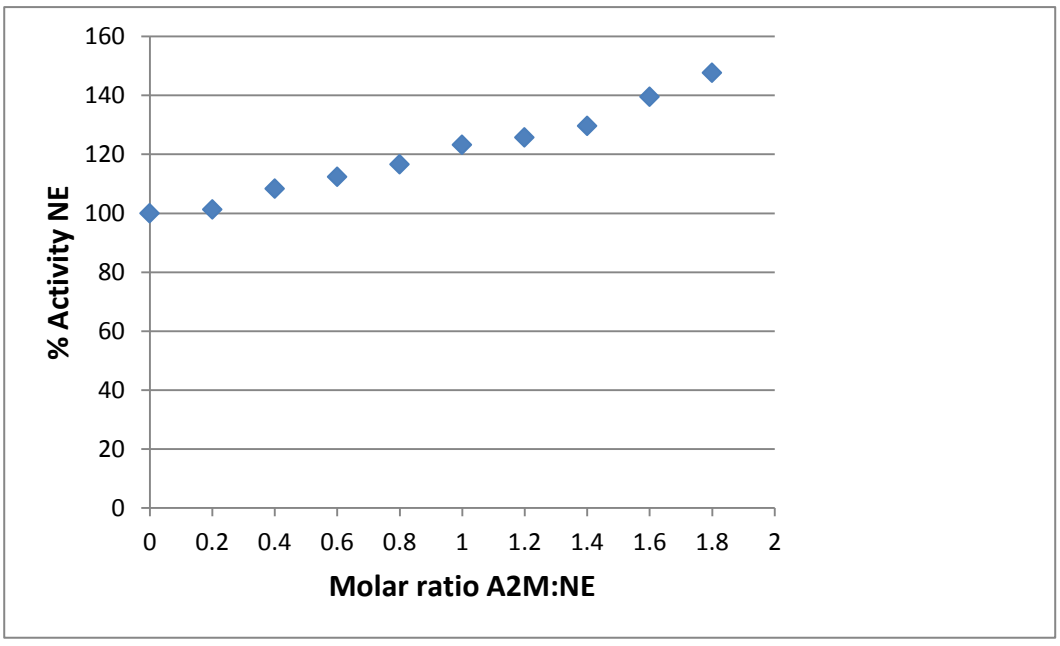

Figure 4.2: The relationship between NE activity and increasing amounts of A2M using SlaaapN as the substrate. The points show the mean values of 3 experiments and the SEM falls within the points plotted.

Figure 4.3- “Inhibition” of NE and PR3 with pure A2M (MSaapvN)

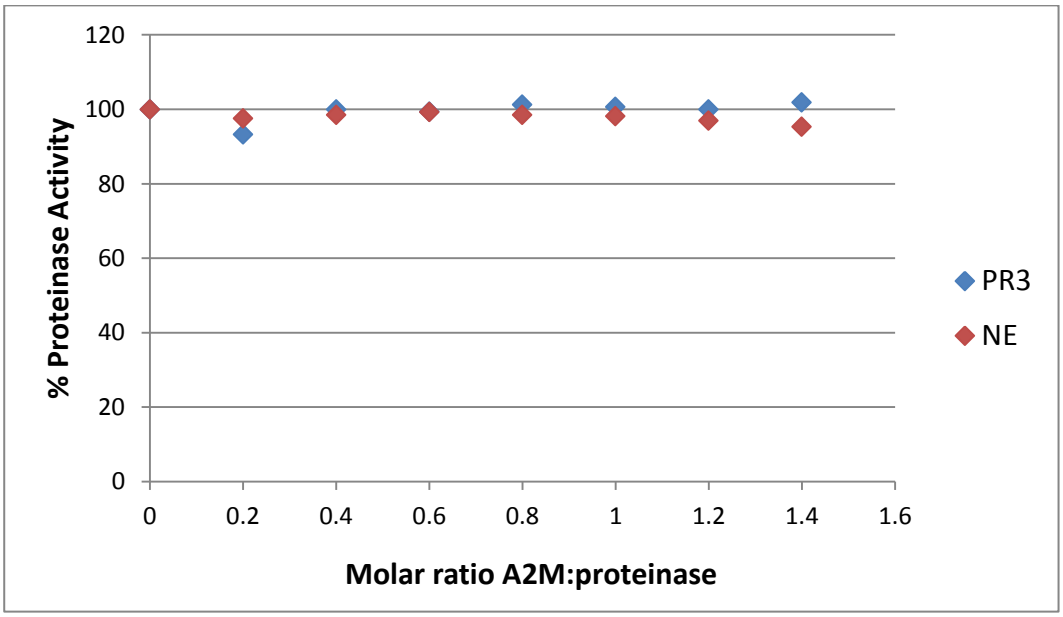

Figure 4.3: NE and PR3 activities in the presence of increasing amounts of A2M using MSaapvN as the substrate. The results from individual experiments for each proteinase are shown, but data for NE and PR3 are shown together for comparison.

4.3.2 A2M ELISA

The serum A2M concentrations as measured by ELISA are shown in Table 4.1. The A1AT concentrations of these serum samples are also shown. A1AT was measured by ELISA as described in section 2.6.1.2.

Table 4.1- A2M concentrations in serum samples of different A1AT genotypes

A1AT genotype	Serum A1AT concentration (µM)	Serum A2M concentration (g/L)
PiMM	30.3	2.198 (3.0µM)
PiMZ	19.8	1.827 (2.5µM)
PiFZ	21.6	1.927 (2.7µM)
PiFM	35.2	1.042 (1.4µM)
PiZZ (1)	4.3	1.260 (1.7µM)
PiZZ (2)	4.9	2.089 (2.9µM)

4.3.3 Inhibition of proteinases with mixtures of pure A2M and pure A1AT

4.3.3.1 Inhibition of NE with mixtures of pure A2M and pure M A1AT

The inhibition slopes of NE activity using mixtures of pure A2M and pure M variant A1AT equivalent to the concentrations found in PiMM, PiFZ and PiZZ sera are shown in Figure 4.4, using SlaaapN as the substrate. The results show that NE was increasingly inhibited as the molar ratio of A1AT:NE increased up to a ratio of 1:1. However, NE activity was not completely inhibited in the presence of A2M, and the residual NE activity was greater with increasing proportional concentrations of A2M. Therefore, the residual NE activity was greatest when using the mixture of proteins equivalent to the relative proportions found in PiZZ serum (15.6% residual activity, Graph C), and least when using the mixture of proteins in the proportions found in PiMM serum (3.5% residual activity, Graph A). The residual NE activity observed when the A1AT was in a molar excess was intermediate when using the mixture of proteins equivalent to the proportions found in PiFZ serum (8.9% residual activity, Graph B).

The results of similar experiments using MSaapvN as the substrate are shown in Figure 4.5 and for comparison the inhibition slope of NE activity with pure M A1AT alone is also shown. These results show that NE activity was fully inhibited by pure M A1AT alone (Graph D), as expected. However, NE activity was not fully inhibited when A2M was present. The residual NE activity observed when A1AT was in a molar excess was greatest when using the mixture of proteins in the proportions found in PiZZ serum (4.5% residual activity, Graph C), and least when using the mixture of proteins in the proportions found in PiMM serum (0.9% residual activity, Graph A). The residual NE activity was intermediate when using the mixture of proteins equivalent to the proportions found in PiFZ serum (1.7% residual activity, Graph B).

Figure 4.4 (A-C)- Inhibition of NE activity with mixtures of A2M and M A1AT in proportions equivalent to PiMM, PiFZ and PiZZ sera (SlaaapN)

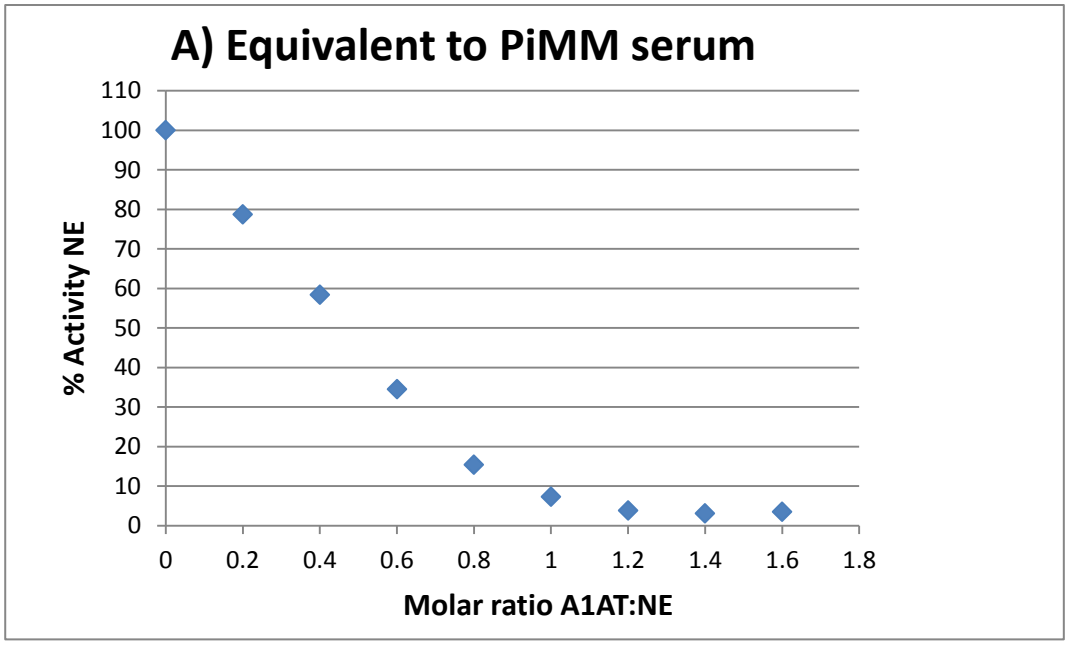

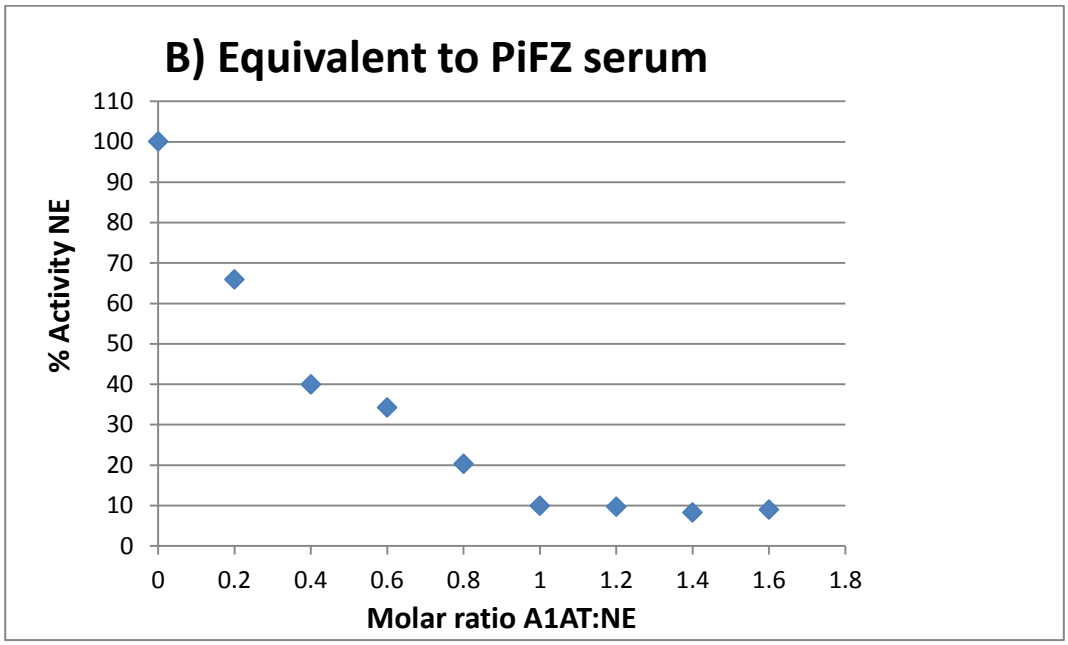

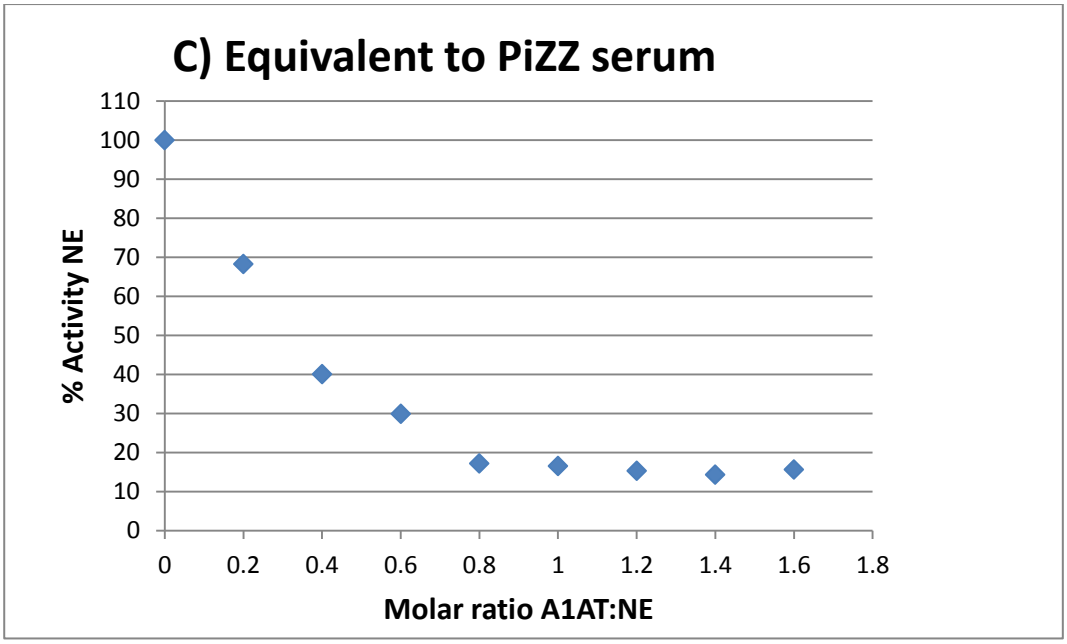

Figure 4.4 (A-C): Inhibition of NE activity using mixtures of M variant A1AT and A2M equivalent to proportions found in PiMM, PiFZ and PiZZ sera. SlaaapN was used as the substrate for these experiments. The results from single experiments are shown.

Figure 4.5 (A-D)- Inhibition of NE activity with mixtures of A2M and M A1AT in proportions equivalent to PiMM, PiFZ and PiZZ sera, and with pure M A1AT (MSaapvN)

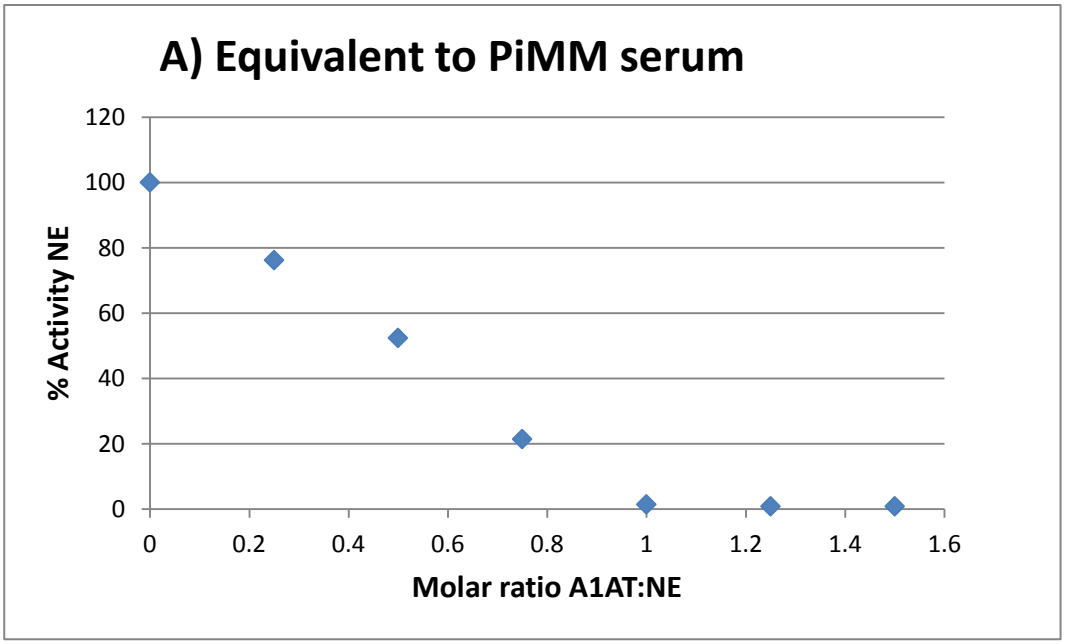

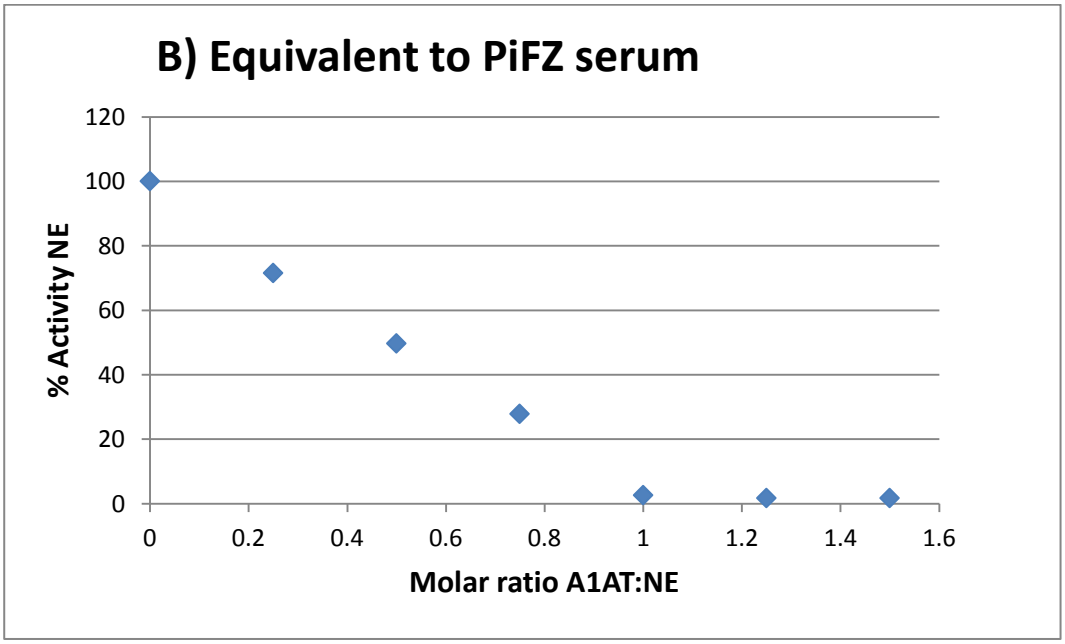

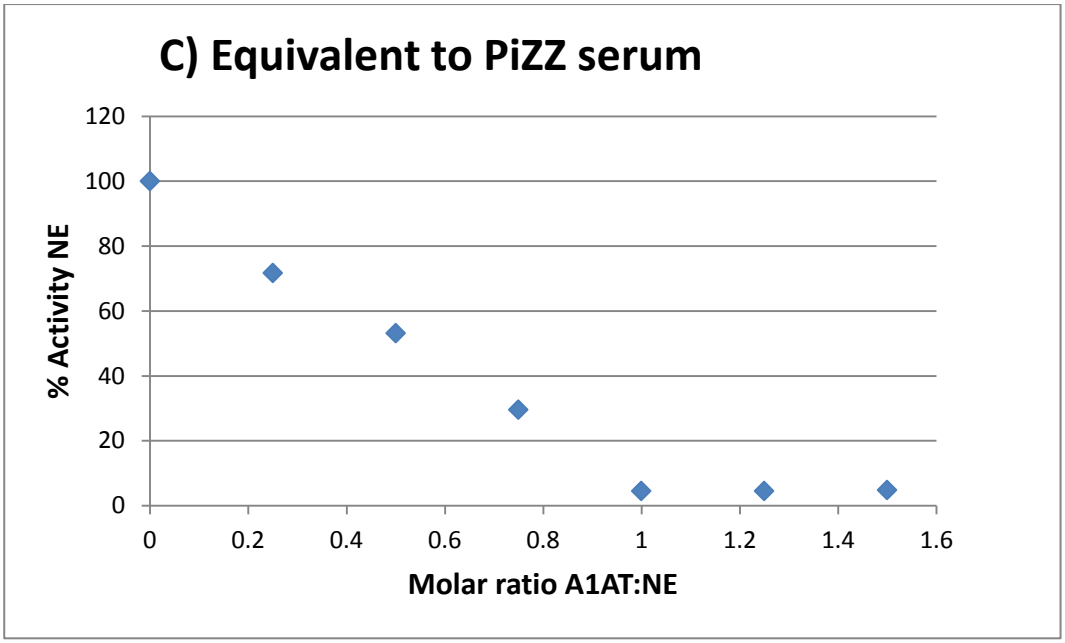

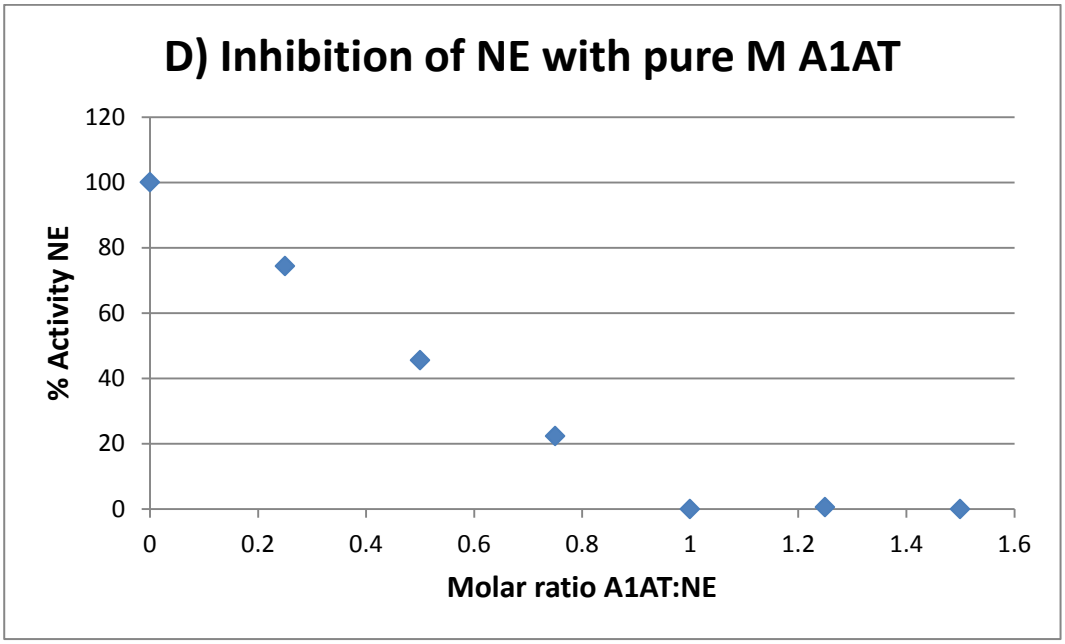

Figure 4.5 (A-D): Inhibition of NE activity using mixtures of M variant A1AT and A2M equivalent to proportions found in PiMM, PiFZ and PiZZ sera. Graph D shows inhibition of NE activity with pure M A1AT. MSaapvN was used as the substrate for these experiments. The results from single experiments are shown. The residual activities of NE when A1AT was in a molar excess were as follows; Graph A 0.9%, Graph B 1.7%, Graph C 4.5% and Graph D 0%.

4.3.3.2 Inhibition of PR3 with mixtures of pure A2M and pure M A1AT

The inhibition slopes of PR3 activity using mixtures of pure A2M and pure M variant A1AT equivalent to proportions found in PiMM, PiFZ and PiZZ sera are shown in Figure 4.6, and MSaapvN was used as the substrate for these experiments. The results show that PR3 activity was increasingly inhibited as the molar ratio of A1AT:PR3 increased up to 1:1, but when A1AT was in a molar excess, PR3 activity was not fully inhibited in the presence of A2M. The residual PR3 activity observed when the A1AT was in a molar excess was similar for the mixtures of proteins equivalent to the proportions found in PiMM (Graph A), PiFZ (Graph B) and PiZZ (Graph C) sera at around 5%.

Figure 4.6 (A-C)- Inhibition of PR3 activity with mixtures of A2M and M A1AT in proportions equivalent to PiMM, PiFZ and PiZZ sera (MSaapvN)

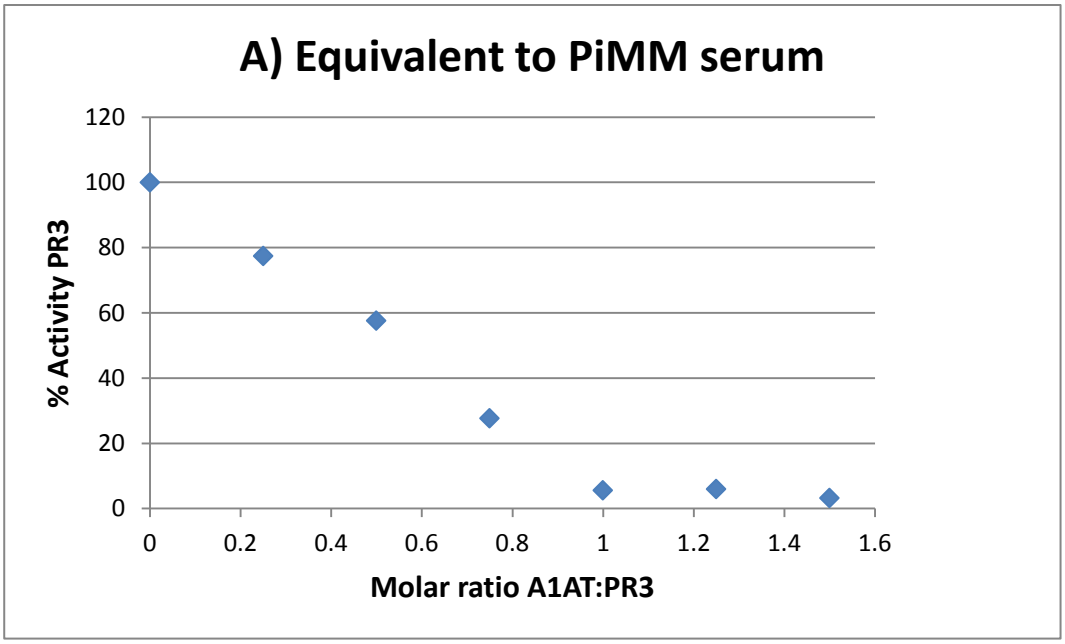

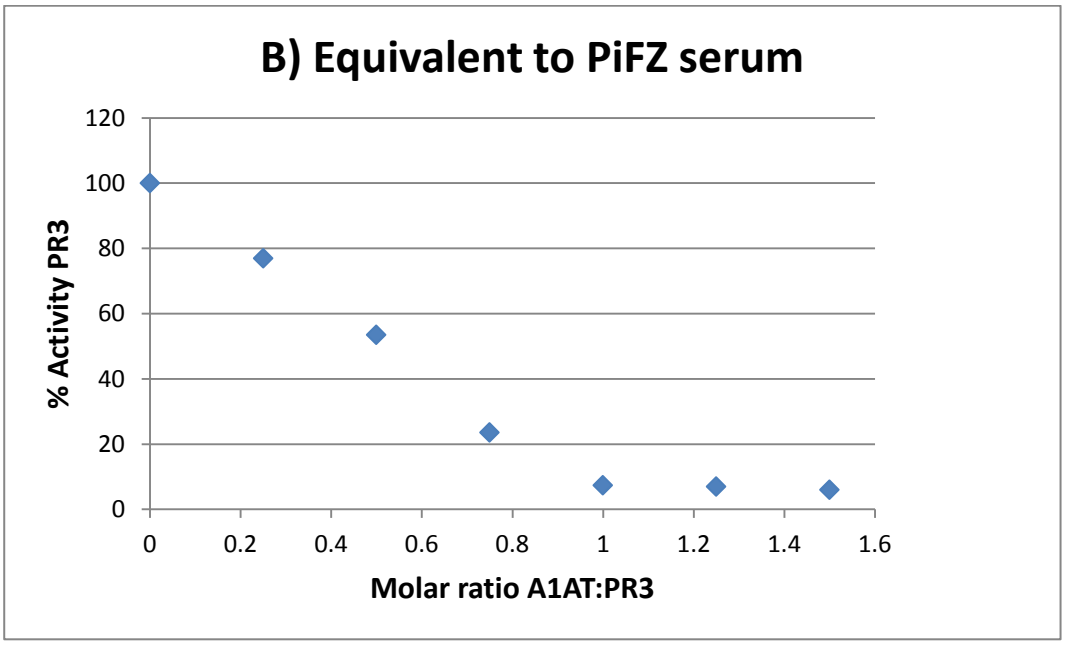

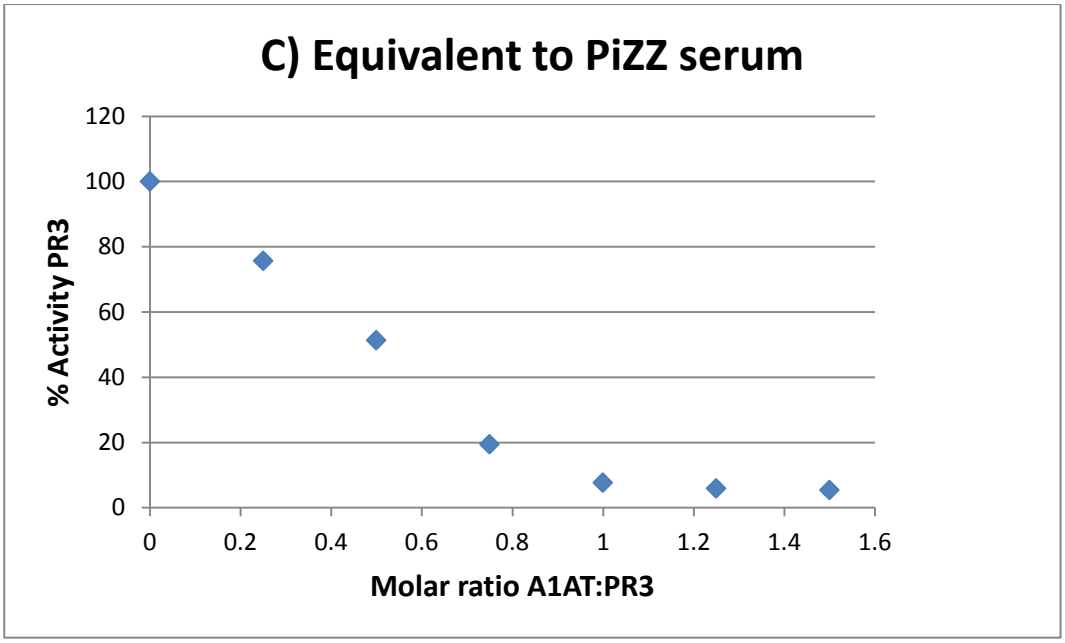

Figure 4.6 (A-C): Inhibition of PR3 activity using mixtures of M variant A1AT and A2M equivalent to proportions found in PiMM, PiFZ and PiZZ sera. MSaapvN was used as the substrate for these experiments. The results from single experiments are shown. The residual activities of PR3 when A1AT was in molar excess were similar in Graphs A, B and C at around 5%.

4.3.3.3 Inhibition of NE with mixtures of pure A2M and pure Z A1AT

The inhibition slopes of NE activity with mixtures of pure A2M and pure Z variant A1AT equivalent to the proportions of inhibitors found in PiMM, PiFZ and PiZZ sera are shown in Figure 4.7 and SlaaapN was used as the substrate for these experiments. The results show that NE activity was increasingly inhibited as the molar ratio of Z A1AT:NE increased up to 1:1, but again, NE was not fully inhibited in the presence of A2M. The residual NE activity when the Z A1AT was in a molar excess was greater as the concentration of A2M increased. Therefore, the mixture of inhibitors equivalent to the proportions found in PiZZ serum had the greatest residual NE activity (18.3%, Graph C) and the mixture of inhibitors equivalent to the proportions found in PiMM serum had the least (4.9%, Graph A), with the mixture of inhibitors equivalent to proportions found in PiFZ serum being intermediate (9.0%, Graph B). The experiment using pure Z A1AT and pure A2M in the proportions equivalent to PiZZ serum did not replicate the earlier results using serum (Figure 3.4) and no enhancement of NE activity (above that of free NE) was observed, as had been observed with PiZZ serum.

Figure 4.7 (A-C)- Inhibition of NE activity with mixtures of A2M and Z A1AT in proportions equivalent to PiMM, PiFZ and PiZZ sera (SlaaapN)

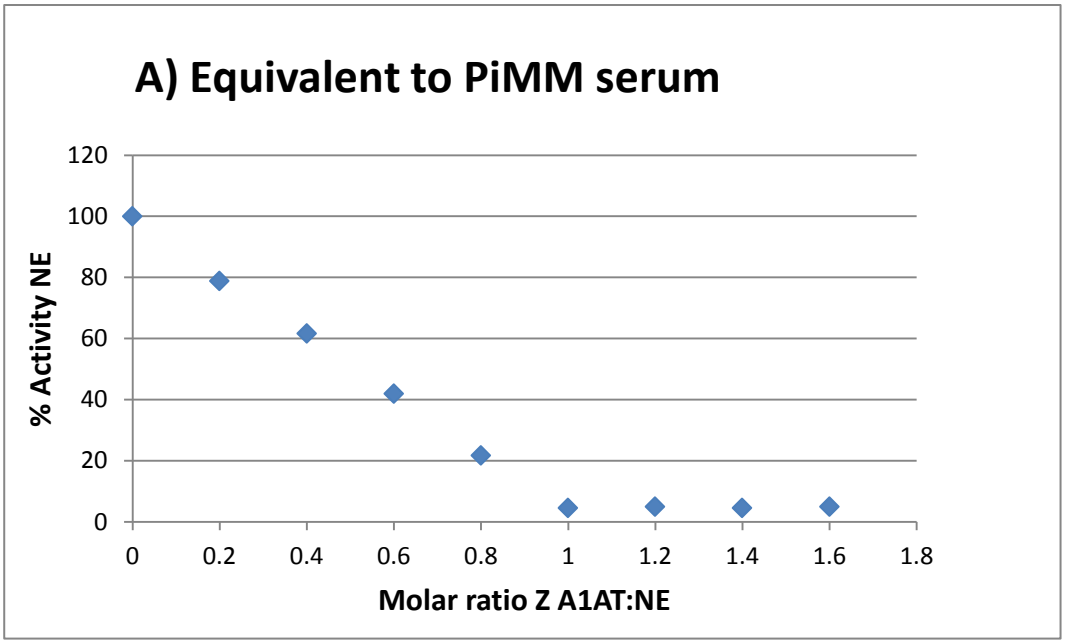

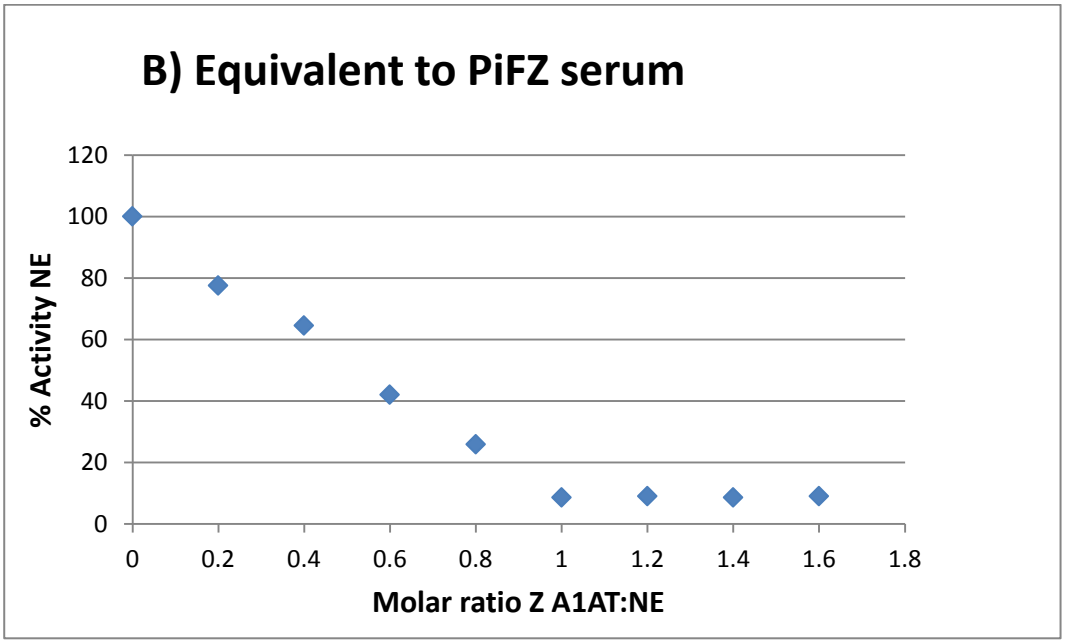

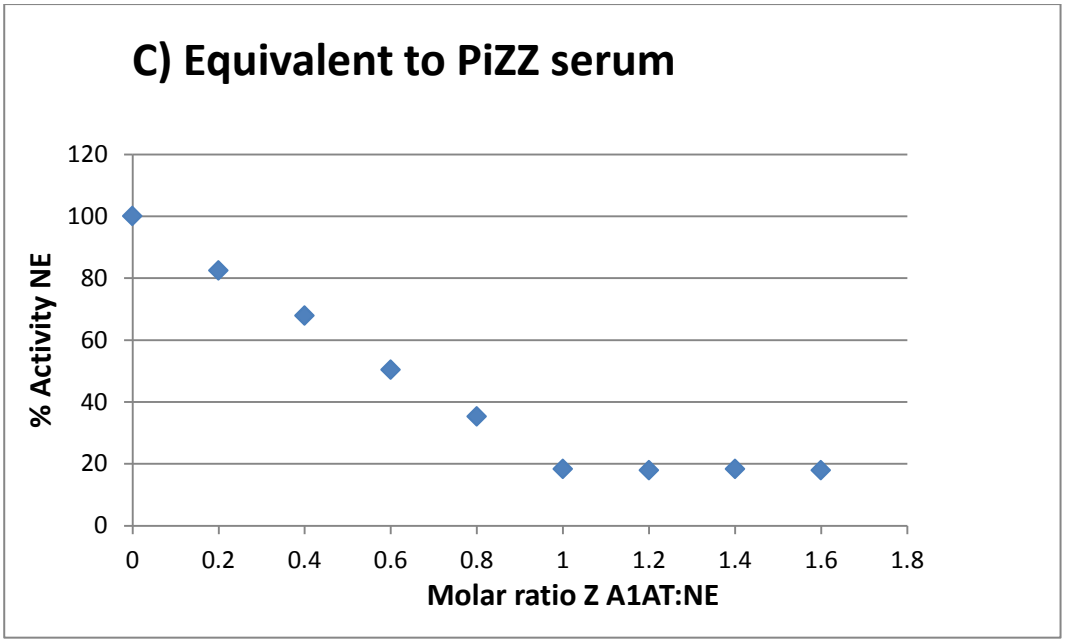

Figure 4.7 (A-C): Inhibition of NE activity using mixtures of Z variant A1AT and A2M in proportions equivalent to those found in PiMM, PiFZ and PiZZ sera. SlaaapN was used as the substrate and results from single experiments are shown. The baseline activities of NE when Z A1AT was in a molar excess were as follows; Graph A 4.9%, Graph B 9.0% and Graph C 18.3%.

4.3.3.4 Inhibition of PR3 with mixtures of pure A2M and pure Z A1AT

The inhibition slopes of PR3 activity using mixtures of pure A2M and pure Z variant A1AT equivalent to the proportions of inhibitors found in PiMM, PiFZ and PiZZ sera are shown in Figure 4.8. MSaapvN was used as the substrate for these experiments. The residual activities of PR3 when Z A1AT was in molar excess were similar in each experiment at around 5% (Figure 4.8, Graphs A-C). In a further experiment where A2M was used at twice the concentration of that found in PiZZ serum, the baseline activity of PR3 remained at around 5% (data not shown).

Figure 4.8 (A-C)- Inhibition of PR3 activity with mixtures of A2M and Z A1AT in proportions equivalent to PiMM, PiFZ and PiZZ sera (MSaapvN)

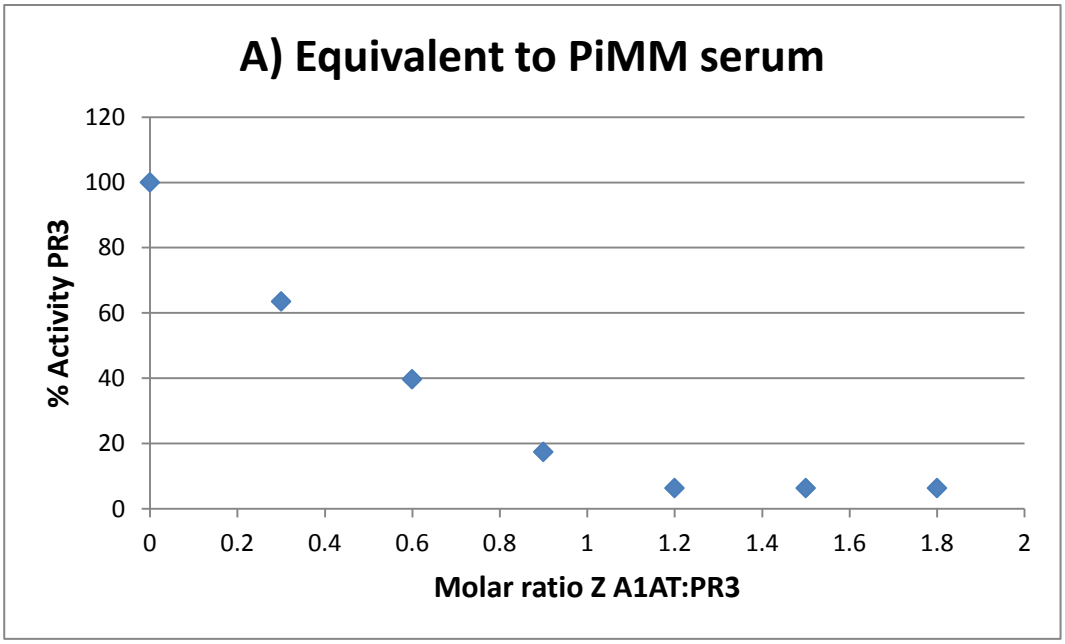

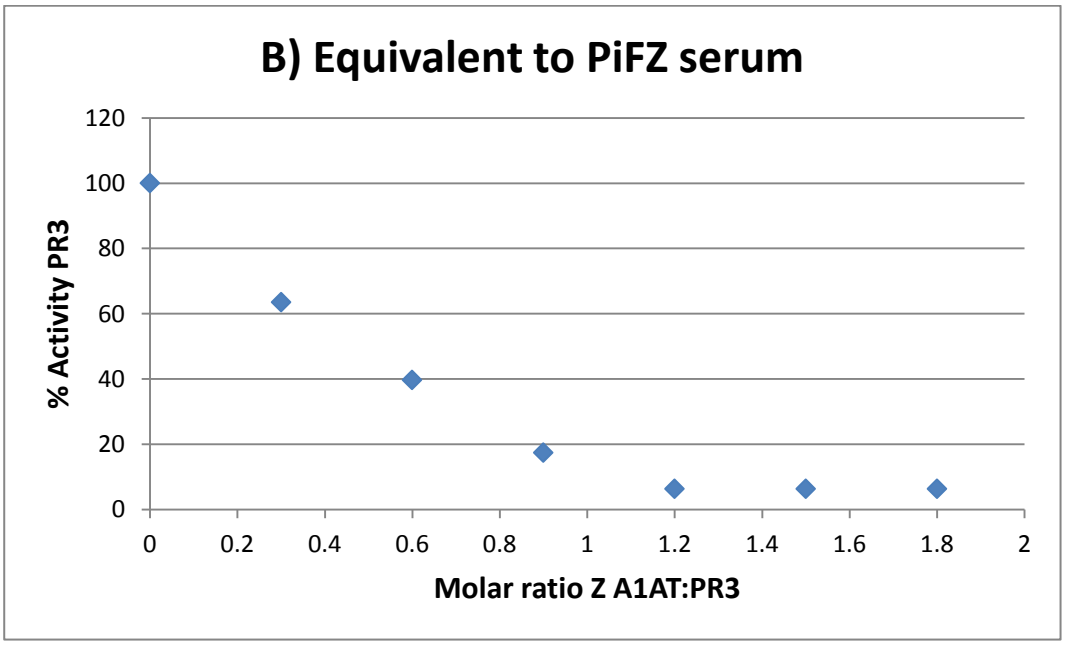

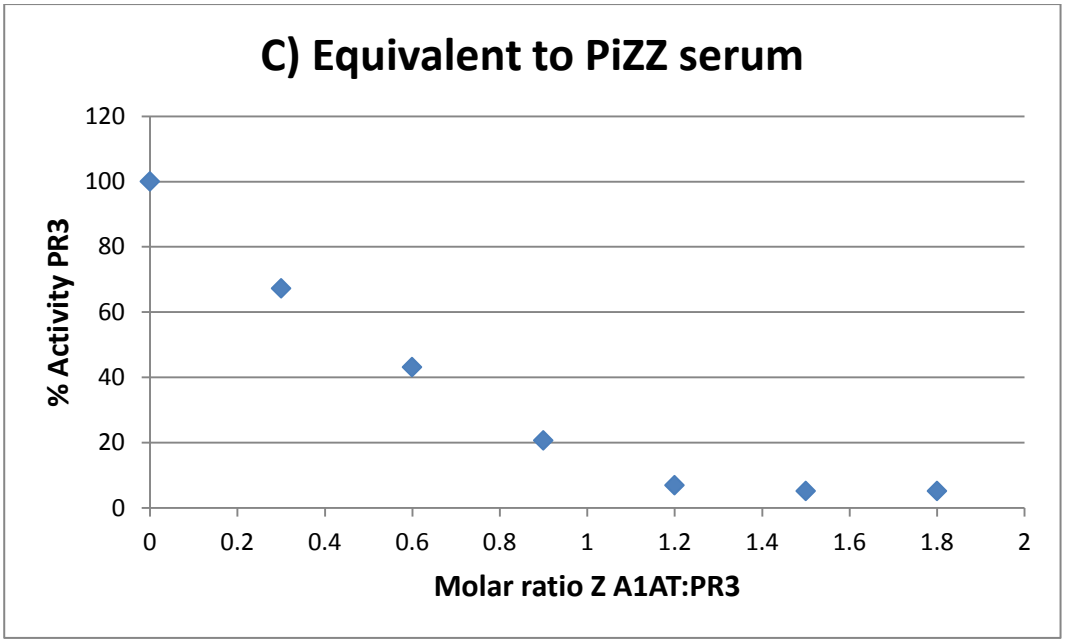

Figure 4.8 (A-C): Inhibition of PR3 activity using mixtures of Z variant A1AT and A2M in proportions equivalent to those found in PiMM, PiFZ and PiZZ sera. MSaapvN was used as the substrate and results from single experiments are shown. The residual activities of PR3 when Z A1AT was in molar excess were similar in Graphs A, B and C at around 5%.

4.4 Discussion

The results shown in Figure 4.2 demonstrate that when SlaaapN was used as the substrate, NE showed enhanced activity as the concentration of A2M increased. This suggests that NE bound to A2M has greater activity than free NE in the presence of this substrate and explains the results obtained in Chapter 3 using PiZZ serum (Figure 3.4), which showed increasing NE activity as the volume of serum increased (and hence the amount of A2M increased). Twumasi *et al* [255] found that maximum activation of NE towards a synthetic substrate occurred when two molecules of NE were complexed to A2M, which may occur when the local concentration of NE is high. They reported that the Km, which reflects the

affinity of the enzyme for the substrate, was not affected by A2M despite the marked enhancement in the catalytic efficiency of the enzyme as measured by Kcat. They hypothesized that the conformational change in A2M during entrapment of the enzyme uncovers a hydrophobic cavity which, in conjunction with a positively charged group, orientates the substrate into a position which is more favourable for the enzyme. Figure 4.3 demonstrates that when MSaapvN was used as the substrate, A2M did not reduce the activities of NE or PR3 up to a molar ratio of 1.4:1. However, no enhancement of proteinase activity was seen when this substrate was used, at least within the concentrations of A2M studied here, highlighting that differences exist in how enzymes interact with different substrates. Potentially, A2M may function predominantly to remove proteinases from the circulatory system [200], rather than inhibiting their activity.

The NE inhibition slopes with mixtures of pure M A1AT and A2M (using SlaaapN as the substrate) shown in Figure 4.4 demonstrate that residual NE activity was seen even when A1AT was in a molar excess, similar (although not equivalent) to results seen with serum. Extrapolation of the initial part of the slope to the x-axis shows that NE was inhibited in a 1:1 molar ratio of A1AT:NE suggesting that A1AT was the predominant inhibitor of NE in these mixtures. The results also confirm that the residual NE activity observed with the serum samples (Chapter 3) was the result of NE bound to A2M since the baseline NE activity was absent when using A1AT alone. The effect was greatest when A1AT and A2M were studied in concentrations equivalent to those found in PiZZ serum compared to concentrations found in PiFZ serum, which in turn was greater than that with concentrations found in PiMM serum. Figure 4.5 shows the same pattern of results when MSaapvN was used as the substrate, but with no enhancement of NE activity with this substrate as described previously. A similar phenomenon has been described elsewhere

using PPE [259] where the residual activity of PPE increased as the ratio of A2M to A1AT increased. Ohlsson *et al* [260] reported that in normal human serum (PiMM), 92% of added NE binds to A1AT and 8% binds to A2M *in vitro*. Deficiency or dysfunction of A1AT (as occurs with mutant variants) would therefore alter these proportions leading to greater amounts of proteinases forming complexes with A2M where they remain active.

The PR3 inhibition slopes with mixtures of pure M A1AT and A2M (Figure 4.6) show that residual PR3 activity was still present when A1AT was in a molar excess. Again, these findings were similar (but not equivalent) to those obtained with serum (Chapter 3) and suggest that the residual PR3 activity observed with the serum samples was the result of PR3 bound to A2M. However, when inhibiting PR3 activity with mixtures of pure A1AT and A2M, the residual activity was not altered by increasing the ratio of A2M to A1AT, unlike the results obtained with serum samples. The exact reason for this discrepancy is unclear, and no previous work has studied the partitioning of PR3 between its two serum inhibitors. However, the observed differences may be due to a degree of inactivation or altered Kass of A1AT in PiFZ and PiZZ sera (see below) and hence greater partitioning of PR3 to A2M in these serum samples where the mutant variants of A1AT are present.

The experiments using pure Z A1AT and pure A2M in proportions found in PiZZ serum (Figures 4.7 and 4.8) did not replicate the earlier results using serum (Chapter 3). One explanation for this discrepancy could be that the pure Z A1AT used in this Chapter was active-site titrated against NE of known activity, and active concentrations were used in these experiments. However, in the serum experiments, active-site titration of Z A1AT was not performed due to the presence of A2M and the impurity of serum, and therefore the

concentration of A1AT was taken as the value measured by ELISA. The Z A1AT in the serum however is unlikely to be 100% active due to some potential complexes with NSPs, and its tendency to form inactive polymers [173] and possible other intermediate conformations, which will influence the partitioning of NSPs more towards binding to A2M.

Brissenden and Cox [261] measured serum A2M concentrations in 178 subjects with emphysema (59 with PiZZ genotype, 5 with A1AT null genotype and 7 with rarer A1ATD genotypes) and 115 healthy controls with a similar age and sex distribution. They found that subjects with A1ATD (regardless of genotype) had significantly greater serum A2M concentrations compared to controls, which was not related to the presence of emphysema. This observation may suggest an even greater shift in the partitioning of NSPs towards binding to A2M in subjects with A1ATD. However, Gaillard *et al* [262] showed that the elastase binding activity of A2M (using PPE) was reduced in subjects with A1ATD compared to subjects with the normal PiMM phenotype, which may further influence the partitioning of NSPs between their serum inhibitors if the same were true for human enzymes.

Although A2M is not a major proteinase inhibitor in the airways (at least in the absence of inflammation), the results described in this Chapter may have clinical significance in circumstances where A1AT is deficient or shows reduced anti-proteinase activity (such as in PiZZ subjects), and proteinases are more likely to be bound to A2M. Although NE bound to A2M can still be inhibited by SLPI in the upper airways [263], SLPI may play a less important role in the anti-proteinase protection of the alveoli. The partitioning of PR3

towards A2M could potentially be of greater significance since free PR3 is inhibited less avidly by A1AT compared to NE [123], and PR3 is not inhibited by SLPI. The studies presented in this Chapter show that PR3 bound to A2M can retain its proteolyic activity (similar to NE) even in the presence of an excess of A1AT. To date, no studies have determined the ability of elafin to inhibit the activity of PR3 bound to A2M.

In future experiments, it would be ideal to use purified A1AT variants (including pure S and F variants not studied here) to replicate the serum experiments described in Chapter 3 more closely. The use of mutant variants of A1AT could potentially allow factors other than concentration to be considered when studying the partitioning of NSPs between their inhibitors. For example, mutant A1AT variants differ from M A1AT in their association rate constants (See Chapter 6) and their susceptibility to form polymers or other conformations which may lead to their inactivation *in vivo*. However, the use of purified active-site titrated Z A1AT in this Chapter did not replicate the results observed using PiZZ serum, as discussed earlier. The data did show a slight increase in partitioning to A2M even when pure Z A1AT was used in comparable active concentrations to those used with M A1AT (see Figures 4.4 and 4.7), indicating that the association rate constant also had an effect on partitioning. The data however did not take into account any polymers or other conformations (intermediate, latent or cleaved forms) of A1AT present in the serum. The reduced partitioning to A2M observed with the pure active Z A1AT protein compared to that observed with PiZZ serum suggests that inactive forms are likely to be present in the serum. The Z A1AT purified from plasma and used in these experiments was found to be approximately 50% inactive following active-site titration. Whether this was the result of the purification process alone or was a reflection of serum activity remains unknown at

present, but highlights a potential difficulty of performing *in vitro* experiments to determine *in vivo* effects.

Overall, the data in this Chapter has confirmed that complexes of NE or PR3 with A2M retain their proteolytic activities (and may show enhanced activities compared to free enzyme), at least towards low molecular weight peptide substrates. In addition, the results have demonstrated that greater concentrations of A2M relative to A1AT are associated with a greater residual enzyme activity, which supports the data presented in Chapter 3. To determine the relevance of these studies to the pathogenesis of emphysema, it is important to study inhibition in the presence of a physiological substrate, and therefore experiments using elastin as a substrate were undertaken and described in Chapter 5.

5 Elastin degradation by serine proteinases

5.1 Introduction

Although the NSPs exhibit a wide range of physiological functions, their excessive activities can result in tissue damage and can potentiate the inflammatory response. In emphysema, the imbalance between the activities of NSPs and their inhibitors leads to the functional loss of elastin and damage to the alveolar structures [76]. Elastin consists of molecules of its soluble precursor tropoelastin [264] that are cross-linked at lysine residues. As a result of its extensive cross-linking and its hydrophobicity, elastin is insoluble and does not undergo significant turnover in healthy tissue [265]. NE can bind to and degrade lung elastin in human emphysema [90], and PR3 can degrade elastin *in vitro* and cause emphysema when administered into the trachea of hamsters [74]. Airway inhibitors such as A1AT and SLPI are less effective against elastin-bound NE compared to free NE [266]. An *in vitro* study [123] has suggested that elastin bound PR3 can be inhibited by A1AT but these findings have yet to be explored *in vivo* or in situations where the A1AT concentration is low or the protein is dysfunctional.

In this Chapter, the inhibition of NE and PR3 activities by serum samples or pure inhibitors has been assessed using labelled elastin as the substrate (elastin-fluorescein). The main aims are to determine the inhibitory capacities of A1AT and A2M in the presence of elastin, and to establish whether complexes of NE or PR3 with A2M are able to degrade elastin.

5.2 Methods

5.2.1 Preparation of elastin-fluorescein

Elastin-fluorescein (Elastin products, USA, purified from bovine neck ligament and labelled with fluorescein-isothiocyanate) was prepared by adding 20mg/ml of elastin-fluorescein (particle size pass 400 mesh, smaller than 37 microns,) to 0.2M Tris base, pH 8.8, 0.01% Triton X-100. The solution was stirred until all particles were wetted. The substrate was then washed on Whatman 41 filter paper (Fisher Scientific, UK) with elastin buffer until the filtrate was colourless. The elastin was then re-suspended in elastin buffer.

5.2.2 Inhibition of NE or PR3 with serum of different A1AT genotypes

Pure NE or PR3 was diluted in elastin buffer to an active concentration of 1.5µM and 20µL was added to an eppendorf 1.5ml tube (Eppendorf, UK). Serum was diluted in elastin buffer so that the concentration of A1AT was 1.5µM and increasing volumes of serum were added to each eppendorf tube. The total volume in each tube was made up to 300µL with elastin buffer and the tubes were incubated for 20 minutes at 37ºC to allow the NE or PR3 to form complexes with inhibitors. The control tube contained buffer alone. After incubation, 200µL of elastin-fluorescein was added and the tubes were incubated on a blood tube rotator at 37ºC for 20 hours. The tubes were then spun in a MSE micro centaur centrifuge at 13,000 RPM for 10 minutes. Next, 100µL of supernatant was taken and added to a 96-well plate and the absorbance was read at 495nm in a Biotek Synergy HT plate reader. Control values were subtracted and inhibition slopes were constructed by plotting the percentage of remaining enzyme activity against the molar ratio of A1AT to NE or PR3.

This method was optimised by introducing the blood tube rotator to ensure adequate mixing of elastin particles in the solution. Also, the incubation time was determined following time course experiments in order to obtain a suitable inhibition slope.

The experiments were also performed with NE or PR3 being added last (after the addition of serum, buffer and elastin) for comparison. This experimental procedure was designed to be more representative of events taking place *in vivo*, where NSPs are released in the presence of local inhibitors and lung elastin.

5.2.3 Inhibition of NE or PR3 with pure A2M or pure A1AT

These experiments were carried out as described for serum samples, except that pure A1AT or A2M was used instead of serum. For the A2M experiments, concentrations of pure A2M and active NE or PR3 were 1.38μM.

5.3 Results

5.3.1 Inhibition of NE or PR3 with PiMM serum

The inhibition slopes of NE (Graph A) and PR3 (Graph B) by PiMM serum using elastin-fluorescein as the substrate are shown in Figure 5.1. In these experiments, elastin was added as the final step following pre-incubation of NE or PR3 with PiMM serum. The results show that PiMM serum increasingly inhibited NE activity as the molar ratio of serum A1AT to NE increased. However, even when the serum A1AT was in a molar excess, 10% residual NE activity towards elastin-fluorescein was observed. In contrast, PR3 activity towards elastin was fully inhibited by PiMM serum when the molar ratio of serum A1AT to PR3 was 1:1.

Figure 5.1-Inhibition of NE or PR3 with PiMM serum (elastin-fluorescein)

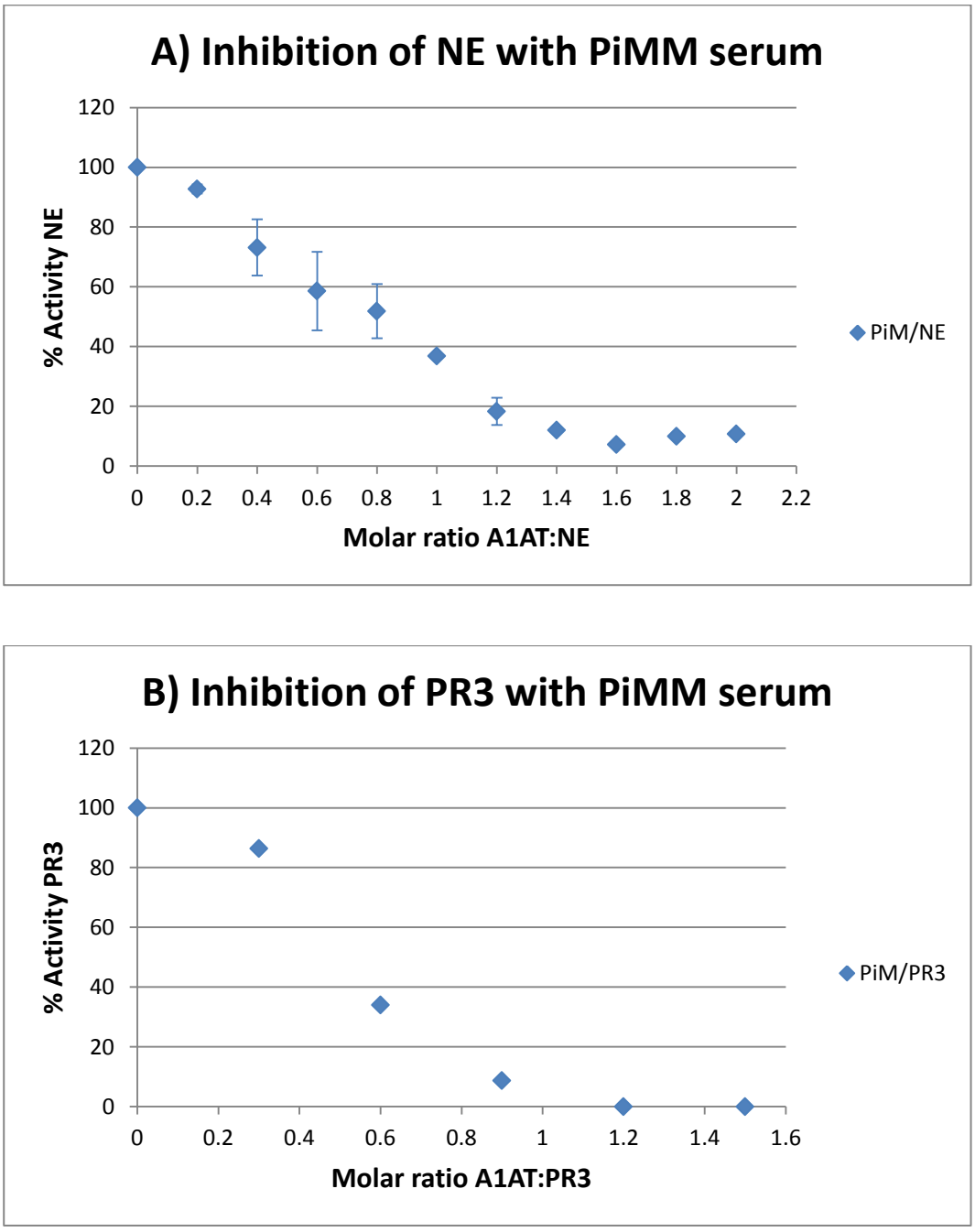

Figure 5.1: Inhibition of NE (A) or PR3 (B) with PiMM serum using elastin-fluorescein as the substrate. Graph A shows the mean results of 3 experiments and error bars show the SEM. Graph B shows the results from a single experiment. The baseline activities when A1AT was in a molar excess were 10% (Graph A) and 0% (Graph B).

The inhibition assays when NE or PR3 were added as the final step to a mixture of PiMM serum, elastin and buffer are shown in Figure 5.2. Individual experiments were performed for each proteinase but the results are presented together for comparison. This experimental procedure is more representative of events taking place *in vivo* when the NSPs are released in the presence of local inhibitors and lung elastin. The results show that both proteinases (but particularly NE) were inhibited less effectively in the presence of elastin.

Figure 5.2-Inhibition of NE or PR3 added to a mixture of PiMM serum, elastin-fluorescein and buffer

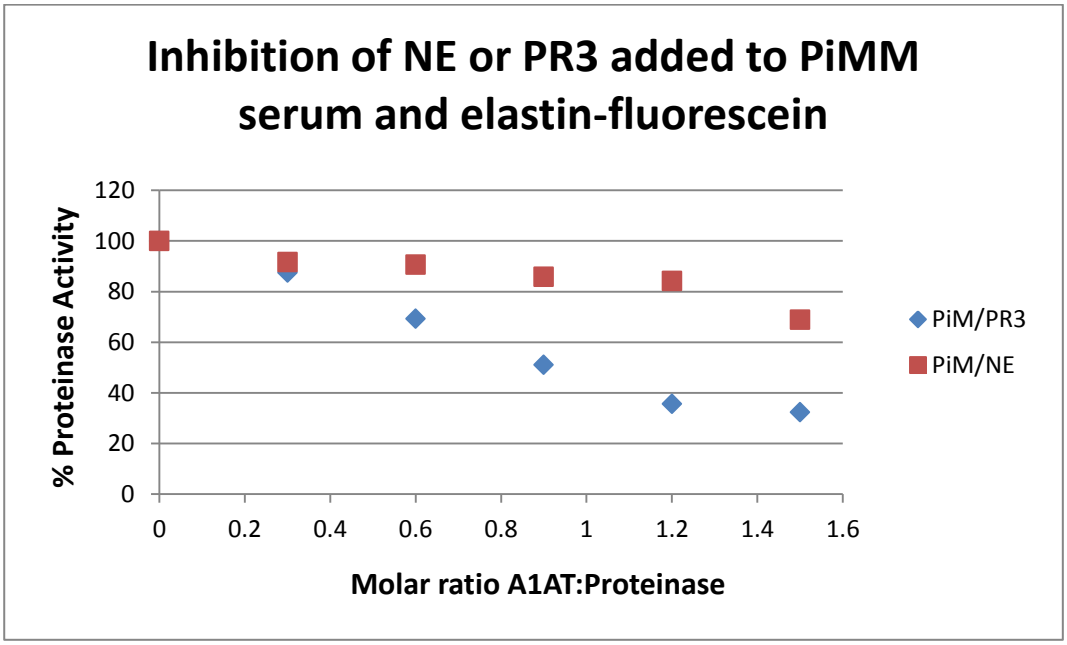

Figure 5.2: Inhibition of NE or PR3 added to a mixture of PiMM serum, elastin-fluorescein and buffer. The results from single experiments are shown.

5.3.2 Inhibition of NE or PR3 with PiZZ serum

The inhibition slopes of NE (Graph A) and PR3 (Graph B) by PiZZ serum using elastin-fluorescein as the substrate are shown in Figure 5.3. In these experiments, elastin was added as the final step following pre-incubation of NE or PR3 with PiZZ serum. The results show that PiZZ serum increasingly inhibited NE activity as the molar ratio of serum A1AT to NE increased. However, even when the serum A1AT was in a molar excess, 12% residual NE activity towards elastin-fluorescein was observed. In contrast, PR3 activity towards elastin was fully inhibited by PiZZ serum when the molar ratio of serum A1AT to PR3 was approximately 1:1.

Figure 5.3- Inhibition of NE or PR3 with PiZZ serum (elastin-fluorescein)

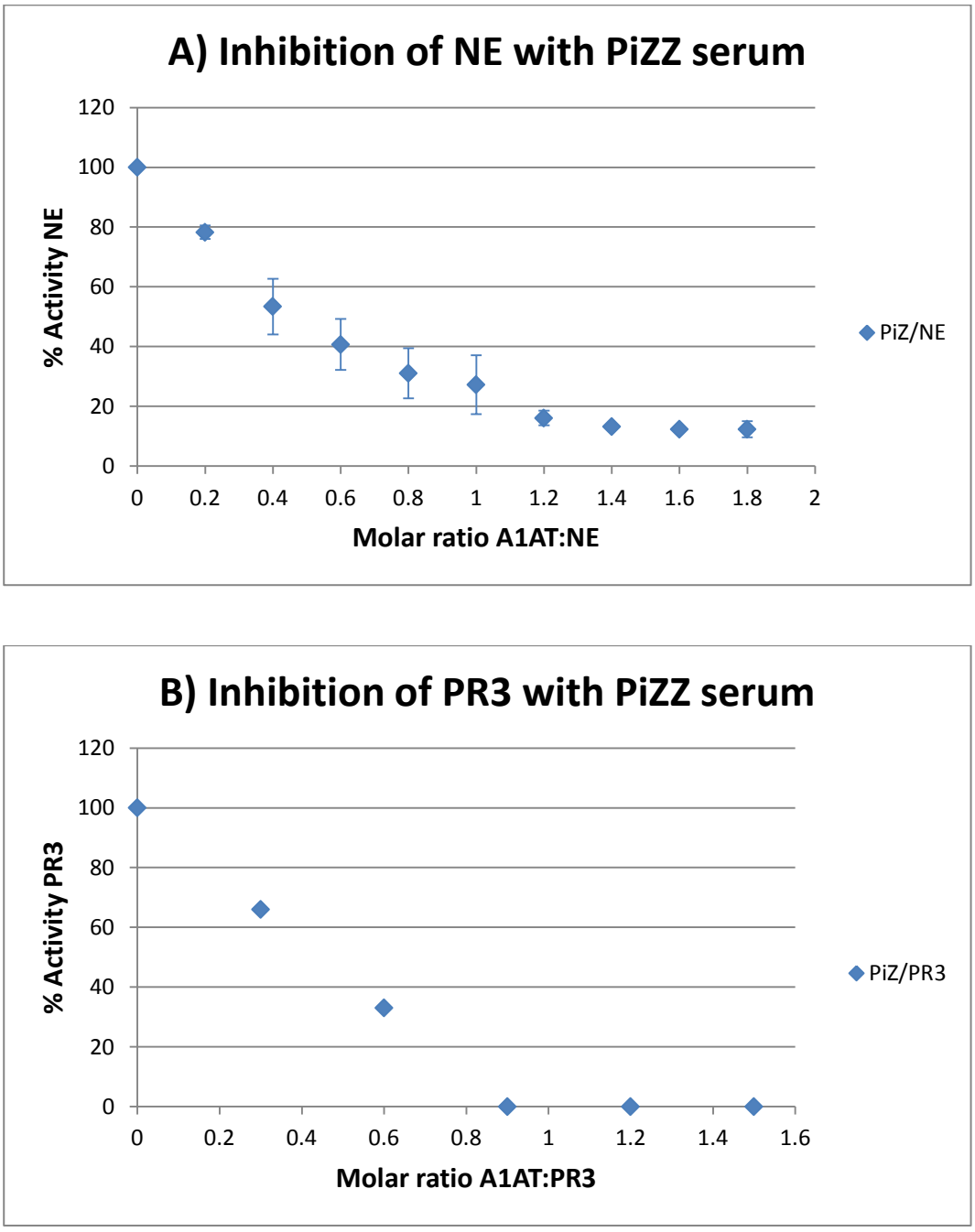

Figure 5.3: Inhibition of NE (A) or PR3 (B) with PiZZ serum using elastin-fluorescein as the substrate. Graph A shows the mean results of 3 experiments and error bars show the SEM. Graph B shows the results from a single experiment. The baseline activities when A1AT was in a molar excess were 12% (Graph A) and 0% (Graph B).

The inhibition assays when NE or PR3 were added as the final step to a mixture of PiZZ serum, elastin and buffer are shown in Figure 5.4. Individual experiments were performed for each proteinase but the results are presented together for comparison. The results show that both proteinases (but particularly NE) were inhibited less effectively in the presence of elastin.

Figure 5.4-Inhibition of NE or PR3 added to a mixture of PiZZ serum, elastin-fluorescein and buffer

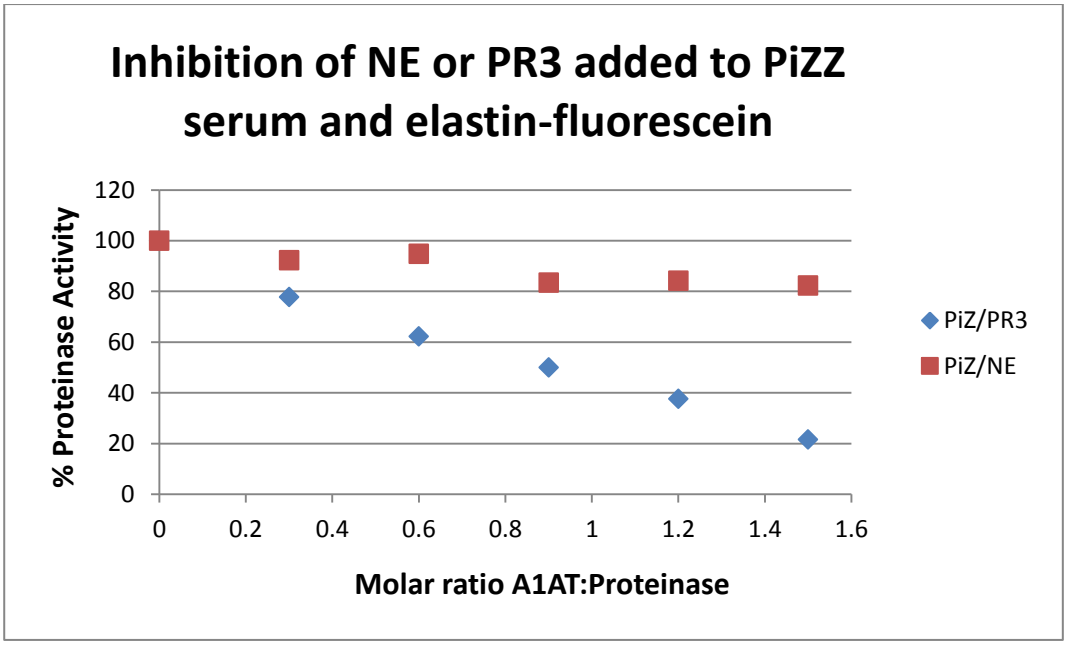

Figure 5.4: Inhibition of NE or PR3 added to a mixture of PiZZ serum, elastin-fluorescein and buffer. The results from single experiments are shown.

The activity of PR3 could be completely inhibited by both PiMM and PiZZ sera with approximately 1:1 stoichiometry when elastin-fluorescein was introduced following pre-incubation of the serum with PR3.

Due to restrictions on time and resources, the experiments with PiFZ and PiSZ sera described below were performed with NE only.

5.3.3 Inhibition of NE with PiFZ serum

The inhibition slope of NE by PiFZ serum using elastin-fluorescein as the substrate is shown in Figure 5.5. In this experiment, elastin was added as the final step following pre-incubation of NE with PiFZ serum. When the serum A1AT was in a molar excess, 12.7% residual NE activity towards elastin-fluorescein was still observed.

Figure 5.5- Inhibition of NE with PiFZ serum (elastin-fluorescein)

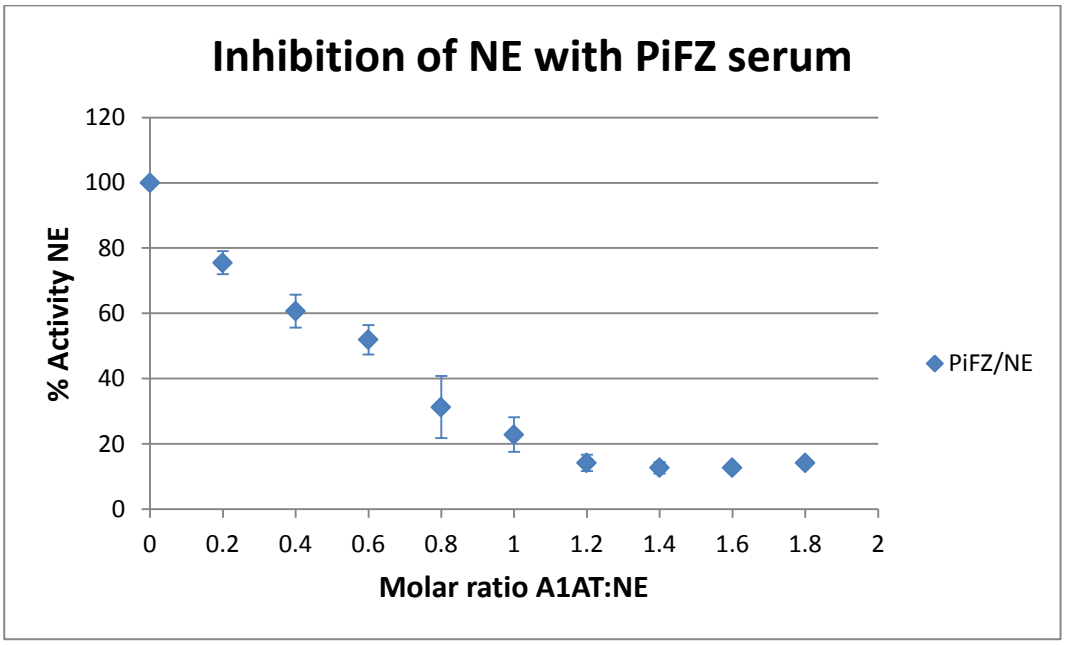

Figure 5.5: Inhibition of NE with PiFZ serum using elastin-fluorescein as the substrate. Points show the mean of three experiments ±SEM. The baseline activity when A1AT was in a molar excess was 12.7%.

5.3.4 Inhibition of NE with PiSZ serum

The inhibition slope of NE by PiSZ serum using elastin-fluorescein as the substrate is shown in Figure 5.6. In this experiment, elastin was added as the final step following pre-incubation of NE with PiSZ serum. When the serum A1AT was in a molar excess, 10.7% residual NE activity towards elastin-fluorescein was still observed.

Figure 5.6- Inhibition of NE with PiSZ serum (elastin-fluorescein)

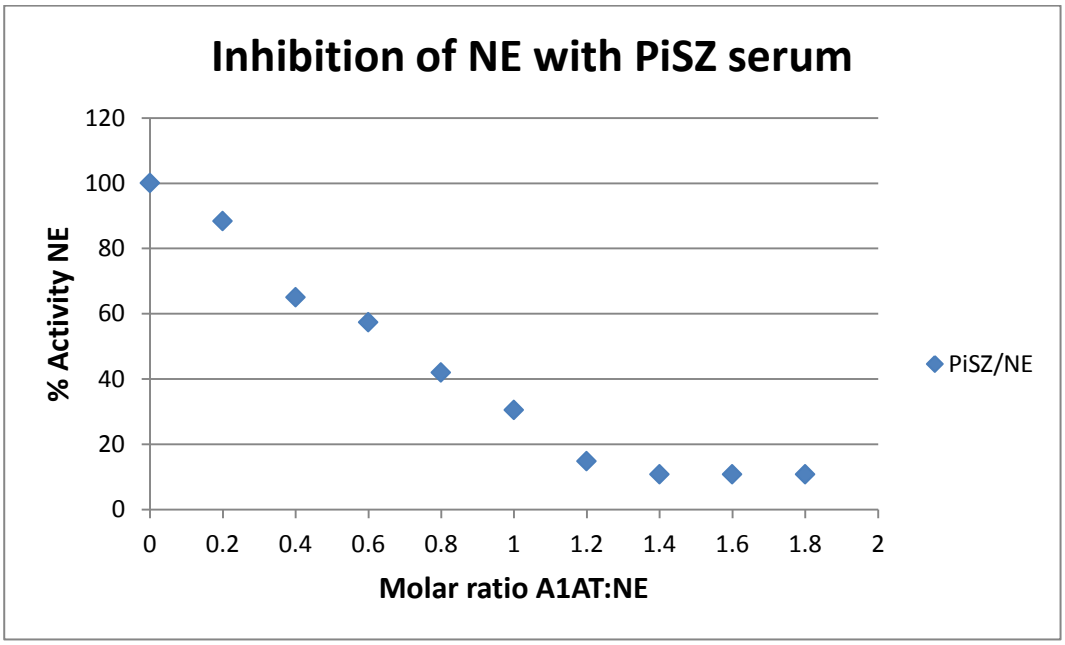

Figure 5.6: Inhibition of NE with PiSZ serum using elastin-fluorescein as the substrate. The results from a single experiment are shown. The baseline activity when A1AT was in a molar excess was 10.7%.

5.3.5 Inhibition of NE by pure A1AT

The inhibition slope of NE by pure A1AT using elastin-fluorescein as the substrate is shown in Figure 5.7. Pure A1AT was able to fully inhibit NE at a molar ratio of 1.2:1. In this experiment, elastin was added as the final step following pre-incubation of NE with pure A1AT.

Figure 5.7- Inhibition of NE by pure A1AT (elastin-fluorescein)

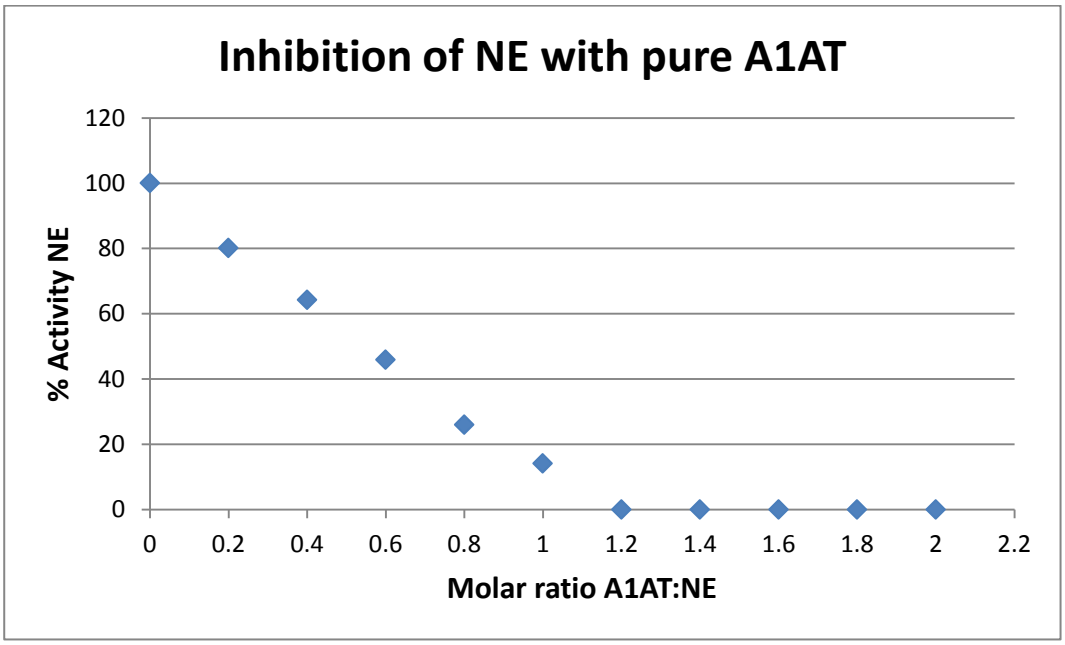

Figure 5.7: Inhibition of NE with pure A1AT using elastin-fluorescein as the substrate. The results from a single experiment are shown. NE activity was completely inhibited by pure A1AT.

5.3.6 Inhibition of NE or PR3 with pure A2M

The inhibition slopes of NE and PR3 by pure A2M using elastin-fluorescein as the substrate are shown in Figure 5.8. In these experiments, A2M was pre-incubated with each proteinase prior to addition of elastin-fluorescein, up to a molar ratio of 3:1. The results show that the activities of both proteinases (but particularly NE) towards elastin were not fully inhibited by A2M.

Figure 5.8-Inhibition of NE or PR3 with pure A2M (elastin-fluorescein)

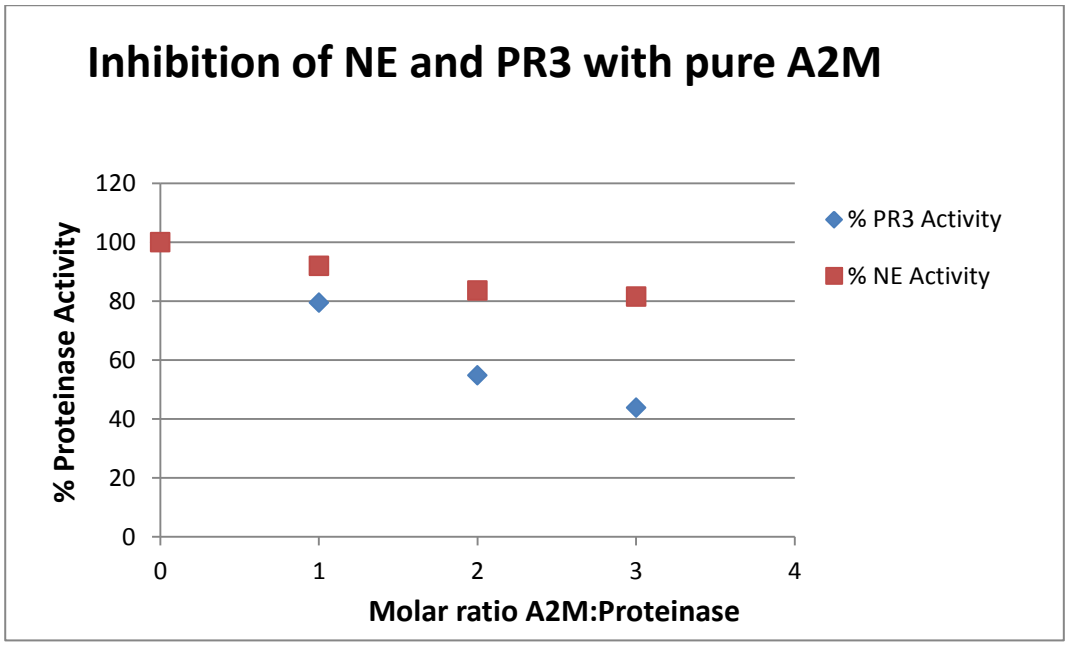

Figure 5.8: Inhibition of NE or PR3 with A2M using elastin-fluorescein as the substrate. Separate experiments were performed for each proteinase and the results from single experiments are shown on the same graph for comparison.

5.4 Discussion

The results presented in this Chapter have shown that NE activity towards elastin-fluorescein was not completely inhibited following pre-incubation with PiMM (Figure 5.1A), PiZZ (Figure 5.3A), PiFZ (Figure 5.5) or PiSZ (Figure 5.6) sera when the A1AT was in a molar excess of the enzyme. The residual NE activity was around 10-15% and could be explained either by elastolytic activity of NE complexes with A2M, or by dissociation of A1AT:NE complexes over the 20 hour incubation period. The hypothesis that NE complexes with A2M are able to degrade elastin is supported by the results in Figure 5.8, which shows that pre-incubation of NE with A2M for 20 minutes up to a molar excess of A2M of 3:1 does not fully inhibit NE activity towards elastin-fluorescein, and a three-fold molar excess of A2M should have theoretically been sufficient to bind all of the free NE (Moore *et al* [254] found that a 1.5 molar excess of A2M was sufficient to bind all free NE under similar experimental conditions). In contrast, pure A1AT could fully inactivate NE when the enzyme and inhibitor were pre-incubated prior to the addition of elastin-fluorescein (Figure 5.7) indicating that significant dissociation of active NE from A1AT did not occur.

It may be expected that when elastin is used as the substrate, NE activity would be completely inhibited by serum samples since elastin has a high molecular mass and should be less accessible to elastolysis by NE bound to A2M. Previous studies [257] however have shown that PPE is capable of digesting chemically solubilised elastin even when complexed with A2M. Furthermore, I have demonstrated that following incubation with a two-fold molar excess of A2M, PPE retains 100% of its activity towards elastin-fluorescein (data not shown). Nevertheless, other studies have shown that NE complexes

with A2M are unable to degrade mature elastin [253, 267]. Some of these discrepancies may relate to experimental conditions, since the elastin used for the experiments described in this Chapter had a particle size of less than 37 microns (pass 400 mesh), and some previously published studies used a particle size of 37-75 microns (200-400 mesh) [268]. Stone *et al* [201] reported that complexes of PPE with A2M retained their elastolytic potential and promoted lung injury in animal studies. Furthermore, NE bound to A2M may be able to degrade the elastin precursor tropoelastin [269], which is secreted into the extracellular space prior to formation of the cross linkages found in elastin [270] and hence could affect the repair process. Therefore NE complexes with A2M could potentially play a role in the development of emphysema, particularly in subjects with A1ATD when NE is more likely to partition to A2M, and further work is therefore required to explore the implications of this possibility.

The NE inhibition assays presented in this Chapter suggest that A1AT is less functional as an inhibitor when elastin-fluorescein is used as the substrate and added following pre-incubation of NE with serum or pure A1AT. Extrapolation of the slopes in Figures 5.1A, 5.3A, 5.5, 5.6 and 5.7 to zero activity shows that NE is inhibited when the molar ratio of A1AT:NE is 1.2-1.4:1. Previous work by Kramps *et al* [271] has also reported that A1AT has a specific inhibitory activity of 40-85% of that observed with synthetic nitroanilide substrates when elastin-fluorescein is used. The authors hypothesized that the lower inhibitory capacity of A1AT when using elastin-fluorescein could potentially be due to dissociation of the enzyme-inhibitor complex during the 20 hour incubation period, resulting in free enzyme which could then bind to elastin. NE bound to elastin is then poorly inhibited by A1AT compared to free NE [266]. However, the results presented here do not support this hypothesis because pure A1AT was able to fully inactivate NE (Figure

5.7) under similar experimental conditions suggesting that significant dissociation did not occur.

The results presented in this Chapter show that PR3 activity towards elastin was completely inhibited by PiMM (Figure 5.1B) and PiZZ (Figure 5.3B) sera. In addition, PR3 activity towards elastin was inhibited more effectively than NE by pure A2M (Figure 5.8). Overall, these results suggest that PR3 complexes with A2M are less likely to play an important role in elastin degradation. Despite these findings, PR3 may still be responsible, at least in part, for the tissue damage associated with emphysema because it is more abundant than NE and has fewer airway inhibitors. These concepts are explored further in Chapter 9.

This Chapter has also highlighted differences in the ability of A1AT to inhibit NSPs in the presence of elastin. Figures 5.2 and 5.4 demonstrate that when proteinases were introduced to a mixture of both elastin and serum (containing the inhibitors A1AT and A2M), NE in particular was inhibited much less effectively in the presence of elastin. These findings are consistent with elastin-bound NE being poorly inhibited by A1AT compared to free enzyme. This concept has been explored in animal studies [272, 273] that demonstrated that in order to protect the lungs from proteolytic damage, synthetic elastase inhibitors needed to be administered prior to the release of elastase. If inhibitors were administered following an elastase challenge, little or no protection was achieved, most probably because the inhibitors failed to inactivate elastin-bound NE. The ineffective inhibition of elastin-bound NE has biological relevance to the pathogenesis of emphysema, and possibly to other disease processes. Thus, further studies investigating the mechanisms of inhibiting

the activity of NE bound to elastin are warranted. However, the results presented here suggest that PR3 may be inhibited by A1AT more effectively than NE in the presence of elastin. An *in vitro* study [123] has reported that the elastolytic rate of PR3 is one eighth that of NE using bovine neck ligament elastin, and that ongoing elastolysis by PR3 can be almost completely inhibited by A1AT, although these findings remain to be verified *in vivo*. These results could potentially be explained by PR3 having fewer binding sites on elastin compared to NE, and PR3 may be able to dissociate more readily from elastin compared to NE [123] and therefore be more susceptible to inhibition by the surrounding A1AT.

The NE inhibition assays using PiMM, PiZZ, PiFZ and PiSZ sera (Figures 5.1A, 5.3A, 5.5 and 5.6) were similar to each other, suggesting that the A1AT in these samples inhibited NE activity towards elastin in a similar manner in molar terms (and likewise for PR3 with PiMM and PiZZ sera). However, since the graphs show molar ratios of A1AT to proteinases and not total concentrations of A1AT, they do not fully reflect the environment in the lungs where lower concentrations of A1AT with an increased susceptibility to polymerisation (and possibly reduced function) would be present in A1ATD subjects.

When comparing the results presented here (using elastin as the substrate) with the results presented in Chapter 3 (using small peptide substrates), it appears that A2M:NE complexes may be less active towards elastin than against low molecular weight peptide substrates. The residual activities of NE (which represent the activities of A2M:NE complexes since the A1AT was in a molar excess) were greater when peptide substrates were used compared to elastin. These findings are consistent with those reported elsewhere [254] and

could possibly be due to a proportion of the complexes containing two molecules of NE, which would not allow simultaneous activity of these two NE molecules towards a macromolecular substrate such as elastin.

The *in vitro* experiments described in this Chapter have some limitations when considering events taking place *in vivo*. Firstly, the elastin used in these experiments was derived from bovine neck ligament which was readily available, although it differs structurally from that found in human lung elastic fibres. Secondly, the experiments were performed using a single buffer at a pH of 8.8 to optimise enzyme activity, which may not represent the inflammatory environment of the lungs. Thirdly, other inhibitors such as SLPI were not present in these experiments, which although not relevant to the PR3 experiments, should be considered in the NE experiments since SLPI can inhibit NE bound to elastin [185] although its inhibitory activity is less than with free NE [266]. Finally, these *in vitro* experiments have considered individual proteinases and their interactions with inhibitors and substrates. In the local environment of the inflamed lung, several proteinases are likely to be present which can interact with each other and with their inhibitors as shown in Figure 1.7. However, despite these limitations, no studies to date have examined the ability of PR3 complexes with A2M to degrade elastin, or the ability of serum from A1ATD subjects to inhibit PR3 activity towards elastin.

Further studies will be necessary to determine whether A2M:NE complexes are important in diseases where excessive activities of NSPs have been implicated. These initial studies could involve the instillation of human A2M:NE complexes into animal lungs to determine whether emphysema-like lesions develop. Although, in view of the tight epithelial

junctions it is probable that a large molecule like A2M may not gain access to the interstitium to damage the lung connective tissue. Alternatively, studies of human samples could involve the measurement of A2M:NE complexes in lung secretions (sputum or BAL) to determine their presence and concentration, and hence destructive potential. However, proteinases trapped by A2M may not readily bind to their specific antibodies [274] due to the inaccessibility of their epitopes which are trapped within the large A2M molecule. Hence, the development of ELISA techniques for the measurement of A2M:NE complexes has proven difficult. Adeyemi *et al* [275] described a technique which necessitated the addition of phenylmethylsulphonyl fluoride (PMSF) to plasma and serum samples in order to measure A2M:NE complexes. However, PMSF is toxic and requires stringent safety precautions in the laboratory. The same research group [276] subsequently reported that pre-incubation of the A2M:NE complex with an anti-human A2M antibody was necessary in order for the complexed NE to bind to its specific antibody. To date, there have been no published methods for measuring A2M:PR3 complexes in biological fluids.

In summary, this Chapter has demonstrated that NE activity towards elastin is not fully inhibited by normal (PiMM), A1ATD (PiZZ) or other A1AT variant (PiFZ, PiSZ) sera, which may be due to elastolytic activity of A2M:NE complexes, or (less likely) to dissociation of A1AT:NE complexes and subsequent poor inhibition of elastin-bound NE. In contrast, PR3 activity towards elastin is fully inhibited by PiMM or PiZZ sera. Overall, the results suggest that PR3 complexes with A2M are unlikely to play a significant role in degradation of mature elastin, and that the inhibitory activity of A1AT towards PR3 is (at least partly) preserved in the presence of elastin.

6 Association rate constants for A1AT variants and proteinases

6.1 Introduction

Previous studies into the association rate constants (Kass) of A1AT have shown that Z variant A1AT is a less competent inhibitor of NE than M variant A1AT [154]. Thus, individuals with the PiZZ genotype not only have lower concentrations of A1AT, but it is also less functional as an inhibitor of NE [155] and, in addition, has an increased tendency to form polymers which are not functional as inhibitors [173]. The S variant of A1AT is reported as having a similar inhibitory activity towards NE compared to the normal M variant [277, 278]. The F and I variants have been less well studied but have been reported to have a reduced ability to inhibit NE, much like that of the Z variant [169, 279].

There have however been few studies of association rate constants for PR3 with A1AT. The M variant of A1AT is a less competent inhibitor of PR3, with Kass values being reported as ten-fold lower than those with NE [117, 280]. To date, no studies into the association rate constants of other A1AT variants with PR3 have been reported.

The work in this Chapter aims to provide new information on the second order association rate constants for A1AT variants and NE or PR3 which are currently not well described. These data will increase our understanding of how these proteinases partition to inhibitors in the presence of neutrophilic inflammation. To study the clinical significance of co-inheritance of a dysfunctional A1AT variant with a deficiency variant, the clinical characteristics of subjects with the PiFZ phenotype have been studied in further detail.

6.2 Methods

6.2.1 Treatment of serum with methylamine to inactivate A2M

In order to measure Kass for A1AT in serum with NE or PR3, it was first necessary to inactivate A2M. This was achieved by treating the serum samples (PiMM, PiZZ, PiSS, PiFZ, PiIZ) with 0.1M methylamine (Fisher Scientific, UK) for 10 minutes at 37°C [281]. Inactivation of A2M by methylamine is a sequential two-step process where thiol ester cleavage is followed by a conformational change in the protein which results in the loss of proteinase binding capacity [282]. The inactivation of A2M was confirmed indirectly by measuring NE and PR3 inhibition by serum samples with and without treatment with methylamine. The substrate used for these experiments was MSaapvN at 0.6mg/ml in 0.1M Hepes, pH 7.5, 9.5% dimethyl sulfoxide (DMSO).

6.2.2 Measurement of Kass for A1AT variants and NE

Pure NE of known activity was diluted to an active concentration of 100nM with NSP assay buffer. Pure A1AT (M or Z variant) or methylamine-treated serum samples (PiMM, PiZZ, PiSS, PiFZ, PiIZ) were also diluted to an A1AT concentration of 100nM and these samples were titrated against NE to determine the percentage of active A1AT. For these experiments, variable amounts of sample containing A1AT were added to 10µL of 100nM NE in a 96-well plate (Costar, USA). The wells were made up to 110µL with buffer and the plates incubated for 30 minutes at room temperature to allow complex formation. The residual NE activity was determined by adding 150µL of MSaapvN at 0.6mg/ml in 0.1M Hepes, pH 7.5, 9.5% DMSO. The OD at 410nm was then read at 5 minute intervals up to 60 minutes using a Biotek Synergy HT plate reader. The activity of A1AT in the sample

was determined by plotting the percentage of remaining NE activity against the A1AT concentration. The linear portion of the slope was extrapolated to the x-axis, and the molar amount of A1AT required to inhibit each mole of NE was calculated. From this calculation, the percentage of A1AT activity was obtained. Each assay was performed in triplicate and the average result was used for all subsequent studies.

Following this initial step, the time-dependent measurements were performed by incubating equimolar amounts of NE and active A1AT (1nM each) in a 1ml polystyrene cuvette with a 1cm pathlength at 23°C. The buffer used for these experiments was NSP assay buffer and the detergent was present in the buffer to minimise the adhesion of free proteinases to plastic and glass surfaces when in dilute solution [240]. Residual NE activity at 1-5 minutes was measured by the addition of 200µL of MSaapvN and measurement of the change in wavelength over 10 minutes using a spectrophotometer (Jasco V550). At each time point, the percentage of NE inhibition was determined. The Kass was calculated by plotting the inverse of NE activity at each time point versus time. From the linear portion of the slope, the half time (t½) of the reaction was calculated using the formula;

$$t½ = \text{y intercept/slope}$$

Kass was calculated using the equation [154];

$$Kass = (\text{Concentration of NE} \times t½)^{-1}$$

6.2.3 Measurement of Kass for A1AT variants and PR3

Pure PR3 of known activity was diluted to an active concentration of 400nM using NSP assay buffer. Pure A1AT (M or Z variant) or methylamine-treated serum samples were also diluted to an A1AT concentration of 400nM and these samples were titrated against PR3 to determine the percentage of active A1AT. For these experiments, variable volumes of sample containing A1AT were added to 10µL of 400nM PR3 in a 96-well plate. The wells were made up to 120µL with buffer and the plate was incubated for 30 minutes at room temperature to allow complex formation. The residual PR3 activity was determined by adding 3µL of Boc-ala-ONp (Sigma, UK) at a concentration of 20mM in methanol. The OD at 347.5nm was then read at 5 minute intervals up to 30 minutes using a Biotek Synergy HT plate reader. The activity of A1AT in the sample was determined by plotting the percentage of remaining PR3 activity against the A1AT concentration. The linear portion of the slope was extrapolated to the x-axis, and the number of moles of A1AT required to inhibit each mole of PR3 was calculated. From this calculation, the percentage of A1AT activity was obtained. Each assay was performed in triplicate and the average result was used for all subsequent studies.

The time-dependent measurements were then performed by incubating equimolar amounts of PR3 and active A1AT (1nM each) in a black opaque polypropylene low binding plate (Sigma, UK) at 23°C with a well volume of 150µL. Residual PR3 activity at 1-5 minutes was measured by stopping the reaction with 3µL of the PR3 specific Förster resonance energy transfer (FRET) substrate Abz-VAD-norV-ADRQ-EDDnp (Alta Biosciences, UK) at a concentration of 1mM [283]. The change in fluorescence (excitation 320nm, emission 420nm) was measured every 2 minutes for 20 minutes using a Biotek Synergy 2 Multi-

Mode Microplate Reader. At each time point, the percentage of PR3 inhibition was determined. The Kass was calculated using the same method as that used for NE.

6.2.4 Determining the clinical significance of the PiFZ phenotype

The clinical characteristics of PiMZ and PiSZ heterozygotes have been studied previously [284, 285]. However, the PiFZ phenotype has been less well studied. In order to increase understanding of its clinical significance, the U.K. A1ATD national registry was searched and six subjects with the PiFZ phenotype were identified. Data was collected from these subjects including; demographic data, A1AT concentration, smoking history, body mass index (BMI), PFTs, frequency of exacerbations, quality of life scores as measured by the St George's Respiratory Questionnaire (SGRQ) and CT scan appearance.

6.3 Results

6.3.1 Treatment of serum with methylamine

In order to measure Kass for A1AT in serum with NE or PR3, it was first necessary to inactivate A2M. The inactivation of A2M by methylamine was confirmed indirectly by performing NE and PR3 inhibition assays with serum samples with and without treatment with methylamine. The results for PiMM (Graphs A and C) and PiZZ sera (Graphs B and D) are shown in Figure 6.1 (data for other sera not shown). The results show that treatment of serum samples with methylamine prior to performing the assay inactivated the A2M, and the inhibition was thus due to A1AT alone. In the graphs where untreated PiZZ serum was used, some enhancement of proteinase activity was seen as the concentration of A2M increased which has been described previously [255] and discussed in Chapter 4.

Figure 6.1 (A-D)- Inhibition of NE and PR3 activity by serum samples with and without treatment with methylamine

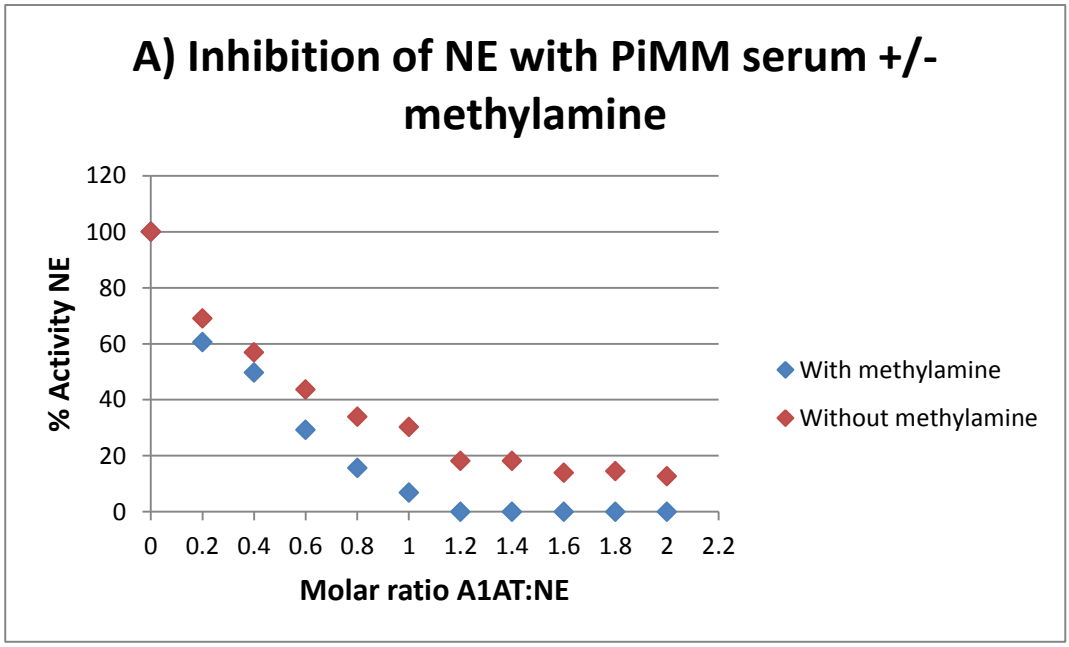

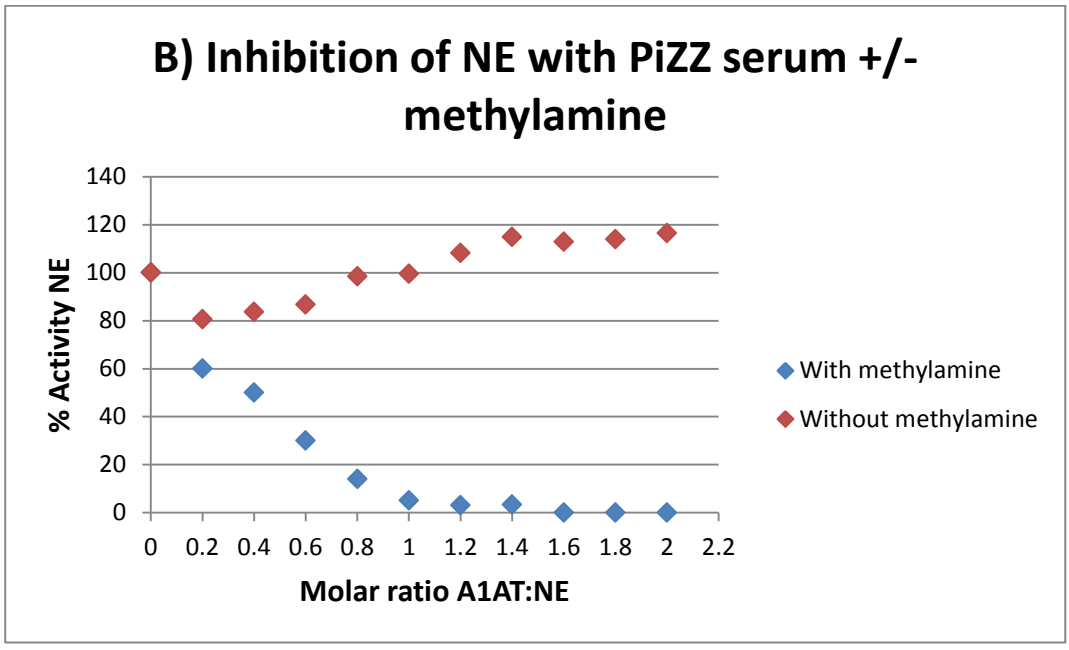

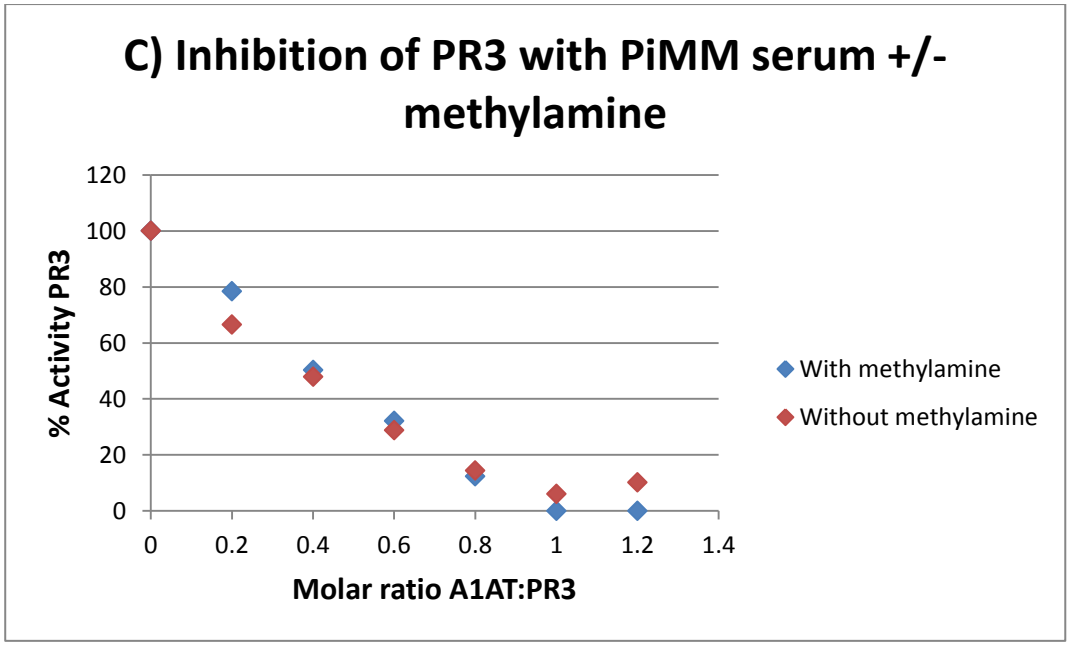

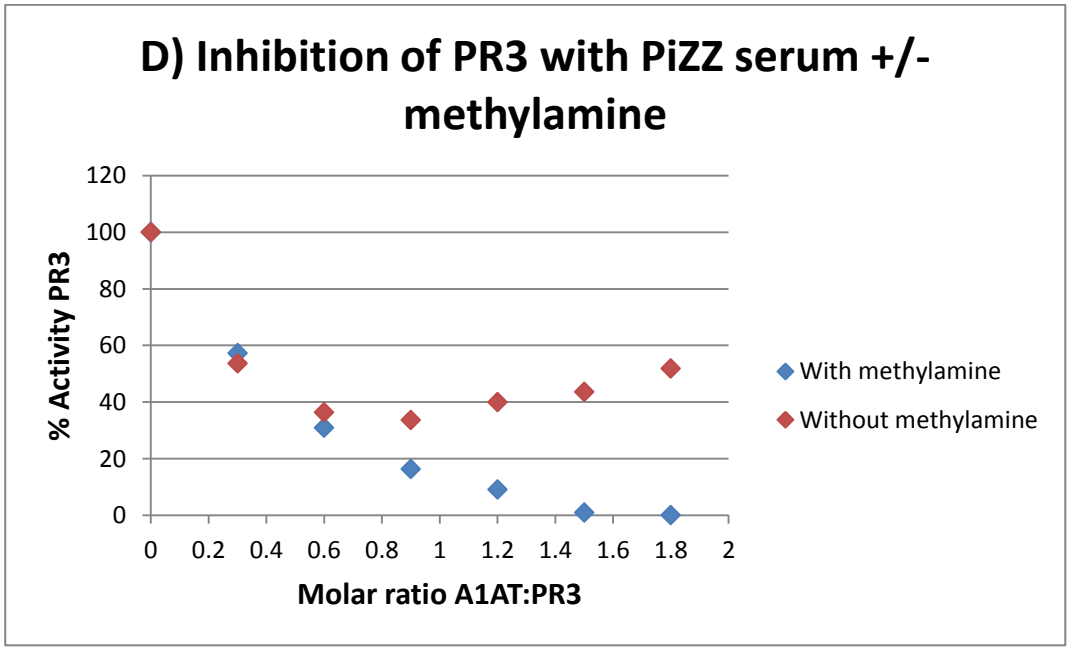

Figure 6.1 (A-D): Inhibition of proteinases using PiMM and PiZZ serum samples with or without treatment with methylamine. Each graph shows the results from single experiments.

6.3.2 Calculation of Kass

After incubating equimolar amounts of proteinase and A1AT for various time points, the residual proteinase activity was measured for each time point, and the percentage of proteinase inhibition was calculated using the formula [154];

$$\% \text{ Inhibitory activity of A1AT} = \frac{(\text{Proteinase activity without A1AT} - \text{Proteinase activity with A1AT}) \times 100}{\text{Proteinase activity without A1AT}}$$

The Kass was calculated by plotting the inverse of the proteinase activity at each time point versus time. An example of the data obtained is shown in Figure 6.2. From the linear portion of the slope, the half time (t½) of the reaction was calculated using the formula;

$$t½ = \text{y intercept/slope}$$

Kass was calculated using the formula;

$$\text{Kass} = (\text{Concentration of proteinase} \times t½)^{-1}$$

Figure 6.2- Calculation of Kass for PR3 and Z A1AT

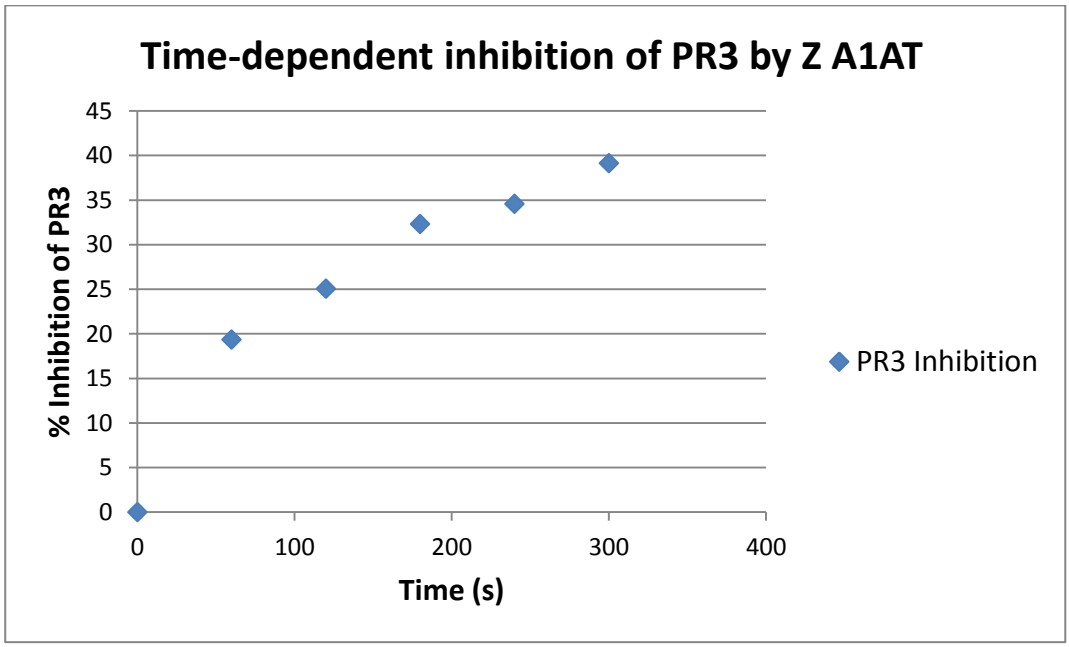

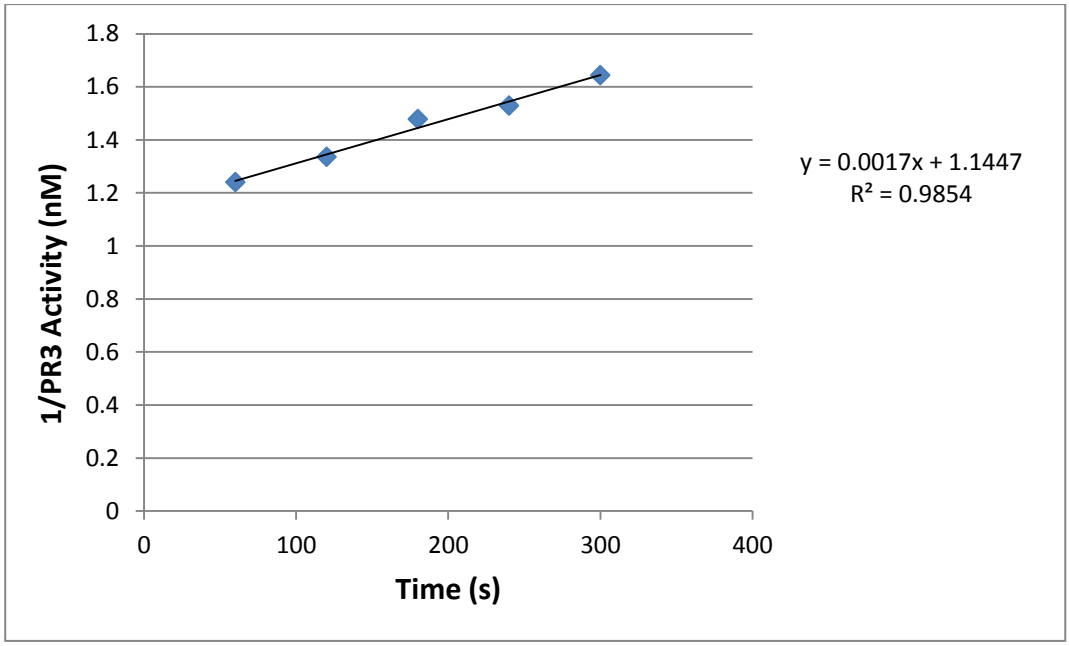

Figure 6.2: The time-dependent inhibition of PR3 with Z A1AT. 1nM each of active PR3 and Z A1AT were incubated at 23ºC for various time points as shown. The reaction was stopped and the residual PR3 activity was measured by the addition of a PR3 specific substrate. Data from a single experiment are shown.

Using the data from Figure 6.2, the t½ = 1.1447/0.0017 = 673 seconds. Therefore Kass = $(1nM \times 673s)^{-1} = 0.001485nM^{-1}s^{-1}$ or $1.49 \times 10^6\ M^{-1}s^{-1}$ from this experiment.

6.3.3 Kass for A1AT variants and NE or PR3

The Kass values for different variants of A1AT with NE or PR3 using this methodology are shown in Table 6.1 and are shown graphically in Figure 6.3. The values show the mean of three experiments and the SEM. Values for NE were greater than PR3 for all A1AT variants studied.

Table 6.1-Kass for A1AT variants and NE or PR3

A1AT variant	**Enzyme**	**Association rate constant (Mean ± SEM) at 23°C (M^{-1} s^{-1})**
M	NE	$1.45\ (0.02) \times 10^7$
S	NE	$1.14\ (0.36) \times 10^7$
Z	NE	$7.34\ (0.03) \times 10^6$
FZ	NE	$5.75\ (1.43) \times 10^6$
IZ	NE	$8.64\ (1.22) \times 10^6$
M	PR3	$9.24\ (0.48) \times 10^5$
S	PR3	$9.51\ (3.00) \times 10^5$
Z	PR3	$1.10\ (0.21) \times 10^6$
FZ	PR3	$1.43\ (0.29) \times 10^6$
IZ	PR3	$1.00\ (0.12) \times 10^6$

Figure 6.3-Kass for A1AT variants and NE or PR3

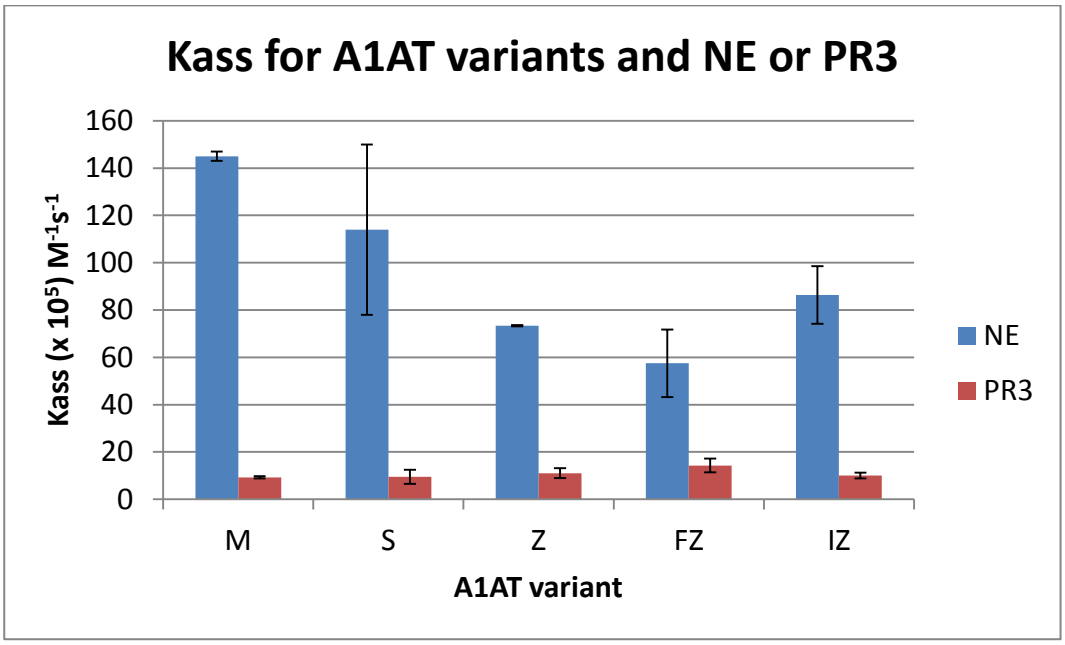

Figure 6.3: Second order association rate constants (Kass) for A1AT variants and NE or PR3. Bars show the mean±SEM. Values for NE were greater than PR3 for all A1AT variants.

6.3.4 Clinical characteristics of subjects with the PiFZ phenotype

The F variant of A1AT is usually associated with a normal serum concentration of A1AT, although the results presented here suggest that it is dysfunctional in its ability to inhibit NE activity. The potential significance of co-inheriting this dysfunctional variant with the main deficiency variant (Z) has been studied briefly here.

The clinical characteristics of the six subjects identified from the U.K. A1ATD national registry with the PiFZ phenotype are shown in Table 6.2. All subjects had A1AT concentrations above the generally accepted protective threshold of 11μM. However, five had evidence of emphysema on their CT scan, which was panacinar emphysema with a lower zone predominance (usually associated with the PiZZ phenotype) in two.

Table 6.2- Clinical characteristics of subjects with the PiFZ phenotype

Clinical Parameter	**Patient 1**	**Patient 2**	**Patient 3**	**Patient 4**	**Patient 5**	**Patient 6**
Age (years)	59	47	70	74	76	53
Sex	M	M	F	M	M	M
A1AT level (μM)	18.7	21.6	24.0	11.8	18.3	19.7
Smoking history (pack years)	24	24	23	19	8	40
BMI (kg/m^2)	23	33	19	29	29	20
FEV1 (% predicted)	29	110	33	99	32	38
FEV1/FVC ratio	0.22	0.77	0.32	0.55	0.31	0.21
KCO (% predicted)	26	100	57	63	87	40
PO_2 on air (KPa, capillary blood gas)	7.3	8.8	7.8	9.3	7.8	8.8
Average number of exacerbations per year	2	0	2	2	4	1
SGRQ (total score)	63	20	75	42	68	26
CT scan appearance	Upper zone emphysema	Normal	Diffuse emphysema in all zones	Basal emphysema	Basal emphysema & bronchiectasis	Diffuse emphysema in all zones

6.4 Discussion

The measurement of second order association rate constants in this Chapter (Table 6.1) has demonstrated that the Z variant of A1AT has an association rate constant which is half that of M variant A1AT for NE, consistent with other published results [154, 155]. In addition, the S variant of A1AT has a similar Kass with NE compared to the M variant, consistent with results published elsewhere [277]. For the current experiments, it was not possible to use serum from F or I homozygotes since no patients have been identified in the U.K. For these reasons, PiFZ or PiIZ heterozygotes were selected since Z A1AT made a relatively small contribution to the overall concentration of A1AT and studies have shown that A1AT from PiMZ heterozygotes has a similar Kass with NE to M A1AT alone [279]. The results presented in this Chapter demonstrate that IZ A1AT had a reduced Kass with NE compared to M A1AT. Mahadeva *et al* [169] previously showed that purified I A1AT had a Kass value with NE comparable to that obtained with Z A1AT, consistent with the findings of the current study. Similarly, the results presented here show that FZ A1AT has a Kass value with NE comparable to that obtained with the Z variant, and are consistent with results published by Cook *et al* [279], who used partially purified F A1AT. These observations support the validity of serum results from PiFZ and PiIZ heterozygotes in the current experiments.

Some variations in published Kass values can be found in the literature [147, 286, 287], which may relate to changes in experimental conditions. Both temperature [279] and pH [288] can affect measured Kass values. For these reasons, the experiments in this Chapter

were performed at a constant pH of 7.4 and temperature of 23°C to allow comparisons to be made between A1AT variants and between enzymes.

Serum contains A2M in addition to A1AT (which could interfere with the assays described) and therefore methylamine was added to inactivate A2M (Figure 6.1). The Kass values for M and Z variants of A1AT with NE and PR3 in these studies were similar when using pure A1AT or methylamine-treated serum, supporting the use of methylamine-treated serum for experiments involving S, F and I variants of A1AT where purified A1AT was not available.

Association rate constants for PR3 and A1AT variants (other than the M variant [117, 280]) have not been published previously. The results presented here show that normal M A1AT has a Kass value for PR3 which is ten times lower than that for NE. Therefore, in the inflammatory environment in lungs where several proteinases may be present, A1AT will preferentially inhibit NE compared to PR3, and active PR3 has the potential to drive the pathophysiological processes that influence COPD and its progression. The data presented here show that other variants of A1AT (Z, S, FZ, IZ) have similar Kass values for PR3 to that of the normal M variant, suggesting a less significant effect of mutations in A1AT on its ability to inhibit PR3. Therefore, mole for mole, these variants are equally capable of forming an enzyme-inhibitor complex with PR3 as the normal M variant, although the lower concentration of A1AT will also influence its ability as an inhibitor. For all A1AT variants studied here, the Kass with NE was greater than that with PR3 (Figure 6.3). For this reason, in addition to the greater amounts of PR3 contained within the neutrophil azurophilic granules, and the fact that PR3 is not inhibited by SLPI, it is

likely that PR3 is more important in the pathophysiology of COPD than has previously been thought, especially in subjects with A1ATD as its activity is likely to persist longer in the neutrophilic environment than NE (especially in the lung).

The association rate constants at 23ºC for both NE and PR3 with A2M have been measured previously (NE 4.1 x 10^7 $M^{-1}s^{-1}$, PR3 1.1 x 10^7 $M^{-1}s^{-1}$) [117, 190]. As discussed in Chapters 3 and 4, proteinases partition between their inhibitors depending on their local concentrations and their association rate constants. When comparing the *in vitro* association rate constants for A1AT and A2M with NE, it would appear that the rates at which M A1AT and A2M associate with NE are similar. However, the *in vivo* significance of these values must also consider that in subjects with the PiMM phenotype, the molar concentration of A1AT is approximately 10 times greater than that of A2M and therefore A1AT is the predominant inhibitor of NE especially in serum. However, PiZZ homozygotes (and PiFZ or PiIZ heterozygotes) have a lower concentration of A1AT with a lower Kass relative to A2M, which alters the partitioning of NE more towards A2M and supports the results presented in Chapter 3. PR3 on the other hand has a greater Kass with A2M compared to all A1AT variants studied here, and therefore if the concentrations of A1AT and A2M were similar (such as in PiZZ subjects), PR3 would preferentially bind to A2M. PR3 complexes with A2M can retain their proteolytic potential towards low molecular weight substrates (Chapter 4) although probably not towards high molecular weight substrates such as elastin (Chapter 5). Nevertheless, the amount of PR3 released from neutrophils is also greater and at present the physiological significance of partitioning remains uncertain.

This Chapter has not considered the contribution of SLPI to the inhibitory capacity of NE in the airways. SLPI is a reversible inhibitor of NE with a Kass of 6.4 x 10^6 $M^{-1}s^{-1}$ and a dissociation rate constant of 2.3 x 10^{-3} s^{-1} at 37ºC [289]. Elafin is also present in the lungs and is a reversible inhibitor of NE and PR3. The association and dissociation rate constants at 25ºC for elafin are 3.6 x 10^6 $M^{-1}s^{-1}$ and 6.0 x 10^{-4} s^{-1} respectively for NE [290] (although greater Kass values have been reported when using different buffers [291]), and 4.0 x 10^6 $M^{-1}s^{-1}$ and 1.7 x 10^{-3} s^{-1} respectively for PR3 [291], which again adds complexities to the local dynamics. The contribution of these inhibitors in the upper airways is considered further in Chapter 9.

The F variant of A1AT has not been studied in detail previously and has been classified as a normal variant since it is present in near normal A1AT concentrations in the circulation. However, co-inheritance of the F allele with a deficiency allele has been described and is associated with an increased susceptibility to emphysema and liver disease [165]. To date, no PiFF homozygotes have been reported in the literature, although there has been one case report of an individual with COPD and the PiFnull phenotype [166]. The U.K. A1ATD national registry contains six PiFZ heterozygotes (Table 6.2). All six subjects had A1AT concentrations above the generally accepted protective threshold of 11µM, comparable with concentrations found in PiMZ heterozygotes who are not believed to be at particular risk of emphysema. Five of the PiFZ subjects had evidence of emphysema on their CT scan which was panacinar emphysema with a lower zone predominance (usually associated with PiZZ homozygotes) in two. These findings could have clinical consequences because measurement of A1AT concentration alone would not identify carriers of the F allele, and PiFZ heterozygotes possibly have an increased risk of

developing emphysema by a concentration-independent mechanism, although referral bias could have influenced these findings.

Many of the mutations of A1AT that have been implicated in the deficiency phenotypes are associated with reduced serum concentrations of A1AT. In many cases, this is the result of the mutation perturbing the structure of the serpin leading to polymerisation [173]. The F mutation does not appear to produce a deficiency phenotype and its susceptibility to polymerisation has not been reported in the literature to date, but instead results in a reduction in Kass which in turn may predispose to disease. This suggests that the position of the mutation (arginine replaced by cysteine at position 223) specifically disrupts the inhibitory mechanism of A1AT. Examination of the structure of A1AT shows that the mutation is in the C-sheet underlying the RCL. With the normal M variant, an arginine at position 223 forms an electrostatic interaction with the side chain of glutamate 354 in the RCL [292]. However, with the F variant, the cysteine at position 223 cannot make this electrostatic interaction and the consequence is likely to be a disruption of the RCL architecture which alters the conformation of the P1-P1' region and may explain the reduced Kass observed here.

In conclusion, this Chapter has demonstrated that A1AT (M, Z, S, F and I variants) has a lower association rate constant for PR3 than NE, and therefore in situations where the concentration of A1AT is insufficient to inhibit both proteinases, NE would be preferentially inhibited. Uninhibited PR3 can replicate the pathological features of COPD associated classically with NE. This Chapter has also highlighted the importance of considering not only the concentration of inhibitors present, but also their function. Some

clinicians may exclude a diagnosis of A1ATD based on a normal A1AT concentration. However, the F variant in particular is associated with normal serum levels of A1AT but is dysfunctional in its ability to inhibit NE activity. Therefore if A1ATD is suspected clinically, phenotyping and genotyping should be requested.

7 *In vitro* effects of A1AT augmentation therapy

7.1 Introduction

Intravenous augmentation therapy by the infusion of pooled human A1AT is currently the most direct and efficient means of elevating A1AT levels in the plasma and in the lung interstitium [293, 294]. Population and *in vitro* studies suggest a minimum plasma threshold A1AT level of 11μM, below which there is insufficient A1AT to protect the lung effectively, leading to an increased risk of developing emphysema [157, 159].

An early study looking at clinical efficacy of augmentation therapy was conducted by Seersholm *et al* [295]. They compared the rate of FEV1 decline amongst 97 former smokers from Denmark with severe A1AT deficiency (PiZZ or Znull) who did not receive augmentation therapy with the rate of decline in 198 severely deficient (PiZZ) German former smokers who received weekly infusions over a mean of 3.2 years. Overall, the rate of decline of FEV1 was lower amongst the treated German patients than amongst the untreated Danish patients (-53 mL per year versus -75 mL per year, p=0.02), with subset analysis showing that the overall difference was mainly due to an effect of augmentation therapy in subjects with an FEV1 between 31 and 65 percent predicted.

The U.S. National Registry of Patients with Severe Deficiency of Alpha 1-Antitrypsin conducted a multi-centre, prospective cohort study sponsored by the National Heart, Lung, and Blood Institute of the National Institutes of Health (NHLBI) [296]. Published data from the Registry showed that survival was enhanced in recipients of augmentation therapy compared with non-recipients [296]. In the subset of patients with FEV1 35 to 49

percent predicted, the rate of FEV1 decline was also slowed in recipients of augmentation therapy. Subsequently, a meta-analysis [297] demonstrated that the protective effect of augmentation therapy (as determined by FEV1 decline) reflected predominantly the results from a subset of patients with FEV1 30 to 65 percent predicted.

Other observational studies indicative of the efficacy of augmentation therapy include those by Lieberman [298] and Stockley *et al* [299]. Lieberman retrospectively determined that the use of augmentation therapy reduced the frequency of lung infections as reported by the patients. Stockley *et al* found that augmentation therapy led to a rise in sputum A1AT concentrations and a fall in sputum leukotriene B4 suggesting an anti-inflammatory effect that may be a surrogate for efficacy.

Interpretation of these data remains complex. Effects on the decline in FEV1 would only be detectable when it is declining fastest. Furthermore, patients receiving regular infusions also get weekly exposure to health care professionals, which could influence exacerbation rate and mortality. These issues clearly affect the robust nature of any conclusions from such observational studies. In addition, the reduction in inflammation alone does not necessarily predict clinical outcome. Therefore, the importance of conducting randomised controlled studies was highlighted.

A randomised controlled trial was first performed by Dirksen *et al* [300], who allocated 28 PiZZ subjects to receive intravenous A1AT infusions for at least 3 years and a further 28 PiZZ subjects to receive placebo infusions. No differences were observed in the rate of

decline in FEV1 between the two groups. However, when analysing the results of CT densitometry, a trend was noted towards a slower annual rate of loss of lung density in those receiving augmentation therapy. This difference did not however achieve the pre-determined level of statistical significance (p=0.07).

The EXAcerbations and Computed Tomography scan as Lung End-points (EXACTLE) study [301] explored the use of CT densitometry and exacerbations for the assessment of the therapeutic effect of augmentation therapy in subjects with A1ATD. This was a randomised, double-blind, placebo-controlled, parallel-group study conducted at three European centres. Seventy seven patients (PiZZ) were randomised to weekly infusions of pooled human A1AT or placebo for 2-2.5 years. CT densitometry demonstrated a significant decline in both groups over the course of the study ($p<0.001$ for both groups), consistent with emphysema progression. There was once again a trend towards benefit in the treated group although this did not reach statistical significance using the primary analysis methodology (p=0.07). No significant differences were found in FEV1 or gas transfer decline between the two groups. Exacerbation frequency was unaltered by treatment, but a reduction in exacerbation severity was observed in the treatment group. A subsequent analysis of this data by Parr *et al* [302] showed that a beneficial effect was present if analysis was confined to the basal region where the emphysema predominates.

The overall results of a combined analysis of these 2 randomised controlled trials (thereby increasing the numbers) concluded that intravenous augmentation therapy reduces the decline in lung density as measured by CT scanning [303].

A1AT replacement therapy delivered by inhalation may be an alternative therapeutic option. In animal studies, inhaled A1AT provides protection against the development of cigarette smoke-induced emphysema [304]. Human phase 2-3 studies of inhaled A1AT in A1ATD subjects with emphysema are currently underway [305], although the primary outcome is exacerbation frequency and severity.

This Chapter aims to study the *in vitro* effects of A1AT augmentation of serum samples from subjects with varying A1AT genotypes (PiSZ, PiFZ, PiZZ) and its effect on partitioning of NE or PR3 between the serum inhibitors A1AT and A2M. These experiments were designed to test the hypothesis that serum from A1ATD individuals augmented with M variant A1AT would give *in vitro* results for inhibiting NSP activities similar to those seen with normal (PiMM) serum. The amount of M A1AT used was initially chosen to mimic the nadir values seen in PiZZ subjects receiving weekly augmentation therapy, although the effect of augmenting to greater thresholds was also explored. PiSZ and PiFZ sera were augmented up to A1AT concentrations found in PiMM homozygotes.

7.2 Methods

7.2.1 Inhibition of NE by serum samples augmented *in vitro* with M A1AT (SlaaapN)

Serum samples were obtained from subjects with PiSZ, PiFZ and PiZZ genotypes and A1AT concentration was determined by ELISA as shown in Table 3.1. Pure M A1AT of

pre-determined activity was added to the serum samples in order to augment the A1AT concentration into a pre-determined range. The PiSZ and PiFZ sera were augmented to A1AT concentrations equivalent to those of PiMM homozygotes (>25μM for the purposes of these experiments). The PiZZ serum was augmented to various A1AT concentrations; 11μM which was taken as the nadir value in subjects receiving weekly augmentation therapy and has been recognised as the "protective threshold," 20μM which is equivalent to the average concentration found in PiMZ heterozygotes, and 30μM which is similar to the average concentration found in PiMM homozygotes. The augmented serum samples were then diluted in NE assay buffer to an A1AT concentration of 1.5μM. Pure NE of pre-determined activity was also diluted to 1.5μM in NE assay buffer and the NE inhibition assays were performed using the methods described in section 3.2.1.1 with SlaaapN (1mg/ml in NE assay buffer) as the substrate. Serum samples with or without added A1AT were assayed on the same plate to allow comparison of the results.

7.2.2 Inhibition of NE by serum samples augmented *in vitro* with M A1AT (elastin-fluorescein)

The same serum samples were used as those in section 7.2.1, except the PiZZ serum was augmented only to 11μM. The samples were then diluted in elastin buffer to an A1AT concentration of 1.5μM. Pure NE of pre-determined activity was diluted to 1.5μM in elastin buffer and the NE inhibition assays were performed using the methods described in section 5.2.2 with elastin-fluorescein as the substrate. Again, serum samples with or without added A1AT were assayed together to allow comparison of the results. Due to limitations on time and resources, these experiments were not performed with PR3.

7.2.3 Inhibition of PR3 by serum samples augmented *in vitro* with M A1AT (MSaapvN)

The same serum samples were used as those in section 7.2.2 but with the PiZZ serum being augmented to 30µM. The samples were then diluted in NSP assay buffer to an A1AT concentration of 1.5µM. Pure PR3 of pre-determined activity was diluted to 1.5µM in NSP assay buffer and the PR3 inhibition assays were performed using the methods described in section 3.2.2.2 with MSaapvN (0.2mg/ml in NSP assay buffer) as the substrate. Again, serum samples with or without added A1AT were assayed together to allow comparison of the results.

7.3 Results

7.3.1 Inhibition of NE by serum samples augmented *in vitro* with M A1AT (SlaaapN)

The results of the NE inhibition assays using PiSZ, PiFZ and PiZZ sera with and without augmentation with M variant A1AT are shown in Figures 7.1, 7.2 and 7.3 respectively, using SlaaapN as the substrate. These results demonstrate that the addition of M A1AT to serum from A1ATD subjects (PiSZ, PiFZ and PiZZ genotypes) changed the pattern of the NE inhibition slopes by reducing the residual NE activity (when the A1AT was in a molar excess). Furthermore, augmentation of PiZZ serum to 20µM led to a greater reduction in the residual NE activity than augmentation to 11µM. No enhancement of NE activity above that of free enzyme was observed in the augmented PiZZ samples studied here.

Figure 7.1- Inhibition of NE with PiSZ serum ± augmentation with M A1AT (SlaaapN)

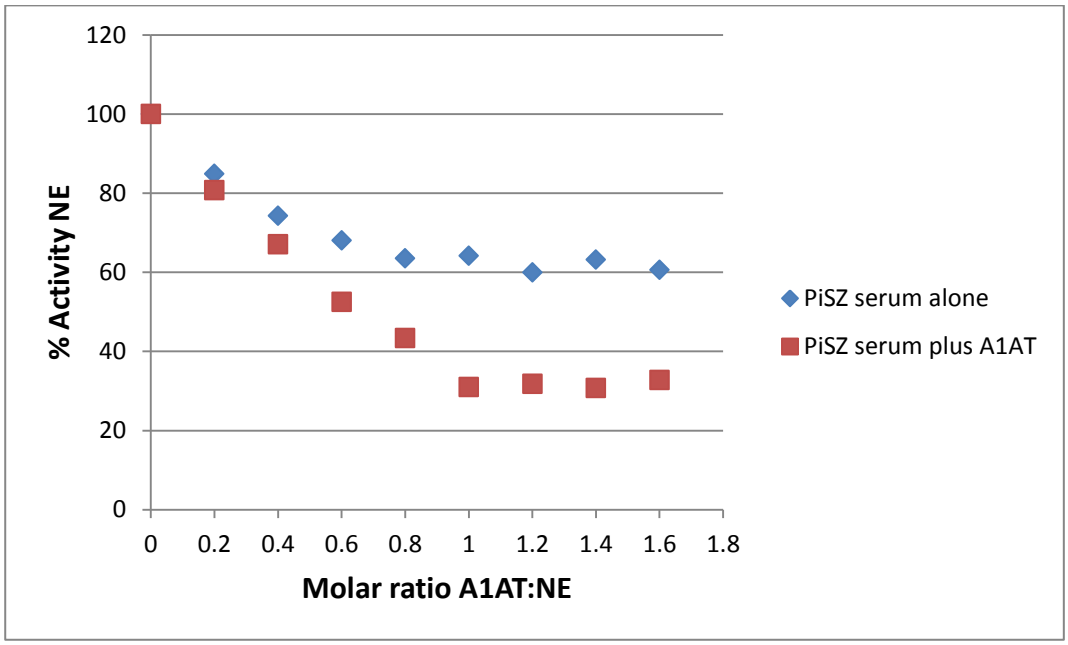

Figure 7.1: Inhibition of NE activity using PiSZ serum with or without augmentation with M A1AT to an A1AT concentration equivalent to that found in a PiMM homozygote. SlaaapN was used as the substrate. Points show the mean of triplicate results from a single plate.

Figure 7.2- Inhibition of NE with PiFZ serum ± augmentation with M A1AT (SlaaapN)

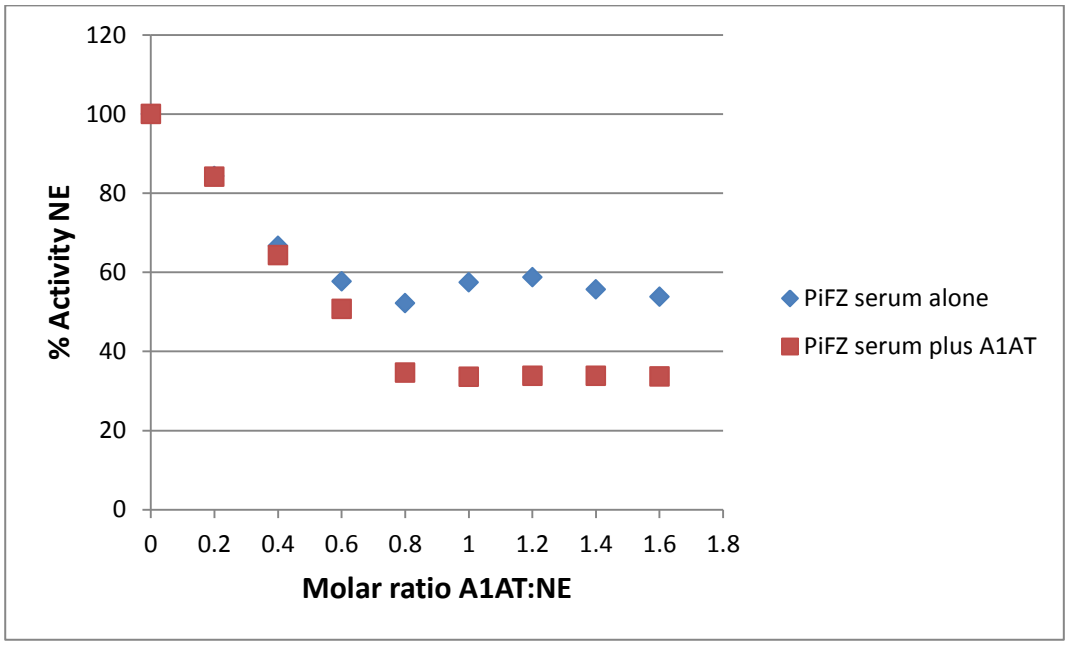

Figure 7.2: Inhibition of NE activity using PiFZ serum with or without augmentation with M A1AT to an A1AT concentration equivalent to that found in a PiMM homozygote. SlaaapN was used as the substrate. Points show the mean of triplicate results from a single plate.

Figure 7.3- Inhibition of NE with PiZZ serum ± augmentation with M A1AT (SlaaapN)

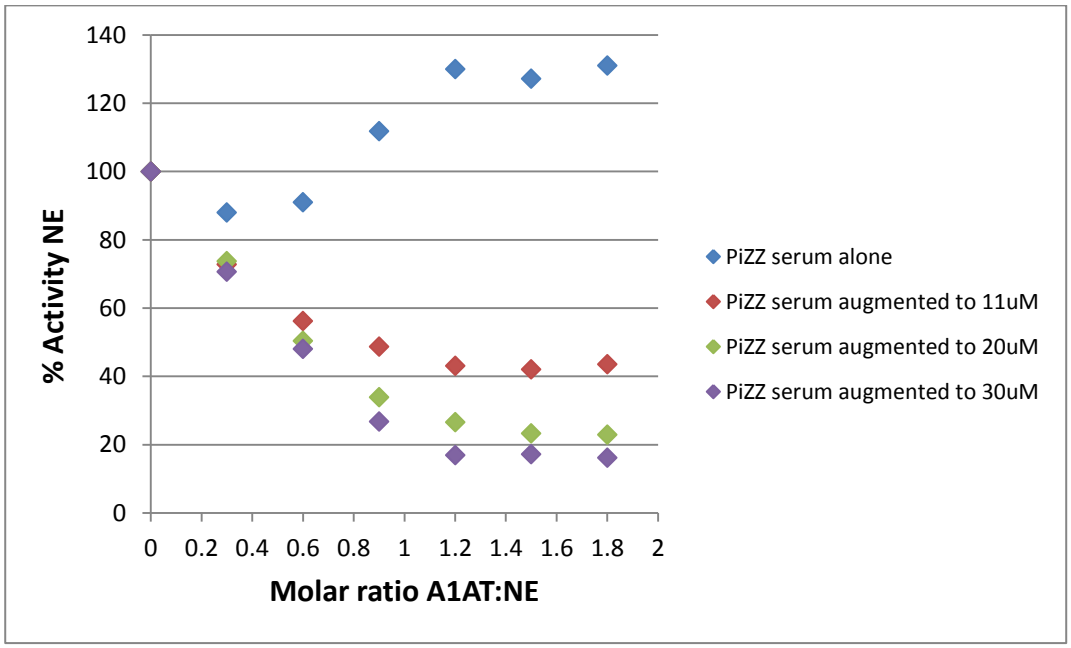

Figure 7.3: Inhibition of NE activity using PiZZ serum with or without augmentation with M A1AT. Augmentation to greater A1AT concentrations reduced the residual activity of NE (when A1AT was in a molar excess). The rationale for the A1AT concentrations used is given in the text. SlaaapN was used as the substrate and the enhanced NE activity observed when PiZZ serum was used alone has been noted previously (Chapters 3 and 4). Points show the mean of triplicate results from a single plate.

7.3.2 Inhibition of NE by serum samples augmented *in vitro* with M A1AT (elastin-fluorescein)

The results of the NE inhibition assays using PiSZ, PiFZ and PiZZ sera with and without augmentation with M variant A1AT and using elastin-fluorescein as the substrate are shown in Figures 7.4, 7.5 and 7.6 respectively. The NE inhibition slopes were similar for PiSZ, PiFZ and PiZZ sera with or without the addition of M A1AT. However, the results show the molar ratios of A1AT to NE, and do not take into account the greater A1AT concentrations in augmented sera compared to non-augmented sera.

Figure 7.4- Inhibition of NE with PiSZ serum ± augmentation with M A1AT (elastin-fluorescein)

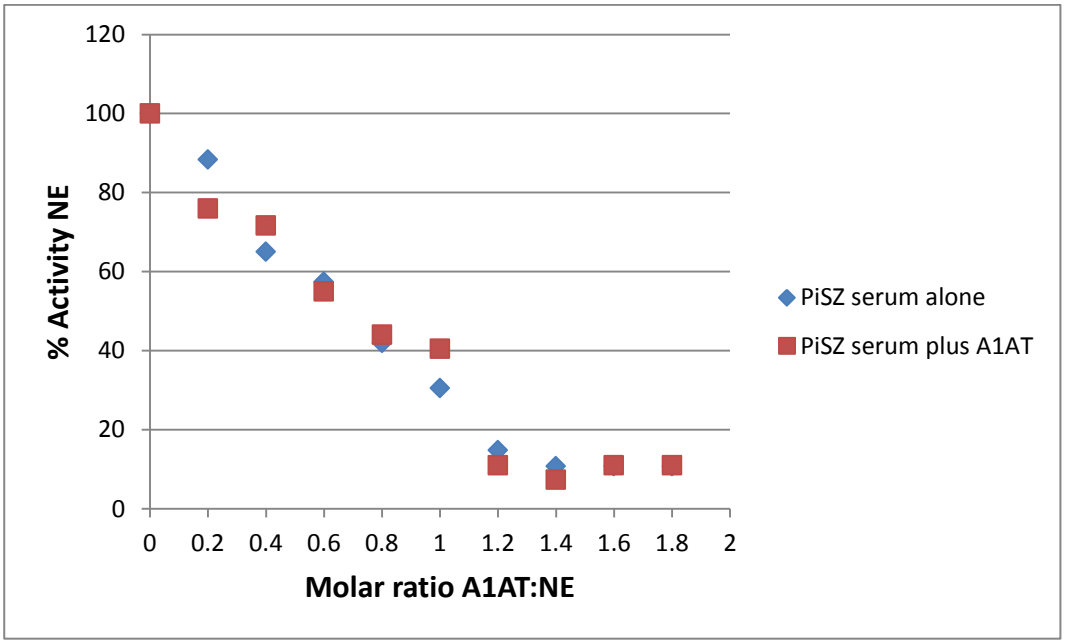

Figure 7.4: Inhibition of NE activity using PiSZ serum with or without augmentation with M A1AT to an A1AT concentration equivalent to that found in a PiMM homozygote. Elastin-fluorescein was used as the substrate. Results from single experiments are shown.

Figure 7.5- Inhibition of NE with PiFZ serum ± augmentation with M A1AT (elastin-fluorescein)

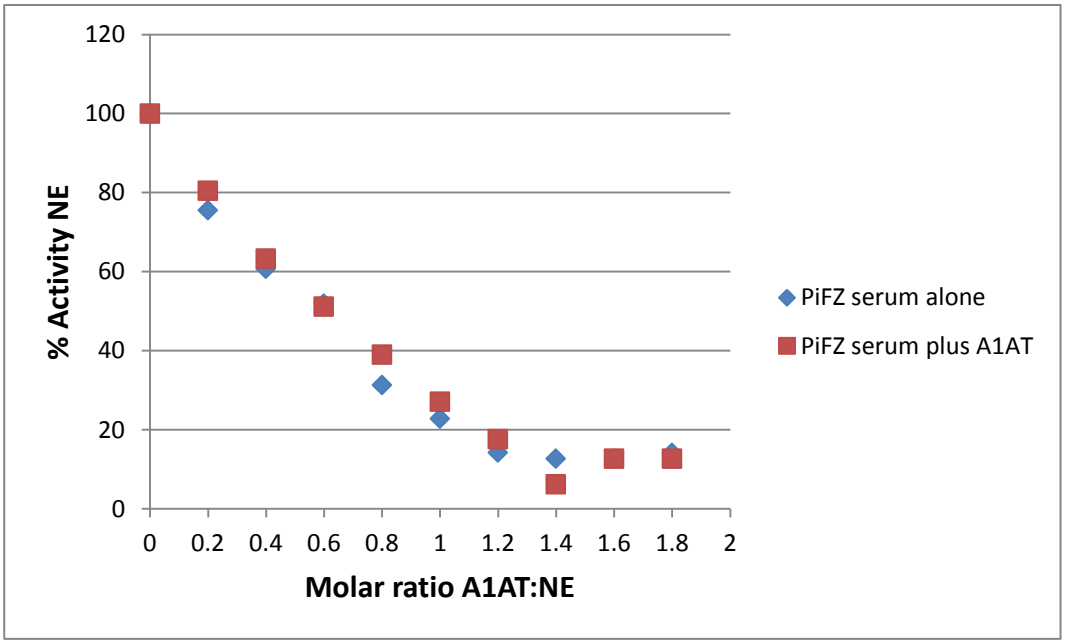

Figure 7.5: Inhibition of NE activity using PiFZ serum with or without augmentation with M A1AT to an A1AT concentration equivalent to that found in a PiMM homozygote. Elastin-fluorescein was used as the substrate. Results from single experiments are shown.

Figure 7.6- Inhibition of NE with PiZZ serum ± augmentation with M A1AT (elastin-fluorescein)

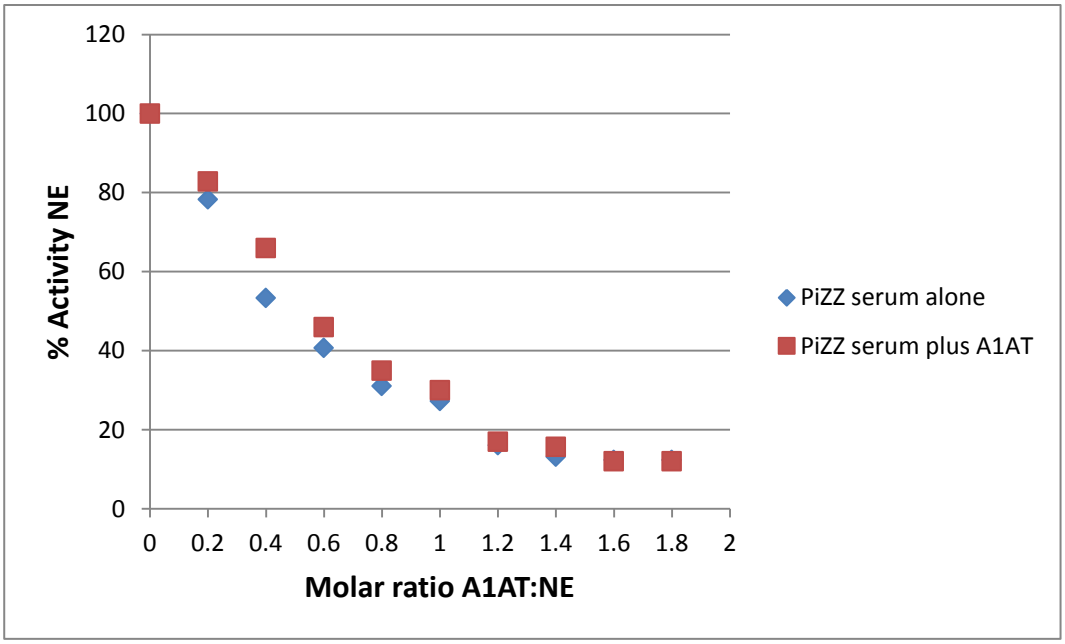

Figure 7.6: Inhibition of NE activity using PiZZ serum with or without augmentation with M A1AT to an A1AT concentration of 11µM. Elastin-fluorescein was used as the substrate and results from single experiments are shown.

7.3.3 Inhibition of PR3 by serum samples augmented *in vitro* with M A1AT (MSaapvN)

The results of the PR3 inhibition assays using PiSZ, PiFZ and PiZZ sera with and without augmentation with M A1AT and using MSaapvN as the substrate are shown in Figures 7.7, 7.8 and 7.9 respectively. The results demonstrate that the addition of M A1AT to serum from A1ATD subjects (PiSZ, PiFZ and PiZZ genotypes) changed the pattern of the PR3 inhibition slopes by reducing the residual PR3 activity (when A1AT was in a molar excess).

Figure 7.7- Inhibition of PR3 with PiSZ serum ± augmentation with M A1AT (MSaapvN)

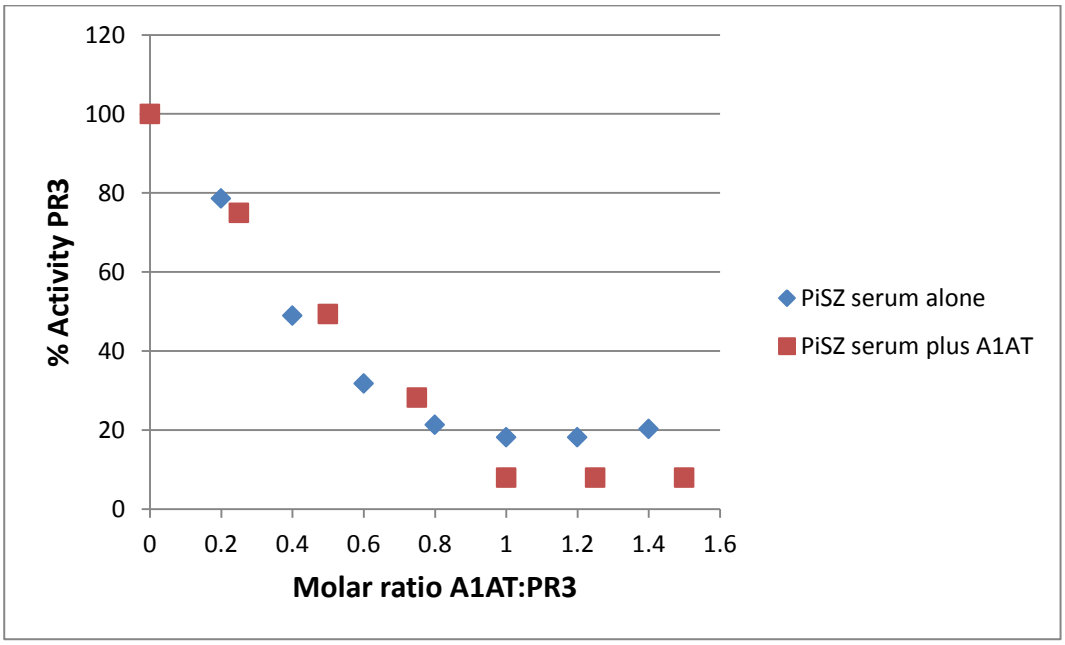

Figure 7.7: Inhibition of PR3 activity using PiSZ serum with or without augmentation with M A1AT to an A1AT concentration equivalent to that found in a PiMM homozygote. MSaapvN was used as the substrate. Points show the mean of triplicate results from a single plate.

Figure 7.8- Inhibition of PR3 with PiFZ serum ± augmentation with M A1AT (MSaapvN)

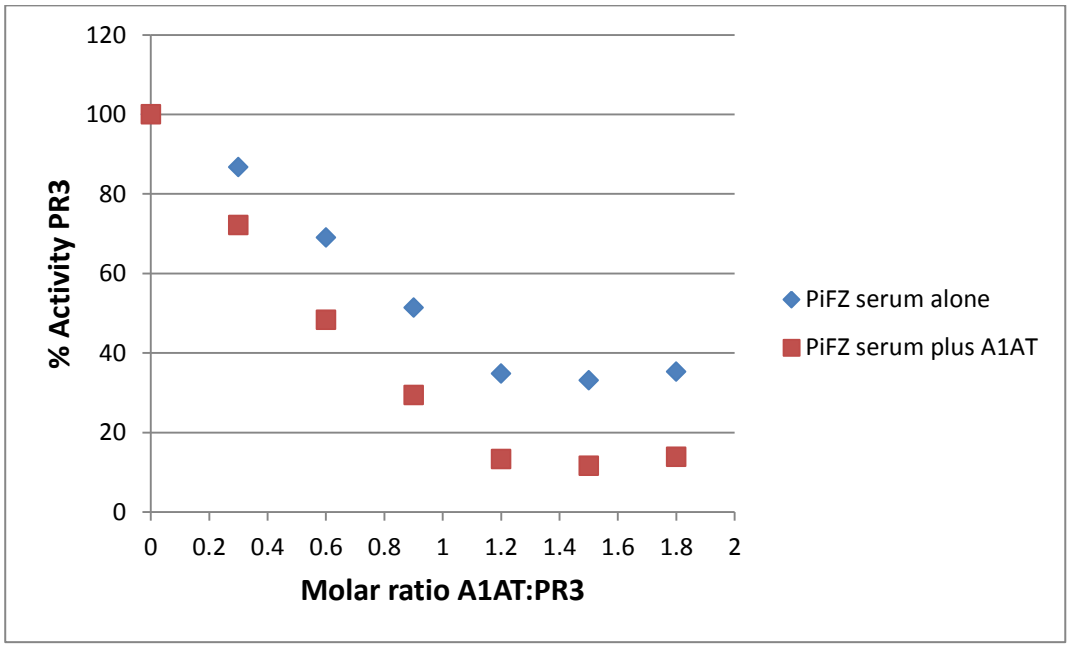

Figure 7.8: Inhibition of PR3 activity using PiFZ serum with or without augmentation with M A1AT to an A1AT concentration equivalent to that found in a PiMM homozygote. MSaapvN was used as the substrate. Points show the mean of triplicate results from a single plate.

Figure 7.9- Inhibition of PR3 with PiZZ serum ± augmentation with M A1AT (MSaapvN)

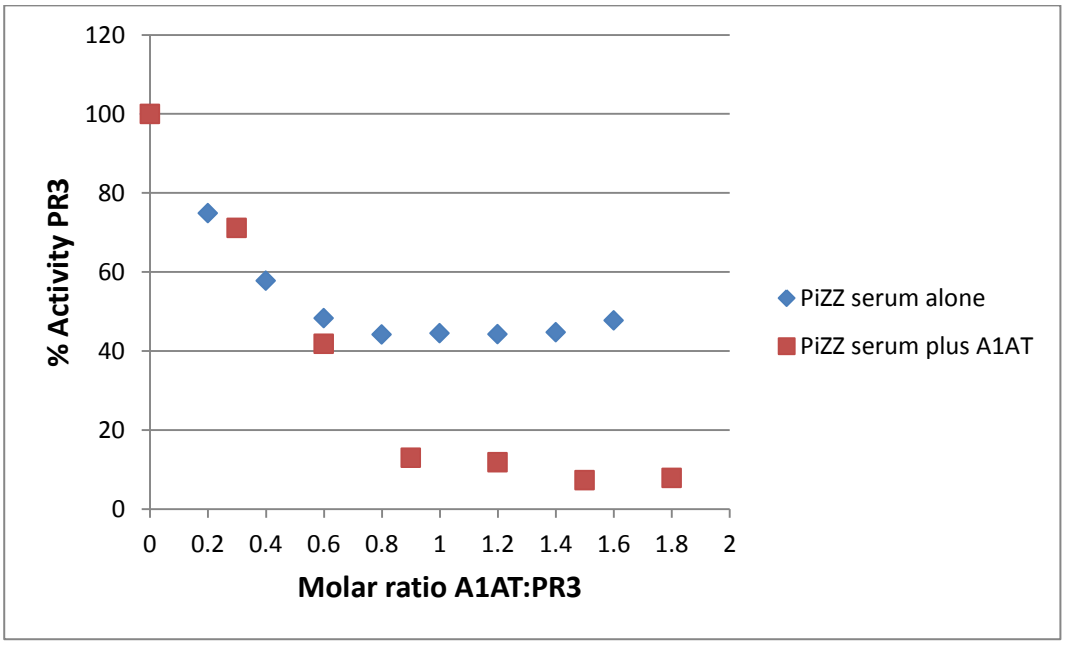

Figure 7.9: Inhibition of PR3 activity using PiZZ serum with or without augmentation with M A1AT to an A1AT concentration equivalent to that found in a PiMM homozygote. MSaapvN was used as the substrate. Points show the mean of triplicate results from a single plate.

7.4 Discussion

The NE inhibition assays using SlaaapN as the substrate (Figures 7.1, 7.2 and 7.3) demonstrate that the addition of M A1AT to serum from A1ATD subjects (PiSZ, PiFZ and PiZZ genotypes) changes the pattern of the NE inhibition slopes. Since the graphs show the molar ratios of A1AT to NE on the x-axis, these changes are not related to concentration of A1AT alone but likely reflect a change in the partitioning between the two proteinase inhibitors A1AT and A2M as described in Chapters 3 and 4. When M A1AT was added to PiSZ and PiFZ sera, there was a reduction in the residual baseline activity of NE (when A1AT was in a molar excess) from around 60% to 30%, approaching

that seen with PiMM serum (Figure 3.1). This change in the partitioning between the inhibitors results in less NE being bound to A2M in the augmented samples (where it shows enhanced activity towards SlaaapN), and a greater proportion being bound to A1AT where it is inactivated. Similarly, when M A1AT was added to PiZZ serum (Figure 7.3), there was a reduction in the residual baseline activity of NE which was greater when the PiZZ serum was augmented to 20μM than to 11μM. Furthermore, following the addition of M A1AT there was no longer any enhancement of NE activity above that of free NE. Again, this is likely to be due to a shift in the partitioning of NE towards binding to A1AT where it is inactivated and therefore less binding to A2M where it shows enhanced activity towards this substrate. In PiZZ homozygotes, not only is the concentration of A1AT reduced in serum (and hence the ratio of A2M:A1AT is increased), the Kass for NE and Z A1AT is lower than the Kass for NE and A2M (Chapter 6) which favours binding of released NE to A2M. Augmentation with M A1AT (which has a similar Kass with NE to that of A2M) therefore shifts the partitioning of released NE towards being inactivated by A1AT. Thus the amount of NE that complexes with A2M would be dramatically reduced which may reduce the clinical consequences.

The NE inhibition assays using elastin-fluorescein as the substrate (Figures 7.4, 7.5 and 7.6) showed that the NE inhibition slopes were similar for PiSZ, PiFZ and PiZZ sera with and without the addition of M A1AT. However, the results show the inhibitory potential of the samples (as shown by molar ratio of A1AT to NE) and not the capacity, since augmented serum has a greater A1AT concentration than non-augmented serum. The results presented in this Chapter are consistent with those presented in Chapter 5, which demonstrated that the pattern of NE inhibition was similar for PiZZ and PiMM sera, and that A1AT was less functional as an inhibitor of NE when elastin-fluorescein was used as

the substrate (extrapolation of the slopes in Figures 7.4, 7.5 and 7.6 to the x-axis suggests that NE is inhibited when the molar ratio of A1AT:NE is 1.2-1.4:1). The lack of difference observed here in the residual baseline activities of NE (when the A1AT was in a molar excess) between augmented and non-augmented samples may potentially be because A2M:NE complexes are less active towards elastin than against low molecular weight peptide substrates. Potentially, a proportion of these complexes may contain two molecules of NE which would not be simultaneously active towards a macromolecular substrate such as elastin, leading to a saturation effect. Although PR3 inhibition assays were not performed using augmented serum with elastin-fluorescein as the substrate, earlier results (Chapter 5) suggested that PiZZ serum could completely inhibit PR3 activity towards elastin with a molar ratio for A1AT:PR3 of 1:1, similar to results found with PiMM serum.

The PR3 inhibition assays using MSaapvN as the substrate (Figures 7.7, 7.8 and 7.9) demonstrate that the augmentation of PiSZ, PiFZ or PiZZ sera alters the pattern of the inhibition slopes in a similar manner to that observed with NE when using a low molecular weight peptide substrate. The baseline activities of PR3 in the augmented serum samples were reduced compared to the non-augmented samples, which again likely represents a change in the partitioning of PR3 between its serum inhibitors, with a greater proportion of PR3 being inactivated by A1AT in the augmented samples. Any physiological significance of active PR3 complexes with A2M remains uncertain at present.

Future studies could explore the inhibitory capacity of serum from A1ATD patients before and after receiving intravenous augmentation therapy to gain a closer insight into the effects of augmentation therapy *in vivo*. Earlier experiments (Chapters 3 and 4) have

suggested that A1AT does not inhibit NE or PR3 bound to A2M, and poorly inhibits NE bound to elastin and therefore augmentation therapy would be less efficacious where enzyme is released in high concentrations and close to connective tissue. However, weekly intravenous augmentation therapy does result in serum A1AT levels that exceed the protective threshold over the full dosing interval and the A1AT maintains its functional activity [286]. The effects of local A1AT concentration on neutrophil cell surface expression of NE and PR3 are explored further in Chapter 8.

In summary, this Chapter has demonstrated that augmentation of A1ATD serum *in vitro* changes the pattern of the NE and PR3 inhibition slopes towards that found with PiMM serum when peptide substrates were used. Greater concentrations of M A1AT were associated with a greater reduction of the residual baseline activities of NE and PR3 and hence a reduction in the proportion of these NSPs bound to A2M (where they retain proteolytic activity). Furthermore, in PiZZ serum, augmentation to an A1AT concentration of 20μM had a greater impact on these characteristics than augmentation to the accepted protective threshold of 11μM.

8 Neutrophil cell surface expression of proteinases

8.1 Introduction

Earlier Chapters have studied the ability of normal (PiMM) and A1ATD (PiZZ) sera to inhibit activity of NSPs and the *in vitro* effects of altering the A1AT concentration by augmentation therapy. In this Chapter, the neutrophil cell surface expression of NE and PR3 has been studied in subjects with A1ATD (PiZZ), usual COPD (PiMM) and healthy controls (PiMM), as well as the local effects of A1AT concentration on neutrophil expression of these NSPs. NSPs bound to the cell membrane of stimulated neutrophils remain catalytically active towards both synthetic peptide and high molecular weight biological substrates such as fibronectin [54, 108, 240, 306]. This activity of membrane-bound NSPs could facilitate penetration through tissue barriers and enable local degradation of extracellular matrix proteins without significant injury to surrounding tissues. However, excessive cell surface NSP activity may also play a role in the pathogenesis of disease.

NE and CG are minimally expressed on quiescent neutrophils [54] whereas PR3 is constitutively expressed on the surface of quiescent neutrophils from healthy controls [108] but may not be active on these cells [307]. This constitutively expressed PR3 is unlikely to originate from the azurophilic granules since other markers of granule exocytosis are not present [308]. The proportion of cells constitutively expressing PR3 on their surfaces has been reported to vary amongst individuals but remains stable in each individual over time, suggesting a genetic background to this feature [308]. This hypothesis has been supported by both family and twin studies [309, 310].

Stimulation of neutrophils by chemoattractants or cytokines results in the mobilisation of the azurophilic granules to the cell surface and increased membrane expression of PR3, NE and CG [51]. Exposure of neutrophils to exogenous NSPs also results in greater membrane expression of NSPs, suggesting that proteinases can spontaneously bind to sites on the neutrophil cell membrane [54]. The mechanism of binding of NE and CG to the neutrophil cell membrane is by a charge-dependent mechanism. These cationic proteineases bind to the negatively charged sulphate groups of heparan sulphate and chondroitin sulphate containing proteoglycans [306]. However, PR3 binding to the cell membrane does not occur in a charge-dependent manner [102]. David *et al* [311] suggested that membrane-bound PR3 co-localises with the adhesion molecule beta-2 integrin (CD11b/CD18). Subsequent experiments have suggested that PR3 binding to the cell membrane is likely to occur via the glycosylphosphatidylinositol (GPI)-anchored neutrophil receptors FcγRIIIb (CD16b) [312] and/or the NB1 (CD177) receptor [313], although the exact mechanism has not been fully elucidated and requires further investigation [314]. A physiological role for membrane-bound PR3 has been suggested by Kim *et al* [315] in mediating phagocytosis of non-opsonized bacteria. In addition, PR3 is expressed on the cell membrane at an early stage of apoptosis, in the absence of degranulation [316]. This PR3 expression decreases macrophage phagocytosis, delaying neutrophil clearance [317] and potentially amplifies inflammatory processes and autoimmunity.

PR3 is a major antigenic target of ANCAs in Wegener's granulomatosis (WG) [115]. ANCAs can bind to PR3 expressed on neutrophil cell membranes and amplify cell

activation. Neutrophil activation occurs when ANCAs cross-link PR3 with FcγRIIa (CD32) inducing the oxidative burst [314, 318, 319]. Witko-Sarsat *et al* reported that individuals with WG had a greater proportion of neutrophils expressing PR3 on their cell membrane compared to healthy controls [310] but did not find any relationship with disease activity or treatment. In contrast, others have reported that neutrophil PR3 expression is greater with acute vasculitis and lower during remission of disease [320, 321]. Overall, cell membrane expression of PR3 seems to be related to WG but the mechanisms of this association remain uncertain. In addition, a deficiency of A1AT (the major circulating inhibitor of PR3) is a risk factor for WG [228]. Campbell *et al* [108] demonstrated that exogenous PR3 could bind to the neutrophil cell membrane in a dose-dependent manner. Therefore, it could be hypothesized that in subjects with a deficiency of A1AT, the concentration of free PR3 in the vicinity of activated neutrophils (following degranulation) would be greater than in subjects with normal concentrations of A1AT (due to local A1AT binding to PR3), and thus PR3 binding to the neutrophil cell membranes may also be greater with A1ATD.

These concepts are explored further in this Chapter by measuring NE and PR3 expression on the cell surface of neutrophils from A1ATD subjects, non-deficient COPD subjects and healthy controls. Experiments have also been performed to study the local effects of A1AT concentration on neutrophil surface expression of NE and PR3. As described above, NSPs on the neutrophil cell membrane may play a role in disease due to their persistent activity.

8.2 Methods

8.2.1 Subject selection

For the experiments where neutrophil cell surface expression of NE and PR3 were measured, nine clinically stable subjects with A1ATD (PiZZ or PiZnull phenotypes) who met the diagnostic criteria for COPD were identified from the UK national registry for A1ATD, and were recruited during outpatient appointments. Nine healthy controls who were partners of patients with A1ATD (and therefore age-matched) were also recruited. The healthy controls had a normal PiMM A1AT genotype, no significant medical history, normal spirometry, were on no regular medication and were non- or ex-smokers. In addition, six clinically stable subjects with usual COPD (PiMM A1AT phenotype) were recruited from outpatient clinics. All subjects had basic demographic data collected, venous blood was collected and neutrophils were extracted (as described in section 2.2.2) and prepared for flow cytometry as described below.

For the experiments studying the local effects of A1AT concentration on neutrophil cell surface expression of NE and PR3, six subjects with A1ATD (PiZZ phenotype) and six healthy controls were recruited. Venous blood was collected both for neutrophil extraction and for plasma.

8.2.2 Preparation of neutrophils for flow cytometry

Neutrophils were used either unstimulated or stimulated with 100nM N-formyl-methionine-leucine-phenylalanine (fMLP; Sigma, UK). The freshly extracted neutrophils were suspended in RPMI 1640 medium (Sigma, UK) in two aliquots; one had fMLP added

for comparison with unstimulated cells. The neutrophil solutions were incubated at room temperature for 30 minutes. Following incubation, the tubes were centrifuged at 460 x g for 10 minutes at room temperature and the supernatants (containing the stimulant in one of the tubes) were removed. The neutrophils were then re-suspended in RPMI 1640 medium without stimulant.

The cells were prepared for flow cytometry in a flexible u-bottomed 96-well plate (Fisher, UK). The wells were labelled and coated with 2% BSA (Sigma, UK) in PBS to minimise cell adhesion to the plate. The neutrophil solutions (200µL) were added to the labelled wells, and the plate was centrifuged at 300 x g for 4 minutes at 4ºC. The supernatants were removed and 50µL of labelled antibodies were added per well. The antibodies used were mouse monoclonal PR3 labelled with fluorescein isothiocyanate (FITC) (abcam, UK) and mouse monoclonal NE antibody (AbD Serotec, UK) labelled with Alexa Fluor 647 using a monoclonal antibody labelling kit (Invitrogen, UK). The antibodies were diluted in 2% BSA in PBS and the optimal dilution of the antibody was determined by performing titration experiments with a range of antibody concentrations. Wells for isotype controls and cells only were included, the latter had only 2% BSA added. The plate was incubated on ice and protected from light for 20 minutes. Following this time period, the cells were washed by adding 2% BSA to all of the wells and spinning the plate in the centrifuge as before. This step was repeated to ensure that any free antibody was removed. The cells were then re-suspended in 2% BSA and added to round bottom tubes suitable for flow cytometry.

Analysis was performed using an Accuri® C6 flow cytometer. Neutrophils were gated based on their forward scatter (FS) and side scatter (SS), and a second gate based on cell width was used to ensure that single cells only were counted. Ten thousand events were recorded for each measurement. The mean fluorescence intensities (MFI) were recorded for cells labelled with PR3 and NE antibodies (following subtraction of the control MFI), and the percentage of cells expressing each proteinase was also measured.

Results presented in this Chapter for PR3 and NE expression on the neutrophil cell membrane are primarily presented in the arbitrary units of MFI (following subtraction of the control MFI). However, the results showing the percentage of cells expressing each proteinase are also discussed for completeness, but not presented graphically.

8.2.3 Determining the effect of A1AT on PR3 and NE expression on the neutrophil cell membrane

Neutrophils were extracted as described in section 2.2.2 and diluted to a concentration of 2 million cells per ml in RPMI 1640 medium. Six 1ml aliquots of the neutrophil solution were measured into 15ml Falcon tubes, which had been coated with 2% BSA to minimise cell adhesion. The tubes were centrifuged at 460 x g for 10 minutes at room temperature and the supernatants were removed to leave a pellet of cells. The cells were then re-suspended in either RPMI 1640 medium (2 tubes), PiZZ plasma (2 tubes) or PiMM plasma (2 tubes). For each pair of tubes, neutrophils were either unstimulated in one tube or stimulated with 100nM fMLP in the second tube. The solutions were incubated at room temperature for 30 minutes and subsequently the tubes were centrifuged at 460 x g for 10 minutes and the supernatants removed. The neutrophils were then re-suspended in RPMI

1640 medium without stimulant and prepared for flow cytometry as described above. Analysis was performed using an Accuri® C6 flow cytometer as described above.

8.2.4 Statistical analysis

Statistical analyses were performed using PASW statistics 18 for Windows. Normality was tested using the Kolmogorov-Smirnov test. For non-parametric data, Mann-Whitney U tests or Wilcoxon signed rank tests were used for comparisons of independent or paired samples respectively. For normally distributed data, independent or paired T-tests were used for comparisons of independent or related samples respectively. When comparing neutrophil cell surface expression of NE and PR3 in the three subject groups, two tailed p-values were used. To test the hypothesis that NE and PR3 expression on the neutrophil cell surface is greater when the surrounding A1AT concentration is reduced, one tailed p-values were used. Results were deemed statistically significant if $p \leq 0.05$.

8.3 Results

8.3.1 Subject demographics

For the experiments where neutrophil cell surface expression of NE and PR3 was measured, there was no difference in sex between the three subject groups (A1ATD, healthy controls and usual COPD). The mean ages of the groups (±SEM) were 60.8±3.2 years for A1ATD subjects, 59.2±4.0 years for healthy controls and 74.2±3.7 years for usual COPD patients. The COPD patients were significantly older than the A1ATD subjects (p=0.018) and the healthy controls (p=0.022). However, importantly, baseline cell membrane expression of PR3 is not thought to be related to age [310].

For the experiments studying the local effects of A1AT concentration on neutrophil cell surface expression of NE and PR3, there was no significant difference in age between the A1ATD subjects and the healthy controls (54.3±3.2 years vs 45.5±3.1 years; p=0.064). However, the A1ATD subjects were predominantly male (83%) and the healthy controls were predominantly female (83%). Nevertheless, these experiments were designed to compare NE and PR3 neutrophil cell surface expression in the presence of either normal (PiMM plasma) or reduced (PiZZ plasma) A1AT concentrations in the same individual, and no direct comparisons were made between the two subject groups.

8.3.2 NE and PR3 expression on the neutrophil cell membrane

8.3.2.1 NE and PR3 expression on unstimulated neutrophils

PR3 expression on the cell surface of unstimulated neutrophils as measured by the MFI was significantly greater in A1ATD subjects (median 2449 MFI, IQR 1503-2593 MFI)

than healthy controls (median 1506 MFI, IQR 879-1884 MFI; 2-tailed p=0.048) and subjects with usual COPD (median 1249 MFI, IQR 749-1840 MFI; 2-tailed p=0.046). However, NE expression was not significantly different between the 3 subject groups (A1ATD 1421 MFI, IQR 1121-3128 MFI; healthy 874 MFI, IQR 416-2140 MFI; COPD 883 MFI, IQR 522-2087 MFI; 2-tailed p>0.05 in all cases). These data are summarised in Figure 8.1.

The percentage of these unstimulated neutrophils expressing PR3 was greater in A1ATD subjects compared to controls (50.0±7.3% vs 27.5±6.3%; 2-tailed p=0.033) but was not significantly different compared to subjects with usual COPD (50.0±7.3% vs 30.1±9.4%; 2-tailed p=0.116). The percentage of unstimulated neutrophils expressing NE was greater in A1ATD subjects compared to those with usual COPD (53.8±10.1% vs 21.5±8.3%; 2-tailed p=0.036) but was not significantly different when compared to healthy controls (53.8±10.1% vs 31.1±10.1%; 2-tailed p=0.161).

Figure 8.1- Cell surface expression of PR3 and NE on unstimulated neutrophils from A1AT deficient subjects, healthy controls and subjects with usual COPD

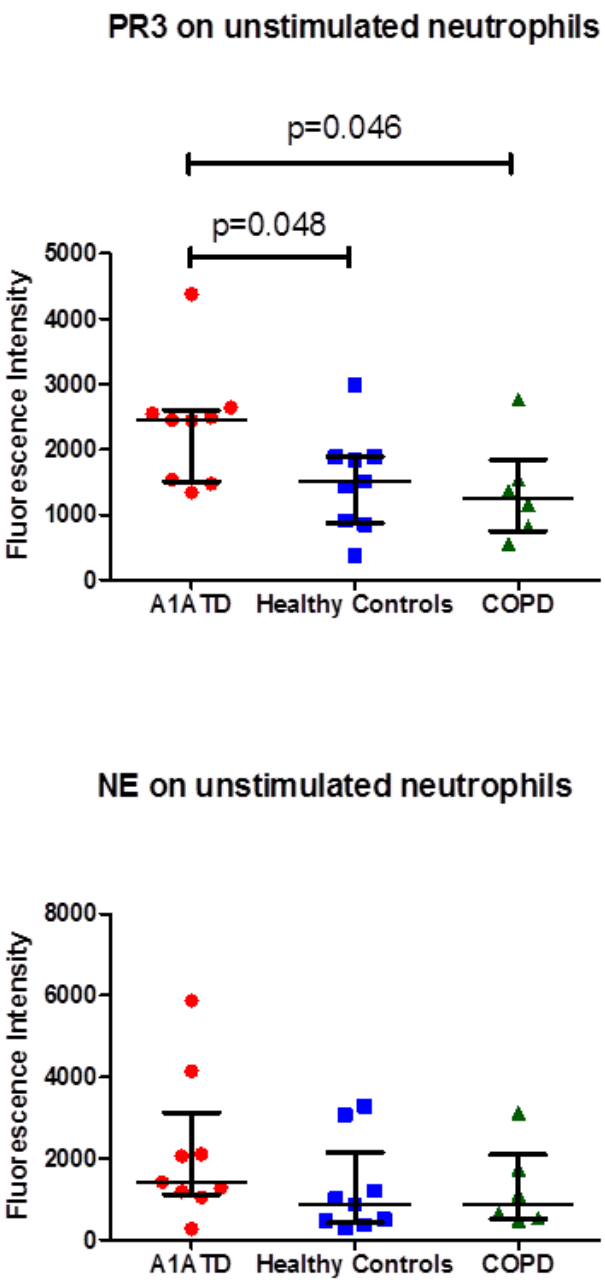

Figure 8.1: Expression of proteinases on the cell surface of unstimulated neutrophils. The y-axis shows the MFI measured by flow cytometry. Each point represents data from a single patient in each of the 3 subject groups. The bars show the median and IQR. Statistically significant differences are highlighted using 2-tailed p-values.

8.3.2.2 NE and PR3 expression on neutrophils following stimulation with fMLP

Following stimulation with 100nM fMLP for 30 minutes, expression of PR3 and NE on the cell membrane as measured by MFI was increased in all subject groups, with the exception of neutrophils from A1ATD subjects where there was no significant increase in NE expression after stimulation. Cell surface expression of PR3 increased proportionally in A1ATD subjects and healthy controls, but showed a greater proportional increase in subjects with COPD. These results are summarised in Figure 8.2 (NS = not significant).

Figure 8.2- Cell surface expression of PR3 and NE before and after stimulation with fMLP

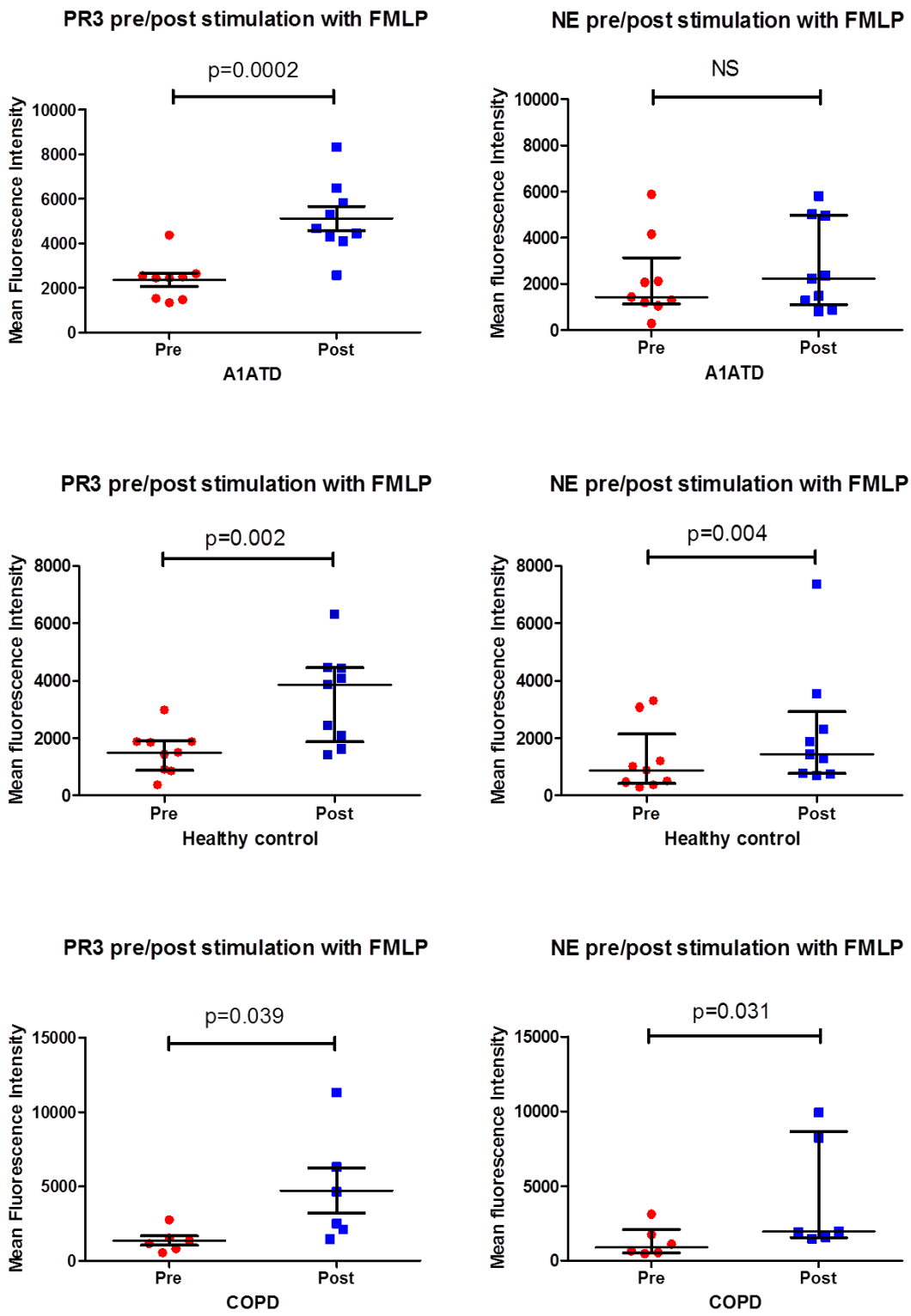

Figure 8.2: PR3 & NE expression on the neutrophil cell surface pre/post stimulation (median and IQR). Different scales are used on the y-axis for each subject group.

PR3 expression on the cell surface of stimulated neutrophils as measured by the MFI was significantly greater in A1ATD subjects (median 4681 MFI, IQR 4205-6149 MFI) compared to healthy controls (median 3856 MFI, IQR 1856-4439 MFI; 2-tailed p=0.042), but was not significantly different when compared to subjects with usual COPD (median 3572 MFI, IQR 1945-7559 MFI; 2-tailed p=0.78). NE expression was not significantly different between the three subject groups (A1ATD 2220 MFI, IQR 1085-4975 MFI; healthy 1431 MFI, IQR 758-2920 MFI; COPD 1938 MFI, IQR 1538-8653 MFI; 2-tailed p>0.05 in all cases). These data are summarised in Figure 8.3.

The percentage of stimulated neutrophils expressing PR3 on their cell surface was not significantly different between the three subject groups (A1ATD 68.2±7.2%, healthy 56.9±7.1%, COPD 67.6±8.5%; 2-tailed p>0.05 in all cases) and the same was true for NE expression (A1ATD 57.0±9.3%, healthy 46.0±9.5%, COPD 59.7±11.7%; 2-tailed p>0.05 in all cases) indicating that the changes were due to increased expression on cells and not solely due to recruitment of more positive cells.

Figure 8.3- Cell surface expression of PR3 and NE on stimulated neutrophils from A1AT deficient subjects, healthy controls and subjects with usual COPD

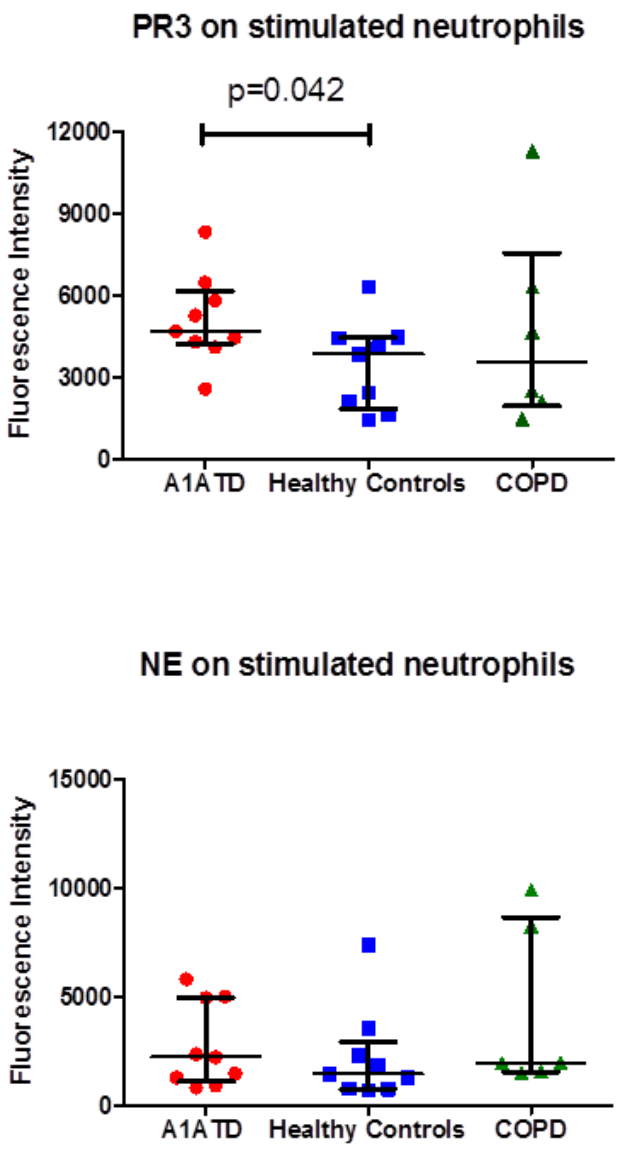

Figure 8.3: Expression of proteinases on the cell surface of neutrophils stimulated with 100nM fMLP. The y-axis shows the MFI measured by flow cytometry. Each point represents data from a single patient in each of the 3 subject groups. The bars show the median and IQR. Statistically significant differences are highlighted using 2-tailed p-values.

8.3.3 The effect of local A1AT concentration on PR3 and NE expression on neutrophil cell membranes

8.3.3.1 NE and PR3 expression on neutrophils from A1ATD subjects following incubation in PiMM or PiZZ plasma

When neutrophils were isolated from A1ATD subjects and incubated in their own plasma, PR3 expression as measured by MFI was significantly greater (median 795 MFI, IQR 614-1106 MFI) than when they were incubated in PiMM plasma containing normal A1AT levels (median 584 MFI, IQR 384-965 MFI; p=0.031). Furthermore, cell surface PR3 expression was greater when neutrophils were incubated in RPMI 1640 medium (in the absence of plasma) compared to both PiZZ and PiMM plasma (median 2469 MFI, IQR 1410-2569; p=0.016 for PiZZ and PiMM plasma). There was no difference in NE expression between the neutrophils incubated in PiZZ or PiMM plasma (PiZZ median 558 MFI, IQR 384-1626 MFI; PiMM median 880 MFI, IQR 288-1486 MFI; p=0.422) or neutrophils incubated in RPMI 1640 medium (median 583 MFI, IQR 230-1170; p=0.219 compared to PiMM plasma, p=0.156 compared to PiZZ plasma). These data are summarised in Figure 8.4.

The percentage of cells expressing PR3 on their cell surface was greater in the presence of PiZZ plasma compared to PiMM plasma (mean 14.3±4.4% vs 7.6±1.9%; p=0.031). Furthermore, the percentage of cells expressing PR3 was greater when the cells were incubated in RPMI 1640 medium than PiZZ and PiMM plasma (mean 41.1±10.1%; p=0.031 for PiZZ plasma and p=0.016 for PiMM plasma). There was no difference in the percentage of cells expressing NE between those incubated in PiZZ and PiMM plasma

(mean 19.6±9.3% vs 27.8±11.8%; p=0.344) or RPMI 1640 medium (15.1±8.3%; p=0.219 compared to PiMM plasma, p=0.156 compared to PiZZ plasma).

Figure 8.4- Cell surface expression of PR3 and NE on neutrophils isolated from A1AT deficient subjects and incubated in PiZZ or PiMM plasma

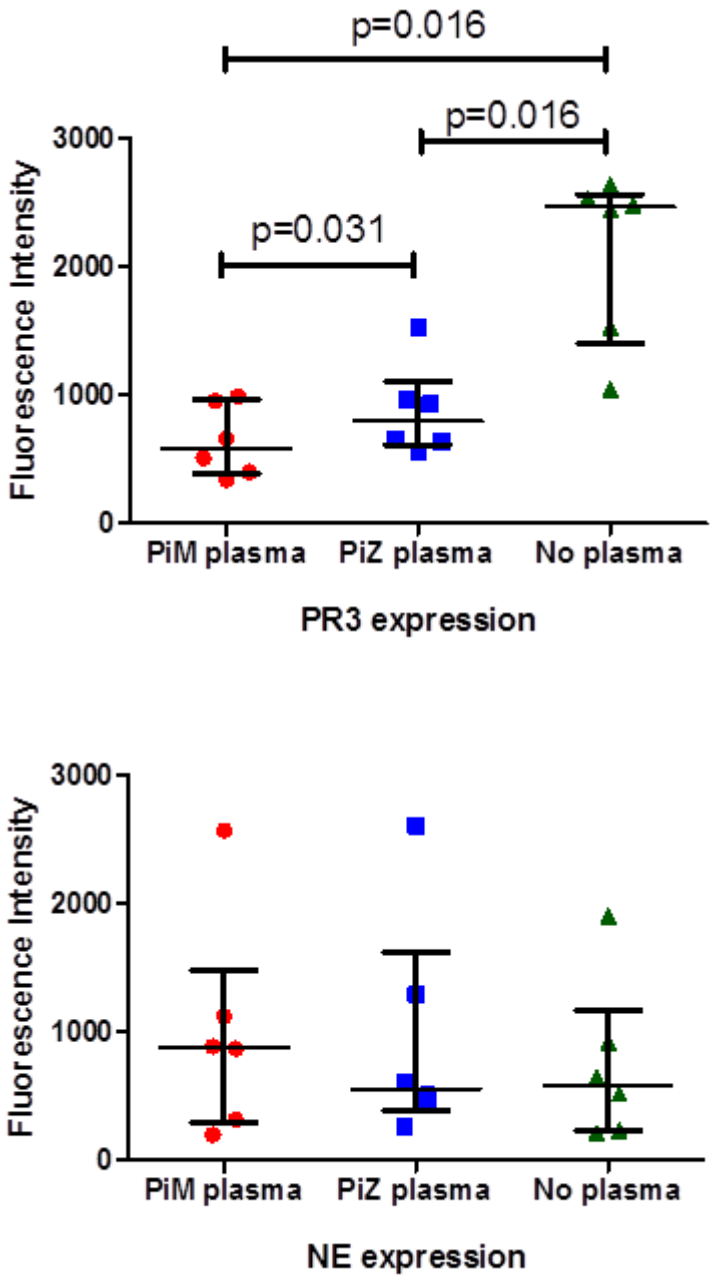

Figure 8.4: Baseline expression (MFI) of proteinases on the cell surface of neutrophils extracted from six A1ATD subjects and incubated in either PiM or PiZ plasma or RPMI 1640 medium prior to labelling with antibodies for flow cytometry. Horizontal lines represent the medians and IQR. Significant differences are labelled.

8.3.3.2 NE and PR3 expression on neutrophils from A1ATD subjects following stimulation with fMLP in the presence of PiMM or PiZZ plasma

When neutrophils from A1ATD subjects were stimulated with fMLP in the presence of either PiZZ or PiMM plasma or RPMI 1640 medium, the PR3 expression was significantly greater compared to unstimulated cells in both PiZZ (p=0.028) and PiMM plasma (p=0.028), and RPMI 1640 medium (p=0.031). However, the increase in PR3 cell surface expression was similar in all groups, being approximately two-fold. Consequently, the cell surface expression of PR3 was significantly greater on the cells stimulated in the presence of PiZZ plasma (median 1390 MFI, IQR 1030-2046 MFI) compared to those stimulated in PiMM plasma (median 986 MFI, IQR 855-1640 MFI; p=0.016). Furthermore, cell surface PR3 expression was greater on neutrophils stimulated in the presence of RPMI 1640 medium (in the absence of plasma) compared to both PiZZ and PiMM plasma (median 3484 MFI, IQR 2856-4444 MFI; p=0.016 for PiZZ and PiMM plasma).

Neutrophil cell surface expression of NE increased significantly following stimulation with fMLP in the presence of RPMI 1640 medium (p=0.016) and PiZZ plasma (p=0.028), but not in the presence of PiMM plasma (p=0.116). There was still however no significant difference in NE expression between the neutrophils activated in the presence of PiZZ or PiMM plasma (PiZZ median 1407 MFI, IQR 602-2766 MFI; PiMM median 1630 MFI, IQR 792-2428 MFI; p=0.5) or RPMI 1640 medium (median 1803 MFI, IQR 853-3323 MFI; p=0.078 compared to PiMM plasma, p=0.344 compared to PiZZ plasma). These data are summarised in Figure 8.5.

The percentage of cells expressing PR3 or NE on their cell surface was not significantly different between cells activated in the presence of PiZZ or PiMM plasma (mean PR3 expression 30.3±6.1% in PiZZ plasma vs 22.6±5.6% in PiMM plasma; p=0.078, and mean NE expression 21.6±6.9% in PiZZ plasma vs 28.6±9.9% in PiMM plasma; p=0.281). However, the percentage of cells expressing PR3 was greater when cells were activated in RPMI 1640 medium than when they were activated in PiZZ or PiMM plasma (59.4±7.4%, p=0.016 for PiZZ and PiMM plasma). In addition, when cells were activated in RPMI 1640 medium, the percentage of cells expressing NE on their surface was greater than when they were activated in PiZZ plasma (41.4±7.4%; p=0.016), but was not different to cells activated in PiMM plasma (p=0.078).

Figure 8.5- Cell surface expression of PR3 and NE on neutrophils isolated from A1AT deficient subjects and activated with fMLP in the presence of PiZZ or PiMM plasma

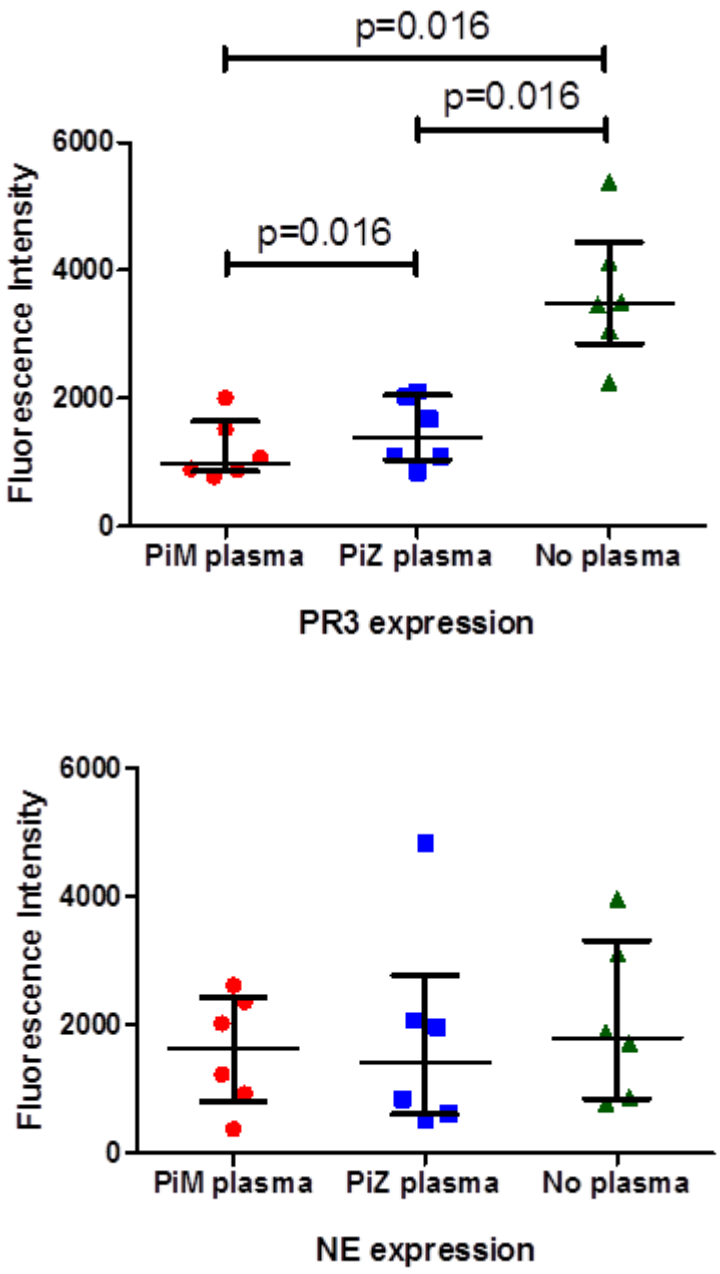

Figure 8.5: Expression of proteinases (MFI) on the cell surface of neutrophils extracted from six A1ATD subjects and activated with fMLP in either PiM or PiZ plasma or RPMI 1640 medium prior to labelling with antibodies for flow cytometry. Horizontal lines represent medians and IQR. Significant differences are labelled.

8.3.3.3 NE and PR3 expression on neutrophils from healthy controls following incubation in PiMM or PiZZ plasma

When neutrophils were isolated from healthy subjects and incubated in either their own or PiZZ plasma (from an A1ATD subject), the PR3 expression was significantly higher on the neutrophils that were incubated in PiZZ plasma (median 924 MFI, IQR 452-1316 MFI) compared to those incubated in PiMM plasma (median 621 MFI, IQR 341-997 MFI; p=0.047). Cell surface PR3 expression was greater when neutrophils were incubated in RPMI 1640 medium (median 897 MFI, IQR 530-1465 MFI) than PiMM plasma (p=0.016), but not PiZZ plasma (p=0.219). There was no difference in NE expression between the neutrophils incubated in PiZZ or PiMM plasma (PiZZ median 1657 MFI, IQR 319-2395 MFI; PiMM median 1199 MFI, IQR 615-1988 MFI; p=0.109) or RPMI 1640 medium (median 627 MFI, IQR 363-2314 MFI; p=0.219 compared to both PiMM and PiZZ plasma). These data are summarised in Figure 8.6.

The percentage of cells expressing PR3 or NE on their cell surface was not significantly different between cells incubated in PiZZ or PiMM plasma (mean PR3 expression 13.0±4.0% in PiZZ plasma vs 9.1±3.4% in PiMM plasma; p=0.281, mean NE expression 42.9±13.9% in PiZZ plasma vs 27.8±12.3% in PiMM plasma; p=0.156). When cells were incubated in RPMI 1640 medium, the percentage of cells expressing PR3 on their surface was greater than when they were incubated in PiMM plasma (17.3±5.9%; p=0.0156), but not different to when they were incubated in PiZZ plasma (p=0.109). The percentage of cells expressing NE on their surface was not significantly different when incubated in RPMI 1640 medium compared to PiZZ or PiMM plasma (30.1±14.3%; p=0.5 for PiZZ and PiMM plasma).

Figure 8.6- Cell surface expression of PR3 and NE on neutrophils isolated from healthy subjects and incubated in PiZZ or PiMM plasma

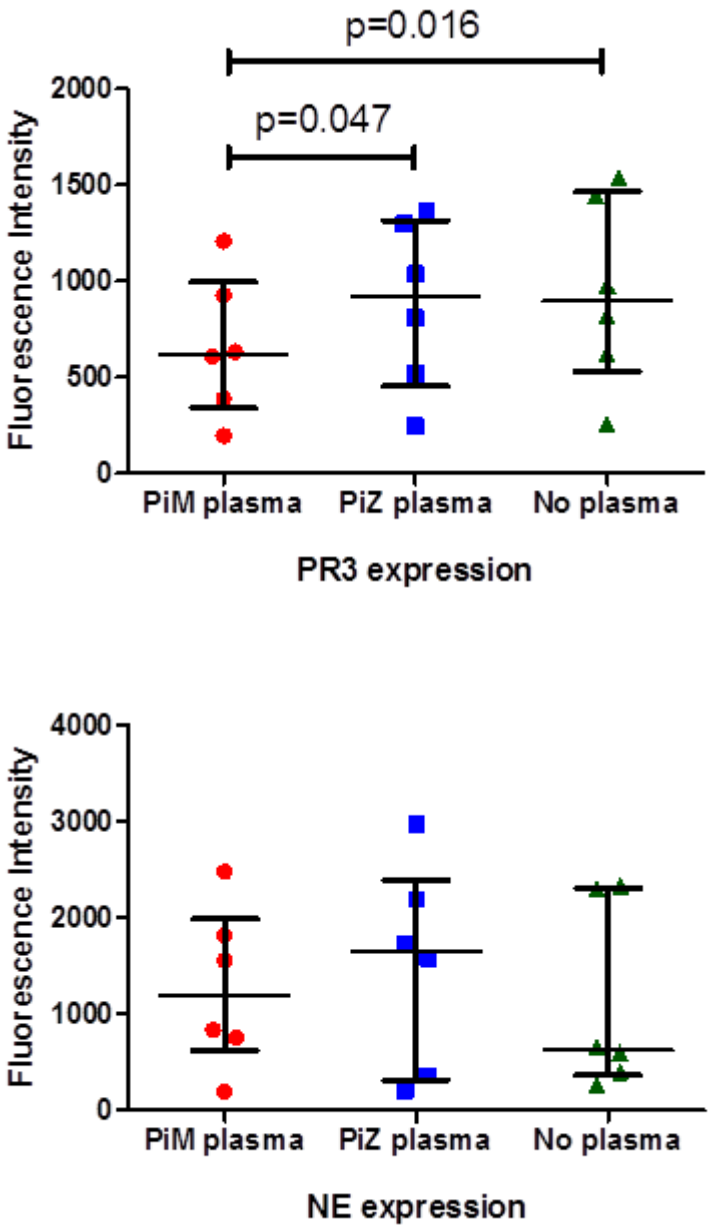

Figure 8.6: Baseline expression (MFI) of proteinases on the cell surface of neutrophils extracted from six healthy subjects and incubated in either PiM or PiZ plasma or RPMI 1640 medium prior to labelling with antibodies for flow cytometry. Horizontal lines represent medians and IQR. Significant differences are labelled.

8.3.3.4 NE and PR3 expression on neutrophils from healthy controls following stimulation with fMLP in the presence of PiMM or PiZZ plasma

When neutrophils from healthy subjects were stimulated with fMLP in the presence of either PiZZ or PiMM plasma or RPMI 1640 medium, the PR3 expression was significantly greater compared to unstimulated cells in both PiZZ (p=0.028) and PiMM plasma (p=0.028), and RPMI 1640 medium (p=0.016). The increase in PR3 cell surface expression was approximately two-fold in the presence of either PiZZ or PiMM plasma, and approximately three-fold in the presence of RPMI 1640 medium. Consequently, the PR3 expression was significantly greater on the cells stimulated in the presence of PiZZ plasma (median 1921 MFI, IQR 866-2525 MFI) compared to PiMM plasma (median 1352 MFI, IQR 695-1529 MFI; p=0.031). Cell surface PR3 expression was greater on neutrophils stimulated in the presence of RPMI 1640 medium (median 2415 MFI, IQR 1505-6018 MFI) than those stimulated in the presence of PiMM plasma (p=0.016), but not PiZZ plasma (p=0.109).

Neutrophil cell surface expression of NE increased significantly following stimulation with fMLP in the presence of PiZZ plasma (p=0.028), PiMM plasma (p=0.046) or RPMI 1640 medium (p=0.016). There was no significant difference in NE expression between the neutrophils activated in the presence of PiZZ or PiMM plasma (PiZZ median 3014 MFI, IQR 580-4553 MFI; PiMM median 2876 MFI, IQR 524-3384 MFI; p=0.156), but neutrophils activated in RPMI 1640 medium (median 3683 MFI, IQR 2329-4474 MFI) had greater NE expression than cells activated in PiMM plasma (p=0.016). These data are summarised in Figure 8.7.

The percentage of cells expressing PR3 on their cell surface was also greater when the cells were activated in the presence of PiZZ plasma compared to PiMM plasma (mean 33.5±8.8% vs 24.5±6.3%, p=0.031). Furthermore, the percentage of cells expressing PR3 was greater when cells were activated in RPMI 1640 medium than when they were activated in PiZZ or PiMM plasma (54.1±10.4%; p=0.031 for PiZZ plasma, p=0.016 for PiMM plasma). There was no difference in the percentage of cells expressing NE between cells activated in the presence of PiZZ plasma or PiMM plasma (mean 46.1±13.3% vs 36.6±14.3%, p=0.281). When cells were activated in RPMI 1640 medium, the percentage of cells expressing NE on their surface was greater than when they were activated in PiMM plasma (56.0±12.2%; p=0.016), but was not different to cells activated in PiZZ plasma (p=0.281).

Figure 8.7- Cell surface expression of PR3 and NE on neutrophils isolated from healthy subjects and activated with fMLP in the presence of PiZZ or PiMM plasma

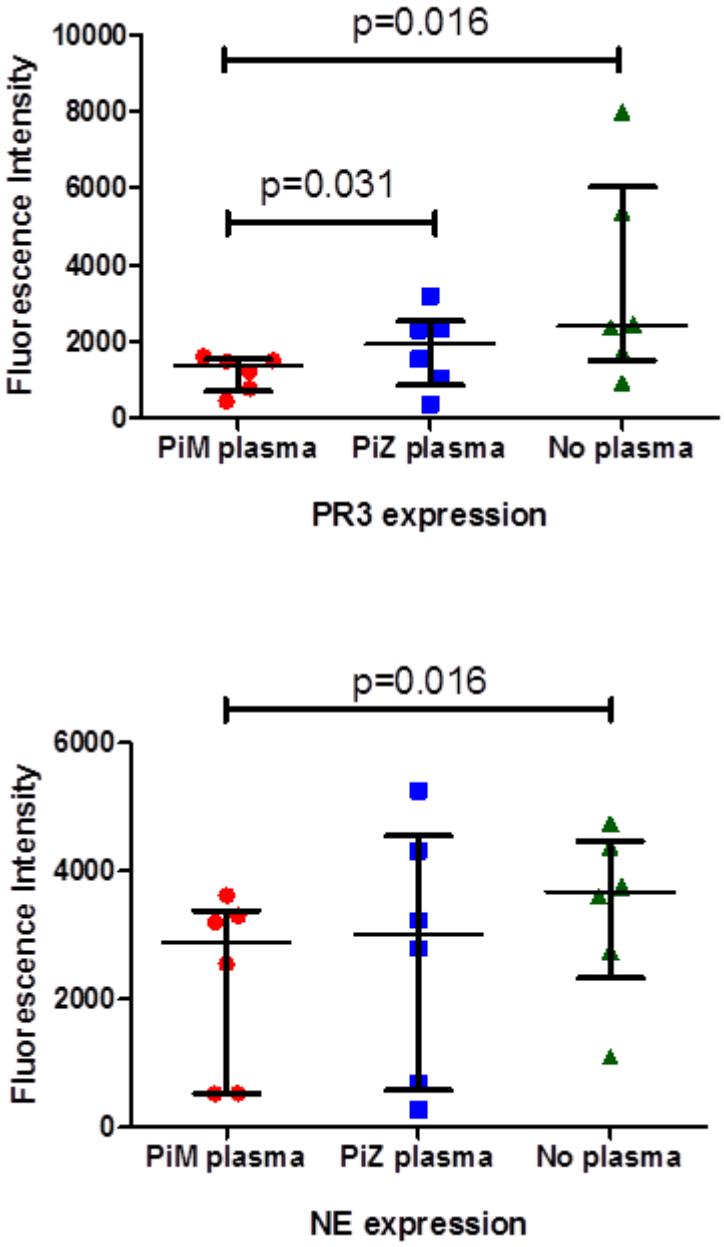

Figure 8.7: Expression of proteinases (MFI) on the cell surface of neutrophils extracted from six healthy subjects and activated with fMLP in either PiM or PiZ plasma or RPMI 1640 medium prior to labelling with antibodies for flow cytometry. Horizontal lines represent medians and IQR. Significant differences are labelled.

8.4 Discussion

This work has confirmed that PR3 is present on the cell membrane of unstimulated neutrophils as previously reported [108]. Neutrophil expression of PR3 (as measured by MFI) was greater in subjects with A1ATD compared to both healthy controls and subjects with usual COPD (Figure 8.1), suggesting that this finding was not solely related to the underlying pulmonary inflammation but was influenced by deficiency of A1AT. This work also found that NE was present on the cell membrane of unstimulated cells in contrast to previously published work [54], although NE expression (as measured by MFI) was not significantly different between the 3 subject groups.

Neutrophil isolation procedures may result in partial cell activation which could modify the expression of NSPs on the cell membranes [322]. The degree of cell activation could depend on the source of the blood and whether it contains primed neutrophils, which are more susceptible to activation than quiescent neutrophils. However, it is unlikely that isolation procedures or the source of the sample would account for the observed differences in PR3 expression between the subject groups for two reasons; firstly, stimulation of the cells with fMLP led to a significant increase in PR3 expression in all subject groups compared to baseline, and secondly, PR3 expression increased proportionally in A1ATD subjects and healthy controls following stimulation with fMLP. However, it could be hypothesized that isolation procedures or the presence of primed neutrophils may have a greater influence on NE expression on the cell membrane, which is not believed to be constitutively expressed [54], and could potentially explain why NE was detected on unstimulated cells and why NE expression on neutrophils from A1ATD

subjects was not significantly different before and after stimulation with fMLP. Indeed, differences between PR3 and NE and their interactions with the cell membrane have been described previously [51].

Following stimulation with fMLP, cell surface expression of PR3 increased proportionally in A1ATD subjects and healthy controls (approximately two-fold) and therefore, PR3 expression (as measured by MFI) remained greater on stimulated neutrophils from A1ATD subjects compared to healthy controls (Figure 8.3), as found with unstimulated cells. However, cell surface expression of PR3 showed a greater proportional increase in subjects with COPD following stimulation with fMLP (3-4 fold, shown in Figure 8.2). Altered neutrophil function in COPD subjects has been reported previously including; increased spontaneous adherence to endothelium under flow conditions [47], enhanced chemotaxis, increased spontaneous extracellular proteolysis [48], and greater production of reactive oxygen species [323], which may be consistent with the enhanced response in PR3 expression seen here.

NE expression increased 2-3 fold on neutrophils from both healthy controls and subjects with usual COPD following stimulation, and these findings are consistent with those of Owen *et al* [54], who reported a 2-3 fold increase in the cell surface expression of NE and CG following stimulation with fMLP with a similar concentration and time course. However, as previously discussed, no significant increase was observed on neutrophils from subjects with A1ATD. Figure 8.3 shows that following stimulation with fMLP, no differences were found in neutrophil expression of NE between subjects with A1ATD, usual COPD and healthy controls, as observed with unstimulated cells.

The current studies have demonstrated that PR3 expression on the neutrophil cell surface was greater when the surrounding concentration of A1AT was lower. Neutrophils extracted and incubated in PiZZ plasma (with a low A1AT concentration) had greater PR3 expression than cells incubated in PiMM plasma (with a normal A1AT concentration), as shown in Figures 8.4 and 8.6. This was true for neutrophils from both subjects with A1ATD and healthy controls, so was independent of the source of the neutrophils. Following stimulation of neutrophils with fMLP in the presence of plasma, PR3 expression was significantly greater than on unstimulated cells in both PiZZ and PiMM plasma, and the proportional increases were similar in both PiZZ and PiMM plasma. Therefore, as found with unstimulated cells, neutrophils stimulated in the presence of PiZZ plasma showed greater PR3 expression than cells stimulated in the presence of PiMM plasma (Figures 8.5 and 8.7). However, neutrophil cell surface expression of NE did not appear to be influenced by the local concentration of A1AT in these studies (as discussed further below), and was not significantly different on cells incubated in either PiZZ or PiMM plasma, or on cells stimulated in the presence of PiZZ or PiMM plasma.

Previous studies have reported conflicting information about the ability of proteinase inhibitors (such as A1AT) to inactivate NSPs on the neutrophil cell membrane. Owen *et al* [54] reported that cell surface-bound NE on fixed cells was resistant to inhibition by naturally occurring proteinase inhibitors such as A1AT and, to a lesser extent, SLPI. Campbell *et al* [108] later reported that membrane-bound PR3 was resistant to inhibition by A1AT and elafin. However, they used unstimulated fixed cells with exogenous PR3 bound to the cell membrane due to the lack of availability of a PR3 specific substrate at the

time of publication. Subsequently, Korkmaz *et al* [324] compared fixed and unfixed neutrophils and showed that NE bound to the cell surface of unfixed activated neutrophils could be fully inhibited by stoichiometric amounts of A1AT, whereas this was not the case when using fixed neutrophils (where the accessibility of epitopes was found to be altered by fixation). They concluded that membrane-bound NE could be removed from the neutrophil membrane following complex formation with A1AT. The same group [307] later studied membrane-bound PR3 and suggested that constitutively expressed PR3 on quiescent neutrophils did not interact with A1AT, whereas PR3 on the surface of stimulated cells could be inhibited by A1AT and cleared from the cell membrane. However, unlike NE, PR3 remained bound to the membrane when inhibited by low molecular weight inhibitors such as elafin, which may be a reflection of the different binding mechanisms of NE and PR3 to the neutrophil cell membrane. The ability of A2M to interact with membrane-bound NSPs remains uncertain.

The ability of A1AT to interact with membrane-bound PR3 and subsequent clearance of the complex would be consistent with the findings of the current studies where greater amounts of A1AT were associated with less neutrophil cell surface expression of PR3. Although this trend was also noted with unstimulated cells, the cell purification process can result in partial cell activation as discussed earlier, and should be considered when interpreting *in vitro* neutrophil studies. This hypothesis is further supported by comparing the MFI values for PR3 expression between the cells incubated in RPMI 1640 medium with those from cells incubated in plasma. The data presented in this Chapter show that MFI values for PR3 expression are greater for cells incubated or stimulated in RPMI 1640 medium compared to cells incubated or stimulated in plasma.

In the studies presented here, there was a similar proportional increase in surface PR3 expression on the neutrophil following stimulation in the presence of different concentrations of A1AT. However, a small study by Matsumoto *et al* [325] showed that neutrophils from 3 healthy controls showed a suppressed increase in membrane PR3 expression when stimulated in the presence of A1AT or healthy plasma. In that study, neutrophils were stimulated with both TNFα and a greater concentration of fMLP (1μM) which could explain the discrepancy with the current results. Previous studies have shown that different stimulants at different concentrations produced variable increases in membrane NSP expression, with increases of up to 30 fold when PMA was used [54] (although this is unlikely to be physiological). The lack of a consistent association between cell surface NE expression and local A1AT concentration in the current studies could therefore potentially be related either to the modest increases of surface NE expression observed when using fMLP 100nM as the stimulant or to the sample sizes studied. However, a genuine lack of association may exist, and paradoxically Owen *et al* [54] found that neutrophils activated [using bacterial lipopolysaccharide (LPS) and fMLP] in the presence of 20% serum expressed greater quantities of cell surface NE compared to cells activated in buffer alone, and the authors suggested that this may be related to the presence of LPS-binding protein in the serum which augments the biological activities of LPS. Therefore, further studies are necessary to establish any relationship between neutrophil surface NE expression and local A1AT concentration.

The association between A1ATD and WG suggests that the proteinase/anti-proteinase imbalance may play a role in the pathogenesis of this disease. Previous studies have shown

that subjects with WG with the PiZZ genotype have more aggressive disease than subjects with the PiMZ or PiMM genotypes [326]. Rooney *et al* [327] studied the local effects of A1AT on anti-PR3 antibody-induced activation of neutrophils. The authors reported that A1AT could inhibit binding of anti-PR3 antibodies and hence reduce activation of neutrophils from subjects with active WG. These observations, in addition to the findings of the current study, may suggest a potential therapeutic role for A1AT augmentation therapy particularly in the sub-group of A1ATD patients with acute episodes of vasculitis due to WG.

In this Chapter, neutrophil cell membrane expression of PR3 and NE has been measured by flow cytometry using both MFI and percentage of positive cells. Unstimulated neutrophils from A1ATD subjects showed greater PR3 expression as measured by both MFI and as a percentage of positive cells compared to healthy controls. However, results from the experiments studying the local effects of A1AT on neutrophil cell surface expression of NE and PR3 showed significant effects detected by MFI but not on the percentage of positive cells. This discrepancy is possibly related to the small sample sizes used, since combining the data from the 2 subject groups (and therefore increasing the numbers) confirmed that the percentage of PR3 positive cells was significantly greater when cells were incubated or stimulated in PiZZ plasma compared to PiMM plasma. However, the differences in percentage of positive cells are not always consistent with the overall differences in MFI suggesting that increased expression may not solely be due to greater numbers of positive cells. In the literature, there is no standard method for presenting data obtained by flow cytometry, as some authors use MFI [49] and others use percentage of positive cells [310]. The data presented here suggest that both parameters are required to understand changes.

The Accuri® C6 flow cytometer used for these studies gives different MFI values to other available cytometers (unpublished personal observations) and therefore comparisons cannot be made between instruments. For these reasons, all of the studies reported here were performed on the same cytometer. The use of the Accuri® C6 flow cytometer has previously been validated in the literature [328, 329] providing confidence of the differences observed between groups reported here.

In summary, this Chapter has demonstrated that PR3 expression on neutrophil cell membranes is greater in subjects with A1ATD compared to healthy controls, and that membrane PR3 expression is greater when the surrounding concentration of A1AT is lower. This could be of clinical importance especially since membrane bound NSPs retain their activity and hence tissue damaging potential. The increased membrane PR3 expression could also potentially play a role in autoimmunity since PR3-ANCA positive vasculitis (Wegener's granulomatosis) is associated with A1ATD where more PR3 surface expression occurs. In the future, a better understanding of the mechanism of PR3 binding to the neutrophil cell membrane may facilitate therapeutic approaches to modulate membrane expression of PR3. These therapeutic approaches may prove valuable both in PR3-ANCA positive vasculitis and other inflammatory diseases (such as COPD with and without A1ATD).

9 The activities of serine proteinases in airway secretions from subjects with A1AT deficiency or usual COPD

9.1 Introduction

An imbalance between the activities of NSPs and their inhibitors (the anti-proteinases) is widely believed to play a role in the pathophysiology of COPD, and this imbalance is even greater in subjects with A1ATD. Previous studies have considered the contribution of NE to the proteinase/anti-proteinase imbalance [330], but to date there has been little direct evidence of the role of PR3, and until recently, research has been hindered by poor availability of specific PR3 substrates and inhibitors.

The studies described in this Chapter were designed to investigate the presence and activity of PR3 compared to NE in sol-phase sputum from subjects with A1ATD or usual COPD, together with the concentrations of their airway inhibitors. Previous Chapters have considered the partitioning of these NSPs between their circulating inhibitors A1AT and A2M. However, this Chapter also considers the contribution of the locally produced airway inhibitors SLPI and elafin, as well as relationships between NSP activities and clinical parameters.

The aim of this Chapter is to provide insight into the contribution of PR3 to the proteolytic activity in the lungs, and hence its potential role and implications as a therapeutic target. The work presented in this Chapter has been published in a peer-reviewed journal [331].

9.2 Methods

9.2.1 Subject selection

Twenty eight clinically stable subjects (at least 8 weeks after any acute infection) with A1ATD (PiZZ phenotype) and a history of chronic bronchitis were identified from the UK national registry for A1ATD, and spontaneously produced sputum was collected as described previously [332]. None of these patients were receiving A1AT augmentation therapy.

Twenty two patients with usual COPD (PiMM phenotype) were recruited from primary care with a clinical diagnosis of COPD, confirmed by spirometry and/or radiological findings to meet the diagnostic criteria [333]. Sputum was collected at the start of an acute exacerbation (day 1) and then after resolution of the episode during convalescence (day 56). In total, 12 day 1 samples and 22 day 56 samples of sufficient volume were available for this study.

All subjects had full demographic data collected including smoking history, full PFTs and HRCT scans performed in the stable clinical state. The A1ATD subjects had their health status assessed using the SGRQ.

9.2.2 Measurement of PR3 and NE activities in sol-phase sputum

Sputum samples were processed as described in section 2.2.3. The enzymatic activities of PR3 and NE in the sol-phase of sputum were evaluated by measuring the hydrolysis of specific substrates using pure proteinases (active site titrated) as standards.

The PR3 activity assays were performed using the FRET substrate Abz-VAD-norV-ADRQ-EDDnp (Alta Biosciences, UK) which was prepared as described previously [283]. This substrate has a catalytic constant Kcat/Km of 3400mM^{-1}s^{-1} and shows no significant hydrolysis by NE [334] or CG (Prof. T Moreau, Rheims, France; personal communication). This was confirmed by adding 3µL of 1mM FRET substrate to 150µL of 10nM solutions of PR3, NE, CG (Sigma, UK) compared to NSP assay buffer as a control. The fluorescence (excitation 320nm, emission 420nm) was read at 5 minute intervals for as long as the curve was linear using a Biotek Synergy 2 Multi-Mode Microplate Reader, and unlike PR3, no change in fluorescence was observed when using pure NE, CG or buffer alone (data not shown). The activity of the CG was confirmed in a separate experiment by using a CG substrate, suc-val-pro-phe-pNa (Bachem, Switzerland).

To measure PR3 activities in sol-phase sputum, standards were prepared by diluting pure PR3 in NSP assay buffer to an active concentration of 10nM and serially diluting the PR3 in the same buffer to 0.63nM, with buffer alone as a blank for the assay. Sol-phase sputum samples were diluted 1 in 60 and the standards and samples (150µL) were added to a black opaque polypropylene low binding plate (Sigma, UK) in duplicate. Subsequently, 3µL of 1mM FRET substrate was added to each well and the fluorescence was measured (excitation 320nm, emission 420nm) at regular intervals for as long as the curve was linear

using a Biotek Synergy 2 Multi-Mode Microplate Reader at 37°C. The activities of PR3 in the samples were obtained by interpolation from the standard curve. Any sample with a value above or below that of the standard curve was repeated at a suitable dilution. Using this FRET substrate, reliable measurements were obtained for PR3 in the range of 0.1-10nM [283]. The intra-assay CV was 3.98% and the inter-assay CV was 13.35%. All results were corrected for the initial sample dilution.

The NE activity assays were performed using SlaaapN as the substrate which has a catalytic constant Kcat/Km of $465M^{-1}s^{-1}$ and shows no significant hydrolysis with PR3 [119]. Pure NE was diluted in NSP assay buffer to 1µM and then serially diluted to 15.6nM, and buffer alone was used as a blank for the assay. Sol-phase sputum samples were studied undiluted with appropriate controls to minimise the effect of the inherent colour of the samples on the OD measurement. The standards, samples and control samples (30µL) were added to a 96 well plate in duplicate and the substrate SlaaapN (150µL of 1mg/ml) was added, except for the control wells where buffer was added instead of substrate. The OD at 410nm was read at regular intervals up to 60 minutes using a Biotek Synergy HT plate reader at 37°C. The activities of NE in the samples were obtained by interpolation from the standard curve after subtraction of control values. The lower limit of detection for this substrate was 15nM and the intra- and inter-assay CVs were 3.48% and 4.76% respectively. Any samples with values below this level were re-assayed using the NE specific FRET substrate Abz-APEEIMRRQ-EDDnp (Alta Biosciences, UK) providing reliable measurements for NE in the range of 0.1-10nM [283]. The intra-assay CV was 3.42% and the inter-assay CV was 4.76%.

9.2.2.1 Determining any effect of Pseudomonas aeruginosa proteinases

The enzymatic activities of both *Pseudomonas aeruginosa* culture supernatants and pure *Pseudomonas* elastase (Merck, UK) were assessed using the above substrates to confirm no cross-reactivity with the assays for human proteinases.

Pseudomonas aeruginosa was grown on chocolate agar plates (Oxoid, UK) from a sputum sample. Colonies were picked off the plate and added to 5ml of LB medium (made using 10g tryptone, 5g yeast and 10g NaCl made up to 1 litre with deionised water and autoclaved to sterilise) and incubated overnight at 37ºC. Following incubation, 1ml of the cloudy medium was measured into a 1.5ml eppendorf tube and centrifuged in a MSE micro centaur centrifuge at 13,000 RPM for 5 minutes. Following centrifugation, a visible pellet had formed and 100µL of supernatant was added per well to a 96-well plate. The substrates used in the above experiments were added to the culture supernatant and any change in fluorescence (for the FRET substrates) or absorbance (for SlaaapN) was measured.

In addition, pure *Pseudomonas* elastase was made at 100µg/ml (3µM) in PPE buffer. The substrates used in the above experiments were added to the pure *Pseudomonas* elastase and any change in fluorescence (for the FRET substrates) or absorbance (for SlaaapN) was measured. NE or PR3 were used as positive controls, and buffer alone was used as a negative control.

9.2.3 Measurement of PR3 and NE concentrations in sol-phase sputum

The concentrations of PR3 and NE in the samples were measured by ELISA using commercially available kits according to the manufacturer's instructions. The PR3 ELISA (Biorbyt, UK) only detects unbound PR3 (information from manufacturer), whereas the NE ELISA (Cambridge Bioscience, UK) detects both free and inhibitor-bound NE (information from manufacturer). The lower limits of detection were 5pM for the PR3 ELISA and 14pM for the NE ELISA. The intra- and inter-assay CVs for these ELISAs were 3.59% and 9.19% respectively for the PR3 ELISA and 5.07% and 13.76% respectively for the NE ELISA.

9.2.4 Measurement of inhibitors in sol-phase sputum

The concentration of A1AT was measured by ELISA as described in section 2.6.1.2. The concentrations of SLPI and elafin were measured using commercially available ELISA kits (R&D systems, UK) according to the manufacturer's instructions. The intra- and inter-assay CVs were 6.37% and 10.76% respectively for the SLPI ELISA and 7.67% and 4.46% respectively for the elafin ELISA. The concentration of A2M was also measured by ELISA using a commercially available kit (Universal Biologicals Cambridge, UK) which was capable of detecting lower concentrations of A2M than the method described in Section 4.2.2 (standards ranged from 0.002-0.5µg/ml; 2.8-690pM). The minimum detectable level of A2M using this ELISA kit was 2ng/ml (2.8pM) and the intra- and inter-assay CVs were 5.10% and 7.01% respectively.

9.2.5 Other measurements in sol-phase sputum

Markers of neutrophilic inflammation were measured when sufficient sample remained, including interleukin (IL)-8, leukotriene (LT)-B4 and myeloperoxidase (MPO). IL-8 and LTB4 were measured using commercially available ELISA kits (R&D systems, UK). The intra- and inter-assay CVs were 5.97% and 7.22% respectively for the IL-8 ELISA and 6.34% and 11.90% respectively for the LTB4 ELISA. MPO activity was measured as described previously [335] by another member of the research group. The intra- and inter-assay CVs for the MPO activity assays were 3.85% and 10.07% respectively.

9.2.6 Statistical analysis

Statistical analyses were performed using PASW statistics 18 for Windows. Normality was tested using the Kolmogorov-Smirnov test. PR3 activity, PR3 concentration, NE activity, NE concentration, IL-8, LTB4, MPO, A1AT, SLPI, FEV1 and SGRQ total score were not normally distributed therefore non-parametric tests were used and data are presented as medians and IQR. Mann-Whitney U tests or Wilcoxon signed rank tests were used for comparisons of independent or related data respectively. Correlations were assessed using Spearman's rank correlation coefficient. Normally distributed data are presented as mean ±SEM and independent or paired T-tests were used for comparisons of data for independent or related measures respectively. To compare variables between A1ATD and COPD subjects after adjusting for baseline differences, the data were log transformed and linear regression was used with group as one of the independent factors. The unstandardized residuals were tested for normality. For statistical purposes, enzyme activity below the lower limit of detection was taken as 0.1nM. Results were deemed statistically significant if $p \leq 0.05$.

9.3 Results

9.3.1 Baseline characteristics

Baseline characteristics of the two subject groups are shown in Table 9.1. The A1ATD subjects were younger, had a lower pack year smoking history, FEV1 (% predicted), FEV1/FVC ratio and KCO (% predicted) compared to the subjects with usual COPD. There were no significant differences in sex distribution or radiological evidence of emphysema between the two groups.

Table 9.1-Baseline characteristics of the subject groups

	A1ATD	**COPD**	**p-value**
Age Mean (SEM)	55 (1.9)	65 (1.9)	0.002
Number of males (%)	22 (79%)	19 (86%)	NS
Smoking history (pack years) Mean (SEM)	21 (3.9)	54 (10.0)	0.004
FEV1 (% predicted) Mean (SEM)	49 (5.9)	72 (5.8)	0.004
FEV1/FVC ratio Mean (SEM)	0.41 (0.04)	0.49 (0.04)	0.031
KCO (% predicted) Mean (SEM)	69 (5.2)	101 (6.1)	0.001
Number with radiological evidence of emphysema on HRCT (%)	22 (79%)	14 (64%)	NS

NS= not significant

9.3.2 PR3 and NE activities in sputum from clinically stable subjects

Detectable PR3 activity was found in all sputum samples from the A1ATD subjects (median 128nM, IQR 33-558nM) and in 64% of samples from subjects with usual COPD (median 22nM, IQR 0-103nM). PR3 activity was greater in A1ATD subjects compared to those with usual COPD (p=0.004) after adjusting for baseline differences in age, pack year smoking history, FEV1 (% predicted) and KCO (% predicted). These results are shown in Figure 9.1. Unbound PR3 concentration measured by ELISA confirmed these differences and values correlated strongly with PR3 activity (Spearman's rho 0.879, p<0.001) indicating that most of the unbound PR3 was enzymatically active, as shown in Figure 9.2.

Detectable NE activity was found in 21% of A1ATD sputum samples (median 0nM, IQR 0-0nM) and 5% of usual COPD samples (median 0nM, IQR 0-0nM). The concentration of NE measured by ELISA (free and bound) was not significantly different (p=0.296) between subjects with A1ATD (median 330nM, IQR 140-813nM) and usual COPD (median 214nM, IQR 84-564nM).

PR3 activity was greater than NE activity in subjects with A1ATD (p=0.004) and those with usual COPD (p=0.015). However, in the A1ATD group, 3 subjects had higher NE activity than PR3 activity. These 3 subjects were colonised with *Pseudomonas aeruginosa* whilst none of the subjects with usual COPD were. The greater PR3 activity in sputum from A1ATD subjects compared to COPD subjects remained even when subjects colonised with *P. aeruginosa* were excluded (p=0.006). Neither *Pseudomonas aeruginosa* culture supernatants nor purified *Pseudomonas* elastase were able to hydrolyse the

substrates used for the NE or PR3 assays, suggesting that the NE and PR3 activities were specific. These results are shown in Figure 9.3 (data for PR3 substrate not shown).

Figure 9.1- PR3 and NE activities in sol-phase sputum

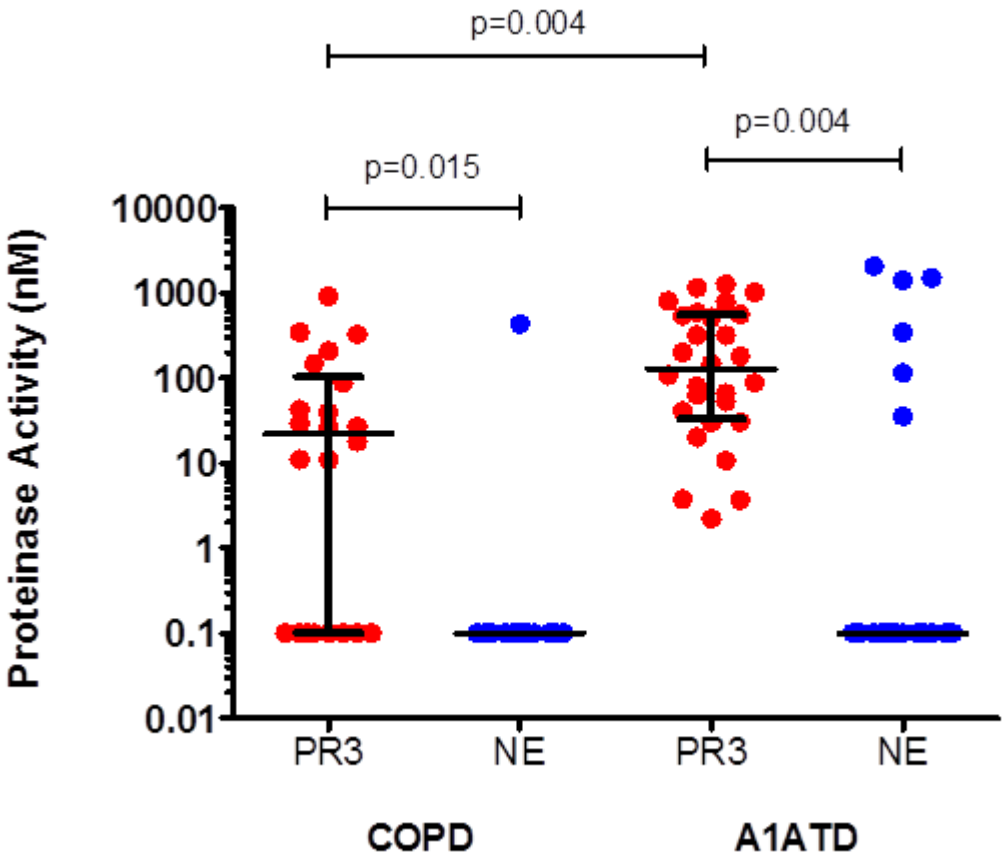

Figure 9.1: PR3 and NE activities in sol-phase sputum spontaneously produced by clinically stable subjects with A1ATD (n=28) and usual COPD (n=22). Each point represents data from an individual subject. Horizontal lines represent the median and IQR. The y-axis shows proteinase activity on a logarithmic scale. Samples with undetectable proteinase activity are indicated at a value of 0.1nM which is the lower limit of detection of the substrates used.

Figure 9.2-Correlation between PR3 activity and PR3 concentration

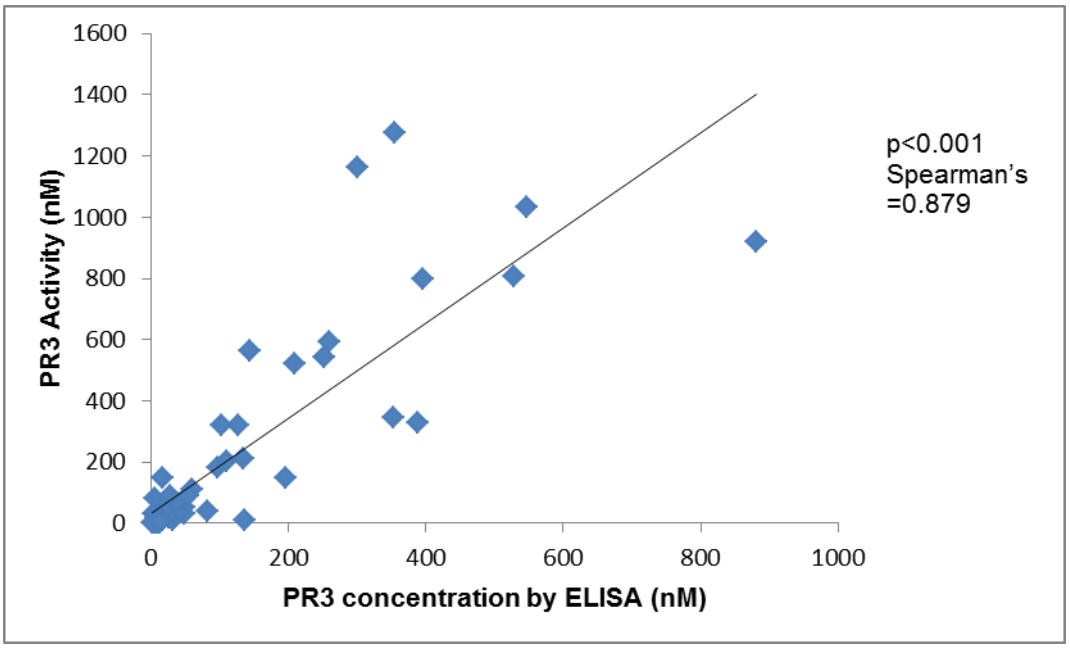

Figure 9.2: Correlation between PR3 activity measured using the specific FRET substrate and unbound PR3 concentration measured by ELISA.

Figure 9.3- The effect of *Pseudomonas* elastase on the substrates used for NE assays

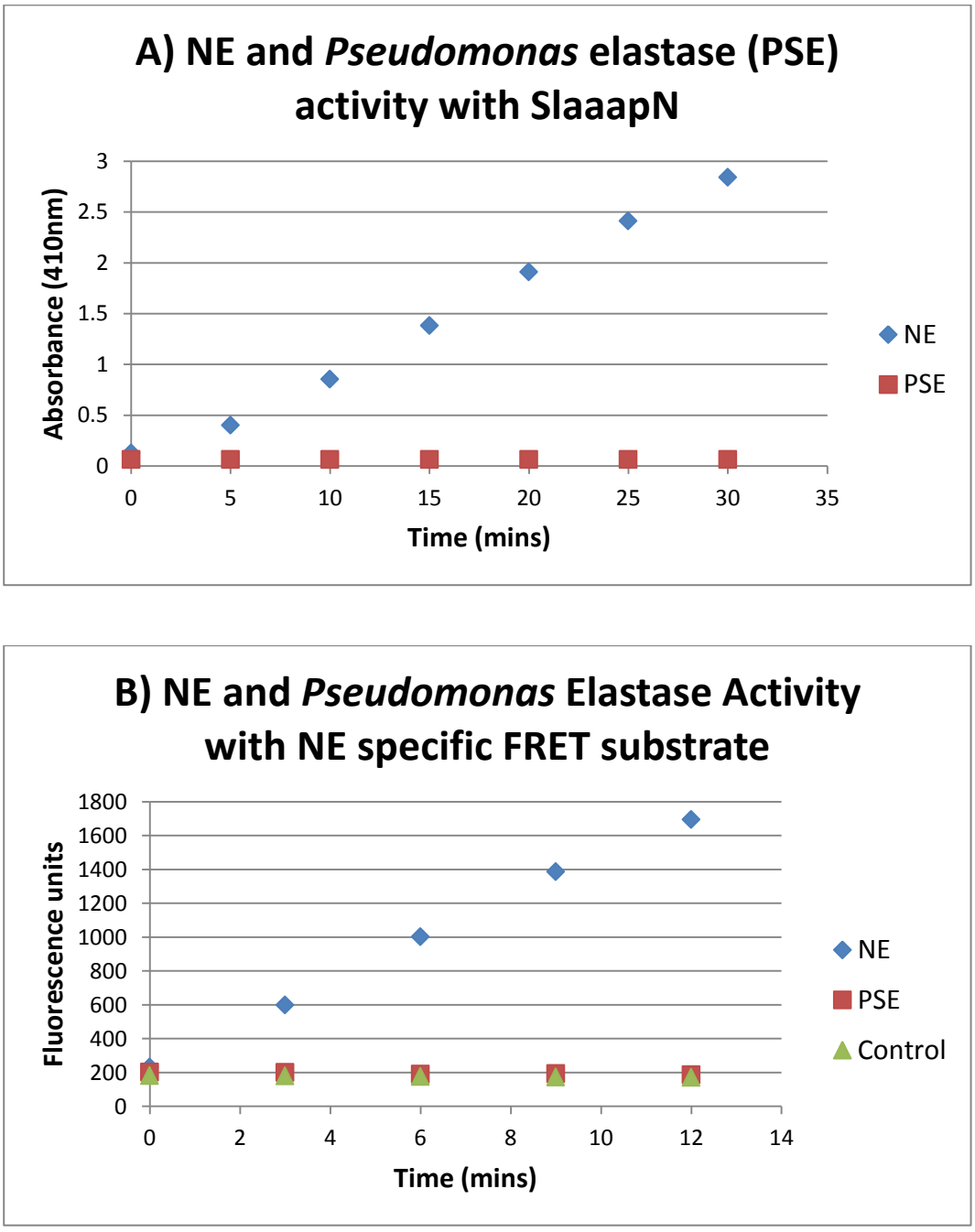

Figure 9.3: Graphs A and B show that pure *Pseudomonas* elastase (PSE) was not able to hydrolyse the NE substrates SlaaapN and the NE specific FRET substrate. Similar results were found using *Pseudomonas aeruginosa* culture supernatants (data not shown).

9.3.3 NSP inhibitory proteins in sputum

As expected, the concentration of A1AT was higher in sputum from subjects with usual COPD compared to those with A1ATD (COPD median 405nM IQR 234-744nM, A1ATD median 51nM IQR 19-83nM: $p<0.001$). In addition, usual COPD subjects also had higher concentrations of SLPI (COPD median 2.8µM IQR 1.7-4.4µM, A1ATD median 1.3µM IQR 0.8-2.7µM: $p=0.002$) and elafin (mean 316±37pM vs 200±39pM: $p=0.039$). However, A2M concentrations were greater in subjects with A1ATD (COPD median 1.2nM IQR 0.4-4.7nM, A1ATD median 3.2nM IQR 0.4-4.7nM: $p=0.046$). The ratio of A1AT/A2M was greater in sputum than in serum in both subject groups, suggesting that diffusion of A2M into the lungs was somewhat limited by its large molecular size. SLPI was quantitatively the predominant NSP inhibitor in sputum from both subject groups. The contribution to the total airway inhibitory capacity of elafin was negligible, being found in sub-nanomolar concentrations in all samples. As shown in Figure 9.4, airway inhibitors of PR3 were quantitatively less than those of NE.

The median concentration of NE measured by ELISA (free and inhibitor-bound) was less than the median total concentration of its cognate inhibitors both in subjects with A1ATD and usual COPD, as shown in Figure 9.5 and would explain why the majority of sputum samples from both subject groups showed no detectable NE activity. It was not possible to measure the total PR3 concentrations since the ELISA available was only able to detect unbound PR3. Nevertheless, the presence of PR3 activity in the sputum samples indicated that the amount of PR3 exceeded the functional concentration of its inhibitors.

Figure 9.4- NSP inhibitory capacity in sputum from stable subjects with A1ATD & COPD

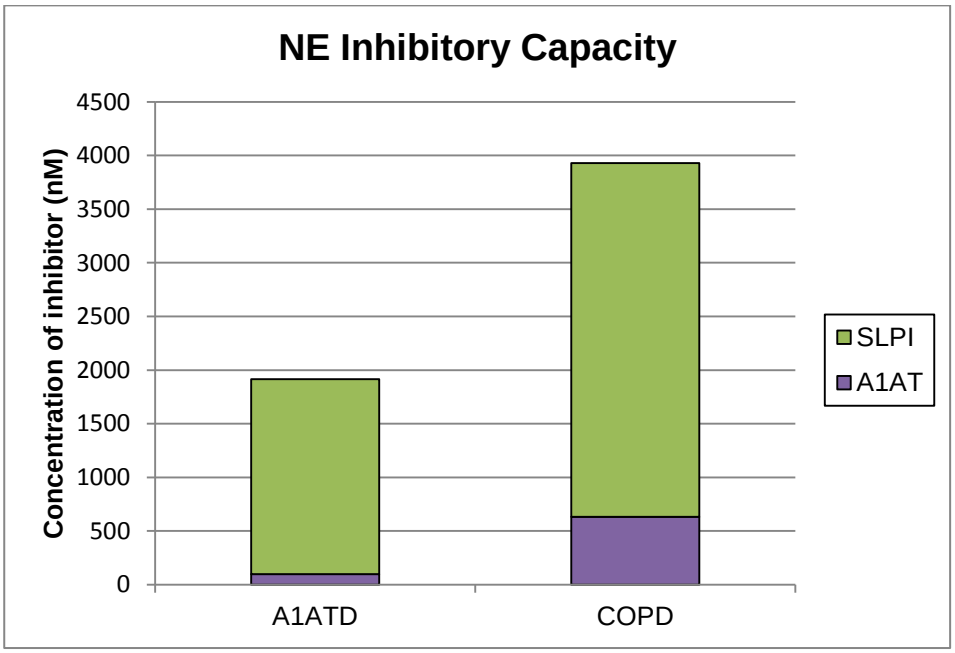

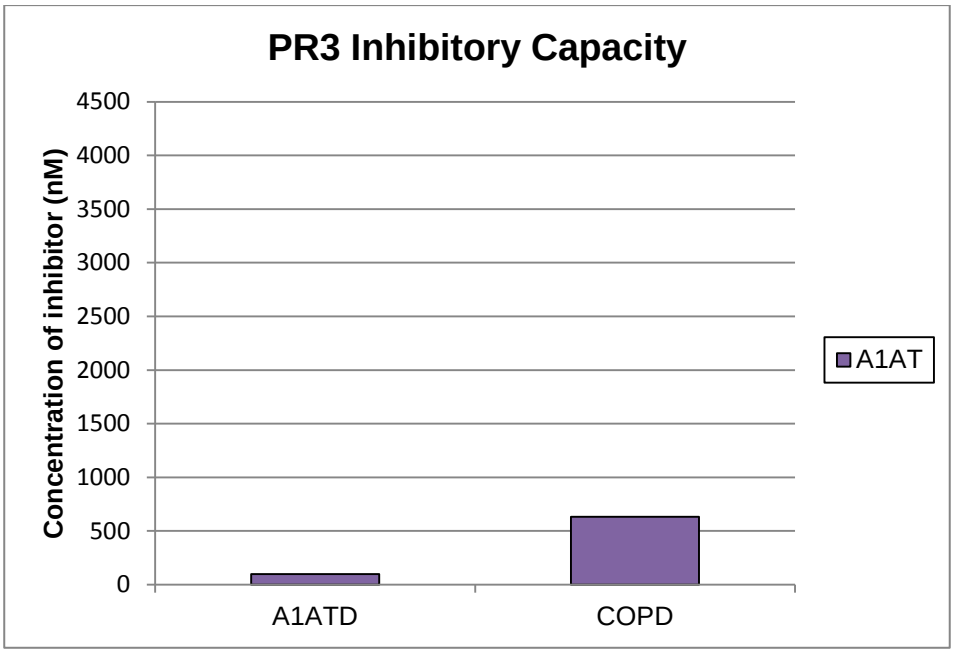

Figure 9.4: Mean concentrations (nM) of airway inhibitors in sol-phase sputum from subjects with A1ATD and usual COPD. The predominant inhibitor of NE in both subject groups was SLPI. The contributions of elafin and A2M in the upper airways were relatively small and are therefore not demonstrable on these graphs. PR3 thus has fewer and significantly reduced quantities of its airway inhibitors than NE.

Figure 9.5- Concentration of NE and its inhibitors in sol-phase sputum

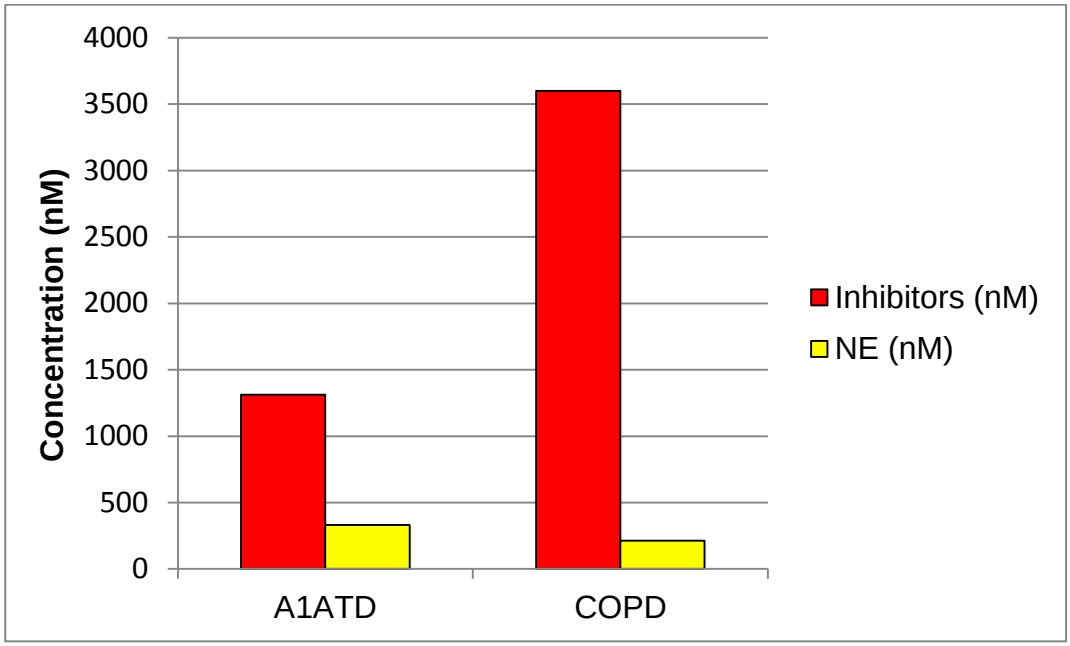

Figure 9.5: Median concentrations (nM) of NE (free and bound to inhibitors) and the median sum of its inhibitors A1AT, SLPI, A2M and elafin in sol-phase sputum from stable subjects with A1ATD and COPD are shown. In both subject groups, the total concentration of NE was well below that of its inhibitors, particularly in subjects with usual COPD. The lack of NE activity in the majority of sputum samples was therefore due to the dominance of its inhibitors.

9.3.4 Relationship between PR3 activity and clinical status

In the 12 subjects with usual COPD who had sputum samples available at the start of an exacerbation and at 8 weeks following the exacerbation when clinically stable, ten day 1 (exacerbation) samples and six day 56 (stable) samples had detectable PR3 activity and the group values were significantly greater during exacerbation than in the stable state

(p=0.037). These data are shown in Figure 9.6. In this sub-group of patients, no significant difference was found in NE activity between exacerbation and stable clinical state (data not shown).

Markers of neutrophilic inflammation were measured in the majority (n=21) of usual COPD samples and in a subset of A1ATD samples (n=11) where sufficient sample remained. The demographics of the COPD subjects where the measurements could be made were not significantly different to those where it could not. The A1ATD subjects who did not have the measurements available were older (59 years vs 50 years: p=0.026) and had a lower KCO (59% predicted vs 82% predicted: p=0.031) than those where measurements were available. However, there were no significant differences in sex, pack year smoking history, smoking status, FEV1 % predicted, FEV1/FVC ratio, residual lung volumes or SGRQ total score between subjects with or without the measurements.

The concentrations of IL-8 (A1ATD median 6.86nM IQR 2.02-12.39nM, COPD median 2.77nM, IQR 1.13-8.24nM: p=0.312), LTB4 (A1ATD median 6.52nM IQR 4.15-20.02nM, COPD median 4.72nM IQR 2.77-17.50nM: p=0.463) and the MPO activities (A1ATD median 0.40 units/ml IQR 0.19-0.57 units/ml, COPD median 0.58 units/ml IQR 0.28-1.65 units/ml: p=0.293) were not significantly different between patient groups.

The correlations between PR3 activity and other parameters are summarised in Table 9.2. PR3 activity correlated positively with NE activity in the A1ATD subjects (Spearman's rho=0.586, p=0.001) even though NE activity was detectable only in 6 subjects. PR3

activity correlated positively with IL-8 quantity in both patient groups (A1ATD Spearman's rho=0.791 p=0.004, COPD Spearman's rho=0.650 p=0.001) and MPO activity (A1ATD Spearman's rho=0.612 p<0.001, COPD Spearman's rho=0.799 p<0.001). In the usual COPD group, PR3 activity also correlated positively with LTB4 (Spearman's rho=0.434, p=0.049).

PR3 activity was found to correlate with the total pathogenic bacterial load in the A1ATD group (Spearman's rho=0.578, p=0.001). Subjects with *Pseudomonas aeruginosa* on quantitative microbiological culture had significantly higher NE activity (p<0.001) and PR3 activity (p=0.025) in their sputum compared to subjects who did not. Higher PR3 activity was also found in samples that grew *Haemophilus influenzae* compared to those that did not (p=0.003) but NE activity was not different.

A significant correlation was also found between PR3 activity and SGRQ total score in the A1ATD subjects (Spearman's rho=0.621, p=0.001). The SGRQ scores were not available for the subjects with usual COPD. No correlations were found between PR3 activity and FEV1 (% predicted) or KCO (% predicted) in either subject group.

Figure 9.6- PR3 activity in COPD patients during an exacerbation and at 8 weeks following the exacerbation when clinically stable

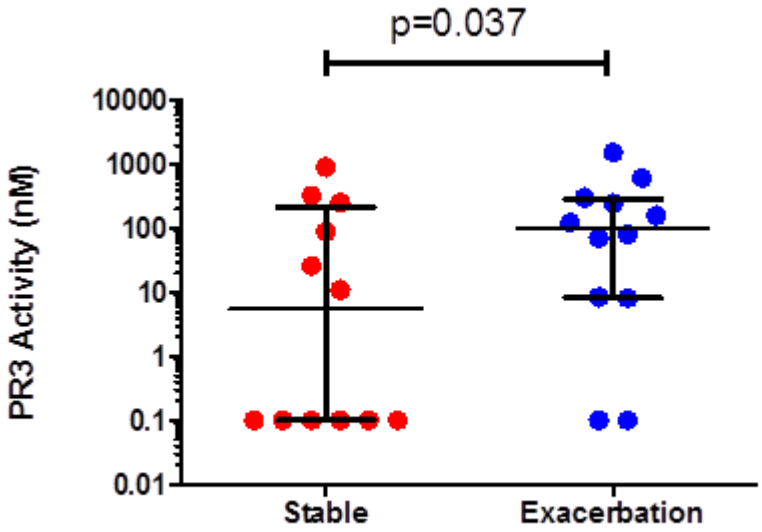

Figure 9.6: PR3 activity in sol-phase sputum from 12 subjects with COPD taken on day 1 of an exacerbation and day 56 when clinically stable. Horizontal lines represent the median and IQR. The y-axis shows PR3 activity on a logarithmic scale.

Table 9.2- Correlations of PR3 activity in sol-phase sputum

Diagnosis	Measurement	Number of Samples with Measurement	Spearman's rho	p-value
A1ATD	MPO	11	0.612	<0.001
	IL-8	11	0.791	0.004
	LTB4	11	0.291	NS
	SGRQ total	25	0.621	0.001
	Total pathogenic bacterial load	28 (18 positive)	0.578	0.001
COPD	MPO	20	0.799	<0.001
	IL-8	21	0.650	0.001
	LTB4	21	0.434	0.049
	Total pathogenic bacterial load	22 (8 positive)	0.291	NS

NS= not significant

9.4 Discussion

The work presented in this Chapter has provided direct evidence that active PR3 is present in sol-phase sputum from clinically stable subjects with chronic bronchitis associated with A1ATD as well as usual COPD. PR3 activity was greater than NE activity in these subjects (Figure 9.1), which likely reflects both the lower airway inhibitory capacity for PR3 (Figure 9.4) and the greater amount of PR3 contained within the azurophilic granules of the neutrophil compared to NE [108]. In addition, the association rate constants of A1AT and elafin for PR3 are orders of magnitude lower than for NE [123] and therefore NE is likely to be preferentially inhibited compared to PR3 in the inflammatory environment. Indeed, NE activity was largely undetectable in the samples studied, which is likely to be due to a dominance of its inhibitors (Figure 9.5). Furthermore, PR3 is not inhibited by SLPI which is present in large amounts in respiratory epithelial lining fluid and is the predominant inhibitor of NE in the upper airways (Figure 9.4). In addition, PR3 is capable of degrading SLPI [127], thus potentially enhancing the biological activities of other NSPs that are usually inhibited by SLPI.

PR3 activity was greater in subjects with A1ATD than in subjects with non-deficient COPD, which highlights the greater proteinase/anti-proteinase imbalance in A1ATD subjects. Figure 9.4 shows that the A1ATD subjects had little anti-proteinase protection against PR3 and would explain why active PR3 was detectable in all sputum samples from this subject group.

PR3 activity was found to be greater during exacerbations than during periods of clinical stability (Figure 9.6). Exacerbations are often associated with an increased neutrophilic

inflammation [44], and would account for the correlations of PR3 activity with other neutrophilic markers (Table 9.2). Of interest, PR3 activity showed a positive correlation with worsening health status as measured by the SGRQ. PR3 activity is thus a marker of increased airway inflammation and exacerbations, which are both associated with impaired health status in subjects with chronic respiratory disease [336, 337] suggesting it is an association rather than cause and effect.

These results do not however demonstrate any relationship between PR3 activity and lung function parameters. In a previous study where PR3 concentration was measured in sputum from 49 subjects with cystic fibrosis (CF), a negative correlation was observed between PR3 concentration and FEV1 (% predicted) [75]. It is possible therefore that the work presented here did not involve sufficient numbers to detect such a relationship between FEV1 and PR3 activity, although other features such as variable bacterial colonisation (see below) will also complicate this potential relationship. The current study also did not find a significant difference in markers of neutrophilic inflammation (IL-8, LTB4 and MPO) between subjects with A1ATD and those with non-deficient COPD. Again, this could be related to the size of the subject groups studied since previous work by Hill *et al* [338] reported that subjects with A1ATD (n=42) had greater inflammation in the upper airways with increased LTB4 and MPO compared to subjects with non-deficient chronic bronchitis (n=39).

The studies presented in this Chapter have directly measured both PR3 and NE activities in biological samples using highly sensitive and specific substrates. Some previously published studies of NSP activities in airway secretions have used non-specific “elastase”

substrates (such as MSaapvN) and potentially measured the combined activities of PR3 and NE [19, 339, 340]. Other studies have indirectly measured PR3 activity by measuring the combined activities of PR3 and NE with and without an NE inhibitor [75]. The direct measurement of individual NSP activities in lung secretions using highly sensitive and specific substrates (as described here) allows the contribution of each NSP to the total proteinase burden to be determined specifically. Although NSPs are released from neutrophils simultaneously upon activation and degranulation, their concentrations can differ due to local factors such as binding to the cell membrane [108], their affinities to endogenous inhibitors at the inflammatory site and their specificities toward peptide or protein substrates [123]. Biological consequences are only likely to occur in the presence (especially persistent presence and quantity) of active enzyme.

The results described in this Chapter are derived from subjects with A1ATD and usual COPD with a chronic bronchitis phenotype. Subjects with chronic bronchitis show a higher airway inflammatory burden compared to subjects who do not expectorate, which is not related to smoking status [19]. Sputum production may also be associated with an accelerated decline in FEV1 in COPD [20]. Therefore, although it is important to understand the role of NSPs in this subgroup of patients, the results presented here may not be generalizable to subjects who are not spontaneous sputum producers. However, spontaneous sputum collection is non-invasive and minimises dilutional errors found with other techniques such as broncho-alveolar lavage [341] and induced sputum collection and may thus provide critical data especially in this important phenotype.

Three of the subjects with A1ATD were colonised with *Pseudomonas aeruginosa* and had significantly higher NE and PR3 activities in their sputum compared to subjects who were not. The presence of *Pseudomonas* proteinases in these sputum samples could not have accounted for these elevated NSP activities (Figure 9.3). However, *Pseudomonas* elastase is able to cleave SlaaapN between the first and second alanine residues, rendering the cleaved substrate ineffective and potentially under-estimating NE activity in the presence of *Pseudomonas* proteinases [342]. However, the NE specific FRET substrate gave results consistent with those using SlaaapN, providing confidence in the activity values reported here.

In addition to the elevated NSP activities in samples that grew *Pseudomonas aeruginosa*, greater PR3 activity was also found in samples that grew *Haemophilus influenzae* compared to those that did not. Hill *et al* [343] have previously shown that in patients with bronchiectasis, *Pseudomonas aeruginosa* provokes a more intense inflammatory response (with elevated NE and MPO activities) compared to *Haemophilus influenzae*, which in turn is greater than that with *Moraxella catarrhalis*. Correlations of PR3 activity with airway bacterial load and airway inflammation (NE and MPO activities) support the role of colonisation in airway neutrophilic inflammation (as indicated previously [343, 344]), but highlights the association with PR3 activity, which has the potential to drive the pathophysiological processes that influence COPD and its progression. This enzyme may therefore be more important in COPD than has previously been thought.

In conclusion, the results presented in this Chapter suggest that PR3 activity should be determined when evaluating the proteinase/anti-proteinase imbalance in the airways.

Whether or not it is central to the pathological process remains to be determined as it remains possible that several proteinases may play a role in the pathogenesis of COPD, either individually, additively or synergistically. In addition to NSPs, both MMPs [345] and cysteine proteinases [212, 214] have been associated with tissue destruction in emphysema both directly and indirectly via their interactions with NSPs and their inhibitors (as shown in Figure 1.7). Strategies to reduce the burden of proteinases in the lungs could potentially offer novel therapies for COPD. Even abrogation of one enzyme may positively abrogate a proteinase cascade involving others. Recently, Jegot *et al* [346] have developed specific PR3 inhibitors. Selective inhibitors of PR3 may thus provide further insight into its role in disease and the inflammatory cascade. Such approaches (based on the studies presented here) could therefore potentially be of therapeutic value in a variety of inflammatory lung diseases, but specifically COPD.

10 Overall discussion and future work

COPD remains a significant medical condition characterised by pulmonary inflammation in response to inhaled substances. At present, the pharmacological therapies available for COPD do not convincingly alter disease progression or mortality, and therefore there is an urgent need for novel therapies. To date, there has been a substantial body of evidence implicating proteinases in the pathophysiology of COPD [100], and notably NE has been a strong focus. However, limited short-term studies of selective NE inhibitors have not been fully effective in controlling neutrophil-mediated damage in the airways [98] and have not demonstrated clinical benefits [99]. Furthermore, other serine proteinases as well as MMPs and cysteine proteinases have been both directly and indirectly implicated in COPD [212, 214, 345], and may play a synergistic or even more central role in tissue destruction than has previously been recognised. In addition, interactions exist between different classes of proteinases, their substrates, their inhibitors and other inflammatory mediators. Thus, the pathophysiology of COPD is complex and uncertainty has led to a reluctance to develop and trial specific anti-proteinase agents.

The results presented in this thesis provide novel data on the biological interactions of NSPs with their inhibitors and substrates, and on the potential importance of PR3 in inflammatory lung disease. These findings along with potential future studies are discussed in further detail below.

10.1 Interactions between NSPs and their inhibitors and substrates

10.1.1 The potential role of proteinase complexes with A2M

The major circulating inhibitors of NE and PR3 are A1AT and A2M which differ in their mechanism of inhibition. Complex formation between A1AT and NSPs results in the enzyme being inactivated. However, "inhibition" of proteinases by A2M does not block the active site of the enzyme and it retains proteolytic activity, at least towards low molecular weight substrates [196]. The results presented in Chapters 3 and 4 demonstrate that NE bound to A2M remains active towards low molecular weight nitroanilide substrates, and shows enhanced activity towards certain substrates, consistent with previous findings [255]. In addition, these results have demonstrated that PR3 bound to A2M also remains proteolytically active towards the small peptide substrate MSaapvN. When these NSPs are introduced to serum, they partition between their major inhibitors depending on both the local concentrations of inhibitors and their association rate constants (as shown in Figure 4.1). Therefore, in situations where A1AT is deficient or dysfunctional, a greater proportion of released NSPs would partition towards A2M and likely remain active *in vivo*.

The potential biological significance of A2M complexes with NSPs was explored in Chapter 5 where elastin was used as a more physiological substrate. The results suggest that A2M:NE complexes are capable of elastin degradation *in vitro*. Firstly, when NE was pre-incubated with PiMM serum (containing a molar excess of A1AT) and elastin was subsequently introduced, some elastin degradation was still observed (Figure 5.1A), which did not occur when pure A1AT was used (Figure 5.7), indicating that the elastin degradation was due to NE bound to A2M. Secondly, when NE was pre-incubated with a

three-fold molar excess of A2M and elastin was subsequently introduced, elastin degradation was again observed (Figure 5.8). The three-fold molar excess of A2M used in these experiments should have theoretically been sufficient to bind all of the free NE, as Moore *et al* [254] found that a 1.5 molar excess of A2M was sufficient to bind all free NE under similar experimental conditions. It does however remain possible that some of the trapped NE could have dissociated from A2M. Although this is unlikely, the absence of free NE could be confirmed in future studies by size exclusion chromatography.

The role of A2M:NE complexes in disease has yet to be fully elucidated, but active A2M:NE complexes have been implicated in the pathogenesis of emphysema in animal models [201], and other studies have shown that A2M:NE complexes may play a role in the adult respiratory distress syndrome in humans [253] and the degradation of cartilage matrix in rheumatoid arthritis [254]. However, other studies have suggested that A2M:NE complexes are unable to degrade macromolecular substrates (such as mature elastin) [267]. Therefore, further studies are necessary to determine whether A2M:NE complexes are important in diseases where excessive activities of NSPs have been implicated. These initial studies could involve the instillation of human A2M:NE complexes into animal lungs to determine whether emphysema-like lesions develop. Additional studies of human samples could involve the measurement of A2M:NE complexes in lung secretions (sputum or BAL), and their relation to clinical outcomes such as PFTs or emphysema severity determined by CT densitometry.

The significance of A2M:PR3 complexes has not been explored previously. Although PR3 bound to A2M remains proteolytically active towards low molecular weight peptide

substrates (Chapters 3 and 4), A2M:PR3 complexes appear to be less likely than A2M:NE complexes to play an important role in elastin degradation. The results presented in Chapter 5 show that both PiMM (Figure 5.1B) and PiZZ (Figure 5.3B) sera were able to completely inhibit PR3 activity towards elastin when the A1AT was in a molar excess, and PR3 activity towards elastin was at least partly inhibited following pre-incubation with A2M (Figure 5.8). Despite these findings, PR3 may still play an important role in the tissue damage associated with emphysema because it is more abundant than NE and has fewer airway inhibitors (Chapter 9).

10.1.2 The effect of elastin on NSP inhibition

The studies in Chapter 5 highlighted differences in how NSPs interact with their inhibitors in the presence of elastin. When NE was pre-incubated with pure A1AT (Figure 5.7), inhibition of NE activity towards elastin occurred when the molar ratio of A1AT:NE was 1.2:1. The studies using serum samples to inhibit NE activity also demonstrated that serum A1AT inhibited NE activity towards elastin when the molar ratio of A1AT:NE was 1.2-1.4:1 following extrapolation of the slope to the x-axis, suggesting that A1AT was less functional as an inhibitor when elastin-fluorescein was used as the substrate. Indeed, previous work by Kramps *et al* [271] reported that A1AT had a specific inhibitory activity of 40-85% of that observed with synthetic nitroanilide substrates when elastin-fluorescein was used, possibly due to a degree of dissociation of the A1AT:NE complex with subsequent poor inhibition of elastin-bound NE. The same was not true of PR3, which was fully inhibited with 1:1 stoichiometry by A1AT in both PiMM and PiZZ sera when elastin-fluorescein was used as the substrate.

Morrison *et al* [266] reported that airway inhibitors such as A1AT and SLPI were less effective against NE bound to elastin compared to free NE. The studies presented in Chapter 5 were consistent with these findings, since NE added to a mixture of both elastin-fluorescein and serum was poorly inhibited even when the concentration of inhibitors was in a molar excess (Figures 5.2 and 5.4), which reflects differential partitioning to the elastin substrate in competition with the inhibitors. This "ineffective" inhibition of NE in the presence of elastin may have biological relevance to the pathogenesis of emphysema which results from damage to elastin in the lung parenchyma. Therefore, further studies will be necessary to investigate this more complex system. However, the studies presented in Chapter 5 suggested that PR3 added to a mixture of both elastin-fluorescein and serum could be inhibited, although less effectively in the presence of elastin (Figures 5.2 and 5.4). A previous *in vitro* study by Ying and Simon [123] reported that the elastolytic rate of PR3 was one eighth that of NE using bovine neck ligament elastin (as was used in the studies presented in this thesis), and that ongoing elastolysis by PR3 was almost completely inhibited by M variant A1AT, although these findings remain to be verified *in vivo* or in situations where the A1AT concentration is low or the protein is dysfunctional (such as in PiZZ homozygotes).

10.1.3 Differences between NE and PR3 and their association rate constants with inhibitors

The M variant of A1AT has been reported to be a less competent inhibitor of PR3 compared to NE, with its Kass with PR3 being ten-fold lower than that with NE [117, 280]. However, the second order association rate constants for other A1AT variants and PR3 had not been described previously. The results presented in Chapter 6 showed that the second order association rate constants for all A1AT variants studied (M, Z, S, FZ, IZ)

were greater for NE than PR3 (Figure 6.3). Therefore, if the concentration of A1AT were to be insufficient to inhibit both proteinases during neutrophilic inflammation, NE would be preferentially inhibited. For this reason, in addition to the greater amounts of PR3 contained within the neutrophil azurophilic granules [108], and the fact that PR3 is not inhibited by the local lung inhibitor SLPI [109], it is likely that PR3 is more important in the pathophysiology of COPD than has previously been thought (especially in subjects with A1ATD) since its activity is likely to persist longer in the neutrophilic environment than NE.

The association rate constants for both NE and PR3 with A2M have been measured elsewhere [117, 190]. The *in vitro* association rate constants for A1AT and A2M with NE are similar. Nevertheless, in subjects with the PiMM phenotype, the molar concentration of A1AT is approximately 10 times greater than that of A2M and therefore released NE is likely to partition predominantly to A1AT in serum. However, PiZZ homozygotes (and PiFZ or PiIZ heterozygotes) have lower concentrations of A1AT with lower association rate constants relative to A2M, which would alter the partitioning of NE more towards A2M where it retains proteolytic activity as discussed earlier. PR3 on the other hand has a greater Kass with A2M compared to all A1AT variants studied here, and therefore if the concentrations of A1AT and A2M were similar (such as in PiZZ subjects), PR3 would preferentially bind to A2M where it will remain active, at least towards low molecular weight substrates. At present, the physiological significance of A2M:PR3 complexes remains uncertain, and further studies will be necessary to determine whether these complexes are able to degrade the elastin precursor tropoelastin, and hence affect the repair process.

In the airways, the chelonianin inhibitors SLPI and elafin are present in addition to A1AT and A2M. SLPI is a reversible inhibitor of NE but does not inhibit PR3 [109]. Furthermore, PR3 can inactivate SLPI [127] thus potentiating the activities of other proteinases usually inhibited by SLPI. Overall, the anti-proteinase protection in the airways against PR3 activity appears to be relatively weak since PR3 has quantitatively fewer airway inhibitors than NE (Figure 9.4). In addition, the association rate constants for A1AT and elafin are lower for PR3 than NE, and therefore these inhibitors would also preferentially associate with NE in the context of neutrophilic inflammation. The potential *in vivo* significance of these observations is discussed in further detail below.

Knowledge of the association rate constants for enzyme-inhibitor interactions and the local concentrations of airway inhibitors could potentially allow a mathematical model to be constructed in order to determine the partitioning of released NSPs between their inhibitors, and the effects of different A1AT variants on this partitioning. For example, Rao *et al* [117] predicted that if both NE and PR3 were released at similar concentrations in the lower respiratory tract, M variant A1AT would distribute between the two NSPs such that 89% of it would be bound to NE and 11% of it would be bound to PR3. A more complex mathematical model could potentially consider the presence of additional inhibitors such as A2M and SLPI, and provide theoretical support to the differences in partitioning of enzymes between their inhibitors observed in Chapter 3.

10.1.4 The *in vitro* effects of augmentation therapy on NSP activities and partitioning between inhibitors

Increasing the A1AT level in deficient subjects increases the total inhibitory capacity. However, the studies described in Chapter 7 demonstrated that the addition of M variant A1AT to serum from subjects with A1ATD (PiSZ, PiFZ or PiZZ genotypes) also alters the partitioning of NSPs between their serum inhibitors even at equivalent concentrations of A1AT. With the augmented serum samples, greater proportions of NE or PR3 became bound to A1AT where they are inactivated, resulting in fewer active complexes between NE or PR3 and A2M. In addition to changes in the partitioning of NSPs between A1AT and A2M, the inhibitory capacity of augmented serum would be greater due to its higher A1AT concentration, the greater Kass of M variant A1AT with NE and a reduced tendency to form inactive polymers. However, A1AT augmentation therapy would still not inhibit elastin-bound NE as discussed previously, and different mechanisms of inhibiting elastin-bound NE should be explored.

10.2 The role of PR3 in A1ATD and COPD

10.2.1 Neutrophil cell surface expression of PR3 and its importance in A1ATD

Previous work has shown that NSPs bound to the cell membrane of stimulated neutrophils remain catalytically active towards both synthetic peptide and high molecular weight biological substrates such as fibronectin [54, 108]. In addition, PR3 expressed on the neutrophil cell membrane is a major antigenic target for ANCAs in WG, and A1ATD is a risk factor for the development of WG [228]. The studies in Chapter 8 showed that PR3 expression on the surface of both unstimulated and stimulated neutrophils was greater in subjects with A1ATD (PiZZ phenotype) compared to healthy controls. In addition,

neutrophil cell surface PR3 expression was greater when the local concentration of A1AT was reduced. However, neutrophil cell surface expression of NE did not appear to be influenced by the local concentration of A1AT in the studies presented here. The greater neutrophil expression of PR3 in A1ATD could potentially contribute to the proteinase/anti-proteinase imbalance observed in this condition, since membrane bound PR3 retains its activity and hence its tissue damaging potential. Furthermore, the proteinase/anti-proteinase imbalance may play a role in the pathogenesis of WG, and previous studies have suggested that subjects with WG with the PiZZ genotype have more aggressive disease than subjects with the PiMZ or PiMM genotypes [326] which likely reflects the amount of neutrophil membrane-bound PR3. In addition, A1AT can inhibit binding of anti-PR3 antibodies to membrane PR3 by steric hindrance [327] and hence reduce activation of neutrophils by this process in subjects with active WG. Overall, these observations may suggest a potential therapeutic role for A1AT augmentation therapy particularly in the sub-group of A1ATD patients with acute episodes of vasculitis due to WG. Clearly, further clinical studies in this sub-group of patients are warranted to determine the efficacy of such an approach.

In the future, a better understanding of the mechanism of PR3 binding to the neutrophil cell membrane may facilitate therapeutic approaches to modulate membrane expression of PR3, which may be beneficial for WG and other conditions where the proteinase/anti-proteinase imbalance plays a role (such as COPD). One strategy may involve blocking the interaction between PR3 and the NB1 receptor. Choi *et al* [347] have identified compounds which can inhibit binding of exogenous PR3 to human neutrophils and reduce TNFα-mediated increases in membrane PR3 on NB1 positive cells. These compounds

could potentially provide a potential therapeutic tool to reduce membrane PR3 expression by preventing its binding to the NB1 receptor.

10.2.2 PR3 activity in airway secretions from subjects with A1ATD and usual COPD

The studies presented in Chapter 9 showed that active PR3 was present in sol-phase sputum from clinically stable subjects with chronic bronchitis associated with A1ATD as well as usual COPD, whereas NE activity was undetectable in the majority of these samples. Therefore, in both groups of patients, the amount of active PR3 was greater than the amount of active NE (Figure 9.1) which most likely reflected the greater anti-proteinase protection against NE in the upper airways (Figure 9.4). In addition, PR3 activity was even greater in subjects with A1ATD than non-deficient subjects with COPD, consistent with the lower concentrations of A1AT and hence the greater proteinase/anti-proteinase imbalance in A1ATD.

PR3 activity was also found to be greater during exacerbations than during periods of clinical stability in subjects with usual COPD (Figure 9.6). Exacerbations are associated with an increased neutrophilic inflammation [44], and these findings are supported by the positive correlations observed between PR3 activity and other neutrophilic markers (Table 9.2). PR3 activity also showed positive correlations with worsening health status and pathogenic bacterial load in A1ATD subjects. Thus, PR3 activity is a marker of increased airway inflammation and exacerbations, both of which are associated with impaired health status in subjects with chronic respiratory disease [336, 337]. The reasons for this association are likely to relate to the overall nature of the inflammation and its systemic

effects. Other factors such as lung function and bacterial colonisation may have independent effects on the perception of health, and more extensive studies with greater patient numbers would be required to determine whether this association represents cause and effect.

In addition to A1AT and the chelonianin inhibitors SLPI and elafin, A2M was found to be present in sol-phase sputum from clinically stable subjects with A1ATD or usual COPD. A2M enters the lungs predominantly by diffusion, however the ratios of A1AT/A2M were greater in sputum than serum in both subject groups, suggesting that diffusion of A2M into the airways was somewhat limited by its large molecular size. The presence of A2M in the lung secretions may still be of pathological significance since A2M complexes with NE or PR3 remain active as discussed previously. Furthermore, proteinases bound to A2M are shielded from other airway inhibitors such as A1AT. Although the studies presented here did not detect a difference in A2M concentration between exacerbations and clinical stability, larger studies [193] have shown that concentrations of A2M in infected samples were greater than in non-infected samples. Therefore, any role of complexes between A2M and NSPs in tissue damage is likely to be greater during exacerbations, and thus may enhance the damaging potential of NSPs.

The results described in Chapter 9 are from subjects with A1ATD or usual COPD with a chronic bronchitis phenotype, and therefore the results may not be generalizable to subjects who do not produce spontaneous sputum. Future studies in A1ATD or COPD could use induced sputum to determine the proteinase burden in the upper airways, or BAL

to sample the distal airways. These studies may provide further insight into the role of PR3 in stable COPD subjects without chronic bronchitis.

The studies described in Chapter 9 have directly measured both PR3 and NE activities in sol-phase sputum using highly sensitive and specific FRET substrates. In the past, the role of PR3 has not been studied in detail due to a lack of availability of specific PR3 substrates and inhibitors. As a result, some previously published studies of NSP activities in airway secretions have used non-specific "elastase" substrates (such as MSaapvN) and potentially measured the combined activities of PR3 and NE [19, 339, 340], thus over-estimating the contribution of NE. Alternatively, previous studies have indirectly measured PR3 activity by measuring the combined activities of PR3 and NE with and without an NE inhibitor [75]. The direct measurement of individual proteinases is important in order to determine the relative contribution of each proteinase to the overall inflammatory burden. This is particularly important in lung secretions from subjects with COPD (and other inflammatory lung diseases where proteinases have been implicated) where several human proteinases of different classes may be present along with bacterial proteinases. Greater knowledge of the roles of each proteinase may identify targets for specific therapeutic inhibitors, although this will require the development of specific direct substrates for the enzymes likely to be present.

Recently, Wysocka *et al* [348] have developed new FRET substrates that allow all three NSPs (NE, PR3, CG) to be quantified at the same time and in the same reaction mixture. These substrates are capable of measuring NSP activities on neutrophil cell membranes and in other biological fluids. Such substrates could be used in future studies of NSP

activities in airway secretions to reduce both time and the amount of sample required, as well as providing information on the relative contributions of the individual NSPs including CG.

10.3 Discussion and future directions

As highlighted above, NSPs are likely to play an important role in the pathophysiology of COPD, and NE in particular has received the most attention in the literature. However, Korkmaz *et al* [349] studied the competition between the NSPs (NE, PR3, CG) for binding to A1AT, and found that NE was the main target of A1AT when identical molar amounts of A1AT and the three NSPs were studied together. Both PR3 and CG were only inhibited once NE had been totally inhibited. The authors also studied BAL from subjects with acute bacterial pneumonia and/or ARDS and again found that NE was the preferred target for inhibitors present in BAL fluid. Interestingly, they found that PR3 (both free and bound to the neutrophil cell membrane) was the least well controlled NSP by the inhibitors present in BAL fluid, perhaps because CG can also be inhibited by SLPI and α1-antichymotrypsin.

To date, the development of anti-proteinase therapies for A1ATD or COPD has not been completely successful. Although A1AT augmentation therapy is used in some countries for subjects with A1ATD, randomised controlled studies to date have not convincingly demonstrated its efficacy in clinical practice [238], although data on emphysema progression using CT densitometry as the outcome have been more suggestive of efficacy [301-303]. It remains possible that treatment with A1AT augmentation therapy predominantly targets NE activity (due to the lower Kass of A1AT with PR3 or CG) and does not control the activities of the other NSPs in the airways whilst NE activity remains,

as suggested by Korkmaz *et al* [349]. In usual COPD, specific inhibitors of NE have failed to show any clinical benefit in short term randomised studies [99]. Again, this may be because NE is the preferred target of endogenous A1AT in these patients, and the uncontrolled activities of other proteinases may be of greater importance.

Novel anti-proteinase agents may include specific inhibitors of PR3 (based on the evidence presented in this thesis), mechanisms for inhibiting NE bound to A2M or elastin, or possibly inhibitors of other classes of proteinases. These areas for future studies are discussed in further detail below.

10.3.1 Inhibitors of PR3

Overall, the results presented both in this thesis and in the literature [75, 349] suggest a potential therapeutic role for inhibitors of PR3 activity in inflammatory lung diseases such as COPD. Specific PR3 inhibitors have not been reported until recently, and their design has been hampered by the fact that all biological inhibitors of PR3 (A1AT, elafin and MNEI) preferentially inhibit NE [123, 179]. Recently, Jegot *et al* [346] were the first to develop a specific PR3 inhibitor derived from MNEI. This inhibitor was capable of inhibiting both free and neutrophil cell membrane-bound PR3. Subsequently, a reversible specific PR3 inhibitor was designed by the same research group based on the sequence of one of its specific FRET substrates [350]. This inhibitor is also able to inhibit free and neutrophil cell membrane-bound PR3, as well as PR3 in induced sputum and BAL fluid. In future studies, specific inhibitors of PR3 will provide further insight into its role in disease and the inflammatory cascade. In addition to their anti-proteinase effects, PR3 inhibitors could potentially have indirect anti-inflammatory effects since PR3 is able to activate

TNFα, IL-8, IL-1β, IL-18 and IL-32 [58, 111-113]. These inhibitors could potentially be of therapeutic value in a variety of inflammatory lung diseases (including COPD) and could be administered either systemically or by inhalation. Therefore, *in vivo* studies of specific PR3 inhibitors will be required to determine their safety and efficacy.

10.3.2 Future directions for NE inhibitors

Future studies should investigate mechanisms of inactivating elastin-bound NE which is poorly inhibited by endogenous inhibitors [266]. Animal studies [272, 273] have shown that in order to protect the lungs from proteolytic damage, synthetic elastase inhibitors needed to be administered prior to the release of elastase. If inhibitors were administered after an elastase challenge, little or no protection was achieved, most probably because the inhibitors failed to inactivate elastin-bound NE. This ineffective inhibition of elastin-bound NE has biological relevance to the pathogenesis of emphysema, and therefore greater knowledge of the mechanisms for inhibiting the activity of elastin-bound NE may lead to the development of more effective agents. In addition, any future developments of NE inhibitors should consider mechanisms of inactivating NE bound to A2M, which is shielded from other biological inhibitors such as A1AT. These complexes may also play a significant role in the elastin degradation associated with emphysema, as discussed in Chapter 5.

10.3.3 Inhibitors of other proteinases

It has been recognised that several proteinases may play a role in the pathogenesis of COPD, either individually, additively or synergistically. In addition to the NSPs discussed in this thesis (NE and PR3), the role of CG in COPD has not been well studied and

therefore its relevance remains largely unknown. However, a dual inhibitor of CG and chymase has been shown to reduce airway inflammation in animal studies [131]. Recently, a fourth NSP has also been identified, NSP4, which shows around 40% sequence homology with NE and PR3 [351]. The physiological and pathological roles of this NSP remain to be determined.

Although direct experimental and clinical observations have predominantly highlighted the importance of NSPs in the pathogenesis of COPD, other classes of proteinases such as MMPs and cysteine proteinases have also been implicated in tissue destruction in emphysema both directly and indirectly. One study of a broad spectrum MMP inhibitor (ilomastat) demonstrated protection against the development of emphysema in cigarette smoke-treated mice [352]. A dual inhibitor of MMPs 9 and 12 has also been shown to reduce small airways fibrosis in smoke exposed guinea pigs [353]. However, a more recent study using MMP-9 knockout mice and human samples suggested that specific inhibition of MMP-9 was unlikely to be an effective therapy against cigarette smoke-induced emphysema [354]. Two human phase IIa studies of an oral inhibitor of MMPs 9 and 12 (AZD1236) administered over a six week period to patients with moderate-to-severe COPD have demonstrated that the drug was generally well tolerated with an acceptable safety profile, but no significant benefits were observed in terms of lung function or other clinical parameters [355, 356], although this time frame is far too short for a disease-modifying study. To date, there have been no human studies of cysteine proteinase inhibitors in COPD.

10.4 Conclusion

COPD remains a major cause of morbidity and mortality worldwide. At present, there is an urgent need for novel therapies to prevent or reverse progression of the disease, although development of such strategies has been limited due to the complex pathophysiology. Our overall knowledge of the relationships between proteinases, their inhibitors and other inflammatory mediators remains limited, and is further hindered by the lack of suitable short-term biomarkers for assessing the potential benefit of therapeutic interventions. The studies presented in this thesis have provided novel data on some of the biological interactions between NSPs and their inhibitors and substrates, and on the potential importance of PR3 in COPD and A1ATD. Selective inhibitors of PR3 are thus required to provide further insight into its role in disease and therapeutic potential in COPD and other inflammatory lung diseases where a proteinase/anti-proteinase imbalance is thought to be central to the pathophysiology.

11 References

1. Pauwels RA, Rabe KF. Burden and clinical features of chronic obstructive pulmonary disease (COPD). *Lancet* 2004: 364(9434): 613-620.

2. Statistics. Deaths by age, sex and selected underlying cause. 2008 [cited 2012]; Available from: www.statistics.gov.uk

3. NICE. Management of chronic obstructive pulmonary disease in adults in primary and secondary care (partial update). 2010 [cited 2012]; Available from: http://guidance.nice.org.uk/CG101/NICEGuidance/pdf/English

4. BTS. Burden of Lung Disease, 2nd Edition. 2006 [cited 2012]; Available from: http://www.brit-thoracic.org.uk/delivery-of-respiratory-care/burden-of-lung-disease-reports.aspx

5. Pellegrino R, Viegi G, Brusasco V, Crapo RO, Burgos F, Casaburi R, Coates A, van der Grinten CP, Gustafsson P, Hankinson J, Jensen R, Johnson DC, MacIntyre N, McKay R, Miller MR, Navajas D, Pedersen OF, Wanger J. Interpretative strategies for lung function tests. *Eur Respir J* 2005: 26(5): 948-968.

6. Jordan RE, Miller MR, Lam KB, Cheng KK, Marsh J, Adab P. Sex, susceptibility to smoking and chronic obstructive pulmonary disease: the effect of different diagnostic criteria. Analysis of the Health Survey for England. *Thorax* 2012: 67(7): 600-605.

7. Doll R, Peto R, Wheatley K, Gray R, Sutherland I. Mortality in relation to smoking: 40 years' observations on male British doctors. *BMJ (Clinical research ed* 1994: 309(6959): 901-911.

8. Tashkin DP, Clark VA, Coulson AH, Simmons M, Bourque LB, Reems C, Detels R, Sayre JW, Rokaw SN. The UCLA population studies of chronic obstructive respiratory disease. VIII. Effects of smoking cessation on lung function: a prospective study of a free-living population. *The American review of respiratory disease* 1984: 130(5): 707-715.

9. Wedzicha JA, Seemungal TA. COPD exacerbations: defining their cause and prevention. *Lancet* 2007: 370(9589): 786-796.

10. Saetta M, Turato G, Maestrelli P, Mapp CE, Fabbri LM. Cellular and structural bases of chronic obstructive pulmonary disease. *American journal of respiratory and critical care medicine* 2001: 163(6): 1304-1309.

11. Gan WQ, Man SF, Senthilselvan A, Sin DD. Association between chronic obstructive pulmonary disease and systemic inflammation: a systematic review and a meta-analysis. *Thorax* 2004: 59(7): 574-580.

12. Agusti AG, Noguera A, Sauleda J, Sala E, Pons J, Busquets X. Systemic effects of chronic obstructive pulmonary disease. *Eur Respir J* 2003: 21(2): 347-360.

13. ATS/ERS. Skeletal muscle dysfunction in chronic obstructive pulmonary disease. A statement of the American Thoracic Society and European Respiratory Society. *American journal of respiratory and critical care medicine* 1999: 159(4 Pt 2): S1-40.

14. Sin DD, Man SF. Chronic obstructive pulmonary disease as a risk factor for cardiovascular morbidity and mortality. *Proceedings of the American Thoracic Society* 2005: 2(1): 8-11.

15. Bolton CE, Ionescu AA, Shiels KM, Pettit RJ, Edwards PH, Stone MD, Nixon LS, Evans WD, Griffiths TL, Shale DJ. Associated loss of fat-free mass and bone mineral density in chronic obstructive pulmonary disease. *American journal of respiratory and critical care medicine* 2004: 170(12): 1286-1293.

16. Schmidt MI, Duncan BB, Sharrett AR, Lindberg G, Savage PJ, Offenbacher S, Azambuja MI, Tracy RP, Heiss G. Markers of inflammation and prediction of diabetes mellitus in adults (Atherosclerosis Risk in Communities study): a cohort study. *Lancet* 1999: 353(9165): 1649-1652.

17. Sinden NJ, Stockley RA. Systemic inflammation and comorbidity in COPD: a result of 'overspill' of inflammatory mediators from the lungs? Review of the evidence. *Thorax* 2010: 65(10): 930-936.

18. MRC. Definition and classification of chronic bronchitis for clinical and epidemiological purposes. A report to the Medical Research Council by their Committee on the Aetiology of Chronic Bronchitis. *Lancet* 1965: 1(7389): 775-779.

19. Gompertz S, Hill AT, Bayley DL, Stockley RA. Effect of expectoration on inflammation in induced sputum in alpha-1-antitrypsin deficiency. *Respiratory medicine* 2006: 100(6): 1094-1099.

20. Vestbo J, Prescott E, Lange P. Association of chronic mucus hypersecretion with FEV1 decline and chronic obstructive pulmonary disease morbidity. Copenhagen City Heart Study Group. *American journal of respiratory and critical care medicine* 1996: 153(5): 1530-1535.

21. Vestbo J. Chronic bronchitis: should it worry us? *Chron Respir Dis* 2004: 1(3): 173-176.

22. Lange P, Nyboe J, Appleyard M, Jensen G, Schnohr P. Relation of ventilatory impairment and of chronic mucus hypersecretion to mortality from obstructive lung disease and from all causes. *Thorax* 1990: 45(8): 579-585.

23. Kim V, Criner GJ. Chronic bronchitis and chronic obstructive pulmonary disease. *American journal of respiratory and critical care medicine* 2013: 187(3): 228-237.

24. Oldham PD. Measurement of the prevalence of emphysema. Problems of definition and sampling. *Proc R Soc Med* 1976: 69(2): 127-128.

25. Webb WR. High-resolution computed tomography of obstructive lung disease. *Radiol Clin North Am* 1994: 32(4): 745-757.

26. Mets OM, de Jong PA, van Ginneken B, Gietema HA, Lammers JW. Quantitative computed tomography in COPD: possibilities and limitations. *Lung* 2012: 190(2): 133-145.

27. Needham M, Stockley RA. Alpha 1-antitrypsin deficiency. 3: Clinical manifestations and natural history. *Thorax* 2004: 59(5): 441-445.

28. Hogg JC, Chu F, Utokaparch S, Woods R, Elliott WM, Buzatu L, Cherniack RM, Rogers RM, Sciurba FC, Coxson HO, Pare PD. The nature of small-airway obstruction in chronic obstructive pulmonary disease. *The New England journal of medicine* 2004: 350(26): 2645-2653.

29. Sturton G, Persson C, Barnes PJ. Small airways: an important but neglected target in the treatment of obstructive airway diseases. *Trends in pharmacological sciences* 2008: 29(7): 340-345.

30. Baraldo S, Turato G, Saetta M. Pathophysiology of the small airways in chronic obstructive pulmonary disease. *Respiration; international review of thoracic diseases* 2012: 84(2): 89-97.

31. King P, Holdsworth S, Freezer N, Holmes P. Bronchiectasis. *Internal medicine journal* 2006: 36(11): 729-737.

32. O'Donnell AE. Bronchiectasis. *Chest* 2008: 134(4): 815-823.

33. Stockley RA. The HRCT scan pursuing real life pathology. *Thorax* 2004: 59(10): 822-823.

34. Whitters D, Stockley RA. Bronchiectasis. *In:* Spiro SG, Silvestri GA, Agusti A, eds. Clinical Respiratory Medicine, Fourth Edition. Elsevier, 2012; pp. 581-587.

35. Scanlon PD, Connett JE, Waller LA, Altose MD, Bailey WC, Buist AS. Smoking cessation and lung function in mild-to-moderate chronic obstructive pulmonary disease. The Lung Health Study. *American journal of respiratory and critical care medicine* 2000: 161(2 Pt 1): 381-390.

36. MacNee W. Predictors of survival in patients treated with long-term oxygen therapy. *Respiration; international review of thoracic diseases* 1992: 59 Suppl 2: 5-7.

37. Celli BR, MacNee W. Standards for the diagnosis and treatment of patients with COPD: a summary of the ATS/ERS position paper. *Eur Respir J* 2004: 23(6): 932-946.

38. Sinden NJ, Stockley RA. Chronic obstructive pulmonary disease: an update of treatment related to frequently associated comorbidities. *Ther Adv Chronic Dis* 2010: 1(2): 43-57.

39. Fitzgerald MF, Fox JC. Emerging trends in the therapy of COPD: novel anti-inflammatory agents in clinical development. *Drug Discov Today* 2007: 12(11-12): 479-486.

40. Rutgers SR, Timens W, Kaufmann HF, van der Mark TW, Koeter GH, Postma DS. Comparison of induced sputum with bronchial wash, bronchoalveolar lavage and bronchial biopsies in COPD. *Eur Respir J* 2000: 15(1): 109-115.

41. Martin TR, Raghu G, Maunder RJ, Springmeyer SC. The effects of chronic bronchitis and chronic air-flow obstruction on lung cell populations recovered by bronchoalveolar lavage. *The American review of respiratory disease* 1985: 132(2): 254-260.

42. Parr DG, White AJ, Bayley DL, Guest PJ, Stockley RA. Inflammation in sputum relates to progression of disease in subjects with COPD: a prospective descriptive study. *Respiratory research* 2006: 7: 136.

43. Stanescu D, Sanna A, Veriter C, Kostianev S, Calcagni PG, Fabbri LM, Maestrelli P. Airways obstruction, chronic expectoration, and rapid decline of FEV1 in smokers are associated with increased levels of sputum neutrophils. *Thorax* 1996: 51(3): 267-271.

44. White AJ, Gompertz S, Stockley RA. Chronic obstructive pulmonary disease . 6: The aetiology of exacerbations of chronic obstructive pulmonary disease. *Thorax* 2003: 58(1): 73-80.

45. Makris D, Moschandreas J, Damianaki A, Ntaoukakis E, Siafakas NM, Milic Emili J, Tzanakis N. Exacerbations and lung function decline in COPD: new insights in current and ex-smokers. *Respiratory medicine* 2007: 101(6): 1305-1312.

46. Rennard SI, Daughton D, Fujita J, Oehlerking MB, Dobson JR, Stahl MG, Robbins RA, Thompson AB. Short-term smoking reduction is associated with reduction in measures of lower respiratory tract inflammation in heavy smokers. *Eur Respir J* 1990: 3(7): 752-759.

47. Woolhouse IS, Bayley DL, Lalor P, Adams DH, Stockley RA. Endothelial interactions of neutrophils under flow in chronic obstructive pulmonary disease. *The European respiratory journal : official journal of the European Society for Clinical Respiratory Physiology* 2005: 25(4): 612-617.

48. Burnett D, Chamba A, Hill SL, Stockley RA. Neutrophils from subjects with chronic obstructive lung disease show enhanced chemotaxis and extracellular proteolysis. *Lancet* 1987: 2(8567): 1043-1046.

49. Sapey E, Stockley JA, Greenwood H, Ahmad A, Bayley D, Lord JM, Insall RH, Stockley RA. Behavioral and structural differences in migrating peripheral neutrophils from patients with chronic obstructive pulmonary disease. *American journal of respiratory and critical care medicine* 2011: 183(9): 1176-1186.

50. Hedstrom L. Serine protease mechanism and specificity. *Chemical reviews* 2002: 102(12): 4501-4524.

51. Korkmaz B, Moreau T, Gauthier F. Neutrophil elastase, proteinase 3 and cathepsin G: physicochemical properties, activity and physiopathological functions. *Biochimie* 2008: 90(2): 227-242.

52. Schechter I, Berger A. On the size of the active site in proteases. I. Papain. *Biochem Biophys Res Commun* 1967: 27(2): 157-162.

53. Segal AW. How neutrophils kill microbes. *Annual review of immunology* 2005: 23: 197-223.

54. Owen CA, Campbell MA, Sannes PL, Boukedes SS, Campbell EJ. Cell surface-bound elastase and cathepsin G on human neutrophils: a novel, non-oxidative mechanism by which neutrophils focus and preserve catalytic activity of serine proteinases. *J Cell Biol* 1995: 131(3): 775-789.

55. Cole AM, Shi J, Ceccarelli A, Kim YH, Park A, Ganz T. Inhibition of neutrophil elastase prevents cathelicidin activation and impairs clearance of bacteria from wounds. *Blood* 2001: 97(1): 297-304.

56. Belaaouaj A. Neutrophil elastase-mediated killing of bacteria: lessons from targeted mutagenesis. *Microbes Infect* 2002: 4(12): 1259-1264.

57. Bank U, Ansorge S. More than destructive: neutrophil-derived serine proteases in cytokine bioactivity control. *Journal of leukocyte biology* 2001: 69(2): 197-206.

58. Wiedow O, Meyer-Hoffert U. Neutrophil serine proteases: potential key regulators of cell signalling during inflammation. *J Intern Med* 2005: 257(4): 319-328.

59. Shafer WM, Pohl J, Onunka VC, Bangalore N, Travis J. Human lysosomal cathepsin G and granzyme B share a functionally conserved broad spectrum antibacterial peptide. *The Journal of biological chemistry* 1991: 266(1): 112-116.

60. Campanelli D, Detmers PA, Nathan CF, Gabay JE. Azurocidin and a homologous serine protease from neutrophils. Differential antimicrobial and proteolytic properties. *The Journal of clinical investigation* 1990: 85(3): 904-915.

61. Brinkmann V, Reichard U, Goosmann C, Fauler B, Uhlemann Y, Weiss DS, Weinrauch Y, Zychlinsky A. Neutrophil extracellular traps kill bacteria. *Science* 2004: 303(5663): 1532-1535.

62. Wartha F, Beiter K, Normark S, Henriques-Normark B. Neutrophil extracellular traps: casting the NET over pathogenesis. *Curr Opin Microbiol* 2007: 10(1): 52-56.

63. Medina E. Neutrophil extracellular traps: a strategic tactic to defeat pathogens with potential consequences for the host. *Journal of innate immunity* 2009: 1(3): 176-180.

64. Remijsen Q, Kuijpers TW, Wirawan E, Lippens S, Vandenabeele P, Vanden Berghe T. Dying for a cause: NETosis, mechanisms behind an antimicrobial cell death modality. *Cell Death Differ* 2011: 18(4): 581-588.

65. Papayannopoulos V, Zychlinsky A. NETs: a new strategy for using old weapons. *Trends Immunol* 2009: 30(11): 513-521.

66. Dubois AV, Gauthier A, Brea D, Varaigne F, Diot P, Gauthier F, Attucci S. Influence of DNA on the activities and inhibition of neutrophil serine proteases in cystic fibrosis sputum. *American journal of respiratory cell and molecular biology* 2012: 47(1): 80-86.

67. Laurell C-B, Eriksson S. The electrophoretic alpha 1 globulin pattern of serum in alpha 1 antitrypsin deficiency. *Scandinavian journal of clinical and laboratory investigation* 1963: 15: 132-140.

68. Gross P, Pfitzer EA, Tolker E, Babyak MA, Kaschak M. Experimental Emphysema: Its Production with Papain in Normal and Silicotic Rats. *Archives of environmental health* 1965: 11: 50-58.

69. Birrer P. Consequences of unbalanced protease in the lung: protease involvement in destruction and local defense mechanisms of the lung. *Agents and actions* 1993: 40: 3-12.

70. Doring G. The role of neutrophil elastase in chronic inflammation. *American journal of respiratory and critical care medicine* 1994: 150(6 Pt 2): S114-117.

71. Bonnefoy A, Legrand C. Proteolysis of subendothelial adhesive glycoproteins (fibronectin, thrombospondin, and von Willebrand factor) by plasmin, leukocyte cathepsin G, and elastase. *Thrombosis research* 2000: 98(4): 323-332.

72. Nakamura H, Yoshimura K, McElvaney NG, Crystal RG. Neutrophil elastase in respiratory epithelial lining fluid of individuals with cystic fibrosis induces interleukin-8 gene expression in a human bronchial epithelial cell line. *The Journal of clinical investigation* 1992: 89(5): 1478-1484.

73. Lucey EC, Stone PJ, Breuer R, Christensen TG, Calore JD, Catanese A, Franzblau C, Snider GL. Effect of combined human neutrophil cathepsin G and elastase on induction of secretory cell metaplasia and emphysema in hamsters, with in vitro observations on elastolysis by these enzymes. *The American review of respiratory disease* 1985: 132(2): 362-366.

74. Kao RC, Wehner NG, Skubitz KM, Gray BH, Hoidal JR. Proteinase 3. A distinct human polymorphonuclear leukocyte proteinase that produces emphysema in hamsters. *The Journal of clinical investigation* 1988: 82(6): 1963-1973.

75. Witko-Sarsat V, Halbwachs-Mecarelli L, Schuster A, Nusbaum P, Ueki I, Canteloup S, Lenoir G, Descamps-Latscha B, Nadel JA. Proteinase 3, a potent secretagogue in airways, is present in cystic fibrosis sputum. *American journal of respiratory cell and molecular biology* 1999: 20(4): 729-736.

76. Janoff A, Sloan B, Weinbaum G, Damiano V, Sandhaus RA, Elias J, Kimbel P. Experimental emphysema induced with purified human neutrophil elastase: tissue localization of the instilled protease. *The American review of respiratory disease* 1977: 115(3): 461-478.

77. Sullivan A, Stockley. R. Proteinases and COPD. Blackwell Publishing Ltd, 2007.

78. Owen CA, Campbell MA, Boukedes SS, Stockley RA, Campbell EJ. A discrete subpopulation of human monocytes expresses a neutrophil-like proinflammatory (P) phenotype. *The American journal of physiology* 1994: 267(6 Pt 1): L775-785.

79. Lestienne P, Bieth JG. Activation of human leukocyte elastase activity by excess substrate, hydrophobic solvents, and ionic strength. *The Journal of biological chemistry* 1980: 255(19): 9289-9294.

80. Snider GL, Lucey EC, Christensen TG, Stone PJ, Calore JD, Catanese A, Franzblau C. Emphysema and bronchial secretory cell metaplasia induced in hamsters by human neutrophil products. *The American review of respiratory disease* 1984: 129(1): 155-160.

81. Sommerhoff CP, Nadel JA, Basbaum CB, Caughey GH. Neutrophil elastase and cathepsin G stimulate secretion from cultured bovine airway gland serous cells. *The Journal of clinical investigation* 1990: 85(3): 682-689.

82. Shapiro SD, Goldstein NM, Houghton AM, Kobayashi DK, Kelley D, Belaaouaj A. Neutrophil elastase contributes to cigarette smoke-induced emphysema in mice. *The American journal of pathology* 2003: 163(6): 2329-2335.

83. Wright JL, Farmer SG, Churg A. Synthetic serine elastase inhibitor reduces cigarette smoke-induced emphysema in guinea pigs. *Am J Respir Crit Care Med* 2002: 166(7): 954-960.

84. Sakamaki F, Ishizaka A, Urano T, Sayama K, Nakamura H, Terashima T, Waki Y, Tasaka S, Hasegawa N, Sato K, Nakagawa N, Obata T, Kanazawa M. Effect of a specific neutrophil elastase inhibitor, ONO-5046, on endotoxin-induced acute lung injury. *American journal of respiratory and critical care medicine* 1996: 153(1): 391-397.

85. Song JS, Kang CM, Rhee CK, Yoon HK, Kim YK, Moon HS, Park SH. Effects of elastase inhibitor on the epithelial cell apoptosis in bleomycin-induced pulmonary fibrosis. *Experimental lung research* 2009: 35(10): 817-829.

86. Hagiwara S, Iwasaka H, Hidaka S, Hasegawa A, Noguchi T. Neutrophil elastase inhibitor (sivelestat) reduces the levels of inflammatory mediators by inhibiting NF-kB. *Inflamm Res* 2009: 58(4): 198-203.

87. Stevens T, Ekholm K, Granse M, Lindahl M, Kozma V, Jungar C, Ottosson T, Falk-Hakansson H, Churg A, Wright JL, Lal H, Sanfridson A. AZD9668: pharmacological characterization of a novel oral inhibitor of neutrophil elastase. *The Journal of pharmacology and experimental therapeutics* 2011: 339(1): 313-320.

88. Kuraki T, Ishibashi M, Takayama M, Shiraishi M, Yoshida M. A novel oral neutrophil elastase inhibitor (ONO-6818) inhibits human neutrophil elastase-induced emphysema in rats. *American journal of respiratory and critical care medicine* 2002: 166(4): 496-500.

89. Smallman LA, Hill SL, Stockley RA. Reduction of ciliary beat frequency in vitro by sputum from patients with bronchiectasis: a serine proteinase effect. *Thorax* 1984: 39(9): 663-667.

90. Damiano VV, Tsang A, Kucich U, Abrams WR, Rosenbloom J, Kimbel P, Fallahnejad M, Weinbaum G. Immunolocalization of elastase in human emphysematous lungs. *The Journal of clinical investigation* 1986: 78(2): 482-493.

91. Betsuyaku T, Nishimura M, Takeyabu K, Tanino M, Miyamoto K, Kawakami Y. Decline in FEV(1) in community-based older volunteers with higher levels of neutrophil elastase in bronchoalveolar lavage fluid. *Respiration; international review of thoracic diseases* 2000: 67(3): 261-267.

92. Betsuyaku T, Nishimura M, Yoshioka A, Takeyabu K, Miyamoto K, Kawakami Y. [Neutrophil elastase and elastin-derived peptides in BAL fluid and emphysematous changes on CT scans]. *Nihon Kyobu Shikkan Gakkai zasshi* 1996: 34 Suppl: 69-74.

93. Carter RI, Mumford RA, Treonze KM, Finke PE, Davies P, Si Q, Humes JL, Dirksen A, Piitulainen E, Ahmad A, Stockley RA. The fibrinogen cleavage product Aalpha-Val360, a specific marker of neutrophil elastase activity in vivo. *Thorax* 2011: 66(8): 686-691.

94. Bellomo R, Uchino S, Naka T, Wan L. Hidden evidence to the West: multicentre, randomised, controlled trials in sepsis and systemic inflammatory response syndrome in Japanese journals. *Intensive care medicine* 2004: 30(5): 911-917.

95. Kadoi Y, Hinohara H, Kunimoto F, Saito S, Goto F, Kosaka T, Ieta K. Pilot study of the effects of ONO-5046 in patients with acute respiratory distress syndrome. *Anesthesia and analgesia* 2004: 99(3): 872-877.

96. Iwata K, Doi A, Ohji G, Oka H, Oba Y, Takimoto K, Igarashi W, Gremillion DH, Shimada T. Effect of neutrophil elastase inhibitor (sivelestat sodium) in the treatment of acute lung injury (ALI) and acute respiratory distress syndrome (ARDS): a systematic review and meta-analysis. *Intern Med* 2010: 49(22): 2423-2432.

97. Luisetti M, Sturani C, Sella D, Madonini E, Galavotti V, Bruno G, Peona V, Kucich U, Dagnino G, Rosenbloom J, Starcher B, Grassi C. MR889, a neutrophil elastase inhibitor, in patients with chronic obstructive pulmonary disease: a double-blind, randomized, placebo-controlled clinical trial. *The European respiratory journal : official journal of the European Society for Clinical Respiratory Physiology* 1996: 9(7): 1482-1486.

98. Ohbayashi H. Neutrophil elastase inhibitors as treatment for COPD. *Expert opinion on investigational drugs* 2002: 11(7): 965-980.

99. Kuna P, Jenkins M, O'Brien CD, Fahy WA. AZD9668, a neutrophil elastase inhibitor, plus ongoing budesonide/formoterol in patients with COPD. *Respiratory medicine* 2012: 106(4): 531-539.

100. Owen CA. Roles for proteinases in the pathogenesis of chronic obstructive pulmonary disease. *International journal of chronic obstructive pulmonary disease* 2008: 3(2): 253-268.

101. Baggiolini M, Bretz U, Dewald B, Feigenson ME. The polymorphonuclear leukocyte. *Agents and actions* 1978: 8(1-2): 3-10.

102. Witko-Sarsat V, Cramer EM, Hieblot C, Guichard J, Nusbaum P, Lopez S, Lesavre P, Halbwachs-Mecarelli L. Presence of proteinase 3 in secretory vesicles: evidence of a novel, highly mobilizable intracellular pool distinct from azurophil granules. *Blood* 1999: 94(7): 2487-2496.

103. Bories D, Raynal MC, Solomon DH, Darzynkiewicz Z, Cayre YE. Down-regulation of a serine protease, myeloblastin, causes growth arrest and differentiation of promyelocytic leukemia cells. *Cell* 1989: 59(6): 959-968.

104. Zimmer M, Medcalf RL, Fink TM, Mattmann C, Lichter P, Jenne DE. Three human elastase-like genes coordinately expressed in the myelomonocyte lineage are organized as a single genetic locus on 19pter. *Proc Natl Acad Sci U S A* 1992: 89(17): 8215-8219.

105. Fujinaga M, Chernaia MM, Halenbeck R, Koths K, James MN. The crystal structure of PR3, a neutrophil serine proteinase antigen of Wegener's granulomatosis antibodies. *J Mol Biol* 1996: 261(2): 267-278.

106. Hajjar E, Korkmaz B, Gauthier F, Brandsdal BO, Witko-Sarsat V, Reuter N. Inspection of the binding sites of proteinase3 for the design of a highly specific substrate. *J Med Chem* 2006: 49(4): 1248-1260.

107. Hajjar E, Broemstrup T, Kantari C, Witko-Sarsat V, Reuter N. Structures of human proteinase 3 and neutrophil elastase--so similar yet so different. *The FEBS journal* 2010: 277(10): 2238-2254.

108. Campbell EJ, Campbell MA, Owen CA. Bioactive proteinase 3 on the cell surface of human neutrophils: quantification, catalytic activity, and susceptibility to inhibition. *J Immunol* 2000: 165(6): 3366-3374.

109. Bergenfeldt M, Axelsson L, Ohlsson K. Release of neutrophil proteinase 4(3) and leukocyte elastase during phagocytosis and their interaction with proteinase inhibitors. *Scandinavian journal of clinical and laboratory investigation* 1992: 52(8): 823-829.

110. Sorensen OE, Follin P, Johnsen AH, Calafat J, Tjabringa GS, Hiemstra PS, Borregaard N. Human cathelicidin, hCAP-18, is processed to the antimicrobial peptide LL-37 by extracellular cleavage with proteinase 3. *Blood* 2001: 97(12): 3951-3959.

111. Coeshott C, Ohnemus C, Pilyavskaya A, Ross S, Wieczorek M, Kroona H, Leimer AH, Cheronis J. Converting enzyme-independent release of tumor necrosis factor alpha and IL-1beta from a stimulated human monocytic cell line in the presence of activated neutrophils or purified proteinase 3. *Proc Natl Acad Sci U S A* 1999: 96(11): 6261-6266.

112. Padrines M, Wolf M, Walz A, Baggiolini M. Interleukin-8 processing by neutrophil elastase, cathepsin G and proteinase-3. *FEBS letters* 1994: 352(2): 231-235.

113. Kim S, Lee S, Her E, Bae S, Choi J, Hong J, Jaekal J, Yoon D, Azam T, Dinarello CA. Proteinase 3-processed form of the recombinant IL-32 separate domain. *BMB Rep* 2008: 41(11): 814-819.

114. Kuckleburg CJ, Tilkens SB, Santoso S, Newman PJ. Proteinase 3 contributes to transendothelial migration of NB1-positive neutrophils. *Journal of immunology* 2012: 188(5): 2419-2426.

115. Kallenberg CG, Heeringa P, Stegeman CA. Mechanisms of Disease: pathogenesis and treatment of ANCA-associated vasculitides. *Nat Clin Pract Rheumatol* 2006: 2(12): 661-670.

116. Cid MC, Segarra M, Garcia-Martinez A, Hernandez-Rodriguez J. Endothelial cells, antineutrophil cytoplasmic antibodies, and cytokines in the pathogenesis of systemic vasculitis. *Current rheumatology reports* 2004: 6(3): 184-194.

117. Rao NV, Wehner NG, Marshall BC, Gray WR, Gray BH, Hoidal JR. Characterization of proteinase-3 (PR-3), a neutrophil serine proteinase. Structural and functional properties. *The Journal of biological chemistry* 1991: 266(15): 9540-9548.

118. Kessenbrock K, Frohlich L, Sixt M, Lammermann T, Pfister H, Bateman A, Belaaouaj A, Ring J, Ollert M, Fassler R, Jenne DE. Proteinase 3 and neutrophil elastase enhance inflammation in mice by inactivating antiinflammatory progranulin. *J Clin Invest* 2008: 118(7): 2438-2447.

119. Wiesner O, Litwiller RD, Hummel AM, Viss MA, McDonald CJ, Jenne DE, Fass DN, Specks U. Differences between human proteinase 3 and neutrophil elastase and their murine homologues are relevant for murine model experiments. *FEBS letters* 2005: 579(24): 5305-5312.

120. Kasahara Y, Tuder RM, Cool CD, Lynch DA, Flores SC, Voelkel NF. Endothelial cell death and decreased expression of vascular endothelial growth factor and vascular endothelial growth factor receptor 2 in emphysema. *American journal of respiratory and critical care medicine* 2001: 163(3 Pt 1): 737-744.

121. Pendergraft WF, 3rd, Rudolph EH, Falk RJ, Jahn JE, Grimmler M, Hengst L, Jennette JC, Preston GA. Proteinase 3 sidesteps caspases and cleaves p21(Waf1/Cip1/Sdi1) to induce endothelial cell apoptosis. *Kidney international* 2004: 65(1): 75-84.

122. Preston GA, Zarella CS, Pendergraft WF, 3rd, Rudolph EH, Yang JJ, Sekura SB, Jennette JC, Falk RJ. Novel effects of neutrophil-derived proteinase 3 and elastase on the vascular endothelium involve in vivo cleavage of NF-kappaB and proapoptotic changes in JNK, ERK, and p38 MAPK signaling pathways. *J Am Soc Nephrol* 2002: 13(12): 2840-2849.

123. Ying QL, Simon SR. Elastolysis by proteinase 3 and its inhibition by alpha(1)-proteinase inhibitor: a mechanism for the incomplete inhibition of ongoing elastolysis. *American journal of respiratory cell and molecular biology* 2002: 26(3): 356-361.

124. Yang JJ, Preston GA, Pendergraft WF, Segelmark M, Heeringa P, Hogan SL, Jennette JC, Falk RJ. Internalization of proteinase 3 is concomitant with endothelial cell apoptosis and internalization of myeloperoxidase with generation of intracellular oxidants. *The American journal of pathology* 2001: 158(2): 581-592.

125. Gabay JE, Scott RW, Campanelli D, Griffith J, Wilde C, Marra MN, Seeger M, Nathan CF. Antibiotic proteins of human polymorphonuclear leukocytes. *Proc Natl Acad Sci U S A* 1989: 86(14): 5610-5614.

126. Renesto P, Halbwachs-Mecarelli L, Nusbaum P, Lesavre P, Chignard M. Proteinase 3. A neutrophil proteinase with activity on platelets. *J Immunol* 1994: 152(9): 4612-4617.

127. Rao NV, Marshall BC, Gray BH, Hoidal JR. Interaction of secretory leukocyte protease inhibitor with proteinase-3. *American journal of respiratory cell and molecular biology* 1993: 8(6): 612-616.

128. Jennette JC, Hoidal JR, Falk RJ. Specificity of anti-neutrophil cytoplasmic autoantibodies for proteinase 3. *Blood* 1990: 75(11): 2263-2264.

129. Korkmaz B, Horwitz MS, Jenne DE, Gauthier F. Neutrophil elastase, proteinase 3, and cathepsin G as therapeutic targets in human diseases. *Pharmacol Rev* 2010: 62(4): 726-759.

130. Sedor J, Hogue L, Akers K, Boslaugh S, Schreiber J, Ferkol T. Cathepsin-G interferes with clearance of Pseudomonas aeruginosa from mouse lungs. *Pediatric research* 2007: 61(1): 26-31.

131. Maryanoff BE, de Garavilla L, Greco MN, Haertlein BJ, Wells GI, Andrade-Gordon P, Abraham WM. Dual inhibition of cathepsin G and chymase is effective in animal models of pulmonary inflammation. *American journal of respiratory and critical care medicine* 2010: 181(3): 247-253.

132. Silverman GA, Bird PI, Carrell RW, Church FC, Coughlin PB, Gettins PG, Irving JA, Lomas DA, Luke CJ, Moyer RW, Pemberton PA, Remold-O'Donnell E, Salvesen GS, Travis J, Whisstock JC. The serpins are an expanding superfamily of structurally similar but functionally diverse proteins. Evolution, mechanism of inhibition, novel functions, and a revised nomenclature. *The Journal of biological chemistry* 2001: 276(36): 33293-33296.

133. Belorgey D, Hagglof P, Karlsson-Li S, Lomas DA. Protein misfolding and the serpinopathies. *Prion* 2007: 1(1): 15-20.

134. Ye S, Cech AL, Belmares R, Bergstrom RC, Tong Y, Corey DR, Kanost MR, Goldsmith EJ. The structure of a Michaelis serpin-protease complex. *Nat Struct Biol* 2001: 8(11): 979-983.

135. Huntington JA, Read RJ, Carrell RW. Structure of a serpin-protease complex shows inhibition by deformation. *Nature* 2000: 407(6806): 923-926.

136. Mast AE, Enghild JJ, Pizzo SV, Salvesen G. Analysis of the plasma elimination kinetics and conformational stabilities of native, proteinase-complexed, and reactive site cleaved serpins: comparison of alpha 1-proteinase inhibitor, alpha 1-antichymotrypsin, antithrombin III, alpha 2-antiplasmin, angiotensinogen, and ovalbumin. *Biochemistry* 1991: 30(6): 1723-1730.

137. Lomas DA, Carrell RW. Serpinopathies and the conformational dementias. *Nat Rev Genet* 2002: 3(10): 759-768.

138. Belorgey D, Irving JA, Ekeowa UI, Freeke J, Roussel BD, Miranda E, Perez J, Robinson CV, Marciniak SJ, Crowther DC, Michel CH, Lomas DA. Characterisation of serpin polymers in vitro and in vivo. *Methods* 2011: 53(3): 255-266.

139. Lomas DA, Evans DL, Finch JT, Carrell RW. The mechanism of Z alpha 1-antitrypsin accumulation in the liver. *Nature* 1992: 357(6379): 605-607.

140. Koj A, Regoeczi E, Toews CJ, Leveille R, Gauldie J. Synthesis of antithrombin III and alpha-1-antitrypsin by the perfused rat liver. *Biochim Biophys Acta* 1978: 539(4): 496-504.

141. Cichy J, Potempa J, Travis J. Biosynthesis of alpha1-proteinase inhibitor by human lung-derived epithelial cells. *The Journal of biological chemistry* 1997: 272(13): 8250-8255.

142. Mornex JF, Chytil-Weir A, Martinet Y, Courtney M, LeCocq JP, Crystal RG. Expression of the alpha-1-antitrypsin gene in mononuclear phagocytes of normal and alpha-1-antitrypsin-deficient individuals. *The Journal of clinical investigation* 1986: 77(6): 1952-1961.

143. Darlington GJ, Astrin KH, Muirhead SP, Desnick RJ, Smith M. Assignment of human alpha 1-antitrypsin to chromosome 14 by somatic cell hybrid analysis. *Proc Natl Acad Sci U S A* 1982: 79(3): 870-873.

144. Travis J, Salvesen GS. Human plasma proteinase inhibitors. *Annu Rev Biochem* 1983: 52: 655-709.

145. Brantly ML, Wittes JT, Vogelmeier CF, Hubbard RC, Fells GA, Crystal RG. Use of a highly purified alpha 1-antitrypsin standard to establish ranges for the common normal and deficient alpha 1-antitrypsin phenotypes. *Chest* 1991: 100(3): 703-708.

146. Sandford AJ, Chagani T, Spinelli JJ, Pare PD. alpha1-antitrypsin genotypes and the acute-phase response to open heart surgery. *American journal of respiratory and critical care medicine* 1999: 159(5 Pt 1): 1624-1628.

147. Beatty K, Bieth J, Travis J. Kinetics of association of serine proteinases with native and oxidized alpha-1-proteinase inhibitor and alpha-1-antichymotrypsin. *The Journal of biological chemistry* 1980: 255(9): 3931-3934.

148. Shock A, Baum H. Inactivation of alpha-1-proteinase inhibitor in serum by stimulated human polymorphonuclear leucocytes. Evidence for a myeloperoxidase-dependent mechanism. *Cell biochemistry and function* 1988: 6(1): 13-23.

149. Gooptu B, Ekeowa UI, Lomas DA. Mechanisms of emphysema in alpha1-antitrypsin deficiency: molecular and cellular insights. *The European respiratory journal : official journal of the European Society for Clinical Respiratory Physiology* 2009: 34(2): 475-488.

150. Yoshida A, Lieberman J, Gaidulis L, Ewing C. Molecular abnormality of human alpha1-antitrypsin variant (Pi-ZZ) associated with plasma activity deficiency. *Proc Natl Acad Sci U S A* 1976: 73(4): 1324-1328.

151. Lomas DA, Mahadeva R. Alpha1-antitrypsin polymerization and the serpinopathies: pathobiology and prospects for therapy. *The Journal of clinical investigation* 2002: 110(11): 1585-1590.

152. Mallya M, Phillips RL, Saldanha SA, Gooptu B, Brown SC, Termine DJ, Shirvani AM, Wu Y, Sifers RN, Abagyan R, Lomas DA. Small molecules block the polymerization of Z alpha1-antitrypsin and increase the clearance of intracellular aggregates. *J Med Chem* 2007: 50(22): 5357-5363.

153. Eriksson S, Carlson J, Velez R. Risk of cirrhosis and primary liver cancer in alpha 1-antitrypsin deficiency. *The New England journal of medicine* 1986: 314(12): 736-739.

154. Ogushi F, Fells GA, Hubbard RC, Straus SD, Crystal RG. Z-type alpha 1-antitrypsin is less competent than M1-type alpha 1-antitrypsin as an inhibitor of neutrophil elastase. *The Journal of clinical investigation* 1987: 80(5): 1366-1374.

155. Llewellyn-Jones CG, Lomas DA, Carrell RW, Stockley RA. The effect of the Z mutation on the ability of alpha 1-antitrypsin to prevent neutrophil mediated tissue damage. *Biochimica et biophysica acta* 1994: 1227(3): 155-160.

156. Blanco I, de Serres FJ, Fernandez-Bustillo E, Lara B, Miravitlles M. Estimated numbers and prevalence of PI*S and PI*Z alleles of alpha1-antitrypsin deficiency in European countries. *Eur Respir J* 2006: 27(1): 77-84.

157. Campbell EJ, Campbell MA, Boukedes SS, Owen CA. Quantum proteolysis by neutrophils: implications for pulmonary emphysema in alpha 1-antitrypsin deficiency. *The Journal of clinical investigation* 1999: 104(3): 337-344.

158. American Thoracic S, European Respiratory S. American Thoracic Society/European Respiratory Society statement: standards for the diagnosis and management of individuals with alpha-1 antitrypsin deficiency. *American journal of respiratory and critical care medicine* 2003: 168(7): 818-900.

159. Turino GM, Barker AF, Brantly ML, Cohen AB, Connelly RP, Crystal RG, Eden E, Schluchter MD, Stoller JK. Clinical features of individuals with PI*SZ phenotype of alpha 1-antitrypsin deficiency. alpha 1-Antitrypsin Deficiency Registry Study Group. *American journal of respiratory and critical care medicine* 1996: 154(6 Pt 1): 1718-1725.

160. Lomas DA, Parfrey H. Alpha1-antitrypsin deficiency. 4: Molecular pathophysiology. *Thorax* 2004: 59(6): 529-535.

161. Owen MC, Carrell RW, Brennan SO. The abnormality of the S variant of human alpha-1-antitrypsin. *Biochimica et biophysica acta* 1976: 453(1): 257-261.

162. Curiel DT, Chytil A, Courtney M, Crystal RG. Serum alpha 1-antitrypsin deficiency associated with the common S-type (Glu264----Val) mutation results from intracellular degradation of alpha 1-antitrypsin prior to secretion. *The Journal of biological chemistry* 1989: 264(18): 10477-10486.

163. Okayama H, Brantly M, Holmes M, Crystal RG. Characterization of the molecular basis of the alpha 1-antitrypsin F allele. *Am J Hum Genet* 1991: 48(6): 1154-1158.

164. Fagerhol MK, Braend M. Serum prealbumin: polymorphism in man. *Science* 1965: 149(3687): 986-987.

165. Kelly CP, Tyrrell DN, McDonald GS, Whitehouse DB, Prichard JS. Heterozygous FZ alpha 1 antitrypsin deficiency associated with severe emphysema and hepatic disease: case report and family study. *Thorax* 1989: 44(9): 758-759.

166. Ringenbach MR, Banta E, Snyder MR, Craig TJ, Ishmael FT. A challenging diagnosis of alpha-1-antitrypsin deficiency: identification of a patient with a novel F/Null phenotype. *Allergy Asthma Clin Immunol* 2011: 7(1): 18.

167. Graham A, Kalsheker NA, Newton CR, Bamforth FJ, Powell SJ, Markham AF. Molecular characterisation of three alpha-1-antitrypsin deficiency variants: proteinase inhibitor (Pi) nullcardiff (Asp256----Val); PiMmalton (Phe51----deletion) and PiI (Arg39----Cys). *Human genetics* 1989: 84(1): 55-58.

168. Baur X, Bencze K. Study of familial alpha-1-proteinase inhibitor deficiency including a rare proteinase inhibitor phenotype (IZ). I. Alpha-1-phenotyping and clinical investigations. *Respiration; international review of thoracic diseases* 1987: 51(3): 188-195.

169. Mahadeva R, Chang WS, Dafforn TR, Oakley DJ, Foreman RC, Calvin J, Wight DG, Lomas DA. Heteropolymerization of S, I, and Z alpha1-antitrypsin and liver cirrhosis. *The Journal of clinical investigation* 1999: 103(7): 999-1006.

170. Salahuddin P. Genetic variants of alpha1-antitrypsin. *Curr Protein Pept Sci* 2010: 11(2): 101-117.

171. Janciauskiene S, Dominaitiene R, Sternby NH, Piitulainen E, Eriksson S. Detection of circulating and endothelial cell polymers of Z and wild type alpha 1-antitrypsin by a monoclonal antibody. *The Journal of biological chemistry* 2002: 277(29): 26540-26546.

172. Elliott PR, Bilton D, Lomas DA. Lung polymers in Z alpha1-antitrypsin deficiency-related emphysema. *American journal of respiratory cell and molecular biology* 1998: 18(5): 670-674.

173. Dafforn TR, Mahadeva R, Elliott PR, Sivasothy P, Lomas DA. A kinetic mechanism for the polymerization of alpha1-antitrypsin. *The Journal of biological chemistry* 1999: 274(14): 9548-9555.

174. Greene CM, McElvaney NG. Protein misfolding and obstructive lung disease. *Proceedings of the American Thoracic Society* 2010: 7(6): 346-355.

175. Alam S, Li Z, Janciauskiene S, Mahadeva R. Oxidation of Z alpha1-antitrypsin by cigarette smoke induces polymerization: a novel mechanism of early-onset emphysema. *American journal of respiratory cell and molecular biology* 2011: 45(2): 261-269.

176. Mahadeva R, Atkinson C, Li Z, Stewart S, Janciauskiene S, Kelley DG, Parmar J, Pitman R, Shapiro SD, Lomas DA. Polymers of Z alpha1-antitrypsin co-localize with neutrophils in emphysematous alveoli and are chemotactic in vivo. *The American journal of pathology* 2005: 166(2): 377-386.

177. Alam S, Wang J, Janciauskiene S, Mahadeva R. Preventing and reversing the cellular consequences of Z alpha-1 antitrypsin accumulation by targeting s4A. *J Hepatol* 2012: 57(1): 116-124.

178. Remold-O'Donnell E, Nixon JC, Rose RM. Elastase inhibitor. Characterization of the human elastase inhibitor molecule associated with monocytes, macrophages, and neutrophils. *J Exp Med* 1989: 169(3): 1071-1086.

179. Cooley J, Takayama TK, Shapiro SD, Schechter NM, Remold-O'Donnell E. The serpin MNEI inhibits elastase-like and chymotrypsin-like serine proteases through efficient reactions at two active sites. *Biochemistry* 2001: 40(51): 15762-15770.

180. Moreau T, Baranger K, Dade S, Dallet-Choisy S, Guyot N, Zani ML. Multifaceted roles of human elafin and secretory leukocyte proteinase inhibitor (SLPI), two serine protease inhibitors of the chelonianin family. *Biochimie* 2008: 90(2): 284-295.

181. Sallenave JM, Si Tahar M, Cox G, Chignard M, Gauldie J. Secretory leukocyte proteinase inhibitor is a major leukocyte elastase inhibitor in human neutrophils. *Journal of leukocyte biology* 1997: 61(6): 695-702.

182. Sallenave JM. Antimicrobial activity of antiproteinases. *Biochem Soc Trans* 2002: 30(2): 111-115.

183. Sponer M, Nick HP, Schnebli HP. Different susceptibility of elastase inhibitors to inactivation by proteinases from Staphylococcus aureus and Pseudomonas aeruginosa. *Biological chemistry Hoppe-Seyler* 1991: 372(11): 963-970.

184. Taggart CC, Lowe GJ, Greene CM, Mulgrew AT, O'Neill SJ, Levine RL, McElvaney NG. Cathepsin B, L, and S cleave and inactivate secretory leucoprotease inhibitor. *The Journal of biological chemistry* 2001: 276(36): 33345-33352.

185. Bruch M, Bieth JG. Influence of elastin on the inhibition of leucocyte elastase by alpha 1-proteinase inhibitor and bronchial inhibitor. Potent inhibition of elastin-bound elastase by bronchial inhibitor. *Biochem J* 1986: 238(1): 269-273.

186. Zani ML, Nobar SM, Lacour SA, Lemoine S, Boudier C, Bieth JG, Moreau T. Kinetics of the inhibition of neutrophil proteinases by recombinant elafin and pre-elafin (trappin-2) expressed in Pichia pastoris. *European journal of biochemistry / FEBS* 2004: 271(12): 2370-2378.

187. Zani ML, Baranger K, Guyot N, Dallet-Choisy S, Moreau T. Protease inhibitors derived from elafin and SLPI and engineered to have enhanced specificity towards neutrophil serine proteases. *Protein Sci* 2009: 18(3): 579-594.

188. Simpson AJ, Maxwell AI, Govan JR, Haslett C, Sallenave JM. Elafin (elastase-specific inhibitor) has anti-microbial activity against gram-positive and gram-negative respiratory pathogens. *FEBS letters* 1999: 452(3): 309-313.

189. Guyot N, Butler MW, McNally P, Weldon S, Greene CM, Levine RL, O'Neill SJ, Taggart CC, McElvaney NG. Elafin, an elastase-specific inhibitor, is cleaved by its cognate enzyme neutrophil elastase in sputum from individuals with cystic fibrosis. *The Journal of biological chemistry* 2008: 283(47): 32377-32385.

190. Virca GD, Travis J. Kinetics of association of human proteinases with human alpha 2-macroglobulin. *The Journal of biological chemistry* 1984: 259(14): 8870-8874.

191. Petersen CM. Alpha 2-macroglobulin and pregnancy zone protein. Serum levels, alpha 2-macroglobulin receptors, cellular synthesis and aspects of function in relation to immunology. *Danish medical bulletin* 1993: 40(4): 409-446.

192. Delain E, Pochon F, Barray M, Van Leuven F. Ultrastructure of alpha 2-macroglobulins. *Electron Microsc Rev* 1992: 5(2): 231-281.

193. Burnett D, Stockley RA. Serum and sputum alpha 2 macroglobulin in patients with chronic obstructive airways disease. *Thorax* 1981: 36(7): 512-516.

194. Stockley RA, Mistry M, Bradwell AR, Burnett D. A study of plasma proteins in the sol phase of sputum from patients with chronic bronchitis. *Thorax* 1979: 34(6): 777-782.

195. Harpel PC. Studies on human plasma alpha 2-macroglobulin-enzyme interactions. Evidence for proteolytic modification of the subunit chain structure. *J Exp Med* 1973: 138(3): 508-521.

196. Sottrup-Jensen L. Alpha-macroglobulins: structure, shape, and mechanism of proteinase complex formation. *The Journal of biological chemistry* 1989: 264(20): 11539-11542.

197. Borth W. Alpha 2-macroglobulin, a multifunctional binding protein with targeting characteristics. *The FASEB journal : official publication of the Federation of American Societies for Experimental Biology* 1992: 6(15): 3345-3353.

198. Kaplan J, Nielsen ML. Analysis of macrophage surface receptors. I. Binding of alpha-macroglobulin . protease complexes to rabbit alveolar macrophages. *The Journal of biological chemistry* 1979: 254(15): 7323-7328.

199. Van Leuven F, Cassiman JJ, Van Den Berghe H. Demonstration of an alpha2-macroglobulin receptor in human fibroblasts, absent in tumor-derived cell lines. *The Journal of biological chemistry* 1979: 254(12): 5155-5160.

200. Ohlsson K, Laurell CB. The disappearance of enzyme-inhibitor complexes from the circulation of man. *Clin Sci Mol Med* 1976: 51(1): 87-92.

201. Stone PJ, Calore JD, Snider GL, Franzblau C. Role of alpha-macroglobulin-elastase complexes in the pathogenesis of elastase-induced emphysema in hamsters. *The Journal of clinical investigation* 1982: 69(4): 920-931.

202. Hayes JA, Korthy A, Snider GL. The pathology of elastase-induced panacinar emphysema in hamsters. *The Journal of pathology* 1975: 117(1): 1-14.

203. D'Armiento J, Dalal SS, Okada Y, Berg RA, Chada K. Collagenase expression in the lungs of transgenic mice causes pulmonary emphysema. *Cell* 1992: 71(6): 955-961.

204. Imai K, Dalal SS, Chen ES, Downey R, Schulman LL, Ginsburg M, D'Armiento J. Human collagenase (matrix metalloproteinase-1) expression in the lungs of patients with emphysema. *American journal of respiratory and critical care medicine* 2001: 163(3 Pt 1): 786-791.

205. Cataldo D, Munaut C, Noel A, Frankenne F, Bartsch P, Foidart JM, Louis R. MMP-2- and MMP-9-linked gelatinolytic activity in the sputum from patients with asthma and chronic obstructive pulmonary disease. *Int Arch Allergy Immunol* 2000: 123(3): 259-267.

206. Ilumets H, Rytila PH, Sovijarvi AR, Tervahartiala T, Myllarniemi M, Sorsa TA, Kinnula VL. Transient elevation of neutrophil proteinases in induced sputum during COPD exacerbation. *Scandinavian journal of clinical and laboratory investigation* 2008: 68(7): 618-623.

207. Betsuyaku T, Nishimura M, Takeyabu K, Tanino M, Venge P, Xu S, Kawakami Y. Neutrophil granule proteins in bronchoalveolar lavage fluid from subjects with subclinical emphysema. *American journal of respiratory and critical care medicine* 1999: 159(6): 1985-1991.

208. Lanone S, Zheng T, Zhu Z, Liu W, Lee CG, Ma B, Chen Q, Homer RJ, Wang J, Rabach LA, Rabach ME, Shipley JM, Shapiro SD, Senior RM, Elias JA. Overlapping and enzyme-specific contributions of matrix metalloproteinases-9 and -12 in IL-13-induced inflammation and remodeling. *J Clin Invest* 2002: 110(4): 463-474.

209. Beeh KM, Beier J, Kornmann O, Buhl R. Sputum matrix metalloproteinase-9, tissue inhibitor of metalloprotinease-1, and their molar ratio in patients with chronic obstructive pulmonary disease, idiopathic pulmonary fibrosis and healthy subjects. *Respir Med* 2003: 97(6): 634-639.

210. Hautamaki RD, Kobayashi DK, Senior RM, Shapiro SD. Requirement for macrophage elastase for cigarette smoke-induced emphysema in mice. *Science* 1997: 277(5334): 2002-2004.

211. Demedts IK, Morel-Montero A, Lebecque S, Pacheco Y, Cataldo D, Joos GF, Pauwels RA, Brusselle GG. Elevated MMP-12 protein levels in induced sputum from patients with COPD. *Thorax* 2006: 61(3): 196-201.

212. Lesser M, Padilla ML, Cardozo C. Induction of emphysema in hamsters by intratracheal instillation of cathepsin B. *The American review of respiratory disease* 1992: 145(3): 661-668.

213. Cardozo C, Padilla ML, Choi HS, Lesser M. Goblet cell hyperplasia in large intrapulmonary airways after intratracheal injection of cathepsin B into hamsters. *The American review of respiratory disease* 1992: 145(3): 675-679.

214. Mason RW, Johnson DA, Barrett AJ, Chapman HA. Elastinolytic activity of human cathepsin L. *Biochem J* 1986: 233(3): 925-927.

215. Shi GP, Munger JS, Meara JP, Rich DH, Chapman HA. Molecular cloning and expression of human alveolar macrophage cathepsin S, an elastinolytic cysteine protease. *J Biol Chem* 1992: 267(11): 7258-7262.

216. Sires UI, Murphy G, Baragi VM, Fliszar CJ, Welgus HG, Senior RM. Matrilysin is much more efficient than other matrix metalloproteinases in the proteolytic inactivation of alpha 1-antitrypsin. *Biochem Biophys Res Commun* 1994: 204(2): 613-620.

217. Gronski TJ, Jr., Martin RL, Kobayashi DK, Walsh BC, Holman MC, Huber M, Van Wart HE, Shapiro SD. Hydrolysis of a broad spectrum of extracellular matrix proteins by human macrophage elastase. *J Biol Chem* 1997: 272(18): 12189-12194.

218. Zhu Y, Liu X, Skold CM, Wang H, Kohyama T, Wen FQ, Ertl RF, Rennard SI. Collaborative interactions between neutrophil elastase and metalloproteinases in extracellular matrix degradation in three-dimensional collagen gels. *Respir Res* 2001: 2(5): 300-305.

219. Okada Y, Watanabe S, Nakanishi I, Kishi J, Hayakawa T, Watorek W, Travis J, Nagase H. Inactivation of tissue inhibitor of metalloproteinases by neutrophil elastase and other serine proteinases. *FEBS Lett* 1988: 229(1): 157-160.

220. Lokshina LA, Golubeva NV, Baranova FS, Orekhovich VN. [Inactivation of blood plasma alpha 1-proteinase inhibitor as affected by 2 splenic thiol proteinases active in a neutral medium]. *Biull Eksp Biol Med* 1987: 103(6): 662-664.

221. Johnson D, Travis J. Inactivation of human alpha 1-proteinase inhibitor by thiol proteinases. *Biochem J* 1977: 163(3): 639-641.

222. Keppler D, Waridel P, Abrahamson M, Bachmann D, Berdoz J, Sordat B. Latency of cathepsin B secreted by human colon carcinoma cells is not linked to secretion of cystatin C and is relieved by neutrophil elastase. *Biochim Biophys Acta* 1994: 1226(2): 117-125.

223. Abrahamson M, Mason RW, Hansson H, Buttle DJ, Grubb A, Ohlsson K. Human cystatin C. role of the N-terminal segment in the inhibition of human cysteine proteinases and in its inactivation by leucocyte elastase. *Biochem J* 1991: 273 (Pt 3): 621-626.

224. King MA, Stone JA, Diaz PT, Mueller CF, Becker WJ, Gadek JE. Alpha 1-antitrypsin deficiency: evaluation of bronchiectasis with CT. *Radiology* 1996: 199(1): 137-141.

225. Brantly M, Nukiwa T, Crystal RG. Molecular basis of alpha-1-antitrypsin deficiency. *The American journal of medicine* 1988: 84(6A): 13-31.

226. Sveger T. alpha 1-antitrypsin deficiency in early childhood. *Pediatrics* 1978: 62(1): 22-25.

227. Edmonds BK, Hodge JA, Rietschel RL. Alpha 1-antitrypsin deficiency-associated panniculitis: case report and review of the literature. *Pediatric dermatology* 1991: 8(4): 296-299.

228. Elzouki AN, Segelmark M, Wieslander J, Eriksson S. Strong link between the alpha 1-antitrypsin PiZ allele and Wegener's granulomatosis. *J Intern Med* 1994: 236(5): 543-548.

229. Hill AT, Campbell EJ, Bayley DL, Hill SL, Stockley RA. Evidence for excessive bronchial inflammation during an acute exacerbation of chronic obstructive pulmonary disease in patients with alpha(1)-antitrypsin deficiency (PiZ). *American journal of respiratory and critical care medicine* 1999: 160(6): 1968-1975.

230. Tanash HA, Riise GC, Hansson L, Nilsson PM, Piitulainen E. Survival benefit of lung transplantation in individuals with severe alpha1-anti-trypsin deficiency (PiZZ) and emphysema. *The Journal of heart and lung transplantation : the official publication of the International Society for Heart Transplantation* 2011: 30(12): 1342-1347.

231. Dickens JA, Lomas DA. Why has it been so difficult to prove the efficacy of alpha-1-antitrypsin replacement therapy? Insights from the study of disease pathogenesis. *Drug design, development and therapy* 2011: 5: 391-405.

232. Flotte TR, Trapnell BC, Humphries M, Carey B, Calcedo R, Rouhani F, Campbell-Thompson M, Yachnis AT, Sandhaus RA, McElvaney NG, Mueller C, Messina LM, Wilson JM, Brantly M, Knop DR, Ye GJ, Chulay JD. Phase 2 clinical trial of a recombinant adeno-associated viral vector expressing alpha1-antitrypsin: interim results. *Human gene therapy* 2011: 22(10): 1239-1247.

233. Yusa K, Rashid ST, Strick-Marchand H, Varela I, Liu PQ, Paschon DE, Miranda E, Ordonez A, Hannan NR, Rouhani FJ, Darche S, Alexander G, Marciniak SJ, Fusaki N, Hasegawa M, Holmes MC, Di Santo JP, Lomas DA, Bradley A, Vallier L. Targeted gene correction of alpha1-antitrypsin deficiency in induced pluripotent stem cells. *Nature* 2011: 478(7369): 391-394.

234. Amariglio N, Hirshberg A, Scheithauer BW, Cohen Y, Loewenthal R, Trakhtenbrot L, Paz N, Koren-Michowitz M, Waldman D, Leider-Trejo L, Toren A, Constantini S, Rechavi G. Donor-derived brain tumor following neural stem cell transplantation in an ataxia telangiectasia patient. *PLoS medicine* 2009: 6(2): e1000029.

235. Kemmer N, Kaiser T, Zacharias V, Neff GW. Alpha-1-antitrypsin deficiency: outcomes after liver transplantation. *Transplant Proc* 2008: 40(5): 1492-1494.

236. Dawkins PA, Dowson LJ, Guest PJ, Stockley RA. Predictors of mortality in alpha1-antitrypsin deficiency. *Thorax* 2003: 58(12): 1020-1026.

237. Martinez FJ, Foster G, Curtis JL, Criner G, Weinmann G, Fishman A, DeCamp MM, Benditt J, Sciurba F, Make B, Mohsenifar Z, Diaz P, Hoffman E, Wise R. Predictors of mortality in patients with emphysema and severe airflow obstruction. *American journal of respiratory and critical care medicine* 2006: 173(12): 1326-1334.

238. Gotzsche PC, Johansen HK. Intravenous alpha-1 antitrypsin augmentation therapy for treating patients with alpha-1 antitrypsin deficiency and lung disease. *Cochrane Database Syst Rev* 2010(7): CD007851.

239. Demkow U, van Overveld FJ. Role of elastases in the pathogenesis of chronic obstructive pulmonary disease: implications for treatment. *Eur J Med Res* 2010: 15 Suppl 2: 27-35.

240. Korkmaz B, Attucci S, Moreau T, Godat E, Juliano L, Gauthier F. Design and use of highly specific substrates of neutrophil elastase and proteinase 3. *American journal of respiratory cell and molecular biology* 2004: 30(6): 801-807.

241. Sroka J, Kordecka A, Wlosiak P, Madeja Z, Korohoda W. Separation methods for isolation of human polymorphonuclear leukocytes affect their motile activity. *European journal of cell biology* 2009: 88(9): 531-539.

242. Freitas M, Porto G, Lima JL, Fernandes E. Isolation and activation of human neutrophils in vitro. The importance of the anticoagulant used during blood collection. *Clinical biochemistry* 2008: 41(7-8): 570-575.

243. Pye A, Stockley RA, Hill SL. Simple method for quantifying viable bacterial numbers in sputum. *J Clin Pathol* 1995: 48(8): 719-724.

244. Pavord ID, Pizzichini MM, Pizzichini E, Hargreave FE. The use of induced sputum to investigate airway inflammation. *Thorax* 1997: 52(6): 498-501.

245. Meneely GR, Kaltreider NL. The volume of the lung determined by helium dilution; description of the method and comparison with other procedures. *J Clin Invest* 1949: 28(1): 129-139.

246. Quanjer PH, Tammeling GJ, Cotes JE, Pedersen OF, Peslin R, Yernault JC. Lung volumes and forced ventilatory flows. Report Working Party Standardization of Lung Function Tests, European Community for Steel and Coal. Official Statement of the European Respiratory Society. *Eur Respir J Suppl* 1993: 16: 5-40.

247. Cotes JE. Lung Function. Blackwell Scientific Publications, Oxford, 1975; pp. 384-386.

248. Berg JM, Tymoczko JL, Stryer L. The Michaelis-Menten Model Accounts for the Kinetic Properties of Many Enzymes. Biochemistry 5th Edition. W H Freeman, New York, 2002.

249. Janoff A, Scherer J. Mediators of inflammation in leukocyte lysosomes. IX. Elastinolytic activity in granules of human polymorphonuclear leukocytes. *J Exp Med* 1968: 128(5): 1137-1155.

250. Barrett AJ. Cathepsin G. *Methods Enzymol* 1981: 80 Pt C: 561-565.

251. Nakajima K, Powers JC, Ashe BM, Zimmerman M. Mapping the extended substrate binding site of cathepsin G and human leukocyte elastase. Studies with peptide substrates related to the alpha 1-protease inhibitor reactive site. *The Journal of biological chemistry* 1979: 254(10): 4027-4032.

252. Barrett AJ, Starkey PM. The interaction of alpha 2-macroglobulin with proteinases. Characteristics and specificity of the reaction, and a hypothesis concerning its molecular mechanism. *Biochem J* 1973: 133(4): 709-724.

253. Wewers MD, Herzyk DJ, Gadek JE. Alveolar fluid neutrophil elastase activity in the adult respiratory distress syndrome is complexed to alpha-2-macroglobulin. *The Journal of clinical investigation* 1988: 82(4): 1260-1267.

254. Moore AR, Appelboam A, Kawabata K, Da Silva JA, D'Cruz D, Gowland G, Willoughby DA. Destruction of articular cartilage by alpha 2 macroglobulin elastase complexes: role in rheumatoid arthritis. *Ann Rheum Dis* 1999: 58(2): 109-113.

255. Twumasi DY, Liener IE, Galdston M, Levytska V. Activation of human leukocyte elastase by human alpha2-macroglobulin. *Nature* 1977: 267(5606): 61-63.

256. Ohlsson K. Comparison of affinity of trypsin for two -macroglobulin fractions and for 1 -antitrypsin in dog serum. *Clin Chim Acta* 1971: 32(2): 215-220.

257. Meyer JF, Bieth J, Metais P. On the inhibition of elastase by serum. Some distinguishing properties of alpha1-antitrypsin and alpha2-macroglobulin. *Clin Chim Acta* 1975: 62(1): 43-53.

258. Lomas DA, Evans DL, Stone SR, Chang WS, Carrell RW. Effect of the Z mutation on the physical and inhibitory properties of alpha 1-antitrypsin. *Biochemistry* 1993: 32(2): 500-508.

259. Gaillard MC, Kilroe-Smith TA. Determination of functional activity of alpha 1-protease inhibitor and alpha 2-macroglobulin in human plasma using elastase. *Journal of clinical chemistry and clinical biochemistry Zeitschrift fur klinische Chemie und klinische Biochemie* 1987: 25(3): 167-172.

260. Ohlsson K, Olsson I. Neutral proteases of human granulocytes. III. Interaction between human granulocyte elastase and plasma protease inhibitors. *Scandinavian journal of clinical and laboratory investigation* 1974: 34(4): 349-355.

261. Brissenden JE, Cox DW. alpha 2-Macroglobulin in patients with obstructive lung disease, with and without alpha 1-antitrypsin deficiency. *Clin Chim Acta* 1983: 128(2-3): 241-248.

262. Gaillard MC, Reichberg SB, Nogueira CM, Kilroe-Smith TA. Differences in elastase-binding activity of alpha 1-protease inhibitor and alpha 2-macroglobulin for asthma patients and control subjects with various alpha 1-protease inhibitor phenotypes. *Clinical chemistry* 1993: 39(4): 675-679.

263. Fryksmark U, Ohlsson K, Rosengren M, Tegner H. Studies on the interaction between leukocyte elastase, antileukoproteinase and the plasma proteinase inhibitors alpha 1-proteinase inhibitor and alpha 2-macroglobulin. *Hoppe-Seyler's Zeitschrift fur physiologische Chemie* 1983: 364(7): 793-800.

264. Heinz A, Jung MC, Jahreis G, Rusciani A, Duca L, Debelle L, Weiss AS, Neubert RH, Schmelzer CE. The action of neutrophil serine proteases on elastin and its precursor. *Biochimie* 2012: 94(1): 192-202.

265. Pierce RA, Mariani TJ, Senior RM. Elastin in lung development and disease. *Ciba Foundation symposium* 1995: 192: 199-212; discussion 212-4.

266. Morrison HM, Welgus HG, Stockley RA, Burnett D, Campbell EJ. Inhibition of human leukocyte elastase bound to elastin: relative ineffectiveness and two mechanisms of inhibitory activity. *American journal of respiratory cell and molecular biology* 1990: 2(3): 263-269.

267. Kueppers F, Abrams WR, Weinbaum G, Rosenbloom J. Resistance of tropoelastin and elastin peptides to degradation by alpha 2-macroglobulin-protease complexes. *Archives of biochemistry and biophysics* 1981: 211(1): 143-150.

268. McGillivray DH, Burnett D, Afford SC, Stockley RA. An evaluation of four methods for the measurement of elastase activity. *Clin Chim Acta* 1981: 111(2-3): 289-294.

269. Galdston M, Levytska V, Liener IE, Twumasi DY. Degradation of tropoelastin and elastin substrates by human neutrophil elastase, free and bound to alpha2-macroglobulin in serum of the M and Z (Pi) phenotypes for alpha1-antitrypsin. *The American review of respiratory disease* 1979: 119(3): 435-441.

270. Ross R, Bornstein P. Elastic fibers in the body. *Scientific American* 1971: 224(6): 44-52.

271. Kramps JA, Morrison HM, Burnett D, Dijkman JH, Stockley RA. Determination of elastase inhibitory activity of alpha 1-proteinase inhibitor and bronchial antileukoprotease: different results using insoluble elastin or synthetic low molecular weight substrates. *Scandinavian journal of clinical and laboratory investigation* 1987: 47(4): 405-410.

272. Janoff A, Dearing R. Prevention of elastase-induced experimental emphysema by oral administration of a synthetic elastase inhibitor. *The American review of respiratory disease* 1980: 121(6): 1025-1029.

273. Stone PJ, Lucey EC, Calore JD, Snider GL, Franzblau C, Castillo MJ, Powers JC. The moderation of elastase-induced emphysema in the hamster by intratracheal pretreatment or post-treatment with succinyl alanyl alanyl prolyl valine chloromethyl ketone. *The American review of respiratory disease* 1981: 124(1): 56-59.

274. Barrett AJ. Leukocyte elastase. *Methods Enzymol* 1981: 80 Pt C: 581-588.

275. Adeyemi EO, Hodgson HJ. Molecular distribution of elastase between its two main inhibitors: direct quantitation of elastase-alpha 2-macroglobulin complex with a novel ELISA technique. *Scandinavian journal of clinical and laboratory investigation* 1990: 50(4): 433-440.

276. Adeyemi EO, Hodgson HJ. Antibody binding to alpha 2-macroglobulin facilitates direct quantitation of elastase-alpha 2-macroglobulin complexes by a simple ELISA technique. *Journal of immunological methods* 1993: 164(2): 189-192.

277. Ogushi F, Hubbard RC, Fells GA, Casolaro MA, Curiel DT, Brantly ML, Crystal RG. Evaluation of the S-type of alpha-1-antitrypsin as an in vivo and in vitro inhibitor of neutrophil elastase. *The American review of respiratory disease* 1988: 137(2): 364-370.

278. Nukiwa T, Brantly ML, Ogushi F, Fells GA, Crystal RG. Characterization of the gene and protein of the common alpha 1-antitrypsin normal M2 allele. *Am J Hum Genet* 1988: 43(3): 322-330.

279. Cook L, Burdon JG, Brenton S, Knight KR, Janus ED. Kinetic characterisation of alpha-1-antitrypsin F as an inhibitor of human neutrophil elastase. *Pathology* 1996: 28(3): 242-247.

280. Duranton J, Bieth JG. Inhibition of proteinase 3 by [alpha]1-antitrypsin in vitro predicts very fast inhibition in vivo. *American journal of respiratory cell and molecular biology* 2003: 29(1): 57-61.

281. Musumeci V, Vincenti A, Bizzi B. A method for the differential determination of plasma antithrombins. *J Clin Pathol* 1976: 29(1): 63-68.

282. Eccleston ED, Howard JB. Reaction of methylamine with human alpha 2-macroglobulin. Mechanism of inactivation. *The Journal of biological chemistry* 1985: 260(18): 10169-10176.

283. Korkmaz B, Attucci S, Juliano MA, Kalupov T, Jourdan ML, Juliano L, Gauthier F. Measuring elastase, proteinase 3 and cathepsin G activities at the surface of human neutrophils with fluorescence resonance energy transfer substrates. *Nat Protoc* 2008: 3(6): 991-1000.

284. Seersholm N, Kok-Jensen A. Intermediate alpha 1-antitrypsin deficiency PiSZ: a risk factor for pulmonary emphysema? *Respiratory medicine* 1998: 92(2): 241-245.

285. Hersh CP, Dahl M, Ly NP, Berkey CS, Nordestgaard BG, Silverman EK. Chronic obstructive pulmonary disease in alpha1-antitrypsin PI MZ heterozygotes: a meta-analysis. *Thorax* 2004: 59(10): 843-849.

286. Wewers MD, Casolaro MA, Sellers SE, Swayze SC, McPhaul KM, Wittes JT, Crystal RG. Replacement therapy for alpha 1-antitrypsin deficiency associated with emphysema. *The New England journal of medicine* 1987: 316(17): 1055-1062.

287. Mittman C, Barbela T, Lieberman J. Antitrypsin deficiency and abnormal protease inhibitor phenotypes. *Archives of environmental health* 1973: 27(3): 201-206.

288. Dlugosz M, Antosiewicz JM, Trylska J. pH-dependent association of proteins. The test case of monoclonal antibody HyHEL-5 and its antigen hen egg white lysozyme. *J Phys Chem B* 2009: 113(47): 15662-15669.

289. Boudier C, Bieth JG. Mucus proteinase inhibitor: a fast-acting inhibitor of leucocyte elastase. *Biochimica et biophysica acta* 1989: 995(1): 36-41.

290. Ying QL, Simon SR. Kinetics of the inhibition of human leukocyte elastase by elafin, a 6-kilodalton elastase-specific inhibitor from human skin. *Biochemistry* 1993: 32(7): 1866-1874.

291. Ying QL, Simon SR. Kinetics of the inhibition of proteinase 3 by elafin. *American journal of respiratory cell and molecular biology* 2001: 24(1): 83-89.

292. Kim S, Woo J, Seo EJ, Yu M, Ryu S. A 2.1 A resolution structure of an uncleaved alpha(1)-antitrypsin shows variability of the reactive center and other loops. *J Mol Biol* 2001: 306(1): 109-119.

293. Stoller JK, Aboussouan LS. alpha1-Antitrypsin deficiency . 5: intravenous augmentation therapy: current understanding. *Thorax* 2004: 59(8): 708-712.

294. Sandhaus RA. alpha1-Antitrypsin deficiency . 6: new and emerging treatments for alpha1-antitrypsin deficiency. *Thorax* 2004: 59(10): 904-909.

295. Seersholm N, Wencker M, Banik N, Viskum K, Dirksen A, Kok-Jensen A, Konietzko N. Does alpha1-antitrypsin augmentation therapy slow the annual decline in FEV1 in patients with severe hereditary alpha1-antitrypsin deficiency? Wissenschaftliche Arbeitsgemeinschaft zur Therapie von Lungenerkrankungen (WATL) alpha1-AT study group. *Eur Respir J* 1997: 10(10): 2260-2263.

296. Schluchter MD, Barker AF, Crystal RD, Robbins RA. A registry of patients with severe deficiency of alpha 1-antitrypsin. Design and methods. The Alpha 1-Antitrypsin Deficiency Registry Study Group. *Chest* 1994: 106(4): 1223-1232.

297. Chapman KR, Stockley RA, Dawkins C, Wilkes MM, Navickis RJ. Augmentation therapy for alpha1 antitrypsin deficiency: a meta-analysis. *Copd* 2009: 6(3): 177-184.

298. Lieberman J. Augmentation therapy reduces frequency of lung infections in antitrypsin deficiency: a new hypothesis with supporting data. *Chest* 2000: 118(5): 1480-1485.

299. Stockley RA, Bayley DL, Unsal I, Dowson LJ. The effect of augmentation therapy on bronchial inflammation in alpha1-antitrypsin deficiency. *Am J Respir Crit Care Med* 2002: 165(11): 1494-1498.

300. Dirksen A, Dijkman JH, Madsen F, Stoel B, Hutchison DC, Ulrik CS, Skovgaard LT, Kok-Jensen A, Rudolphus A, Seersholm N, Vrooman HA, Reiber JH, Hansen NC, Heckscher T, Viskum K, Stolk J. A randomized clinical trial of alpha(1)-antitrypsin augmentation therapy. *Am J Respir Crit Care Med* 1999: 160(5 Pt 1): 1468-1472.

301. Dirksen A, Piitulainen E, Parr DG, Deng C, Wencker M, Shaker SB, Stockley RA. Exploring the role of CT densitometry: a randomised study of augmentation therapy in alpha1-antitrypsin deficiency. *Eur Respir J* 2009: 33(6): 1345-1353.

302. Parr DG, Dirksen A, Piitulainen E, Deng C, Wencker M, Stockley RA. Exploring the optimum approach to the use of CT densitometry in a randomised placebo-controlled study of augmentation therapy in alpha 1-antitrypsin deficiency. *Respiratory research* 2009: 10: 75.

303. Stockley RA, Parr DG, Piitulainen E, Stolk J, Stoel BC, Dirksen A. Therapeutic efficacy of alpha-1 antitrypsin augmentation therapy on the loss of lung tissue: an

integrated analysis of 2 randomised clinical trials using computed tomography densitometry. *Respir Res* 2010: 11: 136.

304. Pemberton PA, Kobayashi D, Wilk BJ, Henstrand JM, Shapiro SD, Barr PJ. Inhaled recombinant alpha 1-antitrypsin ameliorates cigarette smoke-induced emphysema in the mouse. *Copd* 2006: 3(2): 101-108.

305. ClinicalTrials.gov. International Study Evaluating the Safety and Efficacy of Inhaled, Human, Alpha-1 Antitrypsin (AAT) in Alpha-1 Antitrypsin Deficient Patients With Emphysema. Updated 19/06/2012 [cited 8/8/12]; Available from: http://clinicaltrials.gov/ct2/show/NCT01217671

306. Campbell EJ, Owen CA. The sulfate groups of chondroitin sulfate- and heparan sulfate-containing proteoglycans in neutrophil plasma membranes are novel binding sites for human leukocyte elastase and cathepsin G. *The Journal of biological chemistry* 2007: 282(19): 14645-14654.

307. Korkmaz B, Jaillet J, Jourdan ML, Gauthier A, Gauthier F, Attucci S. Catalytic activity and inhibition of wegener antigen proteinase 3 on the cell surface of human polymorphonuclear neutrophils. *The Journal of biological chemistry* 2009: 284(30): 19896-19902.

308. Halbwachs-Mecarelli L, Bessou G, Lesavre P, Lopez S, Witko-Sarsat V. Bimodal distribution of proteinase 3 (PR3) surface expression reflects a constitutive heterogeneity in the polymorphonuclear neutrophil pool. *FEBS letters* 1995: 374(1): 29-33.

309. Schreiber A, Busjahn A, Luft FC, Kettritz R. Membrane expression of proteinase 3 is genetically determined. *J Am Soc Nephrol* 2003: 14(1): 68-75.

310. Witko-Sarsat V, Lesavre P, Lopez S, Bessou G, Hieblot C, Prum B, Noel LH, Guillevin L, Ravaud P, Sermet-Gaudelus I, Timsit J, Grunfeld JP, Halbwachs-Mecarelli L. A large subset of neutrophils expressing membrane proteinase 3 is a risk factor for vasculitis and rheumatoid arthritis. *J Am Soc Nephrol* 1999: 10(6): 1224-1233.

311. David A, Kacher Y, Specks U, Aviram I. Interaction of proteinase 3 with CD11b/CD18 (beta2 integrin) on the cell membrane of human neutrophils. *Journal of leukocyte biology* 2003: 74(4): 551-557.

312. Fridlich R, David A, Aviram I. Membrane proteinase 3 and its interactions within microdomains of neutrophil membranes. *J Cell Biochem* 2006: 99(1): 117-125.

313. von Vietinghoff S, Tunnemann G, Eulenberg C, Wellner M, Cristina Cardoso M, Luft FC, Kettritz R. NB1 mediates surface expression of the ANCA antigen proteinase 3 on human neutrophils. *Blood* 2007: 109(10): 4487-4493.

314. Hu N, Westra J, Kallenberg CG. Membrane-bound proteinase 3 and its receptors: relevance for the pathogenesis of Wegener's Granulomatosis. *Autoimmunity reviews* 2009: 8(6): 510-514.

315. Kim YC, Shin JE, Lee SH, Chung WJ, Lee YS, Choi BK, Choi Y. Membrane-bound proteinase 3 and PAR2 mediate phagocytosis of non-opsonized bacteria in human neutrophils. *Molecular immunology* 2011: 48(15-16): 1966-1974.

316. Durant S, Pederzoli M, Lepelletier Y, Canteloup S, Nusbaum P, Lesavre P, Witko-Sarsat V. Apoptosis-induced proteinase 3 membrane expression is independent from degranulation. *Journal of leukocyte biology* 2004: 75(1): 87-98.

317. Kantari C, Pederzoli-Ribeil M, Amir-Moazami O, Gausson-Dorey V, Moura IC, Lecomte MC, Benhamou M, Witko-Sarsat V. Proteinase 3, the Wegener autoantigen, is externalized during neutrophil apoptosis: evidence for a functional association with phospholipid scramblase 1 and interference with macrophage phagocytosis. *Blood* 2007: 110(12): 4086-4095.

318. Porges AJ, Redecha PB, Kimberly WT, Csernok E, Gross WL, Kimberly RP. Anti-neutrophil cytoplasmic antibodies engage and activate human neutrophils via Fc gamma RIIa. *J Immunol* 1994: 153(3): 1271-1280.

319. Reumaux D, Vossebeld PJ, Roos D, Verhoeven AJ. Effect of tumor necrosis factor-induced integrin activation on Fc gamma receptor II-mediated signal transduction: relevance for activation of neutrophils by anti-proteinase 3 or anti-myeloperoxidase antibodies. *Blood* 1995: 86(8): 3189-3195.

320. Harper L, Cockwell P, Adu D, Savage CO. Neutrophil priming and apoptosis in anti-neutrophil cytoplasmic autoantibody-associated vasculitis. *Kidney international* 2001: 59(5): 1729-1738.

321. Muller Kobold AC, Kallenberg CG, Tervaert JW. Leucocyte membrane expression of proteinase 3 correlates with disease activity in patients with Wegener's granulomatosis. *Br J Rheumatol* 1998: 37(8): 901-907.

322. Kuijpers TW, Tool AT, van der Schoot CE, Ginsel LA, Onderwater JJ, Roos D, Verhoeven AJ. Membrane surface antigen expression on neutrophils: a reappraisal of the use of surface markers for neutrophil activation. *Blood* 1991: 78(4): 1105-1111.

323. Noguera A, Batle S, Miralles C, Iglesias J, Busquets X, MacNee W, Agusti AG. Enhanced neutrophil response in chronic obstructive pulmonary disease. *Thorax* 2001: 56(6): 432-437.

324. Korkmaz B, Attucci S, Jourdan ML, Juliano L, Gauthier F. Inhibition of neutrophil elastase by alpha1-protease inhibitor at the surface of human polymorphonuclear neutrophils. *J Immunol* 2005: 175(5): 3329-3338.

325. Matsumoto T, Kaneko T, Seto M, Wada H, Kobayashi T, Nakatani K, Tonomura H, Tono Y, Ohyabu M, Nobori T, Shiku H, Sudo A, Uchida A, Kurosawa DJ, Kurosawa S. The membrane proteinase 3 expression on neutrophils was downregulated after treatment with infliximab in patients with rheumatoid arthritis. *Clin Appl Thromb Hemost* 2008: 14(2): 186-192.

326. Esnault VL, Testa A, Audrain M, Roge C, Hamidou M, Barrier JH, Sesboue R, Martin JP, Lesavre P. Alpha 1-antitrypsin genetic polymorphism in ANCA-positive systemic vasculitis. *Kidney international* 1993: 43(6): 1329-1332.

327. Rooney CP, Taggart C, Coakley R, McElvaney NG, O'Neill SJ. Anti-proteinase 3 antibody activation of neutrophils can be inhibited by alpha1-antitrypsin. *American journal of respiratory cell and molecular biology* 2001: 24(6): 747-754.

328. Vines A, McBean GJ, Blanco-Fernandez A. A flow-cytometric method for continuous measurement of intracellular Ca(2+) concentration. *Cytometry A* 2010: 77(11): 1091-1097.

329. Galbraith DW. Simultaneous flow cytometric quantification of plant nuclear DNA contents over the full range of described angiosperm 2C values. *Cytometry A* 2009: 75(8): 692-698.

330. Travis J. Structure, function, and control of neutrophil proteinases. *The American journal of medicine* 1988: 84(6A): 37-42.

331. Sinden NJ, Stockley RA. Proteinase 3 activity in sputum from subjects with Alpha-1-Antitrypsin deficiency and COPD. *Eur Respir J* 2013: 41(5): 1042-1050.

332. Sapey E, Bayley D, Ahmad A, Newbold P, Snell N, Stockley RA. Inter-relationships between inflammatory markers in patients with stable COPD with bronchitis: intra-patient and inter-patient variability. *Thorax* 2008: 63(6): 493-499.

333. GOLD. Global Strategy for the Diagnosis, Management and Prevention of COPD, Global Initiative for Chronic Obstructive Lung Disease (GOLD). 2011.

334. Korkmaz B, Hajjar E, Kalupov T, Reuter N, Brillard-Bourdet M, Moreau T, Juliano L, Gauthier F. Influence of charge distribution at the active site surface on the substrate specificity of human neutrophil protease 3 and elastase. A kinetic and molecular modeling analysis. *The Journal of biological chemistry* 2007: 282(3): 1989-1997.

335. Llewellyn-Jones CG, Harris TA, Stockley RA. Effect of fluticasone propionate on sputum of patients with chronic bronchitis and emphysema. *American journal of respiratory and critical care medicine* 1996: 153(2): 616-621.

336. Brusse-Keizer M, van der Palen J, van der Valk P, Hendrix R, Kerstjens H. Clinical predictors of exacerbation frequency in chronic obstructive pulmonary disease. *Clin Respir J* 2011: 5(4): 227-234.

337. Snoeck-Stroband JB, Postma DS, Lapperre TS, Gosman MM, Thiadens HA, Kauffman HF, Sont JK, Jansen DF, Sterk PJ. Airway inflammation contributes to health status in COPD: a cross-sectional study. *Respiratory research* 2006: 7: 140.

338. Hill AT, Bayley DL, Campbell EJ, Hill SL, Stockley RA. Airways inflammation in chronic bronchitis: the effects of smoking and alpha1-antitrypsin deficiency. *Eur Respir J* 2000: 15(5): 886-890.

339. Lee RL, Rancourt RC, del Val G, Pack K, Pardee C, Accurso FJ, White CW. Thioredoxin and dihydrolipoic acid inhibit elastase activity in cystic fibrosis sputum. *American journal of physiology Lung cellular and molecular physiology* 2005: 289(5): L875-882.

340. Simpson JL, Scott RJ, Boyle MJ, Gibson PG. Differential proteolytic enzyme activity in eosinophilic and neutrophilic asthma. *American journal of respiratory and critical care medicine* 2005: 172(5): 559-565.

341. Zedtwitz-Liebenstein K, Schenk P, Apfalter P, Fuhrmann V, Stoiser B, Graninger W, Schuster E, Frass M, Burgmann H. Ventilator-associated pneumonia: Increased

bacterial counts in bronchoalveolar lavage by using urea as an endogenous marker of dilution. *Crit Care Med* 2005: 33(4): 756-759.

342. Pelletier A, Dimicoli JL, Boudier C, Bieth JG. Nonchromogenic hydrolysis of elastase and cathepsin G p-nitroanilide substrates by Pseudomonas aeruginosa elastase. *American journal of respiratory cell and molecular biology* 1989: 1(1): 37-39.

343. Hill AT, Campbell EJ, Hill SL, Bayley DL, Stockley RA. Association between airway bacterial load and markers of airway inflammation in patients with stable chronic bronchitis. *The American journal of medicine* 2000: 109(4): 288-295.

344. Marin A, Garcia-Aymerich J, Sauleda J, Belda J, Millares L, Garcia-Nunez M, Serra I, Benet M, Agusti A, Anto JM, Monso E, On Behalf Of The Pac-Copd Study G. Effect of Bronchial Colonisation on Airway and Systemic Inflammation in Stable COPD. *Copd* 2012: 9(2): 121-130.

345. Churg A, Zhou S, Wright JL. Series "matrix metalloproteinases in lung health and disease": Matrix metalloproteinases in COPD. *The European respiratory journal : official journal of the European Society for Clinical Respiratory Physiology* 2012: 39(1): 197-209.

346. Jegot G, Derache C, Castella S, Lahouassa H, Pitois E, Jourdan ML, Remold-O'Donnell E, Kellenberger C, Gauthier F, Korkmaz B. A substrate-based approach to convert SerpinB1 into a specific inhibitor of proteinase 3, the Wegener's granulomatosis autoantigen. *The FASEB journal : official publication of the Federation of American Societies for Experimental Biology* 2011: 25(9): 3019-3031.

347. Choi M, Eulenberg C, Rolle S, von Kries JP, Luft FC, Kettritz R. The use of small molecule high-throughput screening to identify inhibitors of the proteinase 3-NB1 interaction. *Clin Exp Immunol* 2010: 161(2): 389-396.

348. Wysocka M, Lesner A, Gruba N, Korkmaz B, Gauthier F, Kitamatsu M, Legowska A, Rolka K. Three wavelength substrate system of neutrophil serine proteinases. *Analytical chemistry* 2012: 84(16): 7241-7248.

349. Korkmaz B, Poutrain P, Hazouard E, de Monte M, Attucci S, Gauthier FL. Competition between elastase and related proteases from human neutrophil for binding to alpha1-protease inhibitor. *American journal of respiratory cell and molecular biology* 2005: 32(6): 553-559.

350. Epinette C, Croix C, Jaquillard L, Marchand-Adam S, Kellenberger C, Lalmanach G, Cadene M, Viaud-Massuard MC, Gauthier F, Korkmaz B. A selective reversible azapeptide inhibitor of human neutrophil proteinase 3 derived from a high affinity FRET substrate. *Biochemical pharmacology* 2012: 83(6): 788-796.

351. Perera NC, Schilling O, Kittel H, Back W, Kremmer E, Jenne DE. NSP4, an elastase-related protease in human neutrophils with arginine specificity. *Proc Natl Acad Sci U S A* 2012: 109(16): 6229-6234.

352. Pemberton PA, Cantwell JS, Kim KM, Sundin DJ, Kobayashi D, Fink JB, Shapiro SD, Barr PJ. An inhaled matrix metalloprotease inhibitor prevents cigarette smoke-induced emphysema in the mouse. *Copd* 2005: 2(3): 303-310.

353. Churg A, Wang R, Wang X, Onnervik PO, Thim K, Wright JL. Effect of an MMP-9/MMP-12 inhibitor on smoke-induced emphysema and airway remodelling in guinea pigs. *Thorax* 2007: 62(8): 706-713.

354. Atkinson JJ, Lutey BA, Suzuki Y, Toennies HM, Kelley DG, Kobayashi DK, Ijem WG, Deslee G, Moore CH, Jacobs ME, Conradi SH, Gierada DS, Pierce RA, Betsuyaku T, Senior RM. The role of matrix metalloproteinase-9 in cigarette smoke-induced emphysema. *American journal of respiratory and critical care medicine* 2011: 183(7): 876-884.

355. Magnussen H, Watz H, Kirsten A, Wang M, Wray H, Samuelsson V, Mo J, Kay R. Safety and tolerability of an oral MMP-9 and -12 inhibitor, AZD1236, in patients with moderate-to-severe COPD: a randomised controlled 6-week trial. *Pulmonary pharmacology & therapeutics* 2011: 24(5): 563-570.

356. Dahl R, Titlestad I, Lindqvist A, Wielders P, Wray H, Wang M, Samuelsson V, Mo J, Holt A. Effects of an oral MMP-9 and -12 inhibitor, AZD1236, on biomarkers in moderate/severe COPD: a randomised controlled trial. *Pulmonary pharmacology & therapeutics* 2012: 25(2): 169-177.

12 Appendices

12.1 Publications relevant to this thesis

12.1.1 Original articles

Sinden NJ and Stockley RA.
Proteinase 3 Activity in Sputum from Subjects with Alpha-1-Antitrypsin Deficiency and COPD.
ERJ 2013; 41(5): 1042-50.

12.1.2 Review articles

Sinden NJ and Stockley RA.
Systemic inflammation and co-morbidity in COPD: A result of "overspill" of inflammatory mediators from the lungs? A review of the evidence.
Thorax 2010; 65(10): 930-6.

Sinden NJ and Stockley RA.
Chronic obstructive pulmonary disease: an update of treatment related to frequently associated co-morbidities.
Therapeutic Advances in Chronic Disease 2010; 1: 43-57.

12.1.3 Conference abstracts

Sinden N, Dafforn T, Stockley R.
Inhibitory profiles of alpha-1-antitrypsin from PiZ & PiSZ individuals and implications for tissue destruction in emphysema.
Thematic poster at European Respiratory Society conference (ERS) 2011.

Sinden N, Ungurs M, Edgar R, Bharadwa P, Stockley R.
Proteinase 3 activity in sputum from alpha-1-antitrypsin deficient subjects.
Spoken presentation at winter British Thoracic Society (BTS) 2011.

Sinden NJ, Stockley RA.
Proteinase 3- A potential therapeutic target in COPD?
Spoken presentation at West Midlands Physicians Association (WMPA) 2012.
Winner of Stephen Whittaker prize

Sinden NJ, Stockley RA.
Alpha 1 antitrypsin deficiency: significance of the PiFZ genotype.
Poster presentation at COPD 8 conference, Birmingham 2012.

Sinden N, Stockley R.
Proteinase 3 activity is present in sputum from subjects with alpha-1-antitrypsin deficiency and COPD.
Poster discussion at ERS 2012.

Sinden N, Dafforn T, Stockley R.
Proteinase 3 and its potential role in emphysema.
Poster discussion at ERS 2012.

Sinden NJ, Sapey E, Walton G, Stockley RA.
Neutrophil cell membrane expression of Proteinase 3 and its relationship to alpha-1-antitrypsin deficiency.
Spoken presentation at winter BTS 2012.

Ungurs MJ, Sinden NJ, Stockley RA
Association between PGRN and airway inflammation in COPD.
Poster at winter BTS 2012.

Ungurs M, Sinden N, Stockley R.
Presence of progranulin in airway inflammation associated with COPD.
Thematic poster at ERS 2013.